Automatisierung und Kalibrierung des sFIDA-Assays zur frühzeitigen Diagnose von neurodegenerativen Krankheiten

Inaugural-Dissertation

zur Erlangung des Doktorgrades
der Mathematisch-Naturwissenschaftlichen Fakultät
der Heinrich-Heine Universität Düsseldorf

vorgelegt von

Yvonne Nelly Herrmann
aus Koblenz

Jülich, Oktober 2016

aus dem Institut für Physikalische Biologie
der Heinrich-Heine-Universität Düsseldorf

Gedruckt mit der Genehmigung der
Mathematisch-Naturwissenschaftlichen Fakultät der
Heinrich-Heine-Universität Düsseldorf

Referent: Prof. Dr. Dieter Willbold
Korreferent: Prof. Dr. Marco Oldiges
Tag der mündlichen Prüfung: 24.11.2016

Danksagungen

An erster Stelle möchte ich mich bei meinem Doktorvater Prof. Dr. Dieter Willbold bedanken. Er gab mir die Möglichkeit an diesem spannenden Thema mit exzellenten Mitarbeitern zu arbeiten und stellte mir auch eine ausgezeichnete Laborausstattung zur Verfügung. Außerdem ein Danke für die interessanten Diskussionen, Denkanstöße und Unterstützung in meinem Projekt.

Mein Dank gilt auch Prof. Dr. Marco Oldiges für die Übernahme der Zweitkorrektur.

Ganz besonders möchte ich mich bei der sFIDA-Gruppe bedanken. Insbesondere bei Dr. Oliver Bannach, Dr. Andreas Kulawik und Dr. Katja Kühbach. Ihr habt mich bei großen und kleinen Problemen unterstützt, immer gute Ratschläge und ein offenes Ohr gehabt. Bei Dr. Oliver Bannach und Dr. Andreas Kulawik möchte ich mich besonders für den Beistand und das Verständnis in den kritischen Phasen bedanken. Dr. Katja Kühbach gilt mein besonderer Dank für das Korrekturlesen meiner Dissertation. Danke auch für die Rettung am Mikroskop und die aufbauenden Worte im Büro, im Labor, im Pinocchio, in der Eisdiele oder beim Kartoffel-Essen.

Christina Linnartz und Loreano Peters haben immer frischen Wind ins Büro gebracht und viel Freude verbreitet. Danke für die Unterstützung und das Ertragen meiner 5 Minuten.

Mein Dank gilt ebenfalls allen anderen Mitgliedern der sFIDA-Arbeitsgruppe, Johannes Willbold, Dr. Kateryna Kravchenko, Dr. Tuyen Bujnicki und Dr. Christian Zafiu für die tolle Zusammenarbeit und die Unterstützung während der Erarbeitung der Manuskripte und meiner Dissertation.

Dr. Maren Hülsemann und Dr. Antonia Klein möchte ich mich für die tolle Zeit in Jülich bedanken. Ich bin froh, dass ihr mir selbst dann noch aus der Ferne Rückhalt gegeben habt.

Ich danke Tamar, Judith, Maren und Christina die immer zur richtigen Zeit aufmunternde Worte gefunden haben.

Ganz besonders möchte ich mich bei meinen engsten Freunden, Wiebke, Hanna, Felicitas, Andreas und Miriam bedanken, die mir zu jeder Zeit zu gehört haben und mir immer gesagt haben "Du schaffst das!".

I also need to thank my host-sister Natasha Roberts for all the hours on Skype listening to me and sending the love, strength, smiles and care packages I needed.

Schließlich möchte ich mich bei Sonja und Georg für die offenen Ohren bedanken und bei meiner Schwester Nadine besonders für die Kraft, die sie mir gegeben hat. Schließlich gilt mein größter Dank meinen Eltern für die permanente Unterstützung bei jedem Schritt auf meinem Lebensweg.

Abstract

Protein misfolding diseases including Alzheimer's disease (AD) and Parkinson disease (PD) are characterized by pathological accumulation of aggregated proteins. In AD, the aggregation of the amyloid β peptide (Aβ) is believed to trigger the disease, whereas in PD the protein α-synuclein (α-syn) is prone to disease-related aggregation. According to the current state of knowledge, soluble oligomers of these proteins are probably the major neurotoxic species and presumably the most direct biomarker in both diseases. The sFIDA assay (surface-based fluorescence intensity distribution analysis) is a highly sensitive technology to determine the concentration of oligomeric Aβ and α-syn as AD and PD biomarker, respectively. The aim of this work was to develop and analyse standard molecules for the sFIDA assay. Further optimization of the sFIDA assay was introduced by automating the preparative procedure on a liquid handling system.

Sensitive detection of stabilized Aβ oligomers as standard molecules in the sFIDA assay was demonstrated by a calculated lower limit of detection of 18 fM oligomers spiked into cerebrospinal fluid (CSF). The development and use of novel standard molecules based on silica nanoparticles coated with Aβ (Aβ-SiNaPs) was described. These Aβ-SiNaPs were further used to identify EDTA as the most suitable anti-coagulant for Aβ oligomer quantitation in blood plasma.

The implementation of the sFIDA assay on a robotic liquid handling system enhanced the robustness and the performance of the assay. By sFIDA automation, parallel processing of a high number of samples was possible without increasing the workload for the operator and the chance of human error. For the investigation of the automated sFIDA performance, crucial assay parameters such as limit of detection, coefficient of variation and linearity were determined. In comparison to manual operation, the lower limit of detection could be reduced to the sub-femtomolar range (0.85 fM).

Finally, silica nanoparticles coated with α-synuclein (α-syn-SiNaPs) were produced to establish a standard molecule for oligomer-based diagnostics of PD. The α-syn-SiNaPs were spiked into CSF and buffer (PBS) and could be detected down to a limit of 2.5 fM.

In conclusion, the results from this work lay the foundation to apply the sFIDA technology in high-throughput validation of oligomeric proteins as biomarkers for AD, PD, and other protein misfolding diseases.

Zusammenfassung

Proteinfehlfaltungserkrankungen, darunter die Alzheimersche Demenz (AD) und Parkinson-Krankheit (PD), zeigen als pathologisches Merkmal die Akkumulation von aggregierten Proteinen. In der AD wird die Aggregation von amyloid-β (Aβ) als Auslöser der Krankheit betrachtet. Während in der PD das Protein α-synuclein (α-syn) zu Fehlfaltung und Aggregation neigt.

Nach derzeitigem Kenntnisstand gelten die löslichen Oligomere dieser Proteine als die Spezies mit der stärksten toxischen Wirkung und sind dadurch vermutlich ein direkter Biomarker für beide Krankheiten. Der sFIDA-Assay (surface-based fluorescence intensity distribution analysis) ist eine hoch sensitive Methode zur Bestimmung der Konzentration von Aβ- und α-syn-Oligomeren als Biomarker für jeweils AD und PD. Das Ziel der vorliegenden Arbeit war die Entwicklung und Analyse von Standardmolekülen im sFIDA-Assay. Eine weitere Optimierung des sFIDA-Assays stellt die Automatisierung der Assay-Präparation auf einem *liquid handling system* dar.

Der sensitive Nachweis von stabilisierten Aβ-Oligomeren als Standardmolekül im sFIDA-Assay wurde durch die Berechnung der Nachweisgrenze von 18 fM der Oligomere verdünnt in Cerebrospinal Flüssigkeit (CSF) gezeigt. Die Entwicklung und Verwendung von einem neuen Standard in Form von Silica-Nanopartikeln mit kovalent gebundenen Aβ (Aβ-SiNaPs) wurde vorgestellt. Diese Aβ-SiNaPs wurden verwendet, um EDTA als geeignetsten Gerinnungshemmer für die Quantifizierung von Aβ-Oligomeren in Blutplasma zu identifizieren.

Die Implementierung des sFIDA-Assay auf einem automatisierten *liquid handling system* steigert die Robustheit und Sensitivität des Assays. Durch die Automatisierung ist die parallele Verarbeitung von einer hohen Anzahl von Proben möglich ohne die Arbeitsbelastung der Anwender und das Risiko von menschlichen Fehlern zu erhöhen. Für die Untersuchung des automatisierten sFIDA-Assays wurden folgende Assay-Parameter untersucht: Nachweisgrenze, Variationskoeffizient und Linearität. Im Vergleich zur manuellen Durchführung wurde die Nachweisgrenze von Aβ-SiNaPs in CSF im sub-femtomolaren Bereich (0.85 fM) erreicht.

Schließlich wurden die Silica-Nanopartikel mit α-synuclein (α-syn-SiNaPs) hergestellt, um ein Standardmolekül zur Diagnose der PD auf Basis von Oligomeren zu etablieren. Die α-syn-SiNaPs wurden in CSF und Puffer verdünnt und eine Nachweisgrenze von 2.5 fM wurde erreicht.

Zusammenfassend dienen die Ergebnisse dieser Arbeit als Grundlage zur Verwendung der sFIDA-Technologie im Hochdurchsatz. Dadurch wird die Validierung von Proteinen in Form von Oligomeren, die als Biomarker für AD, PD und anderen Proteinfehlfaltungserkrankungen dienen können, ermöglicht.

Inhaltsverzeichnis

Abkürzungsverzeichnis

α-syn	α-synuclein
Aβ	Amyloid-β
Aβ_{1-40}	Amyloid-β_{1-40} (mit Aminosäuren 1-40)
Aβ_{1-42}	Amyloid-β_{1-42} (mit Aminosäuren 1-42)
ACH	*Amyloid cascade hypothesis* (Amyloid-Kaskaden-Hypothese)
AD	Alzheimersche Demenz
ADDL	*Aβ-derived diffusible Ligands*
AICD	APP intracellular domain (APP intrazelluläre Domäne)
APOE4	Apolipoprotein-E ϵ4 Allel
APP	Amyloid precursor protein (Amyloid-Vorläuferprotein)
BACE 1	β-*site APP cleaving Enzym 1*
Bsp	Beispiel
cLLD	*Capacitive liquid level detection*
CSF	*Liquor cerebrospinalis* (Zerebrospinalflüssigkeit, Liquor)
CTF83	C-Terminale Fragment 83
CTF99	C-terminale Fragment 99
CV	*Coefficient of variance* (Koeffizient der Varianz)
DMSO	Dimethylsulfoxid
EDC	1-Ethyl-3-(3-dimethylaminopropyl)carbodiimid
EDTA	Ethylendiamintetraessigsäure
ELISA	*Enzyme Linked Immunosorbent Assay* (antikörperbasiertes Nachweisverfahren)
EOAD	*Early-onset* AD
FCS	Fluoreszenzkorrelationsspektroskopie
FIDA	*Fluorescence intensity distribution analysis* (Fluoreszenz-Intensität-Distribution-Analyse)
fMRT	Funktionelle Magnetresonanztomographie
HCl	Salzsäure
HMW	*High molecular weight* (hochmolekular)

HPLC ..... *High-performance liquid chromatography* (Hochleistungsflüssigkeitschromatographie)
kDa ..... Kilodalton
LB ..... *Lewy bodies* (Lewy-Körperchen)
LBD ..... *Lewy-Body*-Demenz
LHC ..... *Liquid Handling Control*
LLD ..... *liquid level detection* (Flüssigkeitsstand Detektion)
LMW ..... *Low molecular weight* (geringes Molekulargewicht)
LOAD ..... *Late-onset* AD
LSM ..... Laser-Scanning Mikroskopie
LTP ..... *Long-term potentiation* (Langzeit-Potenzierung)
MCI ..... *Mild cognitive impairment*
mDa ..... Megadalton
MES ..... 2-(N-Morpholino)ethansulfonsäure
min ..... Minuten
ML ..... Microlab
MMSE ..... *Mini-Mental-State-Examination*
MRT ..... Magnetresonanztomographie
NaOH ..... Natriumhydroxid
NFT ..... *Neurofibrillary tangles* (neurofibrillären Bündel)
NHS ..... N-Hydroxysuccinimid
PBS ..... Phosphatgepufferte Salzlösung
PBS-T ..... Phosphatgepufferte Salzlösung mit 0,05% Tween
PD ..... *Parkinson's disease* (Parkinson-Krankheit)
pE3Aβ ..... Pyroglutamat-Aβ (Position 3)
PEG ..... Polyethylenglycol
PET ..... Positronen-Emissions-Tomographie
pLLD ..... *Pressure liquid level detection*
PrP ..... Prion-Protein
PS1 ..... Präsenilin 1
PS2 ..... Präsenilin 2
sFIDA ..... *Surface-based fluorescence intensity distribution analysis* (Oberflächenbasierende Fluoreszenz-Intensität-Distribution-Analyse)
SiNaPs ..... Silica-Nanopartikel
Std ..... Stunden
TEM ..... *Transmission electron microscopy* (Transmissionselektronenmikroskop)

UZ ..... Ultrazentrifuge

VBA ..... *Visual Basic for Applications*

Abbildungsverzeichnis

Tabellenverzeichnis

1. Einleitung

In diesem Kapitel wird die Krankheit Alzheimersche Demenz (AD) vorgestellt. Dabei werden die biologischen Grundlagen zum Verständnis der Krankheit dargestellt und das Verfahren sFIDA zur frühzeitigen Diagnose der AD wird im Detail beschrieben. Es folgt eine Zusammenfassung der Parkinson-Krankheit (*Parkinson disease*, PD), die eine weitere neurodegenerativen Erkrankung ist. Im Anschluss wird die Automatisierung von Prozessen und ihre Verwendung, und damit verbundene Fortschritte und Verbesserungen, im Laborbereich geschildert.

1.1 Alzheimersche Demenz

Die Alzheimersche Demenz (AD) ist eine neurodegenerative Krankheit und gehört außerdem zu den Proteinfehlfaltungserkrankungen (Soto, 2003; Brettschneider et al., 2015). Die AD wurde vom deutschen Psychiater Alois Alzheimer erstmalig im Jahre 1906 beschrieben. Als charakteristische Symptome der AD gelten die Abnahme von kognitiven Funktionen, wie Orientierung und Wortfindung, und der Verlust des episodischen Gedächtnisses (Alzheimer, 1911; Herrup, 2015).

AD ist die häufigste Form der Demenz mit einem Anteil von 60 bis 80% der Demenzkranken (Lansdall, 2014). In Abhängigkeit des Alters der Betroffene wird die AD in zwei Typen kategorisiert:

- Typ 1: früher Beginn der Erkrankung (*early-onset* AD, EOAD)
- Typ 2: später Beginn der Erkrankung (*late-onset* AD, LOAD)

Die EOAD-Patienten haben einen Anteil von 1 bis 6% der AD-Patienten und das Alter der Betroffenen liegt zwischen 30 und 65 Jahren (Bekris et al., 2010). Der Krankheitsverlauf der EOAD mit relativ schneller Verschlechterung weist vielseitige Störungen der höheren kortikalen Funktionen auf (World Health Organization, 2015). Demgegenüber beginnt die LOAD ab dem 65. Lebensjahr und hat einen langsamen Krankheitsverlauf mit Gedächtnisstörungen als Hauptmerkmal (World Health Organization, 2015; Bekris et al., 2010).

Zusätzlich wird zwischen familiärer und sporadischer AD unterschieden. Die familiäre AD ist genetisch bedingt und 5% der AD-Patienten gehört zu dieser Gruppe (Luo et al., 2016). Der größte Anteil der Patienten (bis 95%) entwickelt die Krankheit sporadisch, wobei das fortgeschrittene Alter als größter Risikofaktor gesehen wird (Finder and Glockshuber, 2007; Roychaudhuri et al., 2009; Sakono and Zako, 2010).

Einer Prognose zur Folge werden 2050 weltweit bis zu 80 Millionen Menschen an AD erkrankt sein (Humpel, 2011). Die Betroffenen, sowie deren Angehörige, werden stark durch die Krankheit belastet, und die Patienten benötigen vor allem im späten Stadium Betreuung. Dadurch wird das Gesundheitssystem mit hohen Kosten zur Versorgung und Pflege der AD-Patienten konfrontiert (Lansdall, 2014; Gilbert, 2014; Swomley et al., 2014).

Der Krankheitsverlauf der AD wird in drei Phasen unterteilt (Blennow et al., 2010; Nabers et al., 2016):

1. Präklinische Phase, in der die kognitiven Beeinträchtigungen nicht stark ausgeprägt sind

2. Prodromalphase, in der Patienten leichte kognitiven Beeinträchtigungen (*mild cognitive impairment*, MCI) aufweisen (Blennow et al., 2010)

3. Endphase der AD, in der Patienten stark ausgeprägte kognitive Beeinträchtigungen aufweisen

Zurzeit ist die korrekte Diagnose der AD mit bis zu 90% möglich, wobei folgende Kriterien einbezogen werden: medizinische Vorgeschichte, physikalische Untersuchungen, Labortests, bildgebende Verfahren (*brain imaging*) und neuropsychologische Beurteilungen (Humpel, 2011). Im Abschnitt 1.1.2 werden die eingesetzten Verfahren zur Diagnose der AD im Detail beschrieben. Die Diagnose der AD kann nur *post-mortem* anhand pathologischer Merkmale verifiziert werden (Humpel, 2011).

Die pathologischen Hauptmerkmale der AD sind die amyloiden Plaques und NFTs im Gehirn der Patienten (Alzheimer, 1911; Lansdall, 2014; Swomley et al., 2014; Thal et al., 2015). Die amyloiden Plaques bestehen aus unlöslichen, extrazellulären Ablagerungen, die überwiegend aus Aβ bestehen (Serrano-Pozo et al., 2011; Lansdall, 2014). NFTs bestehen aus einer hyperphosphorylierten Form des tau-Proteins und liegen intrazellulär vor.

1.1.1 Amyloid-β

1.1.1.1 Synthese von Aβ

Aβ ist ein Protein mit 36 bis 43 Aminosäuren und entsteht durch die Endoproteolyse des *Amyloid Precursor Proteins* (APP). APP ist ein Typ I Membranprotein, das durch unterschiedliche Splicing-Vorgänge in drei Isoformen APP_{695}, APP_{751} und APP_{770} gebildet wird (Sandbrink et al., 1996). In den Neuronen ist besonders das APP_{695} vorzufinden (Gralle and Ferreira, 2007).

Es gibt zwei proteolytische serielle Prozessierungswege des APPs (siehe Abbildung 1.1). Der nicht-amyloidogene Verlauf wird durch die α-Sekretase eingeleitet (Hiltunen et al., 2009; Hicks et al., 2012). Diese Sekretase prozessiert das APP innerhalb der Aβ-Region und verhindert so die Bildung von Aβ (Allinson et al., 2004). Dabei entstehen die lösliche Ektodomäne sAPPα und das C-terminale Fragment 83 (CTF83) . Die γ-Sekretase prozessiert das entstandene CTF83, sodass p3 und die APP intrazellulär Domäne (AICD) als Produkt entstehen. Die Funktion von p3 ist noch nicht aufgeklärt, und die AICD wird höchstwahrscheinlich abgebaut (Hicks et al., 2012). Die γ-Sekretase ist ein Multiprotein-Komplex, der die Protein-Untereinheiten Präsenilin 1 und 2 (PS1 and PS2) enthält.

Die serielle Prozessierung des APP im amyloidogenen Verlauf durch die β- und γ-Sekretase führt zur Freisetzung von Aβ in verschiedenen Isoformen. Die β-Sekretase besteht aus dem β-*site APP cleaving Enzym 1* (BACE 1) und spaltet das APP in die Produkte: lösliche Ektodomäne sAPPβ und das C-terminale Fragment 99 (CTF99). Das CTF99 wird von der γ-Sekretase prozessiert, sodass eine AICD und unterschiedliche Isoformen des Aβ-Proteins entstehen können. Die zwei häufigsten Isoformen sind $Aβ_{1-40}$ und $Aβ_{1-42}$, die im Verhältnis 10:1 gebildet werden (Hicks et al., 2012). Außerdem entstehen Aβ-Varianten, die am N-Terminus verkürzt sind. Davon ist das Pyroglutamat-Aβ (pE3Aβ) die häufigste Form. Diese Isoform beginnt mit dem Pyroglutamat der dritten Position am N-Terminus von Aβ.

Die löslichen Ektodomänen sAPPα und sAPPβ, die durch den nicht-amyloidogenen bzw. den amyloidogenen Prozessierungsweg entstehen, haben eine neuroprotektive Funktion (Allinson et al., 2004; Hiltunen et al., 2009; Hicks et al., 2012).

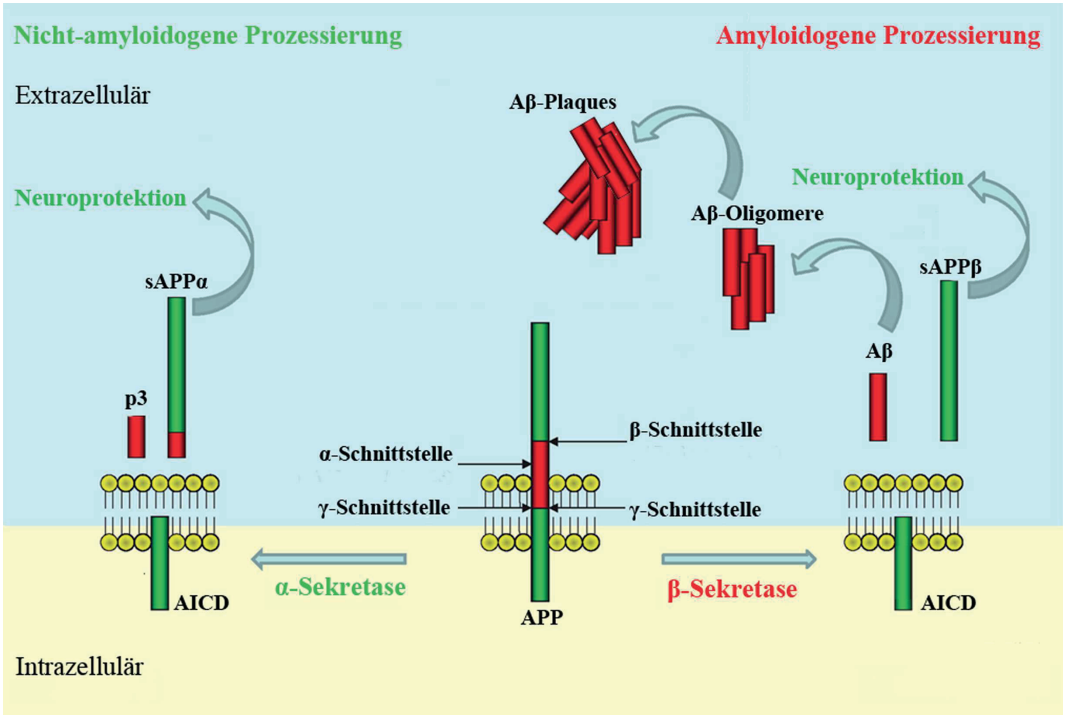

Abbildung 1.1: Nicht-amyloidogene und amyloidogene Prozessierung des APP.
APP besitzt Schnittstellen für die α-, β- oder γ-Sekretase. Die α-Sekretase leitet den nicht-amyloidogenen Weg ein und spaltet das APP in die Produkte sAPPα und das C-terminale Fragment 83 (CTF83) (links). Nach der Prozessierung des CTF83 durch die γ-Sekretase, entstehen als Produkte das p3-Fragment mit unbekannter Funktion und eine APP intrazellulär Domäne (AICD). Die amyloidogene Prozessierung (rechts) beginnt mit der Prozessierung von APP durch die β-Sekretase, wodurch das lösliche sAPPβ und das CTF99 als Produkte entstehen. Danach werden die Produkte Aβ mit $39-42$ Aminosäuren und eine AICD durch die Spaltung des sAPPβ durch die γ-Sekretase gebildet. (Abbildung in Anlehnung an Hicks et al. 2012)

Es gibt Hinweise auf verschiedene Funktionen von Aβ, wie die antimikrobielle Aktivität (Soscia et al., 2010) und die Wirkung als Antioxidans gegen oxidativen Stress (Zou et al., 2002; Baruch-Suchodolsky and Fischer, 2009). Außerdem konnte gezeigt werden, das Aβ ein Transkriptionsfaktor sein kann (Bailey et al., 2011; Tabaton et al., 2011) oder eine Rolle bei der Regulation vom Transport von Cholesterin spielt (Igbavboa et al., 2009; Baruch-Suchodolsky and Fischer, 2009). Trotzdem ist die Funktion von Aβ und der verschiedenen Produkte aus den zwei möglichen Wegen zur Prozessierungen von APP nicht vollständig aufgeklärt (Hiltunen et al., 2009).

In der familiären Form der AD wurden Mutationen im APP-Gen auf Chromosom 21 und in den Präsenilin-Genen auf Chromosom 14 (*psen-1*) und Chromosom 1 (*psen-2*) vorgefunden (Bekris et al., 2010). Für das APP-Gen wurden 32 verschiedene *missense* Mutationen in 85 Familien identifiziert und diese Mutationen wurden in 10% bis 15% der familiären AD Patienten vorgefunden. Die Gene *psen-1* und *psen-*

2 kodieren für die Proteine PS1 und PS2, die Untereinheiten der γ-Sekretase sind. Durch die Mutationen in diesen Genen kann die proteolytische Prozessierung des APP verändert und das Gleichgewicht vom APP-Metabolismus kann gestört sein. Es kann zur Erhöhung der Gesamtmenge an Aβ kommen und das vermehrte Vorkommen von Aβ-Isoformen, die zu Aggregation neigen (Finder and Glockshuber, 2007; Musiek and Holtzman, 2015).

Für die sporadische AD wurde noch kein kausatives Gen identifiziert. Das Apolipoprotein-E ϵ4 Allel (APOE4) wird in viele genetischen Studien mit der sporadischen AD in Zusammenhang gebracht (Bekris et al., 2010; Blennow et al., 2010).

1.1.1.2 Aggregation von Aβ

Die Expression des Vorläuferproteins APP und die Prozessierung zu Aβ ist ein normaler physiologischer Stoffwechselweg, sodass sich Aβ auch in der Zerebrospinalflüssigkeit (*liquor cerebrospinalis*, CSF) und im Gehirn von gesunden Menschen befindet (Hardy and Selkoe, 2002; Shoji et al., 1992; Haass et al., 1992). Dabei liegt Aβ in seiner monomerischen Form vor und hat einen amphiphilen Charakter, wobei der N-Terminus hydrophil ist und der C-Terminus, der als Teil des APP in der Membran vorliegt, hydrophobe Aminosäuren besitzt (Finder and Glockshuber, 2007).

Wie bereits in Abschnitt 1.1.1.1 erwähnt entstehen verschiedene Isoformen des Aβ, die auch unterschiedlichen Aggergationsverhalten vorweisen. Das $A\beta_{1-42}$ liegt schnell in der β-Faltblatt-Struktur vor (Finder and Glockshuber, 2007) und neigt zur stärkeren Aggregation zu Oligomeren *in vivo* als $A\beta_{1-40}$ (Haass and Selkoe, 2007). Eine weitere Isoform die zur starken Aggregation neigt ist das Pyroglutamat-Aβ und wurde vermehrt im Gehirn von AD-Patienten vorgefunden (Thal et al., 2015). Die Isoform $A\beta_{1-39}$ verbleibt länger in einer *random-coil*-Konformation bevor es zu Oligomeren mit hohem Anteil an β-Faltblättern aggregiert (Finder and Glockshuber, 2007).

Das Modell nach Finder und Glockshuber (2007) beinhaltet die Fibrillisierung von Aβ über den *Seeding*-Mechanismus (siehe Abbildung 1.2). In der lag-Phase wird zunächst ein Nuklei aus Aβ-Molekülen gebildet, der die Bildung von Protofibrillen und schließlich Fibrillen begünstigt. Es können sich Einheiten von Fibrillen lösen, die wiederum als Nuklei agieren und die Aggregation zu Fibrillen beschleunigen. Die lag-Phase kann entfallen oder wird verkürzt, wenn bereits geformte Aβ-Nuklei zu einem Aβ-Gemisch dazu gegeben werden und die Aggregation zu Fibrillen wird initiiert (Harper et al., 1997; Finder and Glockshuber, 2007; Thal et al., 2015).

Protofibrillen sind löslich und weisen eine stabförmige Struktur auf. Die Struktur setzt sich aus der Anordnung von Aβ-Monomeren in der β-Faltblatt-Konformation zusammen (Finder and Glockshuber, 2007). Protofibrillen gelten als Vorläufer zu der thermodynamisch stabileren Fibrillen. Diese Aggregationsform ist nicht löslich und besitzt eine filamentöse Struktur. Die untersuchten amyloiden Plaques von AD-Patienten sind große, extrazellulär vorliegende Aggregate, die hauptsächlich aus Aβ-Fibrillen bestehen (Finder and Glockshuber, 2007; Golde et al., 2011; Gilbert, 2014).

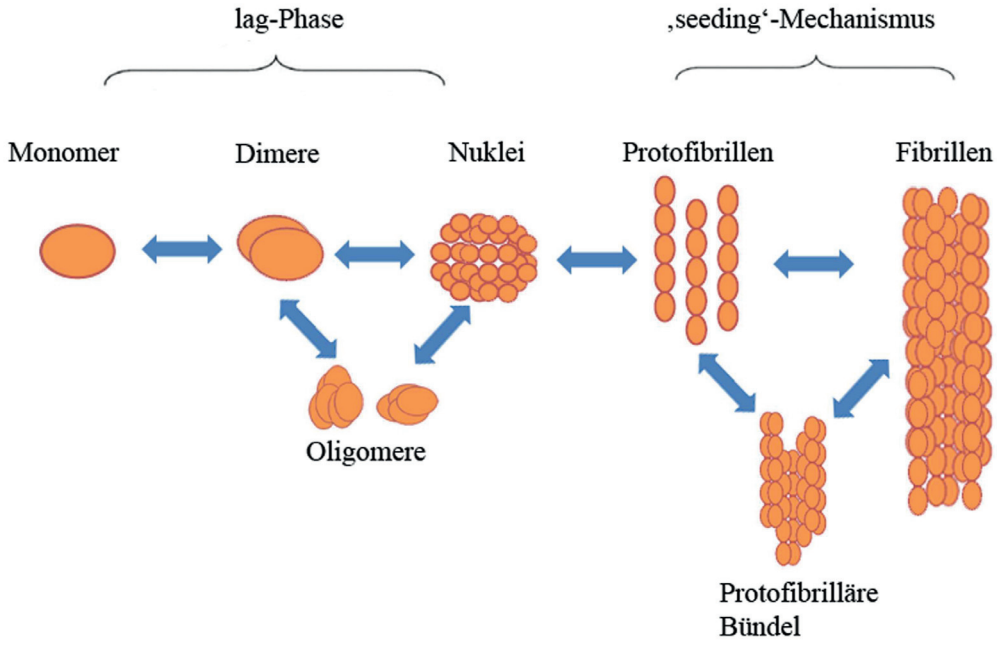

Abbildung 1.2: Schema zur Aggregation des Aβ.
Aβ-Monomere bilden zunächst Dimere und kleine, lösliche Oligomere. In der lag-Phase entstehen außerdem die sogenannten Nuklei, diese aggregieren über den Seeding-Mechanismus zu Protofibrillen und daraus bestehende Bündel. Schließlich werden Fibrillen gebildet. (Abbildung in Anlehnung an Finder and Glockshuber 2007 und Verma et al. 2015)

Die Initiierung der Aggregation von Aβ durch Aβ-Nuklei könnte demnach durch einen Prionen-ähnlichen Mechanismus erklärt werden (Brettschneider et al., 2015). Prion wurde von Prusiner 1982 als Begriff für einen proteinartigen, infektiösen Partikel eingeführt. Der infektiöse Partikel besteht überwiegend oder vollständig aus einer fehlerhaft gefalteten und aggregierten Form des Prion-Proteins (PrP) (Walker and Jucker, 2015). Die fehlerhafte Faltung kann spontan entstehen oder durch genetische Faktoren begünstigt werden (Goldmann, 2008; Walker and Jucker, 2015). Daraufhin wird eine Kettenreaktion ausgelöst, indem bei Kontakt zwischen normal gefalteten und fehlerhaft gefalteten Proteinen die Konformationsänderung des nor-

mal gefalteten zum fehlerhaft gefalteten Protein stattfindet (Olanow and Brundin, 2013; Stöhr et al., 2012; Brettschneider et al., 2015). Es kommt zu Ablagerungen von fehlerhaft gefalteten Prion-Protein, sodass es zum Verlust von Neuronen kommt und dadurch die Struktur des Gehirns schwammartig wird (Walker and Jucker, 2015). Die bekanntesten Prion-Krankheiten sind Bovine spongiforme Enzephalopathie (BSE) beim Rind, Traberkrankheit (*scrapie*) bei Schafen und Creutzfeldt-Jakob Krankheit beim Menschen (Uversky et al., 2008; Aguzzi, 2007; Walker and Jucker, 2015)

Das erhöhte Vorkommen und die Ausbreitung von Aβ-Aggregaten in transgenen, Aβ-exprimierenden Mäusen konnte gezeigt werden, wenn bereits aggregierte Aβ-Spezies aus synthetischer oder biologische Quelle in das Gehirn oder in die Bauchhöhle injiziert wurde (Stöhr et al., 2012; Eisele et al., 2009; Heilbronner et al., 2013).

Die Untersuchung der unterschiedlichen Aggregationsformen von Aβ ist schwierig, da sich die verschiedenen Spezies in einem dynamischen Gleichgewicht befinden, das sich bei Veränderung der chemischen Umgeben (Temperatur, pH-Wert Aβ-Konzentration, etc.) verschieben kann (Benilova et al., 2012; Finder and Glockshuber, 2007). Während der Analyse können die Spezies weiter aggregieren oder wieder dissoziieren (Herskovits et al., 2013). Zusätzlich kommen einzelne Spezies nur in sehr geringen Konzentrationen vor, was die Analyse weiter erschwert (Bruggink et al., 2012).

1.1.1.3 Amyloid-Kaskaden-Hypothese

Die Identifizierung von Aβ als Hauptbestandteil der senilen Plaques hat zur der Amyloid-Kaskaden-Hypothese (*Amyloid Cascade Hypothesis* (ACH)) geführt (Hardy and Selkoe, 2002; Armstrong, 2011). Die Hypothese beschreibt die Pathogenese der AD und wurde immer weiterentwickelt und neueren Erkenntnissen angepasst. Zu Anfang wurde angenommen die Ablagerungen von Aβ in Form von senilen Plaques führt zu den Symptomen der AD wie die Bildung neurofibrillären Bündel, das Absterben von Neuronen und das Auftreten von Demenz (Hardy and Higgins, 1992). Zurzeit werden die löslichen Aβ-Oligomere als die hochtoxische Spezies angesehen (Gralle and Ferreira, 2007; Bruggink et al., 2013; Jongbloed et al., 2015).

In der folgenden Abbildung 1.3 wird die ACH verdeutlicht, wonach die familiäre AD durch Mutationen in APP- oder Präsenilin-Genen ausgelöst wird. Während bei der sporadischen AD die Risikofaktoren, wie Alter und Umwelt am Anfang der Kaskade stehen. Die beiden Formen der AD beginnen mit dem vermehrten Vorkommen von Aβ durch verstärkte Produktion und/oder verringertem Aβ-Abbau

(Blennow et al., 2010). Dadurch entsteht ein Ungleichgewicht im Stoffwechselweg und die fehlerhafte Faltung sowie die Aggregation des Aβ wird begünstigt. Dementsprechend nimmt die Konzentration von neurotoxischen Aβ-Oligomeren zu und die Bildung von weiteren Aggregationsformen, wie Fibrillen, führt dann zur Entstehung von unlöslichen Plaques im Gehirn. Die vorhandenen Aggregationsformen von Aβ verändern die Aktivität von Kinasen und Phosphatasen, wodurch es zur Bildung von NFTs kommt. Außerdem kommt es zu entzündlichen Reaktionen und erhöhten oxidativen Stress im Gehirn. Die Fehlfunktion von Neuronen und Synapsen, sowie Defiziten bei der Funktion von Neurotransmittern und beeinträchtigte Langzeit-Potenzierung (LTP), führen zu den Symptomen der AD wie Orientierungslosigkeit und Gedächtnisverlust.

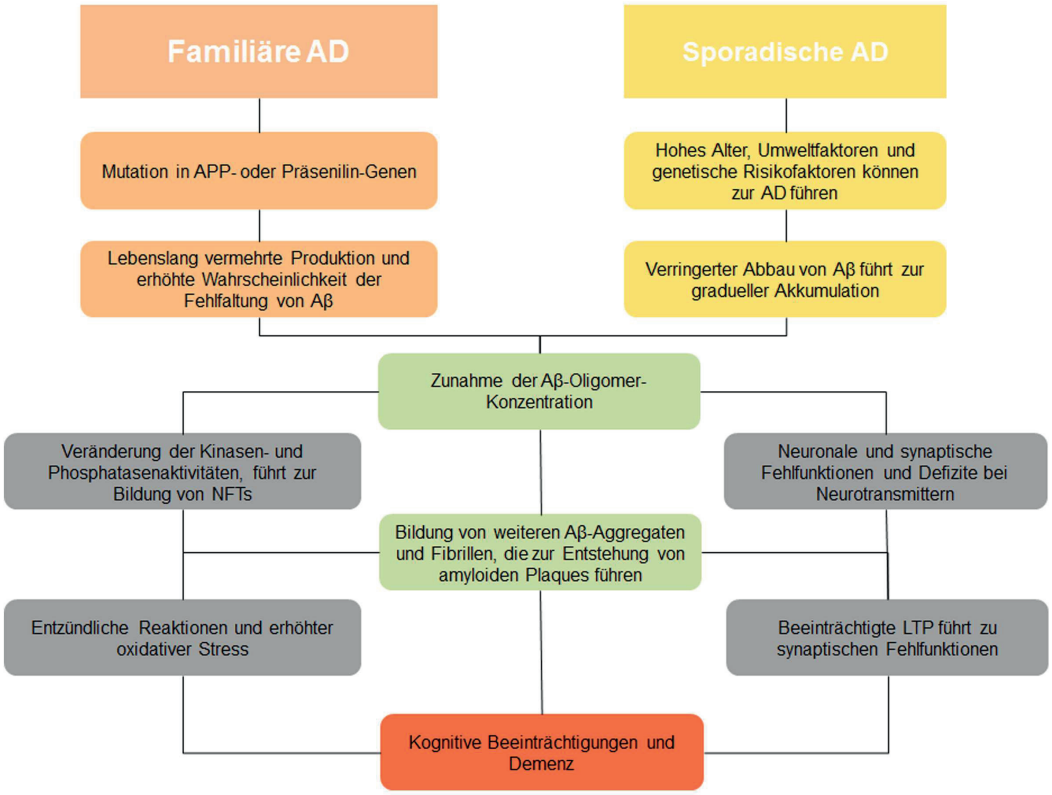

Abbildung 1.3: Amyloid-Kaskaden-Hypothese zur Entstehung und dem Fortschritt der AD.
Das Kaskaden-Modell beschreibt in beiden Fällen (familiäre und sporadische AD) zunächst ein Ungleichgewicht zwischen der Aβ-Produktion und dem Abbau, sodass Fehlfaltung und die Aggregation von Aβ begünstigt werden. Die erhöhte Konzentration von Aβ-Oligomeren und weiteren Aggregationsformen führt zu der Bildung von amyloiden Plaques und durch Veränderung von der Kinasen-und Phosphatasenaktivität werden neurofibrillärer Bündel (NFTs) geformt. Das Aufkommen von beeinträchtigter Langzeit-Potenzierung (LTP) führt zu synaptischen Fehlfunktionen. Außerdem kommt es zu Defiziten bei der Funktion von Neurotransmittern und weitere neuronale und synaptische Fehlfunktionen führen zu kognitiven Beeinträchtigungen (Abbildung in Anlehnung an Blennow et al. 2010).

Die ACH bleibt weiterhin eine Hypothese mit Argumenten dafür und dagegen (Herrup, 2015). Die Argumente für die ACH beinhalten die identifizierten genetischen Faktoren und hauptsächlich Studien, die den Einfluss von Aβ-Aggregaten untersuchten. Im Gegensatz dazu gibt es auch eine Reihe von Ergebnissen aus Studien, die Argumente gegen die ACH liefern, da gezeigt werden konnte das nur die Überexpression von Aβ oder die Veränderung der identifizierten Gene nicht immer zur AD führten. Die Abbildung 1.4 gibt eine Übersicht über die Stärken und Schwächen der ACH.

	Stärken	Schwächen
Genetik	• Identifizierte APP und PSEN Gene in familiären AD • APOE4 Varianten beeinflussen das Risiko für AD und den Aβ-Abbau • Seltene APP Mutation verringert Bildung von Aβ und schützt vor AD	• Keine Mutationen für α-Sekretase oder BACE gefunden • Polymorphismen in Genen von APP, PSEN, BACE und MAPT (tau) haben nur wenige Assoziationen • MAPT Mutation steht in Verbindung zu frontotemporale Demenz
Biochemie	• Aβ entsteht durch Prozessierung von APP durch γ-Sekretase (PSEN) • Bedingungen zur Bildung von $A\beta_{1\text{-}42}$ führt zu vermehrter Aggregation • Zunahme des AD Risikos durch APOE4, Aβ-Abbau wird verlangsamt	• Alleinige Expression von Aβ in transgene Mäusen nicht ausreichend • Andere biochemische Defizite kommen in der AD vor, die Demenz zu verursachen
Tiermodelle	• Überexpression von menschlichem APP in Mäusen führt zu Plaques • Transgene Mäuse mit menschlichem APP zeigen Defizite für Gedächtnisfunktionen • Aβ ist toxisch für Neuronen in Kultur • Überexpression von menschlichem APP in Fruchtfliegen führt zu Neurodegeneration	• Überexpression von menschlichem APP in Mäusen führt nicht zu NFTs, Neuro-degeneration oder Demenz wie in AD • PSEN Transgene haben keine Plaques, NFTs oder Neurodegeneration • Defizite für Gedächtnisfunktionen in Transgenen werden schnell und komplett korrigiert
Pathologie	• Aβ-Plaques kommen häufig im Gehirn von AD-Patienten vor	• NFTs korrelieren besser mit Neuro-degeneration im Gegensatz zu Plaques • Individuen mit erhöhten Plaque Vorkommen können normale kognitive Funktionen haben
Klinische Funde	• Plaques erhöhen das AD Risiko • In manchen Individuen mit Aβ-Ablagerungen und Demenz verbessern sich die kognitiven Funktionen durch Anti-Aβ-Therapien	• Nachdem es zur AD kommt, verbessert sich die kognitive Funktionen nicht wenn Reduzierung von Plaques statt findet • Per Definition, gibt es keine AD ohne Plaques und Ablagerungen in Form von Plaques ohne Demenz bedeutet präklinische AD • Keine klinische Studie in Phase 3 basierend auf ACH war erfolgreich • Inhibierung von γ-Sekretase verstärkt AD Symptome
Epidemiologie		• Nichtsteroidale und entzündungshemmende Medikamente halbieren das AD Risiko

Abbildung 1.4: Stärke und Schwächen der Amyloid-Kaskaden-Hypothese. (In Anlehnung an Herrup 2015)

Die kürzlich veröffentlichten Berichte von Musiek et al. 2015 und Herrup et al. 2015 argumentieren jeweils für und gegen die ACH. Jedoch gibt es den Konsens, dass die AD stark mit der Aggregation von Aβ verbunden ist. Trotzdem wird der Verlust von Neuronen und die Entstehung von Plaques und NFTs als komple-

xe Prozesse gesehen und vermutet das die Ursachen auf unterschiedliche vernetzte Faktoren basieren. Die folgenden Faktoren sollen zur Entstehung von AD beitragen: die lysosomale Fehlfunktion, der Verlust der Homöostase von Calciumionen (Ca^{2+}), Neuroinflammation, die starke Beschädigung durch oxidativen Stress und Probleme im Glukose Metabolismus (Luo et al., 2016). Dementsprechend reicht die ACH in der derzeitigen Form nicht aus, um die Entstehung der AD zu beschreiben.

1.1.2 Diagnose der Alzheimerschen Demenz

1.1.2.1 Klinische Diagnose

Die AD kann erst *post-mortem* durch die mikroskopische Untersuchung des Gehirns zweifellos anhand von amyloiden Plaques und NFTs diagnostiziert werden (Mucke, 2009; Humpel, 2011). Bei der Diagnose von lebenden Patienten bestimmt die Sensitivität und Spezifität eines untersuchten Parameters die Eignung als Diagnosekriterium (Humpel, 2011). Die Sensitivität entspricht dem Anteil der richtig positiv getesteten Patienten [in %], während die Spezifität die Korrektheit der identifizierten Kontrollen [in %] angibt. Zurzeit hat die Diagnose der AD durch die Kombination von verschiedenen, untersuchten Kriterien eine Sensitivität von 70,9 bis 87,3% und die Spezifität liegt zwischen 44,3 und 70,8% (Beach et al., 2012).

Eine frühzeitige Diagnose der AD ist nicht nur für den Patienten und sein Umfeld wichtig, sondern auch um die Entwicklung von Medikamenten und Therapiemöglichkeiten voran zu treiben. Beispielsweise sollte bei einer klinischen Studie zu einem Medikament zur Therapie der AD Probanden ausgewählt werden, die im frühen Stadien (präklinische Phase oder Prodromalphase) der Krankheit sind (Blennow et al., 2010; Bittner et al., 2016; Olsson et al., 2016). Damit während der Studie der Krankheitsverlauf der AD mit und ohne Behandlung verfolgt werden kann. Probanden mit anderen Demenz-Krankheiten könnten das Ergebnis der klinischen Studie beeinflussen, da die eingesetzte Therapie für die AD vorgesehen ist und nicht für andere Demenz-Arten. Eine frühe Diagnose kann des weiteren eine frühzeitige Behandlung der AD ermöglichen, um den Verlauf der AD zu mindern oder sogar vor dem Auftreten der ersten Symptome und dem Absterben von Neuronen die Entwicklung der Krankheit verhindern (Blennow et al., 2010; Golde et al., 2011; Lansdall, 2014).

Ein erster klinischer Test um zunächst eine Demenz festzustellen ist der MMSE (*Mini-Mental-State-Examination*) entwickelt von Folstein in 1975. Hierbei handelt sich um die Untersuchung von kognitiven Funktionen des Patienten durch ein Interview. Es werden verschiedene Fragen und Aufgaben gestellt, deren korrekte Lö-

sung ein Punkt ergeben. Anhand der erreichten Punktzahl werden die Patienten in Kategorien eingeordnet. Maximal können 30 Punkte erreicht werden, die für uneingeschränkte kognitive Funktionen steht. Wenn die Punkte unter 20 liegen, wird der Patient als dement eingestuft (Folstein et al., 1975).

Die Diagnose der AD erfolgt über die Untersuchung von weiteren klinischen und neuropathologischen Kriterien, um die AD von anderen Demenzen zu unterscheiden. Dabei kommen bildgebende Verfahren (*Brain Imaging*) wie Magnetresonanztomographie (MRT) und Positronen-Emissions-Tomographie (PET) zum Einsatz. Diese untersuchen das Gehirn auf charakteristische Muster wie strukturelle und funktionale zerebrale Veränderungen, die auf eine AD hinweisen können (Johnson et al., 2016).

Die Atrophie im Gehirn gilt als ein charakteristisches Muster für AD und wird durch MRT untersucht. In den Gehirnarealen medialen Schläfenlappen, entorhinalen Kortex und Hippocampus wird eine Atrophie meist zu erst festgestellt (Johnson et al., 2016). Zusätzlich kann durch die Verwendung von funktioneller Magnetresonanztomographie (fMRT) die Neuronen-Aktivität indirekt untersucht werden. Im Hippocampus wurde eine Abnahme der Neuronen-Aktivität bei der Verarbeitung von neuen Informationen in klinisch diagnostizierten AD-Patienten festgestellt (Rombouts et al., 2000; Golby et al., 2005; Hämäläinen et al., 2007). In einigen anderen Studien konnte gezeigt werden, dass die Neuronen-Aktivität im präfrontalen Kortex in AD-Patienten zu genommen hat (Grady et al., 2003; Sperling et al., 2003; Solé-Padullés et al., 2009), um höchstwahrscheinlich die Defizite im Hippocampus zu kompensieren (Johnson et al., 2016).

Im PET wird die synaptische Aktivität durch die Untersuchung des Glukose-Metabolismus mittels radioaktiv markiertem ^{18}*F-fluorodeoxyglucose* (FDG) bestimmt (Johnson et al., 2016). Hierbei wurde eine Reduktion vom Glukose-Metabolismus in AD-Patienten festgestellt (Reiman et al., 1996; Minoshima et al., 1997; Santi et al., 2001). Bei der Verwendung von radioaktiv markiertem ^{11}*C-Pittsburgh compound B* (PIB) im PET werden Ablagerungen von unlöslichem Aβ im Gehirn untersucht, wobei diese erhöht in AD-Patienten lokalisiert wurden (Klunk et al., 2004).

Im nächsten Abschnitt 1.1.2.2 wird die Untersuchung von CSF-Proben der Patienten auf bestimmte molekulare Biomarker als weiteres Kriterium zur Diagnose der AD beschrieben.

1.1.2.2 Molekulare Biomarker

Der Begriff Biomarker umfasst objektiv gemessene und evaluierte Werte zur Kategorisierung normaler biologischen Prozesse, pathogenen Prozesse oder pharma-

kologischen Reaktionen auf therapeutische Ansätze (Blennow et al., 2010; Humpel, 2011). Dementsprechend kann ein Biomarker als Indikator für Gesundheit oder Krankheit sowie zum *Monitoring* des Krankheitsverlaufes genutzt werden.

Zur Diagnose der AD wird der Gehalt von Proteinen insbesondere im CSF bestimmt, da das CSF biochemische Veränderungen des Gehirns widerspiegeln kann (Blennow et al., 2010; Olsson et al., 2016). Folgende drei Proteingehalte wurden als molekulare Biomarker in Studien untersucht: $A\beta_{1-42}$, Gesamt-tau und phosphoryliertes tau (Hampel et al., 2010; Bittner et al., 2016; Olsson et al., 2016). Dabei zeigt totales und phosphoryliertes tau eine Zunahme in der Konzentration, während die Konzentration von Aβ im Krankheitsverlauf von AD abnimmt (Hölttä et al., 2013; Bibl et al., 2012).

Das Protein tau ist ein wichtiger Faktor bei der Stabilisierung der Mikrotubuli in neuronalen Axonen (Schaffer et al., 2014). Die Bindung zu den Mikrotubuli wird durch Phosphorylierung (verminderte Affinität) und Dephosphorylierung (verstärkte Affinität) von tau gesteuert. Die hyperphosphorylierte Form von tau führt zu Fehlfaltungen und verminderte Löslichkeit wodurch es zur Aggregation und Bildung von NFTs kommt. Die NFTs treten auch während des normalen Alterungsprozesses im Gehirn auf, dabei jedoch in deutlich geringerer Ausprägung als bei AD-Patienten (Perl and Brody, 1980; Price and Morris, 1999).

Die Analyse von $A\beta_{1-42}$ im CSF von Autopsie-bestätigten AD-Patienten ergab eine geringere Konzentration als bei der Kontrollgruppe, die kognitiv normale Personen enthielt (Sunderland et al., 2003; Shaw et al., 2009). Neben der Untersuchung von $A\beta_{1-42}$ werden die Konzentrationen der Isoformen $A\beta_{1-38}$ und $A\beta_{1-40}$ bestimmt. Die Konzentration dieser Isoformen zeigten geringe und keine signifikanten Unterschiede zwischen den AD-Patienten und der Kontrollgruppe (Olsson et al., 2016). Die Konzentrationen von den untersuchten Aβ-Isoformen beziehen sich auf den gesamten Gehalt des Proteins. Hierbei erfolgt keine Unterscheidung zwischen Aβ-Spezies, wie Monomeren, Oligomeren oder anderen Aggregationsformen.

Neben dem CSF werden geeignete Biomarker im peripheren Blut untersucht, da die Blutentnahme wesentlich einfacher und weniger invasiv als die Entnahme vom CSF ist (Humpel, 2011; Bibl et al., 2012; Doecke et al., 2012). Derzeit sind die Biomarker für AD im Blut (Blutplasma, Serum, etc.) nicht ausreichend validiert und unzureichend im Vergleich zu untersuchten Biomarker im CSF (Humpel, 2011).

Keiner der vorgestellten Biomarker kann mit den bisherigen Verfahren als einziger Indikator für die eindeutige Diagnose der AD und die Abgrenzung zu anderen neurodegenerativen Krankheiten mit Demenz eingesetzt werden. Die Kombination der Untersuchung von Gesamt-tau, phosphoryliertem tau und Aβ erzielt keine ab-

solute Diagnose, aber es wird eine Sensitivität und Spezifität von 85 bis 90 % für die Diagnose der AD erreicht (Olsson et al., 2016).

Die folgende Abbildung 1.5 zeigt ein Modell zu den Biomarkern der AD. Dabei verändern sich die Biomarker von normal bis abnormal (y-Achse) in einer zeitlichen Abfolge in Bezug auf den Krankheitsverlauf (Jack et al., 2010). Die Biomarker können durch die vorgestellten Verfahren charakterisiert werden und verhalten sich je nach Krankheitsstadium unterschiedlich stark „abnormal“. Aβ erreicht frühzeitig abnormale Werte (rote Linie) und endet im Plateau wenn die ersten klinischen Symptome beginnen. Die neuronale Degeneration korreliert mit dem Ausmaß der klinischen Symptome zu einem späteren Zeitpunkt im Krankheitsverlauf. Die Gehirnstruktur verändert sich zu einem späten Zeitpunkt zum abnormalen (hellgrüne Linie), aber sehr ähnlich zu den Biomarkern kognitiven Funktionen und Gedächtnis.

Neben der Anordnung der Biomarker stellt das Modell die Veränderung der Biomarker mit sigmoiden Kurven dar, da die Biomarker keinen statischen Verlauf aufzeigen. Jeder Biomarker verändert sich nicht-linear mit der Zeit. Besonders die Atrophie im Gehirn verändert sich rapide von Patienten mit ersten klinischen Symptomen. Die Verwendung von sigmoiden Kurven bezüglich des Zeitablaufs soll implizieren das der maximale Effekt von jedem Biomarker im Krankheitsverlauf variiert. Zahlreiche Studien haben seit der Veröffentlichung dieses Modells unterstützende Ergebnisse für die zeitliche Anordnung der Biomarker Aβ und neuronale Degeneration geliefert. Zusätzlich wurden Daten veröffentlicht, die den sigmoiden Verlauf der Aβ-Kurve in Bezug auf den Krankheitsverlauf untermauern (Jack Jr. et al., 2013).

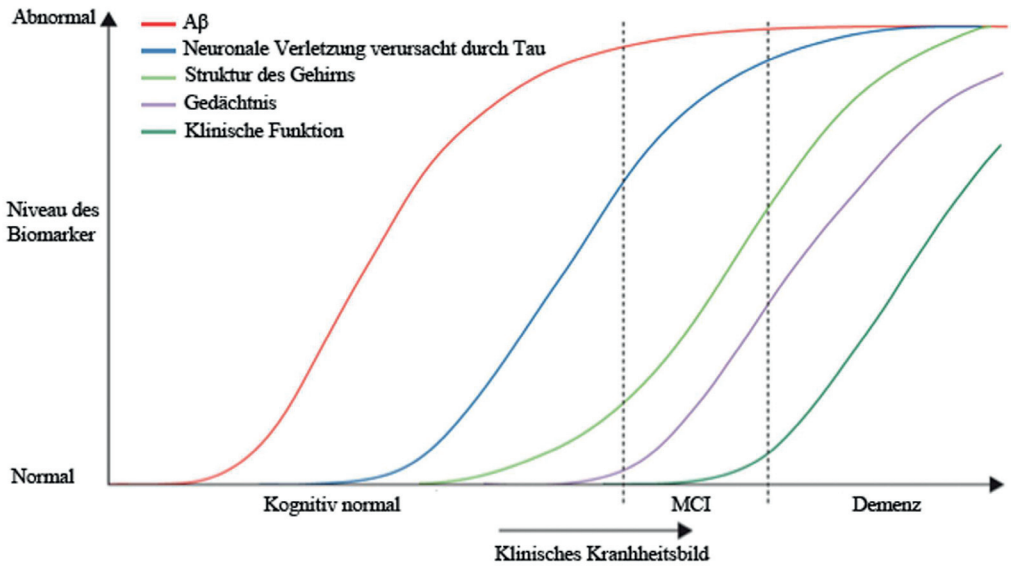

Abbildung 1.5: Modell der dynamischen Biomarker der Pathologie der Alzheimerschen Demenz.
Die Biomarker verändern sich von normal bis abnormal (y-Achse) in einer zeitlichen Abfolge in Bezug auf den Krankheitsverlauf der AD (x-Achse). Es werden unterschiedliche Verfahren zur Bestimmung der Biomarker eingesetzt, beispielsweise wird die Ablagerung von Aβ in PET Aufnahmen bestimmt oder der Proteingehalt im CSF wird gemessen. Neuronale Verletzungen verursacht durch tau werden durch den erhöhten tau-Gehalt im CSF bestimmt. Außerdem können von tau FDG-PET Aufnahmen erstellt werden. Die Atrophie des Gehirns wird durch MRT identifiziert. (Abbildung in Anlehnung an Jack et al. 2010)

Die Veränderungen der Proteinkonzentrationen von Gesamt-tau, phosphoryliertes tau und Aβ im CSF können bereits zu einem frühen Stadium der AD messbar und damit ein Hinweis auf die präklinischen Veränderungen im Gehirn sein. Dementsprechend sind diese Biomarker eine potentielle Möglichkeit die AD frühzeitig zu diagnostizieren (Hölttä et al., 2013).

1.1.2.3 Detektion von Aβ-Oligomeren als Biomarker

Neuste Studien haben gezeigt, dass lösliche Aβ-Oligomere, nicht die Monomere oder unlöslichen Plaques, neurotoxische Wirkung haben und dadurch die Entwicklung der AD beeinflussen, wenn nicht sogar auslösen könnten. Dementsprechend gilt diese Aβ-Aggregationsform als vielversprechender Biomarker für die AD (Jack et al., 2010; Humpel, 2011; Blennow and Zetterberg, 2015).

Die Detektion von Aβ-Oligomeren, bezeichnet auch als *Aβ-derived diffusible Ligands* (ADDL), im CSF wurde bereits mit verschiedenen Verfahren untersucht. Dabei kann die Spezifität zu Aβ-Oligomeren durch die Nutzung von zwei monoklonalen Anti-Aβ-Antikörper genutzt werden. Wenn Antikörper am gleichen Epitop binden und auf einem Aggregat dies auch tun, müssen mindestens zwei Epitope

zugänglich sein (Xia et al., 2009; Fukumoto et al., 2010; Klaver et al., 2011). Unter Anwendung dieses Prinzips in Sandwich-ELISAs wurden einigen Studien erhöhte Konzentrationen von Aβ-Oligomeren in CSF in AD-Patienten bestimmt ((Fukumoto et al., 2010; Hölttä et al., 2013; Savage et al., 2014)). Eine weitere Möglichkeit ist die Verwendung monoklonaler Anti-Aβ-Antikörper, die an Oligomer-spezifische Konformationen binden (Fukumoto et al., 2010; Yang et al., 2015). Hierbei wurde in der Studie von Yang et al. (2015) eine Überlappung der Aβ-Oligomere Konzentrationen von Kontroll-, MCI- und AD-Patienten im CSF gezeigt, wobei die Messungen von Gesamt-tau, phosphoryliertem tau und $A\beta_{1-42}$ eine klare Unterscheidung zwischen AD- und Kontrollgruppe aufwies.

Die Quantifizierung von Aβ-Oligomeren bleibt eine Herausforderung, da die Konzentration der Aβ-Oligomere sehr gering im Vergleich zur Konzentration der Aβ-Monomere im CSF ist, und die genannten Verfahren möglicherweise nicht sensitiv genug sind oder die relevanten Spezies nicht detektieren (Blennow and Zetterberg, 2015). Ein weiteres Verfahren zur sensitiven Detektion einzelner Moleküle ist der sFIDA-Assay, dessen Weiterentwicklung durch Automatisierung das Ziel dieser Arbeit ist. Im Abschnitt 1.2 wird die Entwicklung und die Funktionsweise des sFIDA beschrieben und bisherige Ergebnisse dazu vorgestellt.

1.1.2.4 Notwendigkeit von Standardmolekülen zur Detektion von Aβ-Oligomeren

Gegenwärtig befinden sich eine Reihe von Oligomer-basierten diagnostischer Test in der Entwicklung. Zur Validierung der Verfahren sollte die Inter-/Intra-Assay-Variabilität bestimmt werden. Dabei werden Aspekte wie beispielsweise Sensitivität und die Nachweisgrenze der Tests sowie die Linearität der Konzentrationsreihen in den jeweiligen Verfahren untersucht (Andreasson et al., 2015). Zusätzlich ist der Vergleich von unterschiedlichen Verfahren notwendig, um die Entwicklung für einen sensitiven und spezifischen Nachweis der Aβ-Oligomere voran zu treiben. Hierfür ist die Verwendung von geeigneten und einheitlichen Standardmolekülen mit stabiler und definierter Größe und der eindeutigen Anzahl von Aβ-Epitopen zur Detektion in den unterschiedlichen Verfahren erforderlich.

Bislang wurden Aβ-Oligomere aus synthetischem Aβ hergestellt und ergibt zunächst ein heterogenes Gemisch aus Monomeren, kleinen Oligomeren und Aggregat-Spezies (Freir et al., 2011; Klein, 2002). Die Auftrennung der Aβ-Spezies anhand ihrer Größe kann durch Filtration, Dialyse oder Größenausschlusschromatographie erfolgen (Barghorn et al., 2005; Savage et al., 2014). Es gibt keine einheitliche Vorgehensweise für die Präparation von Aβ-Oligomeren, sodass es vermut-

lich starke Unterschiede bei Größenverteilung und Konformation gibt. Somit ist ein Vergleich von verschiedenen Assays unter Verwendung von Aβ-Oligomere, die auf unterschiedliche Weise hergestellt wurden, nicht möglich.

Schließlich wurden quer-vernetzte $A\beta_{1-40}$-Dimere entwickelt. Hierbei wird $A\beta_{1-40}$ modifiziert, sodass an Position 26 in der Aminosäure-Abfolge ein Cystein statt eines Serin vorliegt ($A\beta_{1-40}$Ser26Cys). Die Cysteine können Disulfidbrücken ausbilden und verbinden zwei $A\beta_{1-40}$-Moleküle (Nuallain et al., 2010; Malley et al., 2014). In den Studien von Xia et al. 2009 und Esparza et al. 2013 wurde $A\beta_{1-40}$Ser26Cys als Kalibrierstandard für Aβ-Oligomere eingesetzt. Da die Aβ-Oligomeren in unterschiedlichen Größen vorliegen können, sind die $A\beta_{1-40}$Ser26Cys-Dimere nur bedingt als Kalibrierstandard für Aβ-Oligomer-spezifischen Assays geeignet.

1.2 sFIDA

sFIDA steht für *surface-based fluorescence intensity distribution analysis* und wurde entwickelt um spezifisch und sensitiv Oligomer- oder Aggregatkonzentrationen analysieren zu können. Das Verfahren basiert auf einer Methode zur Detektion von PrP-Protein in Hirnhomogenaten von BSE-infizierten Rindern und Scrapie-infizierten Hamstern von Birkmann et al. (2006). Es wurden zwei unterschiedliche Fluoreszenz-markierte Anti-PrP-Antikörper eingesetzt, um die PrP-Aggregate durch Fluoreszenzkorrelationsspektroskopie (FCS) im 2-Kanal-Modus detektiert. Die Auswertung erfolgte mittels *fluorescence intensity distribution analysis* (FIDA). Hierbei wurde als spezifisches Signal nur die Ereignisse gewertet, die in beiden Kanälen im FCS detektiert wurden.

In 2007 veröffentlichten Birkmann et al. eine Weiterentwicklung des Verfahrens mit erhöhter Sensitivität. Die PrP-Aggregate wurden mithilfe eines PrP-Antikörper, einem sogenannten Fänger-Antikörper, auf einer Glasoberfläche immobilisiert. Anschließend wurden Antikörper mit unterschiedlichen Fluoreszenz-Markierungen als Detektions-Antikörper eingesetzt und die Oberfläche wurde mittels Fluoreszenzspektroskopie gemessen. Kolokalisierte Signale auf der Oberfläche dienen als readout und wurden durch die zwei verschiedenen Kanäle bestimmt. Dieses Verfahren wurde *surface-based fluorescence intensity distribution analysis* (sFIDA) genannt.

In der Alzheimer-Diagnostik wurde dieses Verfahren 2007 erstmals von Funke et al. zum Nachweis von Aβ-Oligomeren im CSF von AD-Patienten eingesetzt. Es wurden Fänger- und Detektions-Antikörper mit überlappenden Epitopen verwendet, um eine sensitive Quantifizierung von Aβ-Oligomeren zu ermöglichen. Durch das Verfahren konnte eine erhöhte Anzahl von kolokalisierten Signalen im CSF von

AD-Patienten gegenüber der Kontrollgruppe bestimmt werden. Ab 2010 wurde die Messmethode des Verfahrens auf Laser-Scanning Mikroskopie (LSM) umgestellt (Funke et al., 2010).

2013 wurde die Optimierung der Oberfläche und die Analyse von CSF-Proben von AD-Patienten und Kontrollspendern veröffentlicht (Wang-Dietrich et al., 2013). Hierbei wurde die Glasoberfläche mit einer Dextran-Matrix funktionalisiert, um unspezifische Bindungen der Proben auf der Glasoberfläche zu verhindern. Die Fänger-Antikörper wurden dann kovalent an die Dextranoberfläche gebunden. Schließlich wurden nach der Probeninkubation die zwei unterschiedlichen Fluoreszenzmarkierten Anti-Aβ-Antikörper auf die Oberfläche gegeben (siehe Abschnitt 1.6). Während der Messung am LSM wurde die Oberfläche in zwei Kanälen gemessen und die Auswertung der Bilddaten ergeben den *sFIDA readout*. Dieser beinhaltet die Anzahl der Pixel, die in beiden Kanälen oberhalb des Hintergrundsignals liegen. Die untersuchten CSF-Proben von AD-Patienten ergaben einen signifikanten Unterschied im *sFIDA readout* gegenüber der Kontrollgruppe. Die Gruppe der AD-Patienten zeigte einen höheren *sFIDA readout* und somit eine höhere Konzentration von Aβ-Oligomeren im CSF im Vergleich zur gesunden Kontrollgruppe. In dieser Studie konnte keine absolute Konzentration von Aβ-Oligomere durch den *sFIDA readout* bestimmt werden, da entsprechende Standardmoleküle zur Kalibrierung des sFIDA Assays fehlten.

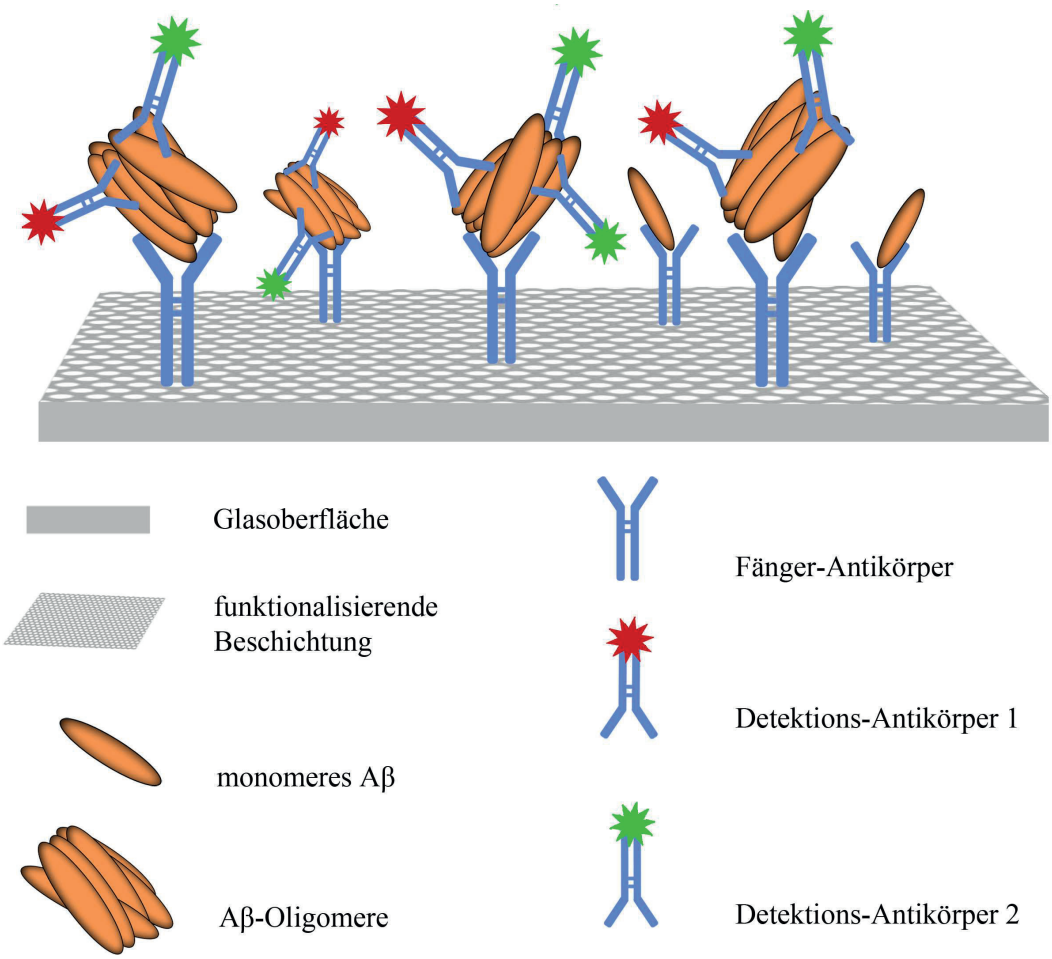

Abbildung 1.6: Schematischer Darstellung der sFIDA-Methode.
Auf der funktionalisierten Glasoberfläche werden kovalent Fänger-Antikörper immobilisiert. Diese binden Aβ-Moleküle aus einer Probe. Anschließend werden zwei Detektions-Antikörper mit unterschiedlichen Fluorochromen dazugegeben. Die Bindung der Detektions-Antikörper kann nur an Aβ-Oligomeren stattfinden, da diese nach dem „Capturing“ freie Epitope besitzen. Danach folgt die Zweifarb-Fluoreszenzmikroskopie zur Detektion der verwendeten Fluorochromen. Bei der Auswertung der Bilddaten werden nur kolokalisierte Pixel mit Intensitäten in beiden Kanälen über einen jeweiligen Schwellwert gezählt. Die Summe dieser Pixel wird als *sFIDA readout* bezeichnet und korreliert mit der Konzentration der Oligomere in der Probe (Abbildung in Anlehnung an Herrmann et al. 2017).

1.3 Oligomere des α-synucleins als Biomarker für die Parkinson-Krankheit

Die Parkinson-Krankheit (PD), auch bekannt unter Morbus Parkinson, ist ebenfalls eine neurodegenerative Erkrankung, die als Symptome vor allem motorische Störungen aufweist (Saracchi et al., 2014). Dazu gehören Muskelstarre, verlangsamte Bewegungen, Muskelzittern und Haltungsinstabilität . Die Krankheit wurde nach dem englischen Arzt James Parkinson benannt, der PD im Jahre 1817 erstmals beschrieb (Parkinson, 2002).

Die Symptome werden durch den Verlust von dopaminergen Neuronen in der *substantia nigra pars compacta* hervorgerufen (Lücking and Brice, 2000; Jankovic, 2008; Jesse et al., 2009). Momentan basiert die Diagnose der PD vorwiegend auf den motorischen Symptomen, die vermehrt beim Verlust von 70% der dopaminergen Neuronen auftreten. Dementsprechend könnte der Einsatz einer möglichen Therapie keine positiven Effekte zeigen, da der Verlust der Neuronen bereits zu weit fortgeschritten ist. Außerdem kommt es zu Falschdiagnosen basierend auf den motorischen Symptome in 15 bis 25% der Fälle (Saracchi et al., 2014). Ähnlich wie bei der AD ist eine eindeutige Diagnose der Erkrankung von PD schwierig und kann meist erst bei Ausprägung der ersten motorischen Störungen erfolgen.

Ein weiteres pathologisches Merkmal ist die Bildung von sogenannten *Lewy bodies* (LB) im Gehirn (Lücking and Brice, 2000; Jesse et al., 2009; Saracchi et al., 2014). Die LBs sind auch charakteristisch für die sogenannte *Lewy-Body*-Demenz (LBD), die als eigenständige Erkrankung auftreten kann (Goedert, 2001; Simonsen et al., 2015). Der Hauptbestandteil der LBs ist das Protein α-synuclein (α-syn).

α-syn ist ein präsynaptisches Protein, das mit Vesikeln und Phospholipid-Membranen im Gehirn interagiert (Lücking and Brice, 2000). Basierend auf Ergebnissen bezüglich der Struktur und dem histologisch nachgewiesenem Vorkommen des α-syn im Gehirn wird angenommen, dass das α-syn einen Einfluss in der Regulation von synaptischer Plastizität und neuronaler Differenzierung hat (Lücking and Brice, 2000; Lashuel et al., 2013). Die Rolle von α-syn in der Pathogenese der PD wird durch die Entdeckung von Mutationen im SCNA Gen unterstützt, die zur familiären Form der PD führen (Saracchi et al., 2014; Mollenhauer, 2014; Dehay et al., 2015).

Für die Untersuchung des gesamten α-syn-Gehaltes in CSF oder Blutplasma werden meist ELISAs eingesetzt (Simonsen et al., 2015). Dabei haben einige Studien einen niedrigen Gesamt-α-syn-Gehalt in PD-Patienten im Vergleich zu der Kontrollgruppe verzeichnet (Tokuda et al., 2006, 2010; Gorostidi et al., 2012; Parnetti et al., 2013, 2014). Jedoch gibt es Studien, die diesen signifikanten Unterschied für den gesamten α-syn-Gehalt in den beiden Gruppen nicht festgestellt haben (Reesink et al., 2010; Park et al., 2011; Foulds et al., 2011; Aerts et al., 2012; Aasly et al., 2014).

Die Bildung von α-syn-Oligomeren tritt bereits früher auf als die klinischen Symptome und diese Aggregationsform gilt als besonders toxisch (Parnetti et al., 2013; Lashuel et al., 2013; Simonsen et al., 2015). Dementsprechend sind die Voraussetzungen gegeben wie bei den Aβ-Oligomeren bezüglich der AD und die oligomerischen α-syn könnten ein Biomarker für die PD sein (Goedert, 2001; Jesse et al., 2009; Lashuel et al., 2013; Saracchi et al., 2014; Simonsen et al., 2015). In einigen

Studien wurden ELISAs modifiziert, um oligomerisches α-syn zu detektieren (Simonsen et al., 2015). Dabei konnten in einer Reihe von Studien ein erhöhter Gehalt von α-syn-Oligomeren in PD-Patienten im Vergleich zu gesunden Kontrollen gemessen werden (El-Agnaf et al., 2006; Tokuda et al., 2010; Park et al., 2011; Sierks et al., 2011; Foulds et al., 2012; Parnetti et al., 2014; Aasly et al., 2014; Hansson et al., 2014; Compta et al., 2014; Førland et al., 2016; Majbour et al., 2016).

Das Prinzip des sFIDA-Assays wurde bereits mit dem PrP-Protein in der Prion-Krankheit und dem Aβ in der AD angewendet. Dementsprechend kann die Verwendung von drei Anti-α-syn-Antikörpern, die an überlappende Epitope oder ähnliche Regionen binden, im sFIDA zur Detektion von α-syn-Oligomeren führen und möglicherweise eine frühzeitige Diagnose der PD ermöglichen. In einer früheren Arbeit konnte von Hübinger et al. 2012 gezeigt werden, dass zwar α-syn-Fibrillen mittels sFIDA detektiert wurden, aber nicht die monomerische Form des Proteins.

1.4 Automatisierung

Automatisierung soll die Qualität eines Prozesses durch Robustheit, Reproduzierbarkeit, Stabilität und Effizienz in Hinblick auf Zeit und Kosten erhöhen (McDowall, 1989; Schnieder, 1999; Lehmann et al., 2015).

Automatisierung im Labor kann in zwei Bereiche eingeteilt werden: Management- und Instrument-Automatisierung. Die Automatisierung des Labor-Managements bezieht sich auf Informationen zu Experimenten und den produzierten Daten (McDowall, 1989). Das Management von Informationen und Daten wird durch die Nutzung von Computern bzw. entsprechender Software automatisiert und ermöglicht eine schnelle Berechnung und Auswertung von Daten (Isenhour, 1985).

Die Instrument-Automatisierung hat das Ziel, die Probenanzahl zu erhöhen und Daten effizient zu produzieren (McDowall, 1989). Um diese Ziel zu erreichen werden Geräte wie Roboter und Automaten eingesetzt. Diese können für unterschiedliche Aufgaben programmiert und eingesetzt werden, um eine flexible Automatisierung zu ermöglichen (Liscouski, 1985). Andere Geräte zur zweckbestimmten Automatisierung sind limitiert auf eine Aufgabe (Beispiel: *Auto-sampler* bei der *High-performance liquid chromatography* (HPLC)). Im Gegensatz zu flexiblen Roboter-Systemen sind diese meist einfacher zu bedienen und kostengünstiger (Liscouski, 1985; Isenhour, 1985).

Die Automatisierung von Prozessen ist heutzutage vor allem in Laboren zur Analytik in der Agrar-, Lebensmittel- und Pharmaindustrie, sowie den Umweltwissenschaften angewandt. Insbesondere die Pharmaindustrie benötigt automatisierte Pro-

zesse, um beispielsweise *drug screening* zur Findung von Wirkstoffen zur Behandlung von Krankheiten effizient zu gestalten (Chapman, 2003). Außerdem wird die Automatisierung in biologischen und biotechnologischen Prozessen wie der DNA- und RNA-Sequenzierung und der Handhabung von Zellkulturen eingesetzt (Meldrum, 2000; Lutkemeyer et al., 2000; Kempner and Felder, 2002; Lehmann et al., 2015).

Im Bereich der Sequenzierung wird vor allem von *high-throughput*-Methoden gesprochen, da eine hohe Anzahl an Proben innerhalb kürzester Zeit verarbeitet und analysiert wird (Bartoloni et al., 1988; Craig and Hoheisel, 1999; Cardona et al., 2009). Diese rasante Entwicklung liegt dem *Human Genome Project* zu Grunde und hat die Automatisierung von verschiedenen Prozessen innerhalb der Sequenzierung vorangetrieben (Craig and Hoheisel, 1999; Cox and Rudolph, 1998).

Die Prozessierung von Zellkulturen wird besonders in *bioscreening* Laboren im großen Maßstab durchgeführt. Die Kultivierung und Aufbereitung von tierischen oder pflanzlichen Zellen, die außerhalb eines Organismus in Nährmedien heranwachsen, ist langwierig und Schritte wie z.B. Medienwechsel, müssen oft wiederholt werden. Dabei ist das Risiko von menschlichem Versagen oder Kontamination sehr hoch. Dementsprechend kann die Qualität der folgenden Versuche durch mangelnde Robustheit oder Stabilität der produzierten Zelllinien leiden (Lehmann et al., 2015). Daher ist es von großem Interesse die Kultivierung von Zellen in einem sterilen und automatisierten System zu ermöglichen, um die nötige Qualität zu gewährleisten.

Im Bereich der Immunoassays gibt es auch eine hohe Tendenz die Schritte bei der Vorbereitung zu automatisieren. Die Anzahl an Waschschritten sind in diesen Verfahren sehr hoch und durch Menschenhand nicht fehlerfrei oder stabil durchführbar (Tecan Group Ltd., 2014; Olsen, C., 2012). Dementsprechend gibt es in den letzten Jahren ein gesteigertes Angebot durch die erhöhte Nachfrage von sogenannten *Plate-Washer*. Diese können meist verschiedene Plattenformate (z.B. Variation der Wellanzahl: 96 oder 384 *Wells*) vollautomatisch (variable Anzahl an Platten) oder teilautomatisch verarbeiten. Die Hersteller empfehlen dabei oft getestete und validierte Werte für die Anzahl der Waschschritte und Intensität des Waschens bei ELISA-Experimenten in ihren Geräten (Tecan Group Ltd., 2014; Olsen, C., 2012; BioTek Instruments, Inc., 2012). Dadurch kann eine standardisierte Ausführung beim Waschen gewährleistet werden. Zusätzlich kann Zeit eingespart werden, die der Experimentator für andere Arbeiten nutzen kann (Tecan Group Ltd., 2014; BIOPRO Baden-Württemberg GmbH, 2013).

Durch das steigende Interesse an der Automatisierung von biologischen Prozes-

sen, wie beispielsweise Assays, werden immer mehr Systeme entwickelt, die neben der Datenerfassung und Analyse, die eigentliche Vorbereitung des Experiments ermöglichen. Dabei geht es neben dem Pipettieren zusätzlich um die Handhabung der Proben vor und nach dem Experiment durch automatisierte Biobank-Systeme (Elliott and Peakman, 2008; Chapman, 2003). Es werden Systeme angeboten, die unterschiedliche Geräte integrieren können und somit die Möglichkeit der Vollautomatisierung bieten. Entscheidend ist dabei, die Komplexität des Experimentablaufs und die verfügbaren finanziellen Möglichkeiten, um einen Prozess im Ganzen zu automatisieren (BIOPRO Baden-Württemberg GmbH, 2013; Chapman, 2003).

1.5 Zielsetzung

In der vorliegenden Arbeit wird zunächst die Verwendung von stabilen Aβ-Oligomere von Crossbeta Bioscience als Standard für die Detektierung von Aβ im sFIDA-Assay untersucht. Die Entwicklung und Verwendung von Silica-Nanopartikeln funktionalisiert mit Aβ (Aβ-SiNaPs) als neuen Standard wird dargelegt. Darüber hinaus wird das Verhalten der Aβ-SiNaPs in der Umgebung von Blutplasma mit verschiedenen Gerinnungshemmern untersucht, um den geeignetsten Gerinnungshemmer für die Verwendung von Blutplasma im sFIDA-Assay zu bestimmen.

Der sFIDA-Assay soll in der vorliegenden Arbeit durch Automatisierung bei der Präparation weiter optimiert werden. Dafür wird ein Pipettierroboter und ein Mikrotiterplatten Washer verwendet. Das sFIDA-Protokoll wird in der Software des Pipettierroboters implementiert und vorgefertigte Waschprotokolle vom Washer werden darüber gesteuert. Dadurch soll die Möglichkeit von menschlichem Versagen minimiert werden und das sFIDA-Assay an Robustheit gewinnen. Die Verwendung der Automatisierung wird im Rahmen eines Spiking-Experimentes mit Aβ-SiNaPs in CSF und PBS untersucht und die Intra-assay Parameter wie Linearität, Variationskoeffizient und Nachweisgrenze werden bestimmt.

Darüber hinaus wird der sFIDA-Assay zur Detektion von α-syn-Oligomeren zur Diagnose von PD im automatisierten System angepasst. Dabei werden die Silica-Nanopartikel mit α-synuclein (α-syn-SiNaPs) funktionalisiert und in einem Spiking-Experiment in CSF und PBS eingesetzt. Hierbei werden die obengenannten Intra-assay Parameter bestimmt, um die α-syn-SiNaPs im sFIDA-Assay zu validieren.

2. Technische Details zur Automatisierung

In diesem Kapitel werden unterschiedliche Aspekte zur Laborautomation des sFIDA-Experiments beschrieben. Es wird der Aufbau der verwendeten Geräte, Pipettierroboter (Microlab Star) und Washer (BioTek Microplate Washer 405 Select LS), sowie die zugehörigen Softwares im Detail erklärt. Die Auswahl verwendeter Laborbedarfsartikel (sogenannte *Labware*) für den Microlab Star und der Ablauf des sFIDA-Assays im automatisierten System werden behandelt.

2.1 BioTek Microplate Washer 405 Select LS

Der BioTek Microplate Washer 405 Select LS, im Folgenden als Washer bezeichnet, kann als unabhängiges Gerät für das Waschen von Mikrotiterplatten im 96- und 384-*Well*-Format verwendet werden (siehe Abbildung 2.1). Der Pipettierroboter kann ebenfalls den Washer ansteuern und vorgefertigte Waschprotokolle aufrufen.

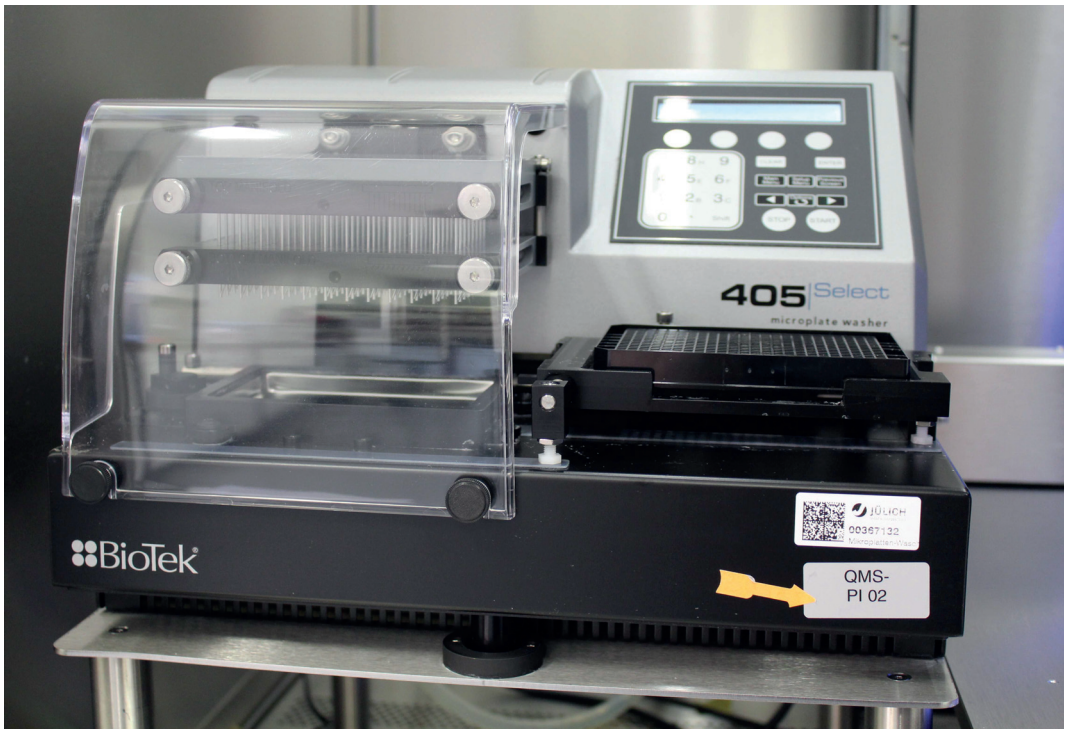

Abbildung 2.1: BioTek Washer 405 Select LS
Washer mit Waschkamm, Mikrotiterplatten-Träger und Touchpad.

2.1.1 Aufbau des BioTek Microplate Washer 405 Select LS

Der Washer besitzt einen 96-Kanal-Waschkamm, der aus 96 angewinkelten Dispensier- und genauso vielen geraden Aspirationnadeln besteht (siehe Abbildung 2.2). So können 96 *Wells* parallel aspiriert und wieder mit Puffer befüllt werden (BioTek Instruments, Inc., 2015a). Es gibt vier Anschlüsse und Schlauchsysteme für Puffer, sodass vier verschiedene Puffer direkt am Gerät zur Verfügung stehen und während der Waschschritte automatisch gewechselt werden können (BioTek Instruments, Inc., 2012). Außerdem gibt es die Möglichkeit die Nadeln in einer wassergefüllten Wanne einzutauchen und zu sonifizieren, um Verunreinigungen an und in den Nadeln zu lösen (BioTek Instruments, Inc., 2015b).

Der Washer ist mit einem abnehmbaren Spritzschutzschild ausgestattet. Des weiteren können mehrere Abfallbehälter (beispielsweise 4 l Behälter) miteinander und dem Washer verbunden werden, sodass ein hohes Abfallvolumen aufgefangen werden kann. Im letzten Abfallbehälter befindet sich ein Überlaufsensor, sodass der Washer eine Meldung abgeben kann, wenn die Abfallbehälter voll sind. Eine Vakuumpumpe baut den benötigten Druck für das Durchlaufen der Flüssigkeit im Washer auf.

Die Waschprotokolle können direkt am Gerät über das *Touchpad* erstellt und ausgewählt werden. Außerdem gibt es die *Liquid Handling Control* (LHC) Software,

um am Computer Waschprotokolle zu erstellen und aufzurufen.

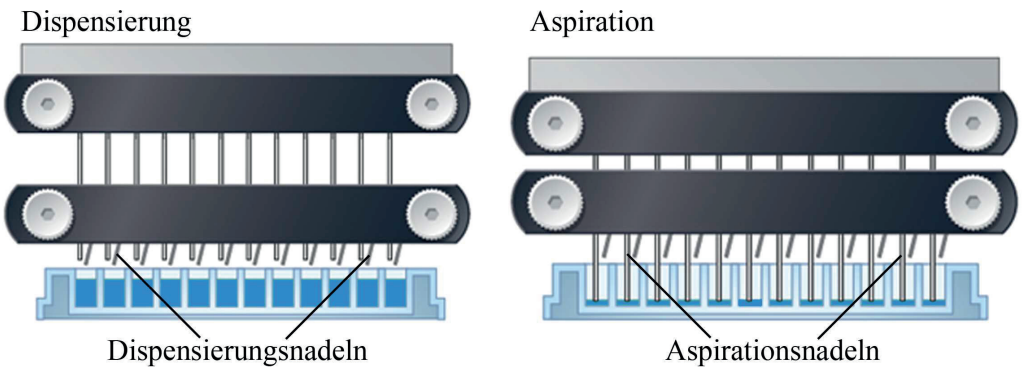

Abbildung 2.2: BioTek Washer Waschkamm
96-Kanal-Waschkamm mit angewinkelten Dispensier- und geraden Aspirationsnadeln (Abbildung in Anlehnung an BioTek Instruments, Inc. 2015a)

2.1.2 Erstellung von Waschprotokollen

Die verwendeten Waschprotokolle wurden am Computer über die LHC-Software erstellt. Es können eine Reihe von Optionen und Parametern ausgewählt und angepasst werden. Es kann der Mikrotiterplatten-Typ ausgewählt, dem Waschprotokoll einen Namen geben und mit weiteren Kommentaren versehen werden. Unter dem Punkt *Add Step* gibt es eine Reihe von Optionen die nacheinander in einem Waschprotokoll ablaufen können. Dabei können Pausen (*Delays*) eingefügt werden, sodass der Anwender Zeit hat um beispielsweise Pufferflaschen zu tauschen oder die Abfallbehälter zu leeren. Außerdem können Schleifen (*Loops*) eingebaut werden, sodass ein Schritt beliebig oft wiederholt wird.

Neben dem Waschschritt (*W-Wash*), in dem bis zu 100 Waschzyklen (Aspiration und Dispensierung) ablaufen können, gibt es die Option die Mikrotiterplatten durch einen einzelnen Aspirationsschritt (*W-Aspirate*) zu leeren oder nur mit Puffer zu befüllen (*W-Dispense*). Wie bereits erwähnt, besitzt dieses Gerät die Möglichkeit vier Puffer gleichzeitig an das Gerät anzuschließen. Wenn zwischen Puffern gewechselt werden soll, muss ein *W-Prime*-Schritt erfolgen. Dieser Schritt gewährleistet einen Pufferwechsel im Washer, sodass für den nächsten Waschschritt der gewünschte Puffer im System vorliegt und nicht Reste vom vorherigen Puffer diesen verdünnen oder kontaminieren.

Der *W-AutoClean*-Schritt sonifiziert die Aspirations- und Dispensierungsnadeln im Wasser. Beim *Shake/Soak*-Schritt kann die Mikrotiterplatte in dem Plattenträger geschüttelt oder für einen Zeitraum inkubiert werden, während die Nadeln des Waschkamms in den gewünschten Puffer getaucht werden.

Innerhalb der beschriebenen Schritte können weitere Optionen wie Anzahl Waschzyklen, Position der Aspirations- und Dispensierungsnadeln, Geschwindigkeit des Flüssigkeitsflusses (*Flow rate*), Dauer und Stärke des Schüttelns, etc. ausgewählt und verändert werden.

Die gewünschten Schritte werden im *Protocol Steps* nach der Auswahl aufgeführt und können in ihrer Reihenfolge weiter verändert werden. Wenn ein Schritt ausgewählt ist, werden die zugehörigen Parameter in *Step Details* angezeigt. Wenn das Waschprotokoll fertig erstellt wurde, kann es in einer Datei abgespeichert werden und beispielsweise in einem weiteren Waschprotokoll aufgerufen werden (*From File...*). So können sehr komplexe Waschprotokolle zusammengestellt, aber auch einzelne Waschschritte verwendet werden.

Im Folgenden werden die Parameter im Detail beschrieben, die später für das sFIDA-Assay verändert wurden. Anhand eines Beispielprotokolls werden Einzelheiten zu den Parametern erklärt.

Bei der Aspiration ist vor allem die Position der Aspirationsnadel ausschlaggebend. Beispielsweise soll vermieden werden in der Mitte des *Wells* kurz vor dem Boden zu aspirieren, da dort starke Scherkräfte wirken können. Entsprechend können die x- und y-Positionen angepasst werden, sodass am Rand des *Wells* aspiriert wird, um mögliche Veränderung an der Oberfläche in der Mitte zu verhindern. Außerdem kann die z-Höhe beim Aspirationsschritt nach oben oder unten angepasst werden, dadurch bleiben je nach z-Höhe unterschiedliche Flüssigkeitsvolumina zurück, die in weiteren Waschzyklen verdünnt werden bevor das ganze Well geleert wird. Durch die Anpassung der x-, y- und z-Positionen während der Aspiration kann die Oberfläche oder die Probe im Well vor starken Einflüssen durch Scherkräfte geschont werden.

Die Position der Dispensionsnadel kann in x-, y- und z-Richtung ausgewählt werden, sodass der Flüssigkeitsstrahl innerhalb des *Wells* an die gegenüberliegende Wand aufkommt und der Boden des *Wells* nicht direkt dem Flüssigkeitsstrahl ausgesetzt ist (siehe Abbildung 2.3). Dadurch kann das z.B. das Zellpräparat vor starken Einflüssen durch den Flüssigkeitsstrahl geschützt werden.

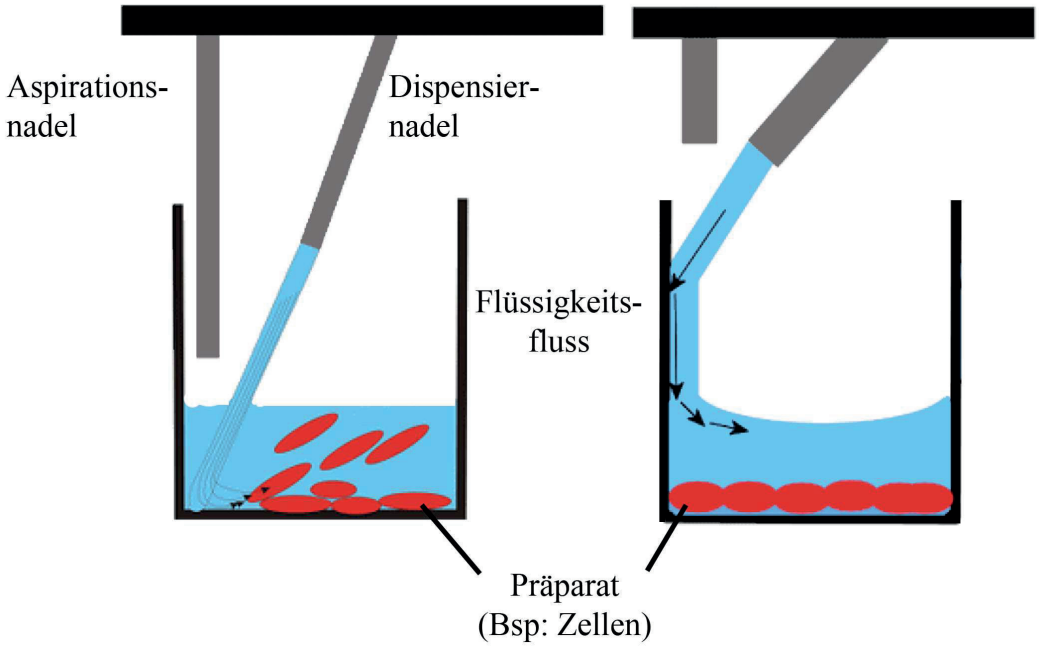

Abbildung 2.3: Position im Dispensierungsschritt
Die Position der Dispensiernadeln kann in x, y und z-Richtung geändert werden, sodass der Flüssigkeitsfluss an der Wellwand abgelenkt wird, um den Wellboden möglichst wenig Scherkräften auszusetzen. Dadurch können beispielsweise zerstörte Zellen oder inhomogene Oberflächen verhindert werden (vgl. links und rechts). (Abbildung in Anlehnung an BioTek Instruments, Inc. 2015a)

Die Abbildung 2.4 zeigt die LHC-Software mit einem Waschprogramm, das das Gerät zunächst mit 300 ml Puffer D spült, um danach jedes Well einer Mikrotiterplatte mit 384 *Wells* dreimal mit Puffer D zu waschen. Der Waschschritt ist blau unterlegt und in den *Step Details* wird aufgeführt mit welchen Einstellungen das Programm abläuft. Es wird kein Puffer vor dem Waschen an die *Wells* abgegeben und es erfolgt kein *Bottom Wash*. Beim *Bottom Wash* wird am Boden der Mikrotiterplatte nicht nur aspiriert sondern während dessen dispensiert.

In dem Waschprotokoll wird die gesamte Mikrotiterplatte gewaschen, wobei der Waschkamm mit 96 Aspirations- und Dispensionsnadeln immer um ein Well versetzt wird, um die gesamte Mikrotiterplatte im 384er-Format zu waschen. Die Aspiration erfolgt bei einer z-Höhe von 22 Schritten (entspricht 2,79 mm über dem Plattenträger), sodass noch ca. 25 µl in dem Well zurückbleiben bevor wieder 85 µl von Puffer D in jedes Well abgegeben werden. Die x-Position hat einen Abstand von -10 Schritten (entspricht 0,46 mm nach links von der Mitte des *Wells*) und die y-Position ist 3 Schritte (entspricht 0,22 mm nach vorne) nach vorne von der Mitte des *Wells* versetzt. Die Verwendung dieser x- und y-Position lässt die Aspiration am Rand des *Wells* erfolgen, um die Mitte des *Wells* vor Scherkräfte zu schützen.

Der Dispensierungsschritt ist mit einer *Flow Rate* von 5 eingestellt und die z-

Höhe liegt bei 100 Schritten über dem Plattenträger (entspricht 12,7 mm über dem Plattenträger). Die y-Position ist in der Mitte des *Wells* und die x-Position hat einen Abstand von 23 Schritten (entspricht 1,05 mm nach rechts) von der Mitte des *Wells*, sodass der Flüssigkeitsfluss nicht direkt auf die Oberfläche trifft. Im letzten Aspirationsschritt (*Final Aspirate*) wird die Aspirationshöhe auf 8 (entspricht 1,02 mm über dem Plattenträger) gesetzt, um das Well möglichst leer (ca. 5 µl zu hinterlassen, sodass direkt der nächste Schritt zur Verarbeitung der Mikrotiterplatte erfolgen kann.

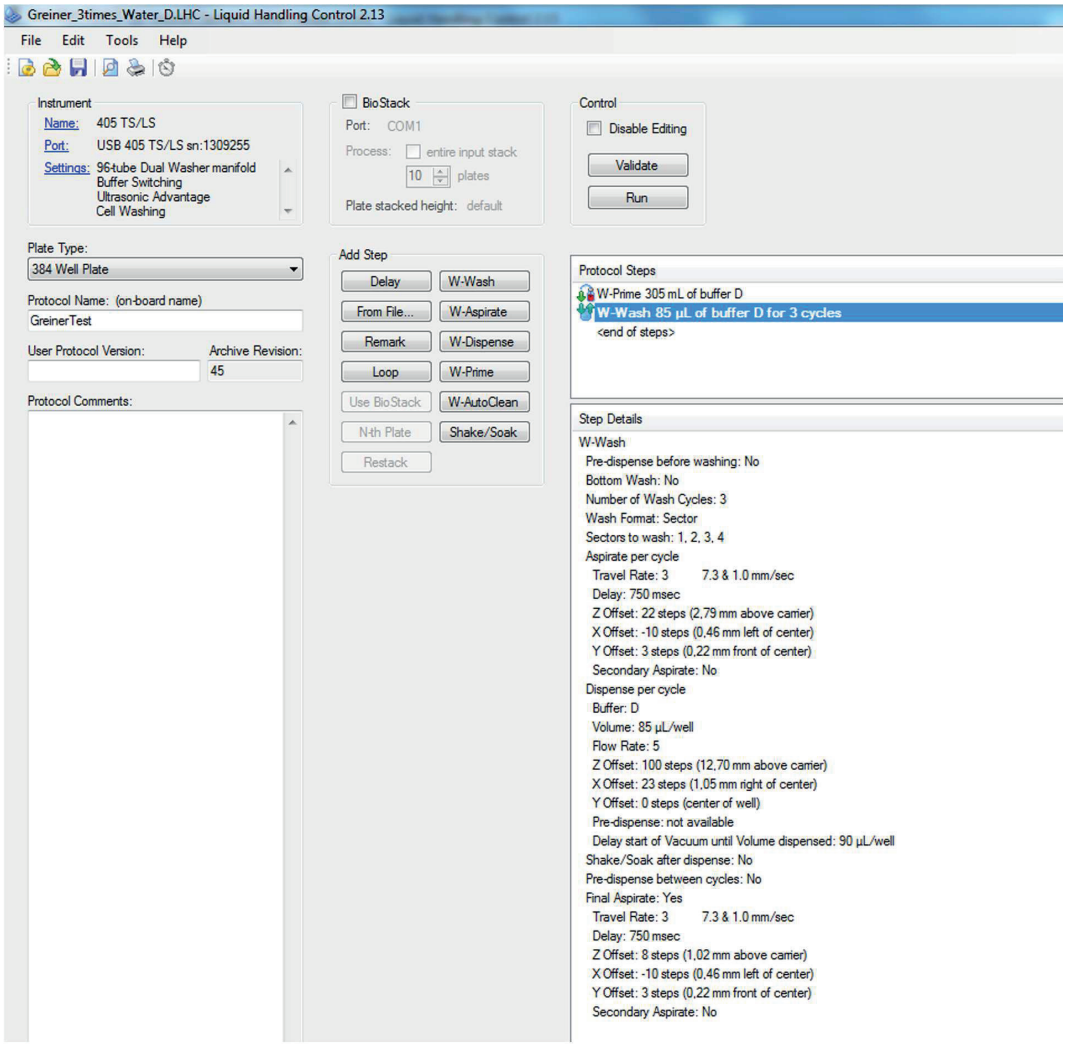

Abbildung 2.4: LHC-Software mit Waschprogramm für 384 *Well* Mikrotiterplatten
Das Gerät wird innerhalb der Software automatisch erkannt und es wird der Mikrotiterplatten-Typ ausgewählt (links). In der Mitte des Software-Dialogs sind die möglichen Waschoptionen und Befehle aufgeführt (*Add Step*). Durch Doppelklick öffnet sich ein Fenster zur Einstellung des ausgewählten Schritts und dieser wird in die *Protocol Steps*abgelegt. Innerhalb dieses Bereichs kann die Reihenfolge der Schritte verändert werden (rechts). Im *Step Details*-Bereich werden die Einstellungen eines ausgewählten Schrittes (blau unterlegt) angezeigt.

2.2 Microlab Star

Der Microlab Star, im Folgenden als ML Star benannt, von der Firma Hamilton ist ein Pipettierroboter (DiLorenzo et al., 2001). Der ML Star ist einer von drei Pipettierroboter der Hamilton Star line. Sie unterscheiden sich in ihrer Länge und damit der Größe des Arbeitsbereiches. Der Starlet ist der kleinste, es folgt der Star und der StarPlus (Hamilton Bonaduz AG, 2015). Die Hamilton Star line kann mit unterschiedlichen Pipettiervorrichtungen (8-Pipettierkanäle, 16-Pipettierkanäle oder 96er Pipettierkopf) ausgestattet werden. Außerdem gibt es zwei Möglichkeiten (iSWAP oder Gripper) um Laborbedarf, die sogenannte Labware, innerhalb des Gerätes oder an Drittgeräte zu transportieren (Hamilton Bonaduz AG, 2010a). Das System ist sehr flexibel und kann unter Beachtung einiger Parameter erweitert oder mit individueller Labware ausgestattet werden. Dementsprechend gibt es viele Möglichkeiten das Gerät auf die eigenen Anforderungen zuzuschneiden; dabei können die Rahmenbedingungen des Experiments oder die Ausstattung im Pipettierroboter die Automatisierung limitieren.

2.2.1 Aufbau des Microlab Stars

Im folgenden wird der Aufbau des ML Star mit der Ausstattung, die in dieser Arbeit verwendet wurde, beschrieben. Der ML Star besitzt einen Arbeitsbereich, das sogenannte Deck, auf dem die Halterungen für Pipettenspitzen, Laborbedarf und Abfallbehälter zur Verfügung stehen (siehe Abbildung 2.5). Der Punkt links vorne (unter dem grünen Startknopf) ist als Nullpunkt bestimmt, von wo aus Positionen in x-, y- und z-Richtung auf dem Deck festgelegt sind.Der Pipettierarm kann in x-Richtung über das Deck fahren und die acht Pipettierkanäle können in y- und z-Richtung Teile des Decks und die darauf platzierte Labware erreichen. Das Deck ist mit Abstandseinheiten versehen, die gleichzeitig als Schiebevorrichtungen fungieren. Dementsprechend müssen die Halterungen Rahmenbedingungen erfüllen, damit Positionen genau festgelegt sind und weder die Halterung noch die darauf stehenden Gegenstände dürfen verrutschen. Denn der ML Star kann nur mit definierten Positionen einen fehlerfreien Ablauf gewährleisten.

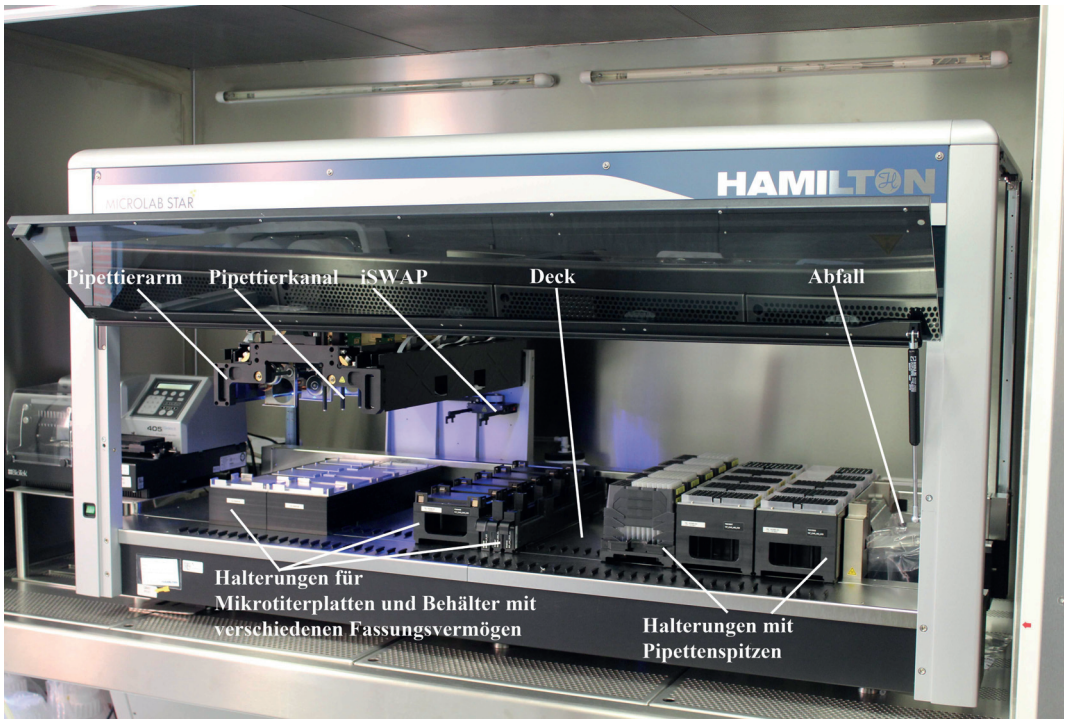

Abbildung 2.5: Allgemeiner Aufbau des Pipettierroboters (Microlab Star)
Der ML Star besitzt einen Pipettierarm, der mit acht Pipettierkanälen ausgestattet ist und einen iSWAP als Transportoption von Mikrotiterplatten besitzt. Auf dem sogenannten Deck werden Halterungen für die Labware und Pipettenspitzen platziert. Es gibt eine weitere Halterung für den Abfall.

Es gibt unterschiedliche Halterungen um verschiedene Pipettenspitzen-Typen, Behälter mit verschiedenen Fassungsvermögen für Flüssigkeiten, Mikrotiterplatten und Mikroreaktionsgefäße auf dem Deck zu platzieren. Wie bereits erwähnt gewährleisten die Halterungen eine definierte Position auf dem ML Star Deck. Dies gilt zusätzlich für die Labware die auf den Halterungen platziert wird. Denn nur wenn die Labware eine definierte Position besitzt, ist es für den ML Star möglich daraus zu pipettieren oder die Labware zu transportieren. In Abschnitt 2.2.3 werden weitere Informationen zu den in dieser Arbeit verwendeten Halterungen und Laborbedarf im ML Star beschrieben.

Der ML Star wurde mit einem Transportierarm, dem sogenannten iSWAP, ausgestattet. Diese Vorrichtung kann Mikrotiterplatten auf dem Deck und zu dem Bio-Tek Microplate Washer 405 Select LS transportieren. Mögliche Waschschritte von Mikrotiterplatten können also in dem Drittgerät ablaufen. Der Washer wurde links neben den ML Star platziert, sodass der iSWAP den Plattenhalter des Washers erreichen kann. Dabei ist die richtige Einstellung des Transportvorgangs sehr wichtig. Denn der iSWAP kann eine Mikrotiterplatte nur ohne Fehler transportieren, wenn die Start- und Ziel-Positionen fest definiert sind und die Mikrotiterplatte dort ohne verrutschen abgelegt werden kann.

Auf der rechten Seite des ML Star befindet sich die Halterung für einen Plastikbeutel für Abfälle (gebrauchte Pipettenspitzen, Flüssigabfall, etc.). Der Plastikbeutel wird darin eingespannt und kann bei Bedarf gewechselt werden.

Der ML Star wird mit der *VENUS two*-Software gesteuert. Innerhalb der Software können Abläufe als Methoden implementiert und entwickelt werden (Hamilton Bonaduz AG, 2010b). Im Abschnitt 2.2.4 werden eine Reihe von Aspekten zur Entwicklung und Implementierung von ML Star Methoden im Detail beschrieben.

2.2.2 Besondere Eigenschaften des Microlab Star

Der Flüssigkeitsstand in einem Behälter kann durch den ML Star detektiert werden. Der ML Star gehört zur Starline, die mit der *Liquid Level Detection* (LLD) ausgestattet ist (DiLorenzo et al., 2001; Hamilton Bonaduz AG, 2010a). Es gibt zwei verschiedene Arten der LLD, zum einem die *capacitive Liquid Level Detection* (cLLD) und die *pressure Liquid Level Detection* (pLLD) . Bei der cLLD detektieren spezielle Hamilton Pipettenspitzen die Leitfähigkeit, wenn sie auf den Flüssigkeitsstand im Behälter treffen. Die Genauigkeit der cLLD hängt von der Behältergröße, dem Volumen und der Polarität/Leitfähigkeit der Flüssigkeit ab. Bei unpolaren Flüssigkeiten muss die pLLD eingesetzt werden. Mit Hilfe dieser Funktion können Fehler, wie fehlendes Volumen im Behälter, detektiert, angezeigt und durch den Anwender behoben werden. Außerdem wurde diese Funktion genutzt, um eine ML Star Methode zur Überwachung der korekten Funktion des Washers zu implementieren (siehe Abschnitt 2.2.8).

2.2.3 Decklayout und Laborbedarf im Microlab Star

Die Auswahl und Verwendung von den im ML Star verwendeten Halterungen und Reaktionsgefäßen werden durch das Experiment bestimmt. Der Umfang eines Experimentes und wie viele Experimente parallel ablaufen sollen, bestimmen die benötigten Volumina der Reagenzien und die Anzahl an Pipettenspitzen. In manchen Experimenten ist das Eingreifen durch einen Anwender gewünscht oder nötig, sodass nicht alle Reagenzien zu Beginn eines Experimentes im ML Star vorbereitet werden können. Im Folgenden werden die verwendeten Halterungen, Reaktionsgefäße und Behälter im sFIDA-Assay beschrieben.

Der Pipettierarm ist mit acht Pipettierkanälen ausgestattet, des Weiteren ist der iSWAP als Transportarm für Mikrotiterplatten eingebaut (siehe Abschnitt 2.2.1). Die Pipettierkanäle können sich in y- und z-Richtung unabhängig voneinander bewegen, sodass jeder Pipettierkanal aus unterschiedlichen Behältern aspirieren und

in andere Behälter Flüssigkeit abgeben kann. Die Abbildung 2.6 zeigt das Deck des ML Star, wie es für den sFIDA-Assay in dieser Arbeit verwendet wurde. Die einzelnen Bestandteile werden im Folgenden detailliert beschrieben.

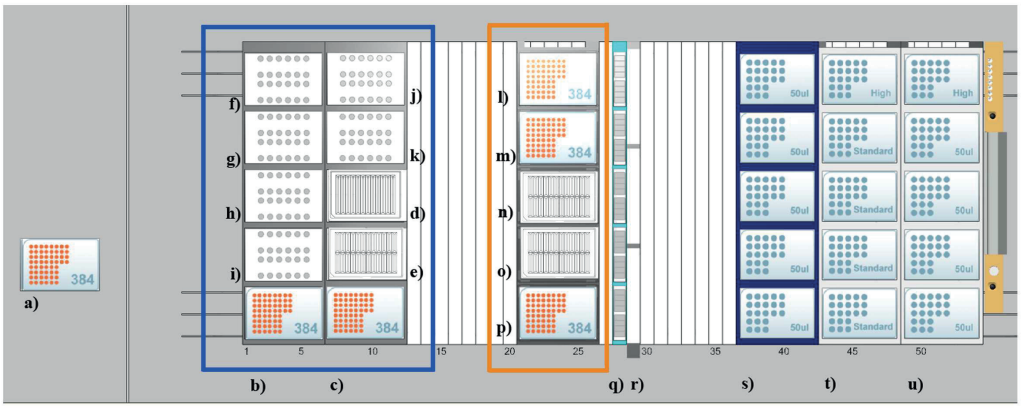

a) Washer Plattenträger
b-c) Mikrotiterplatte im 384-Well Format
d) Behälter im Format von Mikrotiterplatten für maximal Volumen von 21 ml pro Spalte
e) Behälter im Format von Mikrotiterplatten für maximal Volumen von 3.5 ml pro Kammer
f-k) Halterung für Mikroreaktionsgefäße (insgesamt 144 Stück)
l-m) Mikrotiterplatte mit Funktion als Deckel
n-o) Behälter im Format von Mikrotiterplatten mit Funktion als Deckel
p) Mikrotiterplatte für Erstabgabe bei der Aliquotierung von Flüssigkeiten
q) Halterung mit fünf Plätzen für Behälter mit maximal Volumen von 50 ml
r) Halterung mit drei Plätzen für Behäter mit maximal Volumen von 120 ml
s) gestapelte Pipettenspitzen mit maximal Volumen von 50 µl
t-u) Halterung für ‚Standard Gestelle' mit zwei mal ‚High'-Pipettenspitzen (1000 µl) und jeweils vier mal ‚Standard'- (300 µl) und 50 µl-Pipttenspitzen

gekühlte Halterung mit entsprechenden Adaptern für Mikrotiterplatten und Mikroreaktionsgefäße
Halterung für Mikrotiterplatten

Abbildung 2.6: Microlab Star Deck für das sFIDA-Assay
a) Mikrotiterplatte repräsentiert den Plattenträger des Washers. Die Mikrotiterplatten (b-c) haben ein 384-Well Format und werden für das sFIDA-Experiment verwendet. Das kleine (e) und große Reservoir (d) erhalten unterschiedliche Reagenzien. Mikroreaktionsgefäße können in sogenannten Adaptern auf dem Deck bereitgestellt werden (f-k). Der Laborbedarf (l-o) dient als Deckel für die verwendeten Mikrotiterplatten und Behälter, die während des sFIDA-Experiments abgedeckt werden müssen. Die Mikrotiterplatte (p) dient zur Erstabgabe von Volumen bei Aliquotierungen. Die Halterungen (q und r) besitzen fünf Plätze für Behälter mit je 50 ml und drei Plätze für 120 ml Behälter. Die gestapelten Pipettenspitzen mit Maximalvolumia von 300 µl oder 50 µl sind unter s) platziert. Die nächsten Halterungen (t-u) können Standard-Gestelle halten und somit unterschiedliche Pipettenspitzen-Typen bereitstellen (für den sFIDA-Assay: Zwei mal 96er 1000 µl Pipettenspitzen und jeweils vier mal 96er 300 µl und 50 µl Pipettenspitzen). Die blaue Umrandung markiert die Halterung, die gekühlt werden kann. Die orange Umrandung umfasst ein Halterung für Mikrotiterplatten ohne Kühlung.

Der Plattenträger des Washers wird in Abbildung 2.6 durch eine Mikrotiterplatte in dem Deck repräsentiert, da die Mikrotiterplatte an dieser Position platziert wer-

den muss, um optimal im Plattenträger des Washers zu liegen.

Es wurde eine gekühlte Halterung auf dem Deck platziert. In dieser Halterung ist das Schlauchsystem eines Kühlungssystems (Pilot One von Huber) fest integriert und kann nicht vom Deck entfernt werden. Es werden Adapter aus Aluminium verwendet, um die Mikrotiterplatten und/oder Mikroreaktionsgefäße auf der Halterung bereitzustellen. Die Adapter leiten die Temperatur der gekühlten Halterung weiter, sodass beispielsweise Inkubationszeiten mit niedrigeren Temperaturen als Raumtemperatur erfolgen können. Mit den entsprechenden Adapter können die Reagenzien oder Proben in Mikroreaktionsgefäßen auf dem Deck des ML Stars gekühlt werden. Zwei Sorten von Mikroreaktionsgefäße mit unterschiedlichen Fassungsvermögen (1,5 ml und 2 ml) können in diese Adapter gestellt werden. Es sind sechs Plätze der gekühlten Halterungen mit Adaptern für Mikroreaktionsgefäße ausgestattet und vier mit Adaptern für Mikrotiterplatten.

Die Mikrotiterplatten haben ein 384-*Well* Format und werden im ML Star beim Pipettiervorgang spaltenweise von links nach rechts prozessiert. Dabei wird zunächst in jeder Spalte jedes zweite *Well* parallel pipettiert, da die acht Pipettierkanäle nicht dicht nebeneinander pipettieren können. Die Pipettierkanäle brauchen einen gewissen Abstand, sodass die Pipettenspitzen das jeweilige *Well* treffen und nicht auf den Rahmen der Mikrotiterplatte aufkommen. Bei Mikrotiterplatten im 384-*Well*-Format wird von Sektoren gesprochen (siehe Abbildung 2.7). Jeder Sektor besteht aus 96 *Wells* und ist um ein *Well* in x- und in y-Richtung versetzt angeordnet. Vier von diesen Sektoren ergeben das 384-*Well*-Format. Im ML Star wird erst der obere Sektor und dann der untere Sektor innerhalb einer Spalte prozessiert.

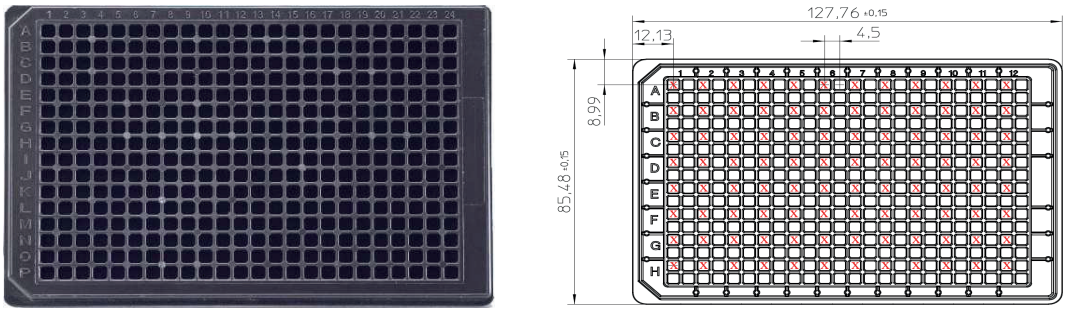

Abbildung 2.7: Mikrotiterplatte im 384-*Well*-Format und schematische Zeichnung
Auf der linken Seite ist eine Mikrotiterplatte im 384-*Well*-Format mit schwarzen Rahmen abgebildet. Rechts ist die dazugehörige schematische Zeichnung der Mikrotiterplatte mit den entsprechenden Maßen in mm. Das Symbol x kennzeichnet den oberen linken Sektor jedes Quadranten der Mikrotiterplatte (Abbildung in Anlehnung an greiner bio-one 2016)

Neben den Mikrotiterplatten, die für das Experiment prozessiert werden, gibt es Mikrotiterplatten, die als Deckel fungieren. Für die verwendeten Mikrotiterplatten gibt es keine passenden Deckel, die der iSWAP abnehmen und auflegen kann.

Dementsprechend wurden weitere Mikrotiterplatten auf dem Deck platziert, die während der Inkubationszeiten auf die Experiment-Mikrotiterplatten gesetzt werden. Zurzeit gibt es die Möglichkeit zwei Mikrotiterplatten parallel in dem ML Star zu verarbeiten. Dazu gibt es zwei weitere Mikrotiterplatten, die als Deckel genutzt werden.

Zusätzlich zu den Mikrotiterplatten gibt es Behälter, sogenannte Reservoirs, die das gleiche Format haben wie Mikrotiterplatten und entsprechend auf denselben Halterungen stehen können. Die Behälter gibt es in unterschiedlichen Ausführungen, sodass eine Reihe von verschiedenen Fassungsvermögen darin vorgelegt werden können (siehe Abbildung 2.8). Die Behälter (B und C) verfügen über 12 Spalten und jede Spalte hat ein maximales Fassungsvermögen von 7 ml bzw. 21 ml. Außerdem gibt es eine weitere Art, die durch eine zusätzliche Abtrennung (horizontal) zwei Kammern in jeder Spalte erhält. Die Kammern können maximal je 3,5 ml Fassungsvermögen enthalten. Im Folgenden werden die unterschiedlichen Behälter entsprechend des Fassungsvermögens als kleines, mittleres oder großes Reservoir bezeichnet.

Der Vorteil dieser Reservoirs gegenüber Mikroreaktionsgefäßen ist, dass die acht Pipettierkanäle gleichzeitig aus diesen Behältern aspirieren bzw. in diese Behälter Flüssigkeit abgeben können. Falls das Reagenz in einem Mikroreaktionsgefäß vorliegt, aber alle acht Pipettierkanäle parallel auf die Mikrotiterplatte das Reagenz abgegeben sollen, müssen die Pipettierkanäle einzeln in das Mikroreaktionsgefäß zur Aspiration des Reagenz und können anschließend auf die Mikrotiterplatte die Flüssigkeit abgeben. Dies ist mit einem hohem Zeitverlust verbunden, verglichen mit der Aspiration aus den Reservoirs. Als Nachteil der Reservoirs gilt das größere Totvolumen gegenüber der Mikroreaktionsgefäßen, damit das acht Pipettierkanal-System genügend Volumen vorliegen hat, um gleichmäßig daraus aspirieren zu können.

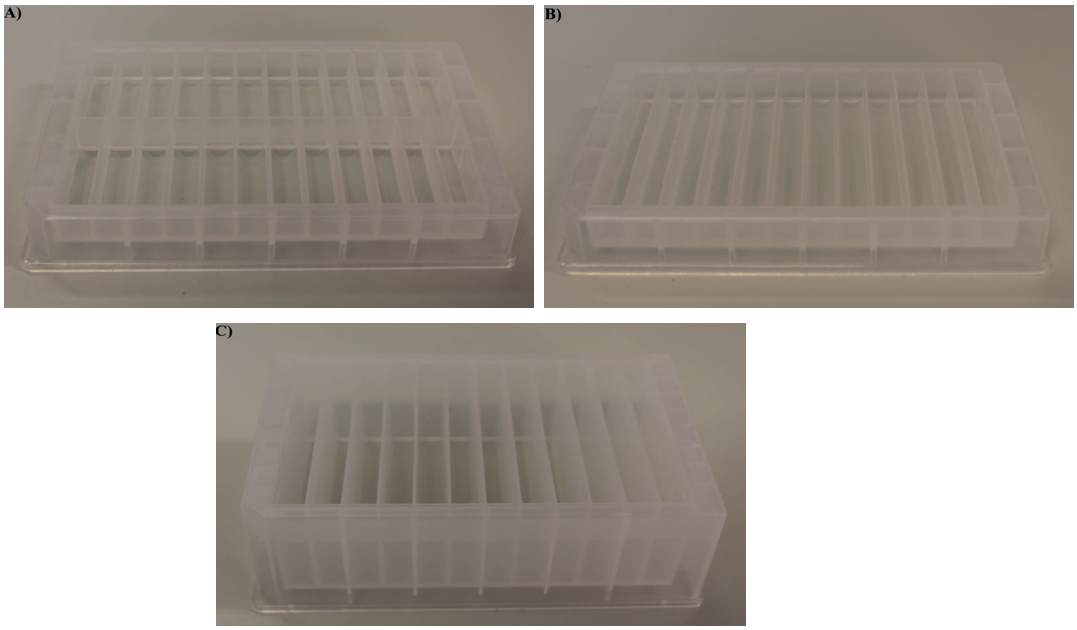

Abbildung 2.8: Reservoirs: Behälter im Mikrotiterplatten-Format
A) Das kleine Reservoir besitzt zwei Kammern in jeder Spalte, die ein Fassungsvermögen von je 3,5 ml haben. B) Das mittlere Reservoir kann ein Fassungsvermögen von 7 ml in jeder Spalte halten und eine Spalte des großen Reservoirs (C) kann ein Fassungsvermögen von 21 ml beinhalten.

In der vorliegenden Arbeit wurden zwei weitere Halterungen für Behälter verwendet: Zum einen eine Halterung mit drei Plätzen für Behälter mit einem Fassungsvermögen von 120 ml und zum anderen eine Halterung mit fünf Plätzen für 50 ml Behältern.

Die im Rahmen dieser Arbeit verwendeten Pipettenspitzen sind für maximale Pipettiervolumina von 1000 µl, 300 µl und 50 µl ausgelegt. Die 1000 µl Pipettenspitzen werden in einem Gestell (*Racks*) mit 96 Stück geliefert; und eine Standard-Halterung kann fünf dieser *Racks* auf dem Deck bereitstellen. Die 300 µl und 50 µl Pipettenspitzen können ebenfalls in dieser Halterung platziert werden. In dieser Arbeit wurden im Deck Layout zwei Halterungen für Pipettierspitzen, die mit zwei *Racks* für 1000 µl Pipettenspitzen bestückt sind. Demzufolge gibt es 192 Pipettenspitzen dieser Art. Des weiteren werden hier je vier *Racks* 300 µl und 50 µl Pipettenspitzen werden bereitgestellt, sodass je 384 Pipettenspitzen von diesen beiden Arten auf dem Deck zur Verfügung stehen.

Die 50 µl Pipettenspitzen werden insbesondere für die Probenverteilung im sFIDA-Assay benötigt, da in diesem Schritt niedrige Volumina pipettiert werden und jedes mal ein Wechsel der Pipettenspitzen nötig ist. Durch den hohen Bedarf an Pipettenspitzen von 300 µl und 50 µl gibt es zusätzlich eine Halterung die gestapelte Pipettenspitzen, 300 µl oder 50 µl, auf dem Deck bereitstellen kann. Dabei sind an fünf Positionen jeweils vier der *Racks* mit einer der Pipettenspitzen-Art gestapelt,

sodass insgesamt 1920 Pipettenspitzen zur Verfügung stehen können.

Der Platz, der auf dem Deck noch frei ist, kann für weitere Halterungen für Mikrotiterplatten und Pipettenspitzen genutzt werden. Dies ist nötig, sobald weitere Mikrotiterplatten parallel verarbeitet werden sollen.

2.2.4 Implementierung von ML Star Methoden

In dem folgenden Teil werden Aspekte der Implementierung von ML Star Methoden anhand einfachen eines Beispiels erklärt, in dem eine Konzentrationsreihe über eine Mikrotiterplatte zu erstellt werden soll. Zur Verfügung stehen acht Pipettierkanäle, der iSWAP, zwei Behälter und die Mikrotiterplatte im 384-*Well*-Format. Der erste Behälter ist ein 120 ml Behälter mit Wasser und der zweite Behälter ist ein Mikroreaktionsgefäß mit eingefärbten Wasser.

Die ML Star Methode soll folgenden Ablauf beinhalten: Zuerst verteilen die acht Pipettierkanäle ungefärbtes Wasser auf die Mikrotiterplatte und im Anschluss soll ein gewünschtes Volumen des gefärbten Wassers in die erste Spalte der Mikrotiterplatte abgeben werden. Im Folgenden wird ein Volumen dieser Spalte in die nächste Spalte übertragen, sodass das eine abfallende Konzentrationsreihe des gefärbten Wassers entsteht. Der Verdünnungsfaktor sowie die Anzahl der Spalten, die verarbeitet werden sollen, soll vom Anwender festgelegt werden. Unter der Annahme, dass der Anwender beispielsweise die Absorption jedes *Wells* der Mikrotiterplatte messen möchte, soll die ML Star Methode fortfahren und den Washer nutzen, um die Mikrotiterplatte zu waschen und leer zurückzugeben.

Zunächst wird die VENUS two-Software gestartet und eine neue ML Star Methode erstellt. Wenn auf die Deck-Ansicht gewechselt wird, gibt es die Möglichkeit das Gerät (ML Star) auszuwählen; unter *Labware* gibt es eine Auswahl an Halterungen und standardisierten Laborbedarfsartikeln die auf das Deck abgelegt werden können. Des Weiteren gibt es unter *Sequences*, im Folgenden als Sequenzen bezeichnet, die verfügbaren Positionen der abgelegten Gegenstände (siehe Abbildung 2.9). Die Sequenzen werden in der ML Star Methode genutzt, um die involvierten Labware zu identifizieren. Es ist eine Art von Variable in der die Position auf dem Deck, Anzahl an möglichen Positionen und Art des Gegenstandes abgelegt ist.

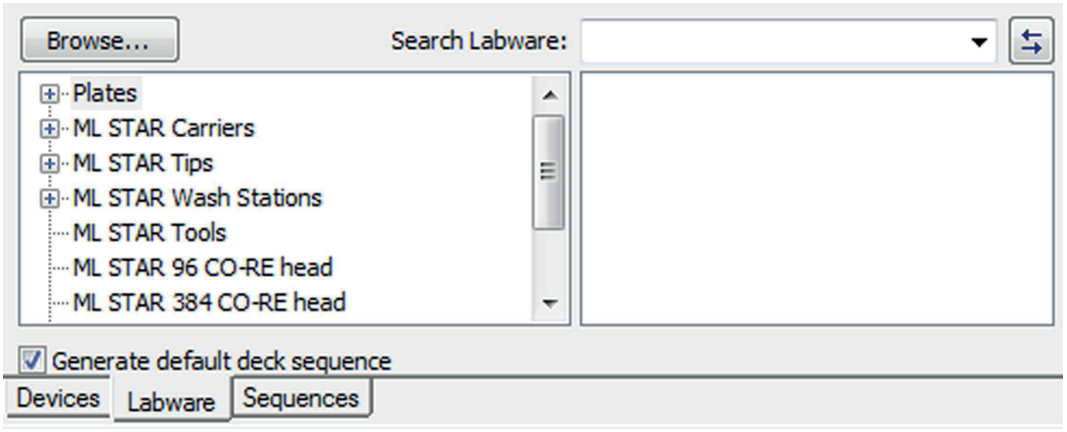

Abbildung 2.9: Reiter-Ansicht für die Labware
Unter der Deck-Ansicht können über die drei Reiter das Geräte, die Labware und die Sequenzen ausgewählt und bearbeitet werden. Bei dem Reiter für die Labware steht ein Katalog von Halterungen und Laborbedarfsartikeln zur Auswahl.

Für das Beispiel werden zunächst die Halterungen für benötigte Pipettenspitzen (1000 µl und 300 µl Pipettenspitzen), ein 120 ml Behälter, ein Mikroreaktionsgefäß und eine Mikrotiterplatte auf dem Deck platziert. Entsprechend müssen die genannten Gegenstände auf den vorgesehenen Halterungen verteilt werden. Es werden automatisch Sequenzen erstellt, die jedoch verändert und umbenannt werden können (siehe Abbildung 2.10). Die Sequenzpositionen können sortiert und bearbeitet werden, sodass ein Laborbedarfsartikel mit mehreren Sequenzpositionen in beliebiger Reihenfolge prozessiert werden kann. Außerdem können Sequenzpositionen von unterschiedlichen Laborbedarfsartikeln ausgewählt und als eine Sequenz abgespeichert werden. Diese Sequenz wird in der gespeicherten Reihenfolge prozessiert.

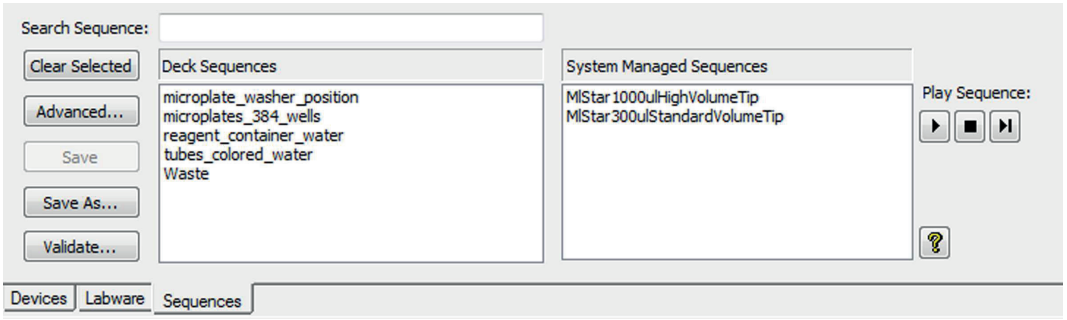

Abbildung 2.10: Reiter-Ansicht für Sequenzen
Die Sequenzen für die einzelnen Laborbedarfsartikel können unbenannt werden und über *Play* durchlaufen werden, sodass in einer Simulation erkennbar wird, in welcher Reihenfolge die Sequenzpositionen prozessiert werden.

In der folgenden Abbildung 2.11 sind die unterschiedlichen Ansichten des Decks dargestellt. Die Deck-Ansicht für den Labware-Reiter zeigt die ausgewählten Gegenstände und ihre Positionen auf dem Deck (siehe 2.11 a)). Unter b) wird die Deck-

Ansicht im Sequenz-Modus angezeigt, dabei sind die relevanten Sequenzpositionen für die beschriebene ML Star Methode rot eingefärbt. Die einzelnen Laborbedarfsartikel bzw. die zugehörigen Sequenzpositionen sind in einzelnen Sequenzen abgespeichert und können so im Programm explizit angesprochen werden.

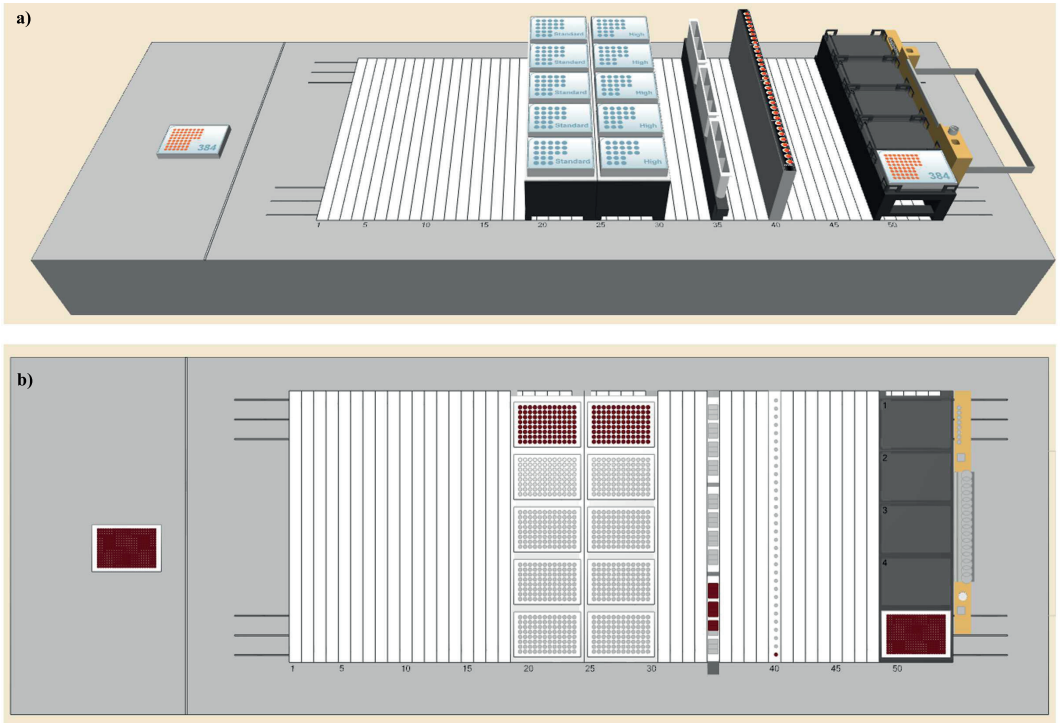

Abbildung 2.11: Deck-Ansicht für Labware und Sequenzen
a) Die Deck-Ansicht im Labware-Reiter. Es können aus einem Katalog Halterungen und unterschiedliche Laborbedarfsartikel ausgewählt und auf dem Deck platziert werden. b) Die Deck-Ansicht für die Sequenzen. Die rot gefärbten Positionen werden in der beschriebenen ML Star Methode prozessiert.

Wenn die entsprechenden Gegenstände auf dem Deck platziert worden und die Sequenzen vorhanden sind, kann mit der Implementierung des Experimentablaufs begonnen werden. Dabei wird auf die Methoden-Ansicht gewechselt. Auf der rechten Seite sind unterschiedliche Befehle kategorisiert und aufgelistet (siehe Abbildung A.1).

Am Anfang jeder ML Star Methode muss ein Initialisierungsbefehl erfolgen. Hierbei werden die vorhanden Eigenschaften wie die Pipettierkanäle und der iSWAP initialisiert und deren Fahr- und Bewegungsabläufe getestet. Danach werden in der Methode eine Reihe von Variablen erstellt (siehe Abbildung 2.12):

- volumeWater = Volumen des ungefärbten Wassers
- volumeColor = Volumen des gefärbten Wassers
- numberCycles = Anzahl Zyklen (bzw. Anzahl Konzentrationen)

- volumeToAspirate = Volumen beim Aspirieren für die Aliquotierung des ungefärbten Wassers
- numberOfDispenses = Anzahl von Dispensierungsschritten, die mit dem aspirierten Volumen erfolgen können
- endOfMicrotiterplate = maximale Anzahl der *Wells* (basierend auf der Anzahl der Spalten)
- nextPositionToAspirate = Position auf der Mikrotiterplatte, die im nächsten Schritt prozessiert werden soll

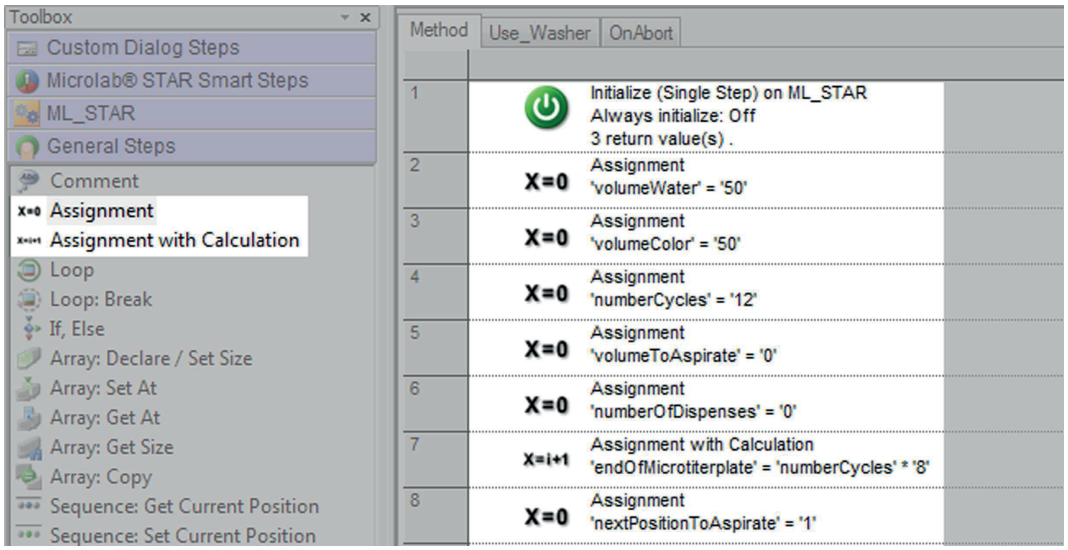

Abbildung 2.12: Initialisierung des Microlab Star und Variablen
Initialisierung des ML Star und Initialisierung der benötigten Variablen (rechts). Ausschnitt aus der Befehlsliste mit Befehlen zum Erstellen von Variablen (links).

Diese werden am Anfang mit bestimmten Werten initialisiert, dürfen aber teilweise durch einen bereitgestellten Dialog vom Anwender überschrieben werden. Dabei gibt es Einschränkungen durch die Beschaffenheit der verwendeten Pipettenspitzen und der Mikrotiterplatte. Die Volumina von ungefärbtem und gefärbtem Wasser dürfen nicht 1000 µl bzw. 300 µl überschreiten und die Summe der je Verdünnung pipettierten Volumina darf nicht mehr als 130 µl ergeben, um das Maximalvolumen der *Wells* der Mikrotiterplatte nicht zu überschreiten. Zusätzlich darf die Anzahl der Spalten in diesem Fall nicht größer als 24 sein.

In dem Dialog zur Eingabe von Parametern durch den Anwender werden zunächst Textfelder erstellt, die dazu auffordern entsprechende Zahlen einzugeben. Daneben werden die Eingabefelder bereitgestellt, diese können als *Numeric input* festgelegt werden (siehe Abbildung 2.13). Hierbei können Minima und Maxima der erlaubten Werte festgelegt werden. Nachdem der Anwender die Eingaben gesetzt und mit *OK* bestätigt hat, sollten die Eingaben geprüft werden, bevor die ML

Star Methode weiter abläuft. In diesem Fall wird jedoch angenommen, dass der Anwender sinnvolle Eingaben getätigt hat, sodass das maximale Volumen jedes *Wells* der Mikrotiterplatte nicht überschritten wird.

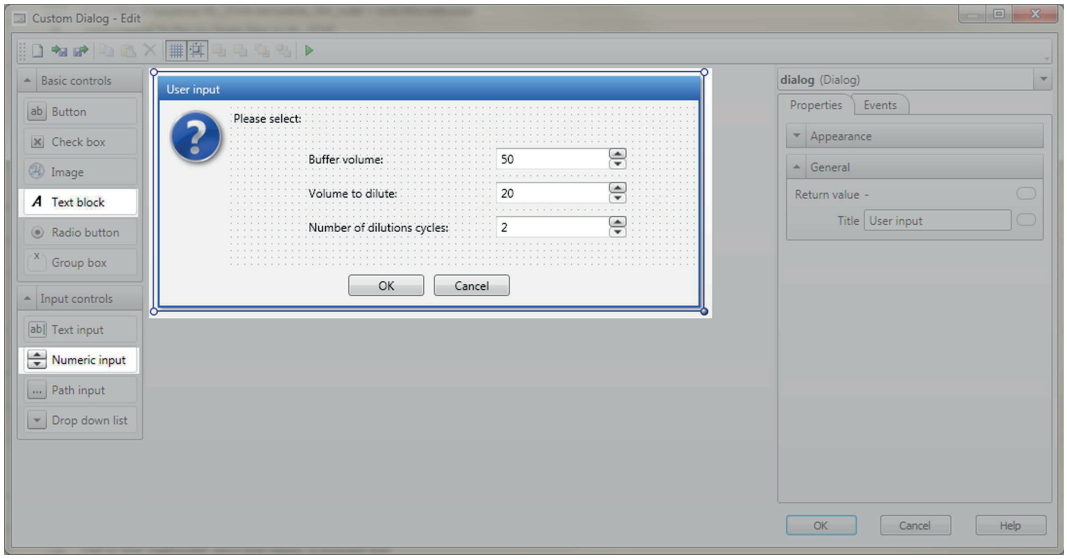

Abbildung 2.13: Erstellung eines Dialogs zur Eingabe von Parametern durch Anwender des Microlab Star
Zum Erstellen eines Dialogs wird ein vorgefertigtes Fenster (mitte) bereit gestellt, das durch Drag-Drop von Elementen (links) gestaltet wird.

Die obengenannten Variablen wurden mit den Anwendereingaben überschrieben und können in den nächsten Schritten genutzt werden. Zunächst soll das ungefärbte Wasser auf die Mikrotiterplatte verteilt werden. Dabei werden die 1000 µl Pipettenspitzen genutzt, diese werden durch den *Tip Pick Up*-Befehl aufgenommen. Anhand der angegeben Spaltenanzahl wird die maximale Anzahl berechnet und das entsprechende Well als Endpunkt der Mikrotiterplatten-Sequenz gesetzt. Anschließend wird ein Schleifen-Befehl (*loop*) gestartet, der über die Mikrotiterplatte iteriert (siehe Abbildung 2.14).

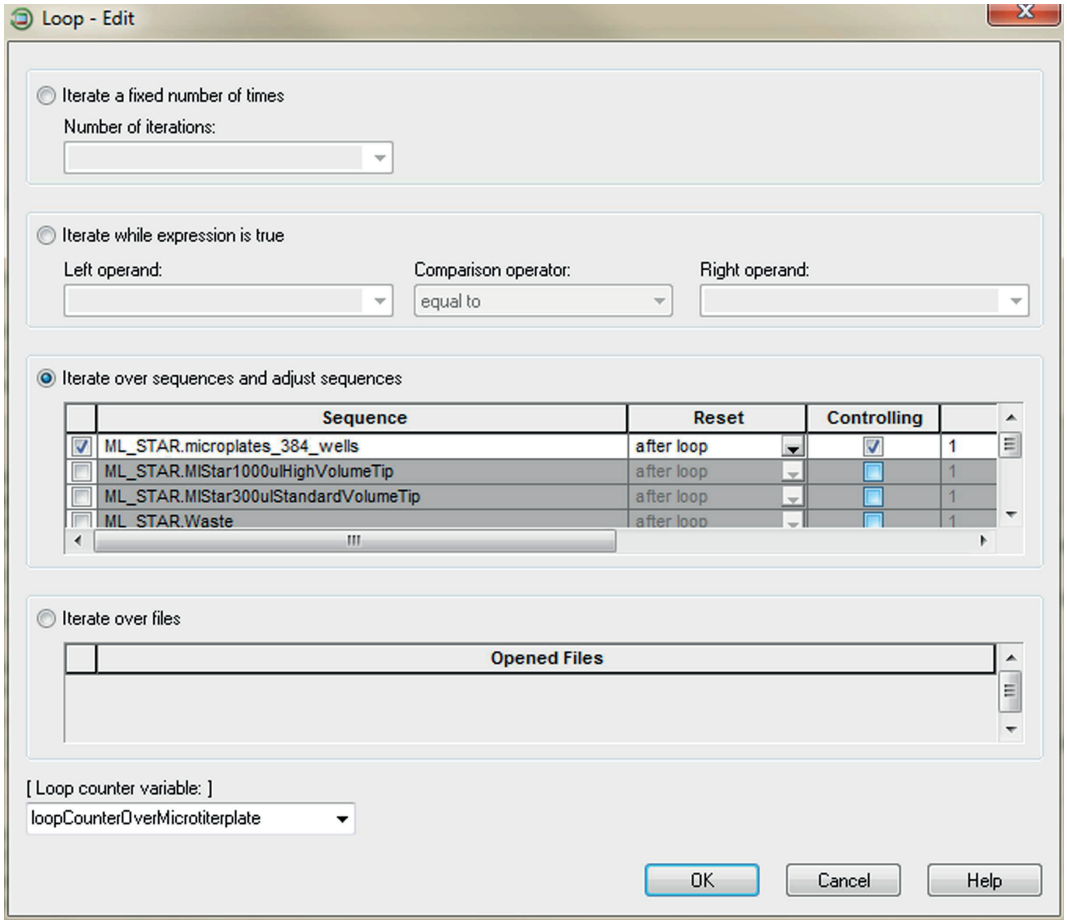

Abbildung 2.14: Iteration über die Mikrotiterplatte durch einen Schleifen-Befehl im Microlab Star
Die Iteration findet über die Sequenz der Mikrotiterplatte statt (mitte). Außerdem gibt es die Möglichkeit eine Anzahl der Iterationen festzulegen oder eine sogenannte *while*-Schleife zu erstellen, die solange iteriert bis eine Bedingung erfüllt ist. Eine Variable für das Hochzählen während der Iteration wird erstellt (unten), diese kann innerhalb der Schleife genutzt werden.

Innerhalb der Schleife werden die folgenden Befehle ausgeführt, um das ungefärbte Wasser in die vorgesehen *Wells* zu verteilen. Dafür wird ein vorgefertigter Befehl genutzt, um das Volumen zu berechnen das aspiriert werden soll . Hier wird angegeben, welche Pipettenspitzen genutzt werden und welches Volumen in jedem Schritt auf welche Sequenz (hier Mikrotiterplatte) abgegeben werden soll. Bei dieser Art des Pipettierens ist es nötig ein *Pre-* und *Post-Aliquot*-Volumen anzugeben. Damit wird das präzise Pipettieren des Volumens durch Aliquotierung gewährleistet. In diesem Schritt werden folgenden Variablen erstellt: volumeAspiration, die dem Aspirationsvolumen entspricht und numberOfDispense, die der Anzahl der Dispensierungsschritte entspricht.

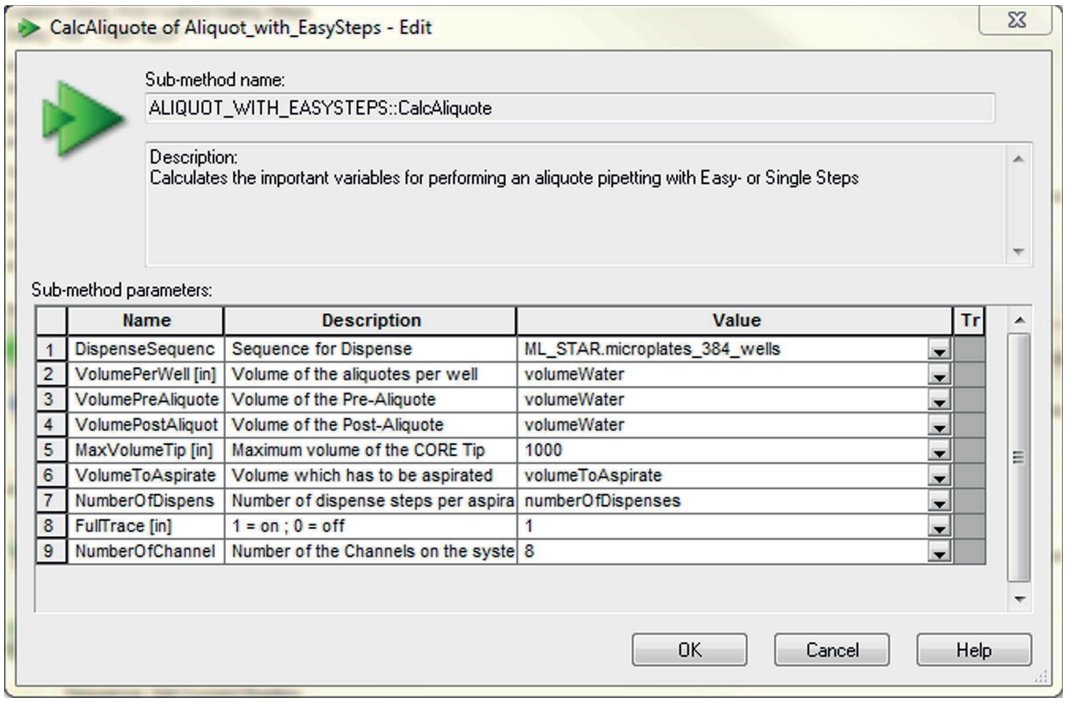

Abbildung 2.15: Eingabe und Berechnung von Parametern für die Aliquotierung im Microlab Star
Dieser Befehl berechnet das Aspirationsvolumen und die Anzahl Dispensierungen anhand der Eingabe von zu pipettierender Sequenz, Volumen und verwendeten Pipettenspitzen für die Aliquotierung. Die berechneten Werte werden in Variablen gesetzt und in der weiteren Befehlsabfolge der Aliquotierung verwendet.

Im Aspirationsschritt wird zunächst die Sequenz (hier 120 ml Behälter) ausgewählt aus der die Aspiration erfolgen soll (siehe Abbildung 2.16). Es wird die vorher erstellte Variable volumeAspiration eingegeben und ausgewählt mit welchem Piptenspitzentyp und Art des Pipettierens verwendet werden soll. Außerdem wird eine sogenannte *Liquid class* (Flüssigkeitsklasse) ausgewählt, die für jeden Pipettenspitzentyp und Art des Pipettierens erstellt werden. Innerhalb dieser Flüssigkeitsklassen können auf Basis der Viskosität der Flüssigkeit unterschiedliche Parameter eingestellt werden. Dies wird in Abschnitt 2.2.5 im Detail beschrieben.

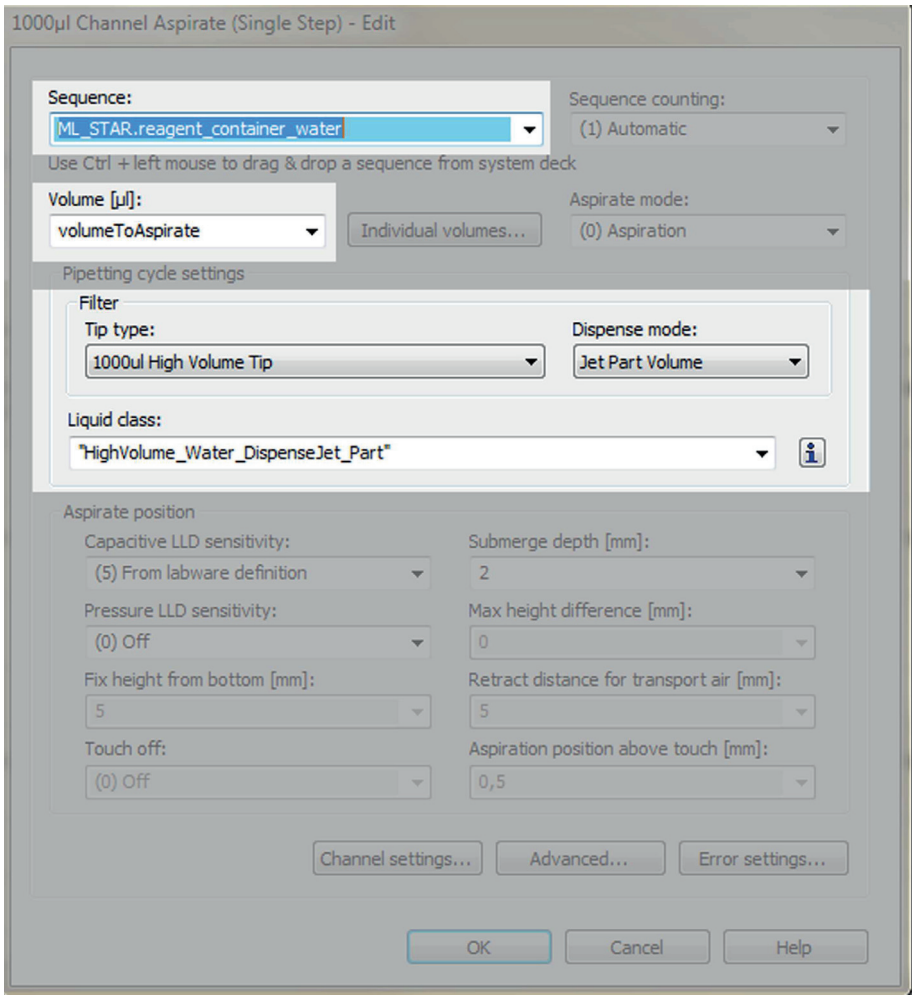

Abbildung 2.16: Befehl zur Aspiration im Microlab Star
Im Aspirationsbefehl wird die Sequenz angegeben aus der die Aspiration stattfinden soll. Im Folgenden wird das gewünschte Volumen angegeben und die Flüssigkeitsklasse zur Aspiration und Dispensierung ausgewählt. Dafür muss der Pipettenspitzentyp ausgewählt werden. Außerdem können noch Einstellungen zur Position der Pipettenspitze angegeben werden (hier ausgegraut).

Wenn der Aspirationsbefehl fertig gestellt ist, wird ein Dispensierungsbefehl (siehe Abbildung2.17) für das *Pre-Aliquot*-Volumen in den 120 ml Behälter erstellt. Hierbei ist zu beachten, dass die Sequenz des 120 ml Behälter wieder auf eins gesetzt wird, da die Sequenz des 120 ml Behälters während der Aspiration vollständig durchlaufen wurde. Schließlich wird eine weitere Schleifen durchlaufen in der über die Anzahl der Dispensierungsschritte (numberOfDispense) iteriert wird. In jedem Schritt werden 100 µl der farblosen Flüssigkeit spaltenweise in die Wells der Mikrotiterplatte gegeben. Wenn das Ende der Schleife für die Dispensierungsschritte erreicht ist wird in einem weiteren Dispensierungsbefehl das *Post-Aliquot*-Volumen in den 120 ml Behälter abgegeben. Solang die Schleife die über die Mikrotiterplatte nicht am Ende der gesetzten *Well*-Anzahl gelangt, werden die Schritte wiederholt und die Mikrotiterplatte erhält 100 µl in jedes vorgesehene *Well*.

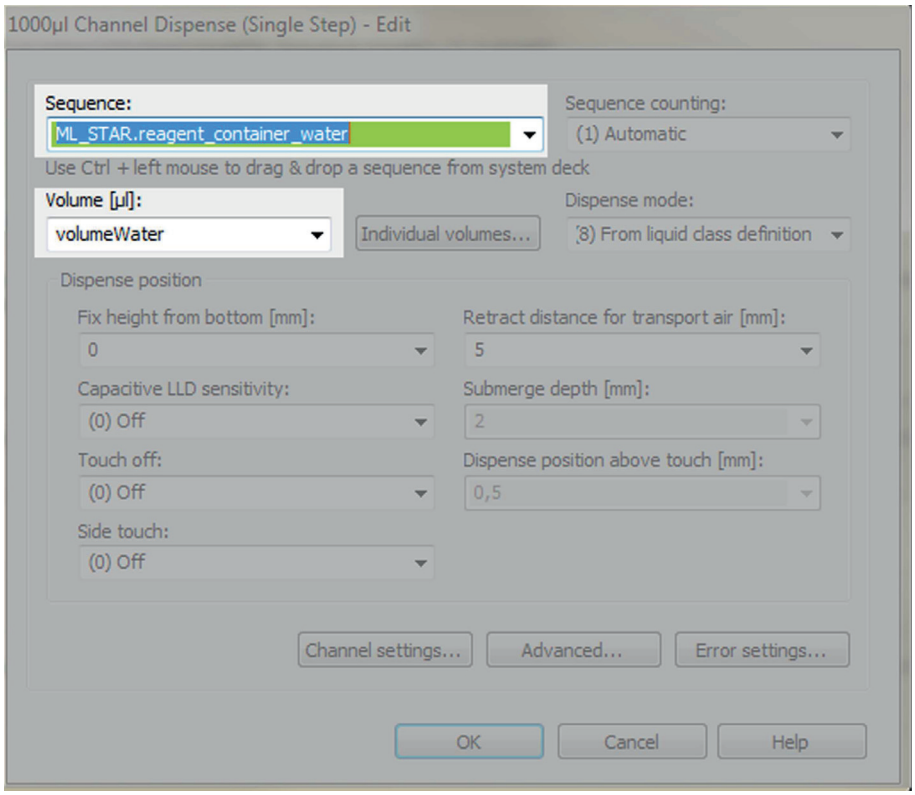

Abbildung 2.17: Befehl zur Dispensierung im Microlab Star
Im Dispensierungsbefehl wird die Sequenz zur Abgabe ausgewählt. Danach wird das Abgabevolumen angegeben. Die Art der Dispensierung ist basierend auf der Flüssigkeitsklasse die im vorangegangen Aspirationsbefehl ausgewählt wurde.

Im Anschluss werden die 1000 µl Pipettenspitzen in den Abfall gegeben (*Tip Eject*-Befehl) und 300 µl Pipettenspitzen werden aufgenommen.

Alle acht Pipettierkanäle können nicht gleichzeitig in das Mikroreaktionsgefäß, um das gefärbte Wasser mit einem Volumen von beispielsweise 30 µl zu aspirieren. Dementsprechend wird nur ein Pipettierkanal genutzt, der über die ersten acht Positionen der Mikrotiterplatte das Volumen des eingefärbten Wassers (volumeColor) abgibt (siehe Abbildung A.2). Im Anschluss wird die Pipettenspitze abgeworfen und alle acht Kanäle nehmen Pipettenspitzen auf. Es wird die Start- und Endposition der Mikrotiterplatte neu gesetzt.

In dem darauffolgenden Schleifen-Befehl wird über die Mikrotiterplatte iteriert und jedes mal werden die Pipettenspitzen gewechselt, deswegen sind die *Tip Pick Up*- und *Tip Eject*-Befehl innerhalb der Schleife. Die Art der Aspiration ist diesmal *DispenseJetEmtpy*, d.h. bei der Dispensierung wird das gesamte Volumen von der Aspiration abgegeben. Es folgt keine Aliquotierung wie in den Schritten davor. Die Aspiration von dem Volumen volumeColor erfolgt in den ersten acht Positionen der Mikrotiterplatte. Es folgt ein Dispensierungsbefehl, dieser prozessiert die nächsten Positionen der Mikrotiterplatten-Sequenz und gibt das Volumen ab. Schließlich

werden die Pipettenspitzen abgeworfen. Die aktuelle Sequenz-Position wird ausgelesen und die Zahl acht wird abgezogen, da acht Positionen in einer Dispensierung verbraucht wurden. In der nächsten Aspiration werden die *Wells* prozessiert in denen zuvor dispensiert wurde. Die neu errechnete Zahl wird als Anfangsposition der Mikrotiterplatten-Sequenz gesetzt und die Schleife iteriert weiter.

In der letzten zu prozessierenden Spalte muss ein Sonderfall berücksichtigt werden, denn wenn in den letzten Spalte dipensiert wurde, hat die Sequenz der Mikrotiterplatte keine Positionen mehr zur Verfügung. Trotzdem soll das Volumen in jedem *Well* gleich sein, deswegen muss aus der letzten Spalte das *volumeColor* heraus pipettiert werden. Dementsprechend wird eine Bedingungsschleife in Form eines sogenannten *If, Else*-Befehls gesetzt. Wenn die aktuelle Position der Mikrotiterplatten-Sequenz null ist, also die letzte zu prozessierende Spalte erreicht wurde, wird von der errechneten maximal *Well*-Anzahl acht (acht Pipettierkanäle) abgezogen und als neue Position der Mikrotiterplatten gesetzt. Direkt im Anschluss werden Pipettenspitzen aufgenommen und das gewünschte Volumen aspiriert. Schließlich werden die Pipettenspitzen und das aufgenommene Volumen in den Abfallbehälter geworfen und ein Abbruchbefehl (*Loop: Break*) beendet die Iterations-Schleife.

Danach wird eine Zeitschaltuhr (*Timer: Start*) auf unendlich erstellt und gestartet (*Timer: Wait for*). Bis zum Stoppen hat der Anwender nun Zeit beipielsweise die Absorption der *Wells* auf der Mikrotiterplatte zu messen, bevor das Programm fortgesetzt wird.

Nach dem Stoppen der Zeitschaltuhr wird eine sogenannte *Submethode* aufgerufen. Diese enthält die Befehle, um die Mikrotiterplatte zum Plattenträger des Washer zu transportieren (siehe Abbildung 2.18) und über die zugehörige Befehlsbibliothek für die LHC-Software wird der Washer gesteuert. Im Detail wird dies in Abschnitt 2.2.7 beschrieben. Nach erfolgreichem Abschluss des Waschprogramms wird die Mikrotiterplatte zurück auf das Deck des ML Stars transportiert und die ML Star Methode ist beendet.

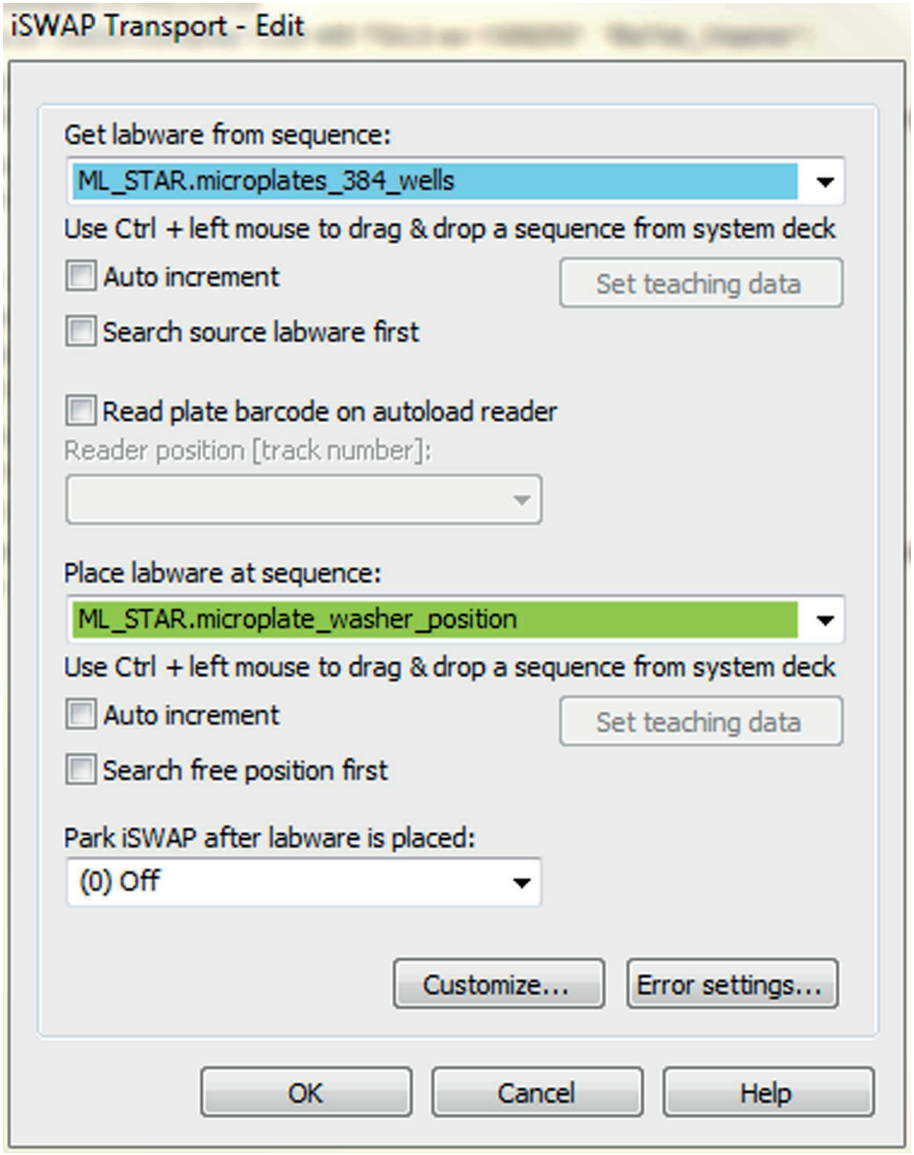

Abbildung 2.18: Befehl zum Transport von Mikrotiterplatten im Microlab Star
Der iSWAP-Befehl zum Transport von Mikrotiterplatten enthält die Startposition (blau) und Zielinformation (grün) in Form einer Sequenz.

Die Abfolge der einzelnen Befehle für die Konzentrationsreihe auf der Mikrotiterplatte können in eine ML Star Submethode ausgelagert werden und andere Stelle als ein Befehl in den Ablauf eines komplexeren Experiments aufgerufen werden. Im Abschnitt A.1 ist die Implementierung der Beispielmethode hinterlegt.

Zum Starten der ML Star Methode wird die *Run Control* geöffnet und auf *Play* gedrückt. Zunächst wird der ML Star initialisiert, falls er noch nicht verwendet wurde. Danach öffnet sich die Anwendereingabe und die weiteren Schritte laufen ab. In der *Run Control* wird das Deck angezeigt und Positionen, die als nächstes prozessiert werden, leuchten grün auf. Außerdem kann ein sogenanntes *Trace file* geöffnet werden, das jeden Schritt genau protokolliert. Dieses *Trace file* kann gedruckt oder gespeichert werden, um das Experiment zu dokumentieren.

2.2.5 Erstellung von *Liquid Classes* im Microlab Star

Um Flüssigkeit präzise pipettieren zu können, müssen einige Parameter der Viskosität der Flüssigkeit angepasst werden. Beim nauellen Pipettieren kann durch Anpassung von Druck und Schnelligkeit der Kolben der Pipette so gesteuert werden, dass bei der Aufnahme einer viskosen Flüssigkeit keine Luft aufgezogen wird. Außerdem kann der Anwender das aufgezogene Volumen per Auge kontrollieren und bei Bedarf korrigieren. Damit auch im ML Star Flüssigkeiten mit verschiedener Viskosität präzise pipettiert werden können, werden sogenannte Flüssigkeitsklassen (*Liquid Classes*) erstellt. Die Flüssigkeitsklassen bieten eine Reihe von Parametern die für die Aspiration sowie die Dispensierung angepasst werden können. Es gibt für jede Art der Pipettenspitzen und für die Art der Dispensierung (einfache Abgabe/Aliquotierung) jeweils eigene Flüssigkeitsklassen.

Die folgende Abbildung 2.19 zeigt eine Flüssigkeitsklasse die bei der Aliquotierung von sehr kleinen Volumina von wässrigem Puffer mit 300 µl-Pipttenspitzen eingesetzt wird. Im oberen Teil der Flüssigkeitsklasse wird ausgewählt ob einzelne Pipettierkanäle oder ein Pipettierkopf genutzt wird. Hinzu kommt die Benennung der Flüssigkeit und ein Auswahlmenü für die Art der Pipettenspitzen und der Dispensierung.

Es folgen die Parameter (*Liquid parameters*) die für die Aspiration sowie die Dispensierung angepasst werden können. Hierbei handelt es sich um die Geschwindigkeit bei der Aufnahme und Abgabe (*Flow rate*) sowie beim Mischen der Flüssigkeit vor der Aufnahme (*Mix flow rate*). Zusätzlich kann ein Transportvolumen in Form von Luft (*Air transport volume*) eingegeben werden, um ein herauslaufen der Flüssigkeit aus der Pipettenspitze zu verhindern. Das Ausstoßvolumen von Luft (*Blowout volume*) kann entsprechend so eingestellt werden, dass am Ende Luft ausgestoßen wird, um möglichst die vollständige Flüssigkeit abzugeben. Für die Aliquotierung werden diese Parameter auf null gesetzt, da die Pipettenspitze ein größeres Volumen der Flüssigkeit aufnehmen, um mehrmals das gewünschte (kleinere) Volumen abzugeben.

Folgende Richtlinien gelten für das Pipettieren viskoser Flüssigkeiten: Die Wechselgeschwindigkeit (*Swap speed*) wird heraufgesetzt, damit keine Flüssigkeit an der Pipettenspitze zurück bleibt, wenn die Pipettenspitze aus der Flüssigkeit heraustritt. Die Absetzzeit (*Settling time*) wird erhöht, sodass nach der Aspiration die Pipettenspitze einige Zeit in der Flüssigkeit verweilt, damit das gewünschte Volumen aufgezogen wird. Das sogenannte Überaspirationsvolumen (*Over-aspirate volume*) wird genutzt um die Pipettenspitzen vor dem eigentlichen Aspirationsbefehl mit der Flüssigkeit im inneren zu benetzen. Das Volumen wird direkt wieder abgege-

ben, aber an den Wänden der Pipettenspitzen liegt nun ein Flüssigkeitsfilm, um die präzise Aspiration von viskosen Flüssigkeiten zu erleichtern.

Die Beendigungsgeschwindigkeit (*Stop flow rate*) und das sogenannte Rückgangsvolumen (*Stop back volume*) sind Parameter, die bei der Dispensierung relevant sind. Die Geschwindigkeit beim Beenden der Dispensierung kann gleich gewählt werden wie die Geschwindigkeit der Dispensierung, sodass die Dispensierungen direkt und konstanter Geschwindigkeit beendet wird. Bei viskosen Flüssigkeiten kann die Geschwindigkeit beim Beenden der Dispensierung langsamer gewählt werden, sodass die präzise Abgabe gewährleistet wird. Damit sich bei der Dispensierung keine Tropfen bilden, wird das Rückgangsvolumen zur Aspiration von Luft eingestellt. Sobald die Pipettenspitze zurückfährt und außerhalb der Flüssigkeit liegt, wird das gewünschte Volumen von Luft aufgezogen.

Weitere Parameter können für die LLD bestimmt werden und unter dem Reiter Korrekturgerade (*Correction Curve*), können die Volumina, die aspiriert werden sollen, auf erhöhte Werte korrigiert werden. Denn neben der Viskosität, nimmt auch die Umgebung (Luftfeuchtigkeit, Temperatur, etc.) Einfluss auf das Pipettieren und kann Ungenauigkeiten beim Pipettieren verursachen. Wenn der Fehler im Volumen aber denselben Faktor ausmacht, kann durch die Anwendung einer Korrekturgeraden der Fehler beim Pipettieren ausgeglichen werden.

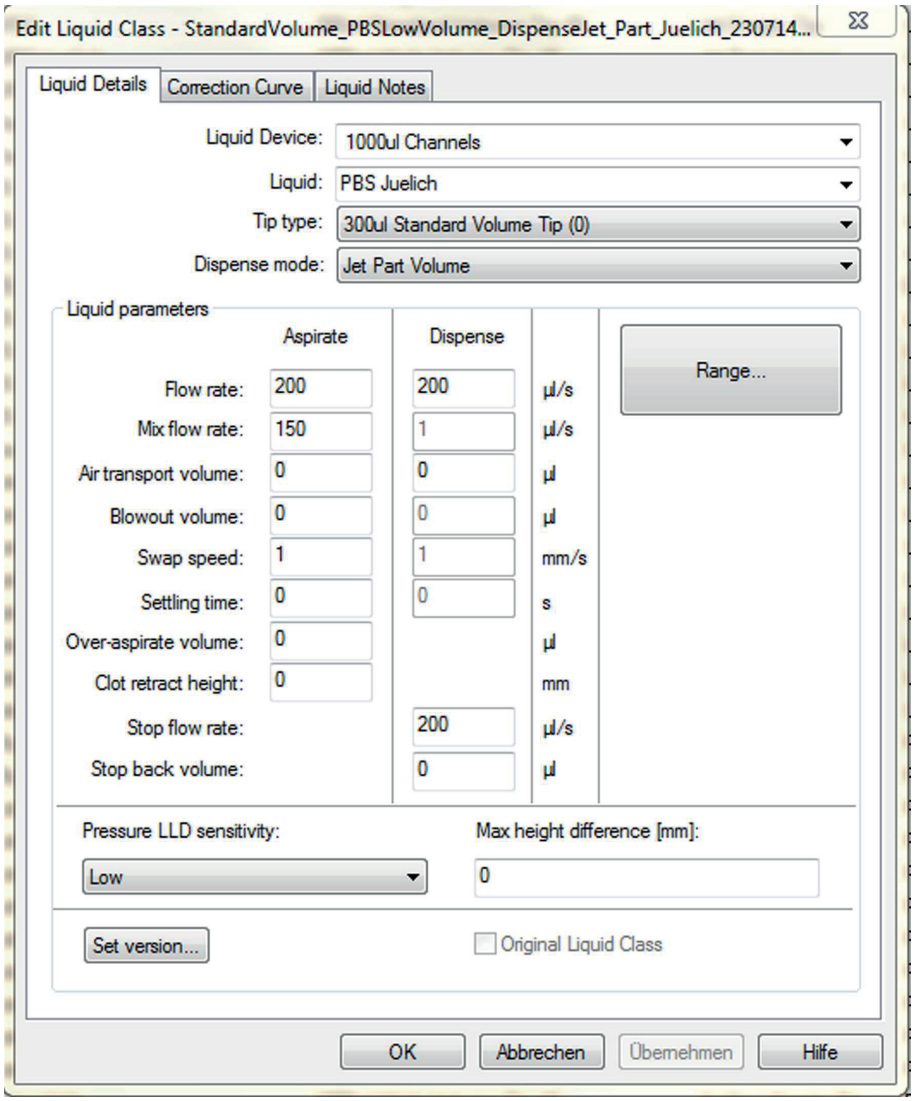

Abbildung 2.19: Parameter der *Liquid Class* zur Aliquotierung mit 300 µl-Pipettenspitzen Eine Flüssigkeitsklasse zur Aliquotierung von einer wässrigen Flüssigkeit (PBS) mit 300 µl Pipettenspitzen. Die Parameter bei der Aspiration und Dispensierung wurden so eingestellt, dass die Pipettierung des gewünschten Volumens von 15 µl präzise erfolgt.

Die Flüssigkeitsklassen decken die Aspekte des Pipettierens ab, die sonst per Hand und Auge gesteuert werden. Der Mensch realisiert beim Pipettieren von flüchtigen oder sehr viskosen Flüssigkeiten, die Fehler die entstehen können und passt das Pipettier-Verhalten an. Der ML Star bietet über eine Reihe von Parametern die Möglichkeit in Abhängigkeit der Flüssigkeit und des gewünschten Pipettiervorgangs ein präzises Pipettieren zu erreichen.

2.2.6 Experiment-Planung und Daten-Import an die Microlab Star Methode

In der *VENUS two*-Software gibt es für den Anwender die Möglichkeit Dialoge zur Eingabe von relevanten Daten zu erstellen. Da manche Experimente jedoch viele Eingaben erfodern, und die nicht nur für den Anwender sondern auch für den Programmierer zu hohem Aufwand führen könnte, wurde im Rahmen dieser Arbeit die Eingabe von Daten durch den Import einer Excel-Datei realisiert. So ist eine übersichtliche und leichte veränderbare Eingabe aller relevanter Daten möglich. Hierfür gibt der Anwender zunächst Rahmenbedingungen (Anzahl Proben, Anzahl an Konzentrationsreihen, etc.) in eine vorgefertigte Excel-Tabelle ein. Die Eingaben werden durch ein VBA-Makro verarbeitet (geschrieben von Dr. Katja Kühbach) und weitere benötigten Informationen berechnet. Die Werte, die für die ML Star Methode von Relevanz sind, werden in einem festen Schema in eine weitere Excel-Tabelle mit festen Kopfzeilen eingetragen. In der VENUS two-Software werden diese Kopfzeilenüberschriften erkannt und jeweils der Inhalt der entsprechenden Variable zu geordnet. Dieser Vorgang wird über einen Lese-Befehl in der VENUS two-Software gesteuert, sodass auch eine Erweiterung von Anwendereingaben innerhalb der ML Star Methode durch einen Zuweisungsbefehl einfach umgesetzt werden kann.

Eine weitere Excel-Tabelle wird durch ein Matlab-Skript (geschrieben von Dr. Andreas Kulawik) erstellt. Das Skript erhält als Eingabe die Anzahl der Proben und Replikate jeder Probe in dem Experiment. Über ein *Random-seeding* Schritt, werden die Replikate auf die Mikrotiterplatte verteilt. Dabei wird von links nach rechts vorgegangen und innerhalb jeder Spalte Sektor-weise die Mikrotiterplatte befüllt. Der Nutzer kann einen Mindestabstand für die Replikate eingeben, sodass die Replikate einer Probe mit einem bestimmten Abstand auf der Mikrotiterplatte verteilt werden. Dabei kann es passieren, dass zusätzliche *Wells* auf der Mikrotiterplatte als Platzhalter eingeführt werden müssen. Der Nutzer kann eine maximale Anzahl an zusätzlichen Sektoren angeben. Wenn für die Eingabe kein Experiment-Layout erstellt werden kann, muss der Nutzer den Abstand zwischen den Replikaten verkleinern und/oder die Anzahl an weiteren Sektoren erhöhen. Das Matlab-Skript erstellt eine Excel-Tabelle, die von der VENUS two-Software während der Probenverteilung ausgelesen wird. Dabei wird anhand der Position der Probe innerhalb der Sequenz der Mikrotitergefäßen auf dem Deck festgelegt welche Probe jeder der acht Pipettierkanäle einzeln aspiriert und diese gleichzeitig in die vorhergesehene Spalte abgegeben werden.

Zurzeit kann die ML Star Methode für das sFIDA-Experiment zwei Platten par-

allel verarbeiten. Die einzelnen Excel-Tabellen werden für jede Mikrotiterplatte mit festgelegtem Namen zusammen in einer Excel-Datei abgespeichert, sodass beim Verarbeiten jeder Mikrotiterplatte die zugehörigen Daten aus der Excel-Datei eingelesen und verarbeitet werden. Der Anwender hat so also die Möglichkeit zwei unabhängige Experimente auf zwei Mikrotiterplatten mit dem ML Star durchzuführen.

2.2.7 Steuerung des BioTek Microplate Washer 405 Select LS

Der BioTek Microplate Washer 405 Select LS kann vom ML Star gesteuert werden. Der Washer wurde neben dem ML Star platziert, sodass der *iSWAP*-Transportarm die Mikrotiterplatten in den Plattenträger des Washers setzen kann. Die Befehle zur Steuerung des Washers im ML Star werden durch eine *Liquid Handling Control-Library* bereitgestellt (siehe Abbildung A.3). Mit Hilfe dieser Befehlssammlung kann der Washer angesteuert und vorgefertigte Waschprotokolle aufgerufen und gestartet werden. Durch Abfrage des Washer-Status kann der ML Star feststellen, wann der Washer mit dem Waschprotokoll fertig ist, um im Anschluss die Mikrotiterplatte für den nächsten Schritt wieder auf das ML Star Deck zu transportieren. Der Washer-Status kann die drei Zustände *Busy*, *Ready* oder *Error* annehmen, sodass je nach Ausgang des Waschvorgangs das Programm des ML Star reagieren kann. Bei *Busy* wartet der ML Star und wenn der Status *Ready* vom Washer zurückgegeben wird, erfolgt der nächste Schritt in der ML Star Methode. Falls ein Fehler vom Washer (Status=*Error*) zurückgegeben wird, wartet der ML Star auf Eingreifen des Anwenders. Dieser kann den Fehler am Washer beheben und das Waschprotokoll nochmal per Hand starten. Nach erfolgreichem Beenden des Waschprogramms platziert der ML Star die Platte wieder auf das Deck und fährt mit dem nächsten Schritt der ML Star Methode fort. Die folgenden *Submethode* beinhaltet die Abfolge der obengenannten Befehle (siehe Abbildung 2.20).

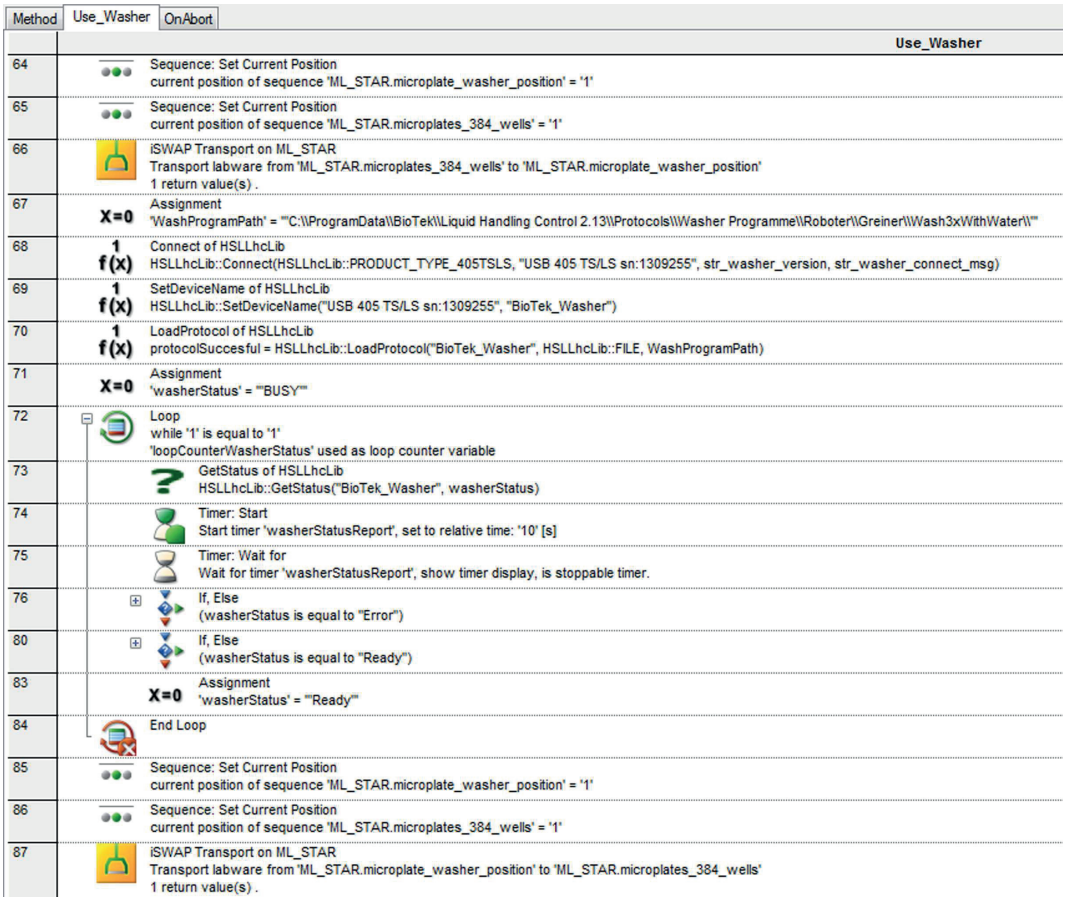

Abbildung 2.20: Befehlabfolge zum Steuern des BioTek Washer durch den Microlab Star Die ML Star Submethode zur Nutzung des Washers beginnt mit dem *Reset* der Sequenz der Mikrotiterplatte. Darauf folgt der iSWAP-Transport der Mikrotiterplatte vom ML Star Deck zur Position im Washer. Das vorgefertigte Waschprotokoll wird in einer Variablen gesetzt und die folgenden Befehle initialisieren den Washer (Zeile 68-70), laden und rufen das Waschprotokoll auf. Innerhalb eines Schleifen-Befehls wird der Status vom Washer alle zehn Sekunden abgefragt. Sobald der Status sich von *Busy* auf *Ready* oder *Error* ändert, wird die Mikrotiterplatte zurück auf das ML Star Deck transportiert.

2.2.8 Wartung vom BioTek Microplate Washer 405 Select LS

Die Wartung des BioTek Microplate Washer 405 Select LS bezüglich der Genauigkeit der Abgabe von Puffer und Aspiration wird durch Verwendung von gefärbtem Wasser und anschließender Absorptionsmessung im Handbuch beschrieben. Dabei wird das gefärbte Wasser durch die Dispensierung vom Washer in die *Wells* einer Mikrotiterplatte abgegeben und anschließend die Absorption gemessen und analysiert. Danach muss das System von dem Farbstoff gesäubert werden. Diese Wartung ist somit aufwendig und kann nicht jede Woche durchgeführt werden. Der ML Star besitzt jedoch die Fähigkeit die Höhe der Flüssigkeit innerhalb der *Wells* durch die cLLD zu bestimmen. Dementsprechend wurde unter Anwendung dieser Technik ein Wartungsprogramm für die Aspirations- und Dispensierungsnadeln entwickelt.

Im Folgenden der Ablauf dieser Wartungsmethode:

1. Mikrotiterplatte wird zum Washer transportiert und im Washer mit Puffer gefüllt (Test der Dispensierungsnadeln)
2. Mikrotiterplatte wird auf das Deck des ML Stars gesetzt und der Flüssigkeitsstand in 96 *Wells* für jede der 96 Washernadeln ein Well über die cLLD bestimmt
3. Mikrotiterplatte wird zum Washer transportiert und im Washer leer aspiriert (Test der Aspirationsnadeln)
4. Mikrotiterplatte wird auf das Deck des ML Stars gesetzt und wieder der Flüssigkeitsstand in 96 *Wells* über die cLLD bestimmt
5. Excel-Datei mit den Werten der vorher bestimmten Flüssigkeitsstände für die Aspirations- und Dispensierungsnadeln an den 96 Positionen der Mikrotiterplatte wird erstellt

Wenn der Flüssigkeitsstand in einem der 96 *Wells* zu stark abweicht, ist das ein Hinweis darauf, dass die Nadel an dieser Position verstopft sein könnte: Bei einer verstopften Dispensierungsnadeln wäre der Flüssigkeitsstand niedriger als in den anderen *Wells*, bei einer verstopften Aspirationsnadel höher. Da die so bestimmten Füllstände jedoch eine gewisse Variabilität über die gesamte Mikrotiterplatte aufweisen, wurden noch keine Richtwerte festgelegt, die in dieser Wartungsmethode erreicht werden müssen, um den Washer als voll funktionsfähig einstufen zu können. Falls der Flüssigkeitsstand nach der Dispensierung sehr nahe am Boden des Mikrotiterplatte bestimmt wird, ist dies ein eindeutiger Hinweis auf eine Verstopfung der entsprechenden Dispensierungsnadel. Der Ablauf der gesamten Wartungsmethode dauert ca. 20 Minuten und ist mit wenig Aufwand verbunden. Demzufolge kann der Washer ohne Einsatz von gefärbtem Wasser und hohem Zeitaufwand gewartet werden.

2.3 Ablauf des sFIDA-Assays

Im Folgenden wird der Ablauf des sFIDA-Assays unter Verwendung des Microlab Star und des BioTek Microplate Washer 405 Select LS im Detail beschrieben.

Der Anwender bereitet zunächst das Deck des ML Stars und die benötigten Puffer für den Washer vor. Danach wird die ML Star Methode *sFIDA-Greiner-Standard-Method* aufgerufen und die Anzahl Platten und weitere Nutzereingaben über

die Excel-Datei an den ML Star übergeben (siehe Abschnitt 2.2.6). Im Abschnitt A.2 ist die gesamte Implementierung der ML Star Methode hinterlegt.

In der Abbildung 2.21 werden die ersten Schritte gezeigt, die vor der Übernacht-Inkubation von Ethanolamin erfolgen: Der ML Star verteilt durch Aliquotierung je 100 µl 5 M Natriumhydroxid (NaOH) in die benötigte Anzahl *Wells* der Mikrotiterplatte im 384-*Well*-Format. Das 5 M NaOH wurde zuvor in einem 50 ml Behälter auf dem Deck (erste Position von außen) bereitgestellt. Nach einer Inkubationszeit von 15 Minuten wird die Mikrotiterplatte an den Washer übergeben und das Waschprotokoll mit dreimal Wasser (Puffer D) aufgerufen. Danach erfolgt die Aliquotierung von 1 M Salzsäure (HCl) aus einem 50 ml Behälter (zweite Position von außen). Es werden je 100 µl 1 M HCl in jedes *Well* aliquotiert und 15 Minuten inkubiert. Nach Ablauf der Inkubationszeit erfolgt erneut das dreimalige Waschen mit Wasser, anschließend ein Waschschritt mit 70% Ethanol (zweimal) im Washer. Bei jedem Flüssigkeitswechsel ist es nötig den Washer mit 300 ml der als nächstes verwendeten Flüssigkeit zu *primen*, sodass Reste der Flüssigkeit aus dem vorangegangene Schritt aus dem Washer-System entfernt werden.

Die Lösung aus Ethanolamin und Dimethylsulfoxid (DMSO) wird hergestellt und in der 12. Spalte des großen Reservoirs bereitgestellt. Es werden je 45 µl in jedes *Well* gegeben, wenn die Mikrotiterplatte getrocknet ist.

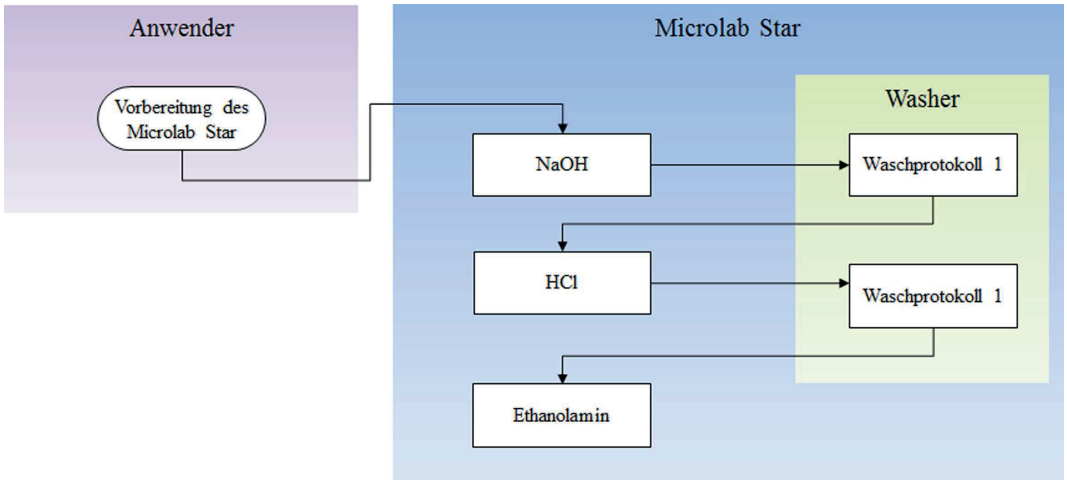

Abbildung 2.21: Ablauf des sFIDA-Assays am ersten Tag im Microlab Star
Am ersten Tag des sFIDA-Assays wird die Mikrotiterplatte mit NaOH und HCl gesäubert und entsprechende Waschprotokolle zur Entfernung der Reagenzien aus den Wells werden im Washer durchgeführt. Schließlich erfolgt nach dem letzten Waschprotokoll und der Trocknung der Mikrotiterplatte, die Inkubation von Ethanolamin/DMSO über Nacht.

Nach der Übernacht-Inkubation von Ethanolamin/DMSO in den Wells folgt der zweite Tag des sFIDA-Assays. Die Abbildung 2.22 verdeutlicht die einzelne Schritte. Der Anwender bereitet das Deck für den zweiten Assay-Tag vor; die Reagenzien

werden zu gegebenem Zeitpunkt frisch für jeden Schritt angesetzt und füllt diese in die vorhergesehene Behälter und setzt diese an die vorhergesehene Positionen.

Die folgenden Waschschritte werden im ML Star durchgeführt, da die verwendeten Reagenzien unverdünnt außerhalb der Richtlinien zur Verwendung im Washer liegen. Der ML Star nimmt das Ethanolamin/DMSO ab und aliquotiert je 80 µl DMSO aus einem 50 ml Behälter (dritte Position von außen) auf die Mikrotiterplatte. Bevor das DMSO wieder durch den ML Star aus den *Wells* entfernt wird, wird die Flüssigkeit zehnmal durch die Spitzen hoch und runter pipettiert, um sie gut zu durchmischen. Dieser Vorgang wird dreimal wiederholt, um das Ethanolamin vollständig aus den *Wells* zu entfernen. Danach wird absolutes Ethanol in einem 120 ml Behälter (erste Position von außen) bereitgestellt und hiermit fünfmal im selben Verfahren wie zuvor mit dem DMSO. Nach dem letzten Waschschritt wird das Ethanol entfernt und die Platte bei Raumtemperatur getrocknet.

Nachdem die Mikrotiterplatte getrocknet ist, wird das Polyethylenglycol (PEG) mit einer Konzentration von 2 mM in DMSO angesetzt und bei 70 $°C$ gelöst. Die angesetzte Lösung wird in der ersten Spalte des kleine Reservoirs bereitgestellt. Es erfolgt die Aliquotierung von 15 µl PEG in jedes *Well* und eine Inkubation von einer Stunde. Die Mikrotiterplatte wird in den Washer transportiert und das Waschprotokoll mit dreimal Wasser wird durchgeführt. Danach erfolgt das Ansetzen einer Lösung bestehend aus 1-Ethyl-3-(3-dimethylaminopropyl)carbodiimid (EDC) und N-Hydroxysuccinimid (NHS) in 2-(N-Morpholino)ethansulfonsäure (MES) (0,1 M und pH-Wert 4,7) durch den Anwender. Die EDC/NHS-Lösung wird in der ersten Spalte des großen Reservoirs vorgelegt und durch den ML Star 30 µl in jedes *Well* pipettiert. Nach 30 Minuten wäscht der Washer dreimal mit MES und parallel werden die Fänger-Antikörper mit der Endkonzentration von 10 ng/µl in phosphatgepufferte Salzlösung (PBS) vorbereitet und 10 Minuten bei 18000 g zentrifugiert. Die hergestellte Fänger-Antikörper-Lösung wird in der zweiten Spalte des kleine Reservoirs für das Pipettieren bereitgestellt. Es werden je 15 µl in die *Wells* der Mikrotiterplatte aliquotiert. Nach einer Stunde Inkubation wäscht der Washer dreimal mit PBS mit 0,05% Tween (PBS-T) und dreimal mit PBS und zieht anschließend die *Wells* leer.

Die SMART-Block Lösung wird in der zweiten Spalten des großen Reservoirs vorgelegt und je 50 µl in jedes *Well* auf die Mikrotiterplatte verteilt. Darauf folgt eine Inkubation von einer Stunde. Danach wird das Waschprotokoll mit dreimal PBS-T und dreimal PBS im Washer aufgerufen, diesmal wird aber das letzte Aspirieren nicht durchgeführt, sodass ca. 80 µl PBS in jedem *Well* der Mikrotiterplatte zurück bleiben.

Im ML Star werden zunächst die Konzentrationsreihen von Standardmolekülen erstellt. Es können maximal drei unterschiedliche Standardmoleküle mit jeweils bis zu acht Konzentrationen pro Experiment eingesetzt werden. Die ML Star Methode erhält durch die Eingabe aus der Excel-Datei die Informationen wie viele und welche Konzentrationen in jeder Konzentrationsreihe enthalten sind. Zunächst wird der Puffer, bspw. PBS, in einem 120 ml Behälter (zweite Position von außen) bereitgestellt und auf die Mikroreaktionsgefäße für die Konzentrationsreihe verteilt. Hierbei nimmt jeder Pipettierkanal ein individuelles Volumen auf, sodass unterschiedliche Verdünnungsschritte möglich sind. Im nächsten Schritt wird aus einem Mikroreatkionsgefäß, das die Stocklösung der Standardmoleküle enthält, das Volumen aufgenommen, um die benötigte Endkonzentration in der ersten Verdünnung zu erhalten. Danach wird seriell die Konzentrationsreihe erstellt und der Vorgang für eventuelle weitere Konzentrationsreihen wiederholt.

Nachdem die benötigten Konzentrationsreihen erstellt worden sind und der Anwender die benötigten biologische Proben in die Mikroreaktionsgefäß-Adapter gesetzt hat, erfolgt die Verteilung der Proben mit je 15 µl in ein *Well* der Mikrotiterplatte. Hierbei erfolgt erst eine Aspiration des Puffers von acht *Wells* von der Mikrotiterplatte, um die *Wells* zu leeren. Danach findet ein Pipettenspitzen-Wechsel statt und jede Pipettenspitze (50 µl Maximalvolumen) nimmt einzeln unterschiedliche Proben mit 15 µl auf. Die Abgabe in die vorher geleerten *Wells* erfolgt mit allen acht Pipettierkanälen gleichzeitig auf die Mikrotiterplatte. Diese Art der Prozessierung bietet genügend Flexibilität, um Proben zufällig auf der Mikrotiterplatte zu verteilen. Nach einer Übernachtinkubation oder einer Inkubationszeit von zwei Stunden wird dreimal mit PBS-T und dreimal mit PBS gewaschen. Bei der letzten Aspiration ist die z-Höhe so angepasst, dass ca. 10 µl in jedem *Well* zurück bleiben.

Die beiden Antikörper zur Detektion werden in PBS mit einer Endkonzentration von jeweils 1,87 ng/ml in PBS angesetzt und eine Stunde bei 100000 g und 4 $^{\circ}C$ zentrifugiert. Der Überstand wird in die dritte Spalte des kleinen Reservoirs vorgelegt und durch Aliquotierung je 20 µl/*Well* auf der Mikrotiterplatte verteilt. Die Abgabe der Detektions-Antikörper erfolgt ca. 5 mm über dem Plattenboden, sodass die Pipettenspitzen nicht kontaminiert werden und weiter verwendet werden können. Nach einer Inkubationszeit von einer Stunde wird fünfmal mit PBS-T und fünfmal mit PBS im Washer gewaschen; nach dem letzten Waschschritt verbleiben ca. 10 µl PBS in jedem *Well*. Danach wird Wasser mit 2 mM Natriumazid in einem 50 ml Behälter (fünfte Position von außen) auf dem Deck bereitgestellt. Es werden 80 µl/*Well* auf die Mikrotiterplatte aliquotiert und wie bei den Detektions-Antikörper wird die Abgabe weit über dem Boden der Mikrotiterplatten stattfinden, sodass

kein Pipettenspitzen-Wechsel stattfinden muss.

Die ML Star Methode zur Durchführung des sFIDA-Experiments ist damit am Ende und eine Benachrichtigung wird per E-Mail an den Anwender verschickt. Zusätzlich erscheint ein Dialog, dass das Experiment beendet ist.

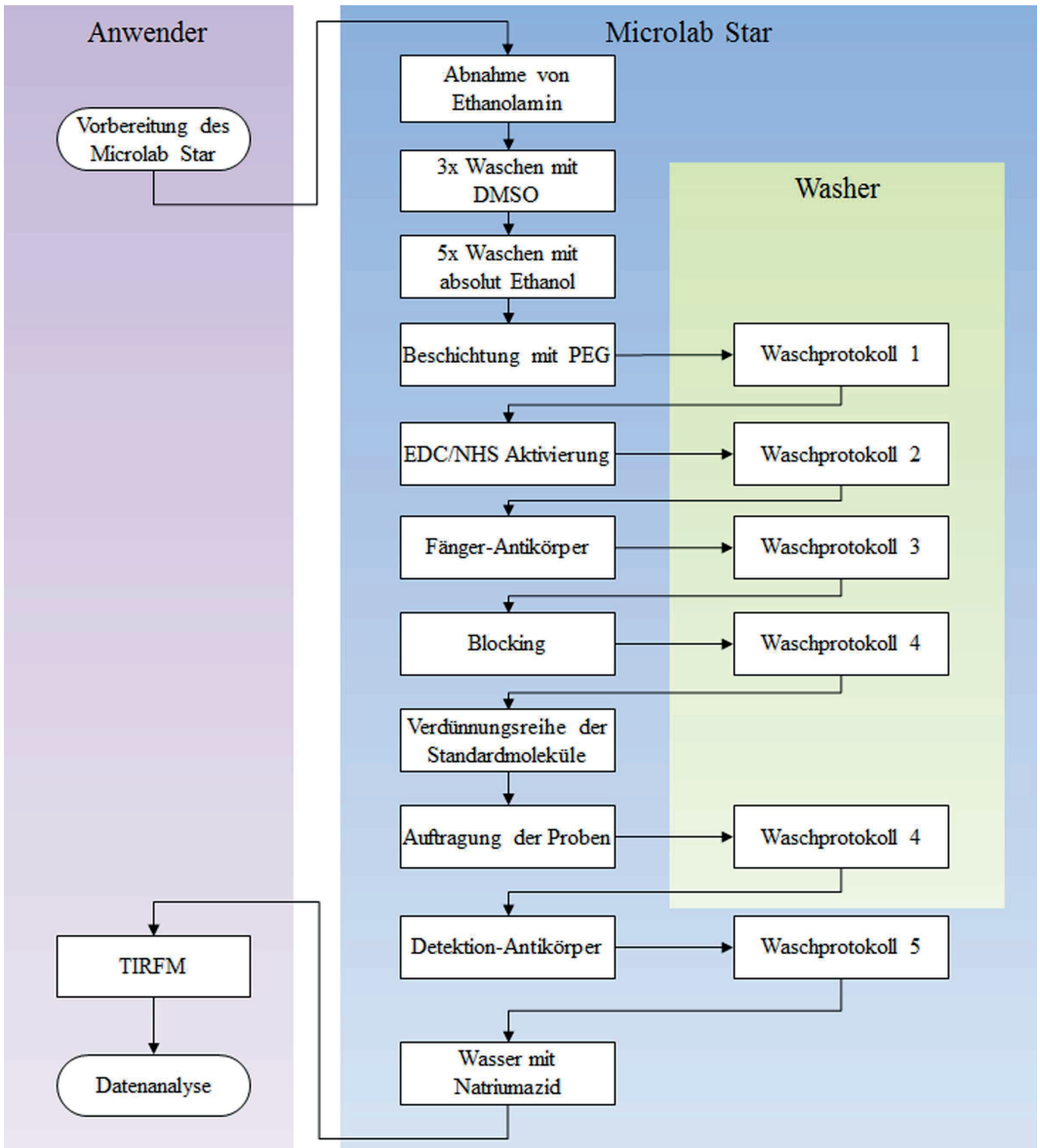

Abbildung 2.22: Ablauf des sFIDA-Assays am zweiten Tag im Microlab Star
Am zweiten Tag des sFIDA-Assays wird das Ethanolamin/DMSO abgenommen und die *Wells* mit DMSO und Ethanol absolut im ML Star gewaschen. Im Folgenden werden die einzelnen Reagenzien zur Funktionalisierung und Aktivierung der Oberfläche und zur Bindung von Fänger-Antikörpern auf der Glasoberfläche durch den ML Star auf die Mikrotiterplatte aliquotiert. Dazwischen erfolgen entsprechende Waschprotokolle im Washer. Schließlich werden die Proben aufgetragen und nach der Inkubationszeit herunter gewaschen. Anschließend werden die Detektions-Antikörper auf die Mikrotiterplatte verteilt. Nach dem letzten Waschprotokoll im Washer, wird der Puffer gegen Wasser mit Natriumazid ausgetauscht. Schließlich erfolgt die Erfassung der Daten am TIRFM und die Analyse der Bilddaten.

2.3.1 Umsetzung des sFIDA-Assays im Microlab Star

Der Ablauf des sFIDA-Assays im ML Star unter Verwendung des Washers wurde in Abschnitt 2.3 im Detail beschrieben. Im folgenden wird der Zeitaufwand und der Materialverbrauch des sFIDA-Assays unter dem Aspekt der Automatisierung genauer untersucht. Dabei dienen im Rahmen dieser Arbeit durchgeführte sFIDA-Assays als Beispiele.

2.3.1.1 Zeitlicher Aufwand

In den folgenden zwei Tabellen 2.1 und 2.2 werden alle Schritte des sFIDA-Assays und die benötigte Zeit aufgeführt. Die aufgeführten Waschprotokolle mit dem Washer beinhalten zusätzlich die benötigte Zeit für den Mikrotiterplatten-Transport vom und zum ML Star. In den Schritten in denen kein Waschprotokoll erwähnt wird, pipettiert der ML Star mit den acht Pipettierkanälen auf die Mikrotiterplatte oder bereitet die Konzentrationsreihen der Standardmoleküle mit einzelnen Kanälen vor. Am Ende werden die Inkubationszeiten und die Zeit zum Trocknen der Mikrotiterplatte hinzugerechnet. Dementsprechend wird der Zeitaufwand für jeden Tage des sFIDA-Assays bestimmt. Der Zeitaufwand im ML Star ist abhängig von der

Tabelle 2.1: Zeitaufwand im Microlab Star am ersten Tag des sFIDA-Assays
Die benötigte Zeit der einzelnen Pipettierschritte und Waschschritte im Washer sind aufgelistet. Es wurden 272 *Wells* der Mikrotiterplatte im ML Star pipettiert und die gesamten 384 *Wells* wurden im Washer gewaschen. Hinzukommen die Inkubationszeiten (NaOH und HCl inkubieren jeweils 15 Minuten) und die Wartezeit zum Trocknen der Platte nachdem Waschschritt mit 70% Ethanol. Bei Verwendung des zweiten Waschprotokolls im Washer muss der Abfallbehälter gewechselt werden, sodass der Abfall vom 70% Ethanol separat aufgefangen werden kann. Dabei kann eine längere Pause entstehen. Das sFIDA-Assay am ersten Tag dauert insgesamt circa 4 Stunden im ML Star.

Schritt	Zeit
NaOH	4,86 min.
Waschprotokoll mit 3x Wasser	5,76 min.
HCl	5,06 min.
Waschprotokoll mit 3x Wasser und 2x 70% Ethanol	10,77 min.
Ethanolamin	12,28 min.
Inkubationszeiten (ohne Übernacht)	30 min.
Trocknung der Mikrotiterplatte	150 min.
Summe	3,65 Std.

Anzahl der *Wells* auf der Mikrotiterplatte. Besonders in dem Schritt der Probenverteilung auf die Mikrotiterplatte ist der Zeitaufwand hoch, da nach jedem Pipettierschritt ein Pipettenspitzen-Wechsel statt finden muss und die Aufnahme von Proben einzeln erfolgen muss, damit die Proben zufällig auf der Mikrotiterplatte

Tabelle 2.2: Zeitaufwand im Microlab Star am zweiten Tag des sFIDA-Assays
Die benötigten Zeiten der einzelnen Pipettierschritte und Waschschritte im Washer sind aufgelistet. Es wurde 256 *Wells* der Mikrotiterplatte im ML Star pipettiert und die gesamten 384 *Wells* wurden im Washer gewaschen. Das sFIDA-Assay am zweiten Tag dauert circa 11 Stunden und 38 Minuten im ML Star.

Schritt	Zeit
Entfernen von Ethanolamin	12,35 min.
Waschschritt im ML Star mit 1x DMSO	20,43 min.
Waschschritt im ML Star mit 5x Ethanol absolut	85,88 min.
Beschichtung mit PEG	3,36 min.
Waschprotokoll mit 3x Wasser	5,78 min.
EDC/NHS Aktivierung	5,06 min.
Waschprotokoll mit 3x MES	5,36 min.
Auftragung der Fänger-Antikörper	3,42 min.
Waschprotokoll mit 3x PBS-T und 3x PBS	9,11 min.
Auftragung von Blocking-Lösung	9,08 min.
Waschprotokoll mit 3x PBS-T und 3x PBS	9,08 min.
Vorbereitung von drei Konzentrationsreihen	20,52 min.
Auftragung der Proben	79,14 min.
Waschprotokoll mit 3x PBS-T und 3x PBS	9,01 min.
Auftragung Detektions-Antikörper	4,12 min.
Waschprotokoll mit 5x PBS-T und 5x PBS	12,3 min.
Auftragung von Wasser mit Natriumazid	6,17 min.
Inkubationszeiten	390 min.
Trocknung der Mikrotiterplatte	150 min.
Summe	11,38 Std.

verteilt werden können. Die Aliquotierungsschritte über die genutzten *Wells* brauchen in der Regel vier bis sechs Minuten. Die Variation in der Zeitspanne kommt dadurch zu Stande, dass je nach Aliquotierungsschritt unterschiedliche Volumina in den *Wells* vorliegen sollen und mit unterschiedlichen Pipettenspitzen gearbeitet wird. Zusätzlich wurden am ersten Tag 272 *Wells* vorbereitet und am zweiten Tag nur noch 256 prozessiert.

Der Zeitaufwand im Washer wächst mit der Anzahl an Waschzyklen und wie oft ein Pufferwechsel statt finden muss, da bei Pufferwechseln immer erst ein sogenannter *Prime*-Schritt erfolgen muss, damit im Waschzyklus der entsprechende Puffer unverdünnt im System vorliegt. Trotzdem erleichtert und reduziert der Washer den Aufwand beim Waschen von Mikrotiterplatten im 384-*Well* Format durch die parallele Verwendung von 96 Aspirations- und 96 Dispensierungsnadeln.

2.3.1.2 Materialverbrauch im Microlab Star

Im Folgenden werden die Verbrauchsmaterialien aufgeführt. Dabei wird zwischen wiederverwendbarem Material und dem Material, das nach Verwendung entsorgt

werden muss, unterschieden. Die folgenden Materialien sind für den einmaligen Gebrauch:

- drei Mikrotiterplatten (Versuchsplatte, Funktion als Deckel und für die Erstabgabe bei der Aliquotierung)
- 30 Mikroreaktionsgefäße (1,5 ml für Proben)
- 10 Mikroreaktionsgefäße (1,5 ml Antikörper, EDC NHS)
- sechs Mikroreaktionsgefäße für die UZ (1,5 ml)
- fünf Mikroreaktionsgefäße (2 ml)
- zwei 15 ml Reaktionsgefäß
- 90 1000 µl Pipettenspitzen
- 316 300 µl Pipettenspitzen
- 256 50 µl Pipettenspitzen

Die folgenden Behälter können gespült und autoklaviert werden, sodass sie für mehrere Versuche verwendet werden können:

- ein kleines Reservoir mit zwei Kammern pro Spalte und Maximalvolumina von je 3,5 ml
- ein großes Reservoir mit Maximalvolumina von 21 ml pro Spalte
- drei 120 ml Behälter
- vier 50 ml Behälter

3. Publizierte Ergebnisse

3.1 Application of an Amyloid-β Oligomer Standard in the sFIDA Assay

Autoren: Katja Kühbach, Maren Hülsemann, Yvonne Herrmann, Kateryna Kravchenko, Andreas Kulawik, Christina Linnartz, Luriano Peters, Kun Wang, Johannes Willbold, Dieter Willbold and Oliver Bannach

Publiziert in: Frontiers in Neuroscience (Open Access (Kühbach et al., 2016))

DOI: https:\\doi.org\10.3389\fnins.2016.00008

Impact Factor (2015): 3.398

Eigener Anteil: 15%

Mitentwicklung der experimentellen Details des sFIDA-Ablaufes, Unterstützung bei der Auswertung des sFIDA-Assays und Unterstützung beim Schreiben des Manuskripts

frontiers in Neuroscience

TECHNOLOGY REPORT
published: 29 January 2016
doi: 10.3389/fnins.2016.00008

Application of an Amyloid Beta Oligomer Standard in the sFIDA Assay

*Katja Kühbach[1], Maren Hülsemann[1], Yvonne Herrmann[1], Kateryna Kravchenko[1], Andreas Kulawik[1], Christina Linnartz[1], Luriano Peters[1], Kun Wang[1], Johannes Willbold[1], Dieter Willbold[1,2] and Oliver Bannach[1,2]**

[1] ICS-6 Structural Biochemistry, Forschungszentrum Jülich GmbH, Jülich, Germany, [2] Institut für Physikalische Biologie, Heinrich-Heine-Universität Düsseldorf, Düsseldorf, Germany

Still, there is need for significant improvements in reliable and accurate diagnosis for Alzheimer's disease (AD) at early stages. It is widely accepted that changes in the concentration and conformation of amyloid-β (Aβ) appear several years before the onset of first symptoms of cognitive impairment in AD patients. Because Aβ oligomers are possibly the major toxic species in AD, they are a promising biomarker candidate for the early diagnosis of the disease. To date, a variety of oligomer-specific assays have been developed, many of them ELISAs. Here, we demonstrate the sFIDA assay, a technology highly specific for Aβ oligomers developed toward single particle sensitivity. By spiking stabilized Aβ oligomers to buffer and to body fluids from control donors, we show that the sFIDA readout correlates with the applied concentration of stabilized oligomers diluted in buffer, cerebrospinal fluid (CSF), and blood plasma over several orders of magnitude. The lower limit of detection was calculated to be 22 fM of stabilized oligomers diluted in PBS, 18 fM in CSF, and 14 fM in blood plasma.

Keywords: Alzheimer's disease, amyloid-β peptide, diagnostic biomarker, early diagnosis, sFIDA, surface-based fluorescence intensity distribution analysis, stabilized oligomers, standard molecule

OPEN ACCESS

Edited by:
Charlotte Elisabeth Teunissen, VU University Medical Center Amsterdam, Netherlands

Reviewed by:
Xifei Yang, Shenzhen Center for Disease Control and Prevention, China
Mary Josephine Savage, Merck and Company, USA

***Correspondence:**
Oliver Bannach
o.bannach@fz-juelich.de

Specialty section:
This article was submitted to Neurodegeneration, a section of the journal Frontiers in Neuroscience

Received: *10 November 2015*
Accepted: *11 January 2016*
Published: *29 January 2016*

Citation:
Kühbach K, Hülsemann M, Herrmann Y, Kravchenko K, Kulawik A, Linnartz C, Peters L, Wang K, Willbold J, Willbold D and Bannach O (2016) Application of an Amyloid Beta Oligomer Standard in the sFIDA Assay. Front. Neurosci. 10:8. doi: 10.3389/fnins.2016.00008

INTRODUCTION

Worldwide 5–7% of people older than 60 years are affected by dementia, with Alzheimer's disease (AD) being the most common type. Due to the aging population, the total number of demented people is predicted to increase even further (Prince et al., 2013). There is neither a cure nor a sufficiently reliable laboratory diagnostic test available for this fatal neurodegenerative disease (Lansdall, 2014). Early diagnosis of AD, however, is of great importance for the development of therapeutics and their future application at an early stage of the disease. It is believed that AD can be treated most effectively in preclinical stages, before cognitive functions become impaired and neurons and synapses are damaged irreversibly (Golde et al., 2011). Hitherto, the definitive diagnosis can only be made after the patients' death based on neuropathological hallmarks, like amyloid plaques, neurodegeneration and neurofibrillary tangles (Ballard et al., 2011).

The main component of amyloid plaques is amyloid β peptide (Aβ), which is formed from the amyloid precursor protein (APP) by β- and γ-secretases (Haass et al., 2012). Once released from the precursor, the Aβ peptide is prone to aggregation and can assemble into oligomeric structures and amyloid fibrils. It is widely accepted that soluble Aβ oligomers but not monomers are highly neurotoxic and that the pathological process in AD starts already years before the onset of clinical manifestation (Braak and Braak, 1991; McLean et al., 1999; Cleary et al., 2004; Lesné et al., 2006).

Currently, the total concentration of $A\beta_{42}$ in cerebrospinal fluid (CSF), which is lower in AD patients compared to healthy persons (Sunderland et al., 2003; Shaw et al., 2009), is used as a biomarker in clinical trials or academic settings to increase the accuracy of AD diagnosis. At the current stage of biomarker development, however, the total concentration of $A\beta_{42}$ in CSF, even in combination with other biomarkers such as tau protein, does not allow a clear distinction of AD patients from healthy controls or patients with other dementias (Humpel, 2011). Therefore, the development of more accurate biomarkers is of utmost importance.

Since Aβ oligomeric species are known to be directly involved in AD pathology or even to trigger the disease (Haass and Selkoe, 2007), Aβ oligomers are considered as promising biomarker for AD (Blennow et al., 2010). The main challenges for Aβ oligomer-based diagnostics in body fluids are the presumably very low concentrations of Aβ oligomers and the high background of monomeric Aβ (Rosén et al., 2013). To meet those requirements, we have previously developed an assay called sFIDA (surface-based fluorescence intensity distribution analysis; Birkmann et al., 2007; Funke et al., 2007, 2010; Bannach et al., 2012). The principle of sFIDA is illustrated in **Figure 1**. The biochemical setup of sFIDA resembles a conventional sandwich ELISA. All Aβ species are immobilized on a functionalized glass surface via Aβ-specific capture antibodies. After immobilization, Aβ aggregates are multiply loaded by at least two detection antibodies, each of them labeled with a different fluorochrome. Because capture and detection antibodies recognize the same or an overlapping epitope on Aβ, Aβ monomers cannot bind any detection antibodies while bound to the capture antibody. In contrast to a classical ELISA, the result of the measurement is not a single readout for the whole sample. Instead, the surface is imaged by high-resolution fluorescence microscopy, such as dual-color total internal reflection fluorescence microscopy (TIRFM). Only those pixels that show signal intensities above the background noise in both channels are counted. Thus, the number of colocalized pixels above the background noise is expected to correlate with the concentration of Aβ oligomers in the sample.

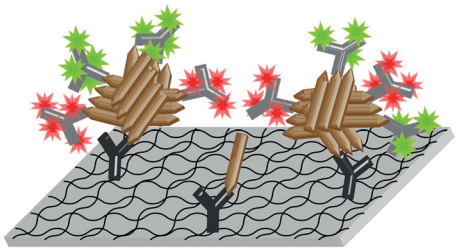

FIGURE 1 | Scheme of the sFIDA assay. Aβ-specific capture antibodies (dark gray Y symbols) are immobilized on a functionalized glass surface. Aβ oligomers (brown rods) present in the sample bind to the capture antibodies and are detected by fluorescence labeled (colored stars) anti-Aβ-antibodies (light gray Y symbols). The surface is then imaged by dual-color microscopy. In this version of the assay, all three of the applied antibodies (one capture and two different detection antibodies labeled with two different fluorochromes) bind to overlapping epitopes at the N-terminus of Aβ, which corresponds to the spiky ends of the brown rods in the scheme above. Thereby, only oligomers with multiple epitopes, but not monomers, are able to bind detection antibodies while bound to the capture and thus yield detectable signals.

Results showing increased sFIDA readouts for AD patients compared to non-demented controls have been reported previously (Wang-Dietrich et al., 2013). However, in this study no reliable Aβ oligomer standard was available to determine absolute concentrations from the assay readout. Due to both the dynamic aggregation and dissociation of Aβ, non-stabilized oligomers are not suited as standard in oligomer-based diagnostic assays.

Here, we demonstrate application of stabilized Aβ oligomers as standard molecules in the sFIDA assay. The sFIDA readout correlates with the applied oligomer concentration over five magnitudes down to a femtomolar range, which will allow the quantification of natural Aβ oligomer concentrations in body fluids.

MATERIALS AND METHODS

Biological Samples and PBS Spiked with Stabilized Oligomers

Four individual human EDTA-anticoagulated plasma samples (Zen-Bio, Research Triangle Park, USA) and one pooled human EDTA-anticoagulated plasma sample from three healthy donors were centrifuged for 15 min at 15,000 × *g*. The supernatant was collected and equal volumes from each sample were combined to obtain one large pool from several donors (from here on referred to as "plasma fraction"). Human cerebrospinal fluid sample (CSF; pooled from healthy donors/mixed gender) was purchased from Biochemed (Winchester, USA). Stabilized Aβ oligomers (Crossbeta Biosciences B.V., Utrecht, the Netherlands), from here on called "oligomers", were serially diluted from the stock solution (10 nM) to concentrations of 1 nM, 100 pM, 10 pM, 1 pM, 100 fM, 10 fM, and 1 fM in PBS (GE Healthcare, Chalfont St. Giles, UK), CSF or the plasma fraction as described above. All concentrations of Aβ oligomers in this publication refer to oligomer particle concentrations, if not stated otherwise. The oligomers consist of approximately 220 $A\beta_{1-42}$ monomers (manufacturer's data); further characterization of the stabilized oligomers, including data on the size homogeneity and stability, are available on the manufacturer's homepage (Crossbeta Biosciences, 2015).

sFIDA

Plate Preparation

384-well plates (SensoPlate Plus with 175 µm glass bottom; Greiner Bio-One, Kremsmünster, Austria) were used for sFIDA. Functionalization of the glass surface was performed as previously described in Janissen et al. (2009). The surface was treated with 5 M NaOH (AppliChem, Darmstadt, Germany) for 15 min, washed three times with water, neutralized with 1 M HCl (AppliChem, Darmstadt, Germany; 15 min), washed again three times with water and then twice with 70% ethanol (VWR International, Langenfeld, Germany). After drying the plate at room temperature, the wells were incubated in

10 M ethanolamine in DMSO (Sigma-Aldrich, St. Louis, USA) overnight. Afterwards, the wells were washed three times with DMSO, twice with 70% ethanol and the plate was dried again at room temperature. A solution of 50 mM SC-PEG-CM (MW 5000 Da, Laysan Bio, Arab, USA) in DMSO was heated shortly to 70°C until the PEG dissolved. After the solution cooled down, 2% (v/v) triethylamin (Fluka, Buchs, Switzerland) were added, the solution was quickly vortexed and 15 µl were applied per well. After an incubation time of 1 h the wells were washed five times with water.

The carboxymethyl groups of SC-PEG-CM on the glass surface were then activated by addition of 30 µl of 100 mM EDC (Fluka, Buchs, Switzerland)/100 mM NHS (Aldrich, Milwaukee, USA) in 0.1 M MES buffer, pH 3.5 (AppliChem) per well for 30 min. After flushing the wells three times quickly with MES buffer, 15 µl of 10 ng/µl capture antibody Nab228 in PBS (the supernatant after centrifuging 10 min at 18,000 g) was added to the surface. After incubating for 90 min, unbound antibody was removed and wells were washed three times with PBST (PBS + 0.05% Tween20, AppliChem Panreac, Darmstadt, Germany) and three times with PBS. Then 50 µl of blocking solution (SmartBlock, CANDOR Biosciences, Wangen, Germany) per well were incubated for 1 h. After washing the wells three times with PBST and three times with PBS, 15 µl sample was applied to each well and incubated overnight. The wells were washed once with PBST and twice with PBS. The detection antibodies 6E10 labeled with Alexa Fluor 488 (Covance, Princeton, USA) and Nab228 labeled with Alexa Fluor 647 (Santa Cruz, Dallas, USA) were combined to each 1.25 µg/ml in PBS and centrifuged for 1 h (100,000 g, 4°C). The supernatant was mixed and added to the wells (15 µl/well, 1 h). Finally, the wells were washed once with PBST and twice with PBS. The buffer was removed and 100 µl of water were applied to each well for image acquisition on TIRFM (AM TIRF MC, Leica microsystems, Wetzlar, Germany).

Image Data Acquisition

Using TIRF microscopy, 25 positions per well were imaged in two different channels (14 bit gray scale; channel 0: excitation at 635 nm, emission filter 705/72 nm; channel 1: excitation at 488 nm, emission filter 525/36 nm). Each image contains 1000 × 1000 pixels and represents an area of 116 × 116 µm. In total, 3.15% of the well surface was imaged.

Image Data Analysis

Prior to data analysis, images showing inhomogeneous surfaces, e.g., due to mechanical damage of the surface or impurities, were excluded from the analysis by automated artifact detection, which is briefly described in the following: Each original image was converted to a binary image by replacing all pixels having intensities above or equal the mean pixel intensity of the regarding image plus one standard deviation with the number one, all others with the number zero. In the next step, erosion was applied to these binary images by using a rectangular structuring element with a size of 31 × 31 pixels. After erosion, the binary image was dilated using the same structuring element as for erosion. Each cluster that consisted of connected pixels with the intensity one in the binary image after dilatation was then analyzed in the original image. Clusters showing either a mean pixel intensity of above 4000, a standard deviation of pixel intensities above 2800, or a skewness of <0 in the original images were defined as artificial and the whole image was excluded from the analysis. Images that had a mean pixel intensity of 16,383 over the whole image in at least one channel were included for image analysis although they were excluded by the artifact detection, because those images are estimated as being saturated, but not artificial.

To account for inhomogeneous illumination, only the central "region of interest" containing 500 × 500 pixels of each image were used for further analysis.

The remaining images were analyzed for colocalization: For both channels, intensity cutoffs for exclusion of background signal were determined. As the background signal might differ from one matrix (i.e., PBS, CSF, and plasma fraction) to another, the cutoff values were determined for each matrix individually, but—in order to compare sFIDA readouts achieved by diluting oligomers in the different matrices—in a reliable and unbiased way. The cutoff for each channel and each matrix was determined from the unspiked control sample to be the value, which is exceeded by only 0.01% of total image pixels. This value represents a reasonable compromise between efficient background removal and retention of assay sensitivity. For cutoffs used in this study, see **Table 1**.

Colocalized pixels with intensity values above the cutoffs in both channels were counted for each image. The number of colocalized pixels was determined for each picture and the average pixel count from all pictures from the same sample was referred to as "sFIDA readout". Please note that the sFIDA readout cannot exceed 250,000, which corresponds to the total number of pixels per analyzed image section.

Calculation of Calibration Curves

For the calibration of assay readout (number of colocalized pixels) to molecule concentration a weighted linear regression analysis was performed with Matlab (The MathWorks, Natick, USA) from experimental data points within the linear detection range (CSF: 100 pM to 10 fM; PBS: 10 pM to 10 fM; plasma fraction: 10 pM to 10 fM) with respective weights calculated as 1/readout. In cases of readout = 0 the weight was determined as 1.

Statistics

In order to statistically assess differences between sFIDA readouts of different concentrations of oligomers diluted in the same matrix, two-way omnibus Kruskal-Wallis test was used for comparison of more than two groups. *Post-hoc*

TABLE 1 | Cutoffs for the different body fluids.

Matrix	Cutoff channel 635 nm	Cutoff channel 488 nm
CSF	3268	2339
PBS	4082	2773
Plasma fraction	4259	2028

Cutoffs were obtained for each channel and matrix by allowing only 0.01% of all pixels to be above background signal for negative controls.

analysis was performed by using two-tailed Mann-Whitney-U test and *p*-value adjustment according to Benjamini and Hochberg (1995) in order to account for multiple testing. By Mann-Whitney-U test, sFIDA readouts from each concentration were compared to the next lower one. Additionally, sFIDA readouts from blank samples were compared to readouts from 10 to 100 fM. The false discovery rate controlling procedure after Benjamini and Hochberg was calculated for 0.05 (for significant results, indicated with *) and 0.01 (for very significant results, indicated with **). Kruskal-Wallis and Mann-Whitney-U test were calculated using the statistical software Origin (OriginLab Corporation, Northampton, USA), false discovery rate controlling procedure after Benjamini and Hochberg was calculated in Microsoft Excel (Microsoft Corporation, Redmond, USA).

RESULTS

Detection of Stabilized Oligomers by sFIDA

In a first set of experiments we sought to find out if the stabilized oligomers can be sensitively detected by the sFIDA assay. Therefore, a log10 dilution series of oligomers in PBS with concentrations ranging from 1 nM to 1 fM was subjected to sFIDA analysis in quadruplicate determination. As can be seen in **Figure 2**, the sFIDA readout correlated well with the applied concentration of stabilized oligomers in the range of 100 pM down to 1 fM. The readouts from 1 nM to 100 pM oligomers in PBS reached saturation, which means that all pixels were above cutoff in both channels. At the lower end of the dilution series, the sFIDA readout of the lowest oligomer concentration (1 fM) did not differ significantly from the readouts from 10 fM oligomers and the blank control. However, there was a significant difference in the sFIDA readouts from 10 fM oligomers and the blank control.

Spiking of CSF, PBS, and EDTA Plasma Fraction with Stabilized Oligomers

After demonstrating the ability to detect even femtomolar concentrations of stabilized oligomers diluted in buffer, we investigated if different body fluid environments affect the sensitivity of oligomer detection by sFIDA. To check for matrix effects that possibly attenuate the specific signal of Aβ oligomers, the oligomers were spiked into CSF and blood plasma from healthy, non-demented control subjects. All samples containing oligomers were determined fourfold by sFIDA analysis, while each blank sample was measured 21-fold. **Figure 3** shows the mean sFIDA readouts for all samples.

The sFIDA readout correlated well with the oligomer concentration down to 1 fM. However, there was no significant difference in the readouts of 10 fM as compared to 1 fM, as well as in the readouts from the blank sample compared to 1 and 10 fM oligomers spiked into CSF. sFIDA readouts from 100 fM and the blank sample differed significantly.

For plasma samples, there was even a very significant difference between the sFIDA readouts of 10 fM and blank sample.

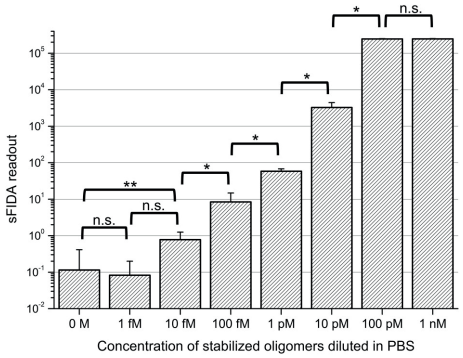

FIGURE 2 | sFIDA readout of stabilized oligomers diluted in PBS. Columns and error bars represent the mean values and standard deviations calculated from a fourfold determination of samples containing oligomers. The blank was determined 21-fold. Cutoffs for each channel were set to discard virtually all background from control samples except for 25 pixels, which are 0.01% of all pixels. This led to the following cutoff values (channel 635 nm/channel 488 nm): 4082/2773. Please note that the number of colocalized pixels (sFIDA readout) is lower than the number of pixels above background in the single channels. n.s., not significant; *$p \leq 0.05$; **$p \leq 0.01$.

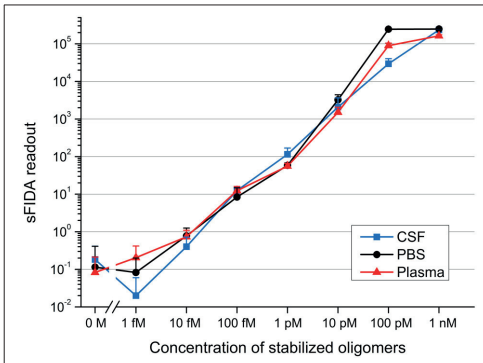

FIGURE 3 | sFIDA readout of stabilized oligomers diluted in CSF, PBS, and a plasma fraction. Shown are mean values and standard deviations from fourfold (samples containing stabilized oligomers) or 21-fold (all blanks) determinations. Cutoffs for channel 635 nm/channel 488 nm: CSF, 3268/2339; PBS, 4082/2773; plasma fraction, 4259/2028.

Lower Limits of Detection and Lower Limits of Quantification for Stabilized Oligomers Diluted in PBS, CSF, and the Plasma Fraction

As the concentration of Aβ oligomers in body fluids like CSF and blood is presumably very low (Bruggink et al., 2013; Hölttä et al., 2013; Savage et al., 2014), the lower limit of detection (LLOD) is an important characteristic of every assay for the determination

of Aβ oligomer concentration. To identify the LLOD for each matrix used in this report, each blank sample was determined 21-fold. The LLOD was calculated as the mean sFIDA readout from all blank samples plus three times the standard deviation. By establishing a calibration curve from the dilution series, the Aβ oligomer concentration corresponding to the calculated sFIDA readout was then determined. The resulting LLODs were 22 fM for stabilized oligomers diluted in PBS, 18 fM in CSF, and 14 fM in the plasma fraction.

The lower limits of quantification (LLOQ) were calculated as the mean sFIDA readout from all blank samples plus ten times the standard deviation. The same calibration curves as used for determination of LLOD were applied, leading to the following concentrations: 32 fM for stabilized oligomers diluted in PBS, 24 fM for dilution in CSF, and 22 fM for dilution in the plasma fraction.

DISCUSSION

In the present work we applied stabilized Aβ oligomers as standard in the sFIDA assay. For dilutions in PBS, CSF from control donors, and blood plasma from control donors, the sFIDA readout correlated with the oligomer concentration over five to six orders of magnitude. Although oligomer concentrations in the upper picomolar range are presumably not physiologically relevant, the observed linearity over several orders of magnitude is useful to check assay functionality and to facilitate assay calibration. The calculated LLODs for oligomers diluted in PBS, CSF, and a plasma fraction were in the range of 14–22 fM particle concentration. We can exclude that endogenous Aβ oligomers, which are possibly present also in healthy subjects, contribute significantly to the assay readout, since the intensity cutoff was determined based on the non-spiked control samples.

For the lower concentrations from 1 pM down to 1 fM, a linear relation between the sFIDA readout and concentrations of Aβ oligomers was observed. We expect that to be the relevant concentration range for analysis of biological samples, as published concentrations of oligomers in CSF are in the femtomolar to low picomolar range (stated as monomeric concentrations of Aβ; oligomeric concentrations are even lower; Bruggink et al., 2013; Hölttä et al., 2013; Savage et al., 2014).

LLODs often refer to the concentration or mass of the total applied peptide, although the actual portion of oligomerized Aβ and the size of Aβ oligomers in the preparations is mostly unknown (Santos et al., 2007; Sancesario et al., 2012). The concentration of 14 fM of the stabilized oligomers used in this study corresponds to 3.1 pM (13.9 ng/L) monomeric $A\beta_{1-42}$. The LLOD given in mass per volume is roughly in the same range or above the limits of detection published for some Aβ oligomer specific ELISA (Fukumoto et al., 2010; Bruggink et al., 2013; Hölttä et al., 2013; Savage et al., 2014). In principle, sFIDA allows detection and quantification of single particles of oligomers consisting of approximately 220 Aβ monomers.

Although the stabilized oligomers used in this study might not accurately reflect the properties of native Aβ oligomers in terms of composition, mass, and structural heterogeneity, they are nevertheless a valuable tool for assay development, assay calibration, and determination of inter- and intra-assay variation due to their stability and homogenous size. While heterogeneous Aβ oligomer standards would resemble endogenous conditions more closely, it is hardly possible to reliably produce such standards with minimal batch-to-batch-variations thus limiting their use in assay validation.

The stabilized oligomers are advantageous with regard to long term stability and they can easily be distributed to compare inter-laboratory results. This enables to thoroughly validate and calibrate an assay, which is a very important feature in assay development. However, the applicability of this standard for biological samples will have to be addressed in future studies. Quantification of very small oligomers in body fluids might emphasize the need for even smaller standard oligomers than the ones used in this study.

We have previously shown that monomers of synthetic Aβ give not rise to significant signals in the sFIDA assay by using overlapping epitopes in the capture and detection system (Wang-Dietrich et al., 2013). When analyzing native CSF samples in diagnostic setups, however, experimental conditions (i.e., pH, incubation times, freeze/thaw cycles) have to be carefully adjusted to avoid false-positive signals due to artificial aggregation of endogenous Aβ monomers.

In the present version of the assay, two N-terminal antibodies were used for capturing and detection of Aβ, i.e., Nab228 (epitope Aβ1-11) and 6E10 (epitope Aβ3-8). By using alternative capture and probe antibodies, it is not only possible to detect oligomers composed of different Aβ isoforms, but also to detect hybrid aggregates composed of different peptides or proteins. Therefore, sFIDA assay can in future be applied for scientific purpose in order to investigate the presence and pathological relevance of different oligomeric species in body fluids or brain homogenates of patients with different neurodegenerative diseases, such as AD. Additionally, after thorough investigation and validation of the assay and the measured targets, sFIDA might either give extra information useful for diagnostics or even measure oligomeric biomarkers that allow a reliable diagnosis, and might be useful for disease monitoring in clinical trials during treatment.

AUTHOR CONTRIBUTIONS

KKU, MH, YH, KKR, AK, CL, LP, KW, JW conducted experiments. KKU, DW, and OB designed experiments and wrote the manuscript.

ACKNOWLEDGMENTS

This work was supported by the Federal Ministry of Education and Research within the projects VIP (03V0641), KNDD (01GI1010A), and JPND/BIOMARKAPD (01ED1203H).

REFERENCES

Ballard, C., Gauthier, S., Corbett, A., Brayne, C., Aarsland, D., and Jones, E. (2011). Alzheimer's disease. *Lancet* 377, 1019–1031. doi: 10.1016/S0140-6736(10)61349-9

Bannach, O., Birkmann, E., Reinartz, E., Jaeger, K. E., Langeveld, J. P., Rohwer, R. G., et al. (2012). Detection of prion protein particles in blood plasma of scrapie infected sheep. *PLoS ONE* 7:e36620. doi: 10.1371/journal.pone.0036620

Benjamini, Y., and Hochberg, Y. (1995). Controlling the false discovery rate: a practical and powerful approach to multiple testing. *J. R. Stat. Soc. B* 57, 289–300.

Birkmann, E., Henke, F., Weinmann, N., Dumpitak, C., Groschup, M., Funke, A., et al. (2007). Counting of single prion particles bound to a capture-antibody surface (surface-FIDA). *Vet. Microbiol.* 123, 294–304. doi: 10.1016/j.vetmic.2007.04.001

Blennow, K., Hampel, H., Weiner, M., and Zetterberg, H. (2010). Cerebrospinal fluid and plasma biomarkers in Alzheimer disease. *Nat. Rev. Neurol.* 6, 131–144. doi: 10.1038/nrneurol.2010.4

Braak, H., and Braak, E. (1991). Neuropathological stageing of Alzheimer-related changes. *Acta Neuropathol.* 82, 239–259. doi: 10.1007/BF00308809

Bruggink, K. A., Jongbloed, W., Biemans, E. A. L. M., Veerhuis, R., Claassen, J. A. H. R., Verbeek, M. M., et al. (2013). Amyloid-β oligomer detection by ELISA in cerebrospinal fluid and brain tissue. *Anal. Biochem.* 433, 112–120. doi: 10.1016/j.ab.2012.09.014

Cleary, J. P., Walsh, D. M., Hofmeister, J. J., Shankar, G. M., Kuskowski, M. A., Selkoe, D. J., et al. (2004). Natural oligomers of the amyloid-β protein specifically disrupt cognitive function. *Nat. Neurosci.* 8, 79–84. doi: 10.1038/nn1372

Crossbeta Biosciences (2015). *Crossbeta Oligomer Publications* [Online]. Available online at: http://www.crossbeta.com/technology/publications/ (Accessed December 07, 2015).

Fukumoto, H., Tokuda, T., Kasai, T., Ishigami, N., Hidaka, H., Kondo, M., et al. (2010). High-molecular-weight β-amyloid oligomers are elevated in cerebrospinal fluid of Alzheimer patients. *FASEB J.* 24, 2716–2726. doi: 10.1096/fj.09-150359

Funke, S. A., Birkmann, E., Henke, F., Görtz, P., Lange-Asschenfeldt, C., Riesner, D., et al. (2007). Single particle detection of Abeta aggregates associated with Alzheimer's disease. *Biochem. Biophys. Res. Commun.* 364, 902–907. doi: 10.1016/j.bbrc.2007.10.085

Funke, S. A., Wang, L., Birkmann, E., and Willbold, D. (2010). Single-particle detection system for Aβ aggregates: adaptation of surface-fluorescence intensity distribution analysis to laser scanning microscopy. *Rejuvenation Res.* 13, 206–209. doi: 10.1089/rej.2009.0925

Golde, T. E., Schneider, L. S., and Koo, E. H. (2011). Anti-aβ therapeutics in Alzheimer's disease: the need for a paradigm shift. *Neuron* 69, 203–213. doi: 10.1016/j.neuron.2011.01.002

Haass, C., Kaether, C., Thinakaran, G., and Sisodia, S. (2012). Trafficking and proteolytic processing of APP. *Cold Spring Harb. Perspect. Med.* 2:a006270. doi: 10.1101/cshperspect.a006270

Haass, C., and Selkoe, D. J. (2007). Soluble protein oligomers in neurodegeneration: lessons from the Alzheimer's amyloid β-peptide. *Nat. Rev. Mol. Cell Biol.* 8, 101–112. doi: 10.1038/nrm2101

Hölttä, M., Hansson, O., Andreasson, U., Hertze, J., Minthon, L., Nägga, K., et al. (2013). Evaluating amyloid-β oligomers in cerebrospinal fluid as a biomarker for Alzheimer's disease. *PLoS ONE* 8:e66381. doi: 10.1371/journal.pone.0066381

Humpel, C. (2011). Identifying and validating biomarkers for Alzheimer's disease. *Trends Biotechnol.* 29, 26–32. doi: 10.1016/j.tibtech.2010.09.007

Janissen, R., Oberbarnscheidt, L., and Oesterhelt, F. (2009). Optimized straight forward procedure for covalent surface immobilization of different biomolecules for single molecule applications. *Colloids Surf. B Biointerfaces* 71, 200–207. doi: 10.1016/j.colsurfb.2009.02.011

Lansdall, C. J. (2014). An effective treatment for Alzheimer's disease must consider both amyloid and tau. *Biosci. Horizons* 7:hzu002. doi: 10.1093/biohorizons/hzu002

Lesné, S., Koh, M. T., Kotilinek, L., Kayed, R., Glabe, C. G., Yang, A., et al. (2006). A specific amyloid-β protein assembly in the brain impairs memory. *Nature* 440, 352–357. doi: 10.1038/nature04533

McLean, C. A., Cherny, R. A., Fraser, F. W., Fuller, S. J., Smith, M. J., Vbeyreuther, K., et al. (1999). Soluble pool of Aβ amyloid as a determinant of severity of neurodegeneration in Alzheimer's disease. *Ann. Neurol.* 46, 860–866.

Prince, M., Bryce, R., Albanese, E., Wimo, A., Ribeiro, W., and Ferri, C. P. (2013). The global prevalence of dementia: a systematic review and metaanalysis. *Alzheimer's Dement.* 9, 63–75. doi: 10.1016/j.jalz.2012.11.007

Rosén, C., Hansson, O., Blennow, K., and Zetterberg, H. (2013). Fluid biomarkers in Alzheimer's disease - current concepts. *Mol. Neurodegener.* 8:20. doi: 10.1186/1750-1326-8-20

Sancesario, G. M., Cencioni, M. T., Esposito, Z., Borsellino, G., Nuccetelli, M., Martorana, A., et al. (2012). The load of amyloid-β oligomers is decreased in the cerebrospinal fluid of Alzheimer's disease patients. *J. Alzheimers Dis.* 31, 865–878. doi: 10.3233/JAD-2012-120211

Santos, A. N., Torkler, S., Nowak, D., Schlittig, C., Goerdes, M., Lauber, T., et al. (2007). Detection of amyloid-β oligomers in human cerebrospinal fluid by flow cytometry and fluorescence resonance energy transfer. *J. Alzheimers Dis.* 11, 117–125.

Savage, M. J., Kalinina, J., Wolfe, A., Tugusheva, K., Korn, R., Cash-Mason, T., et al. (2014). A sensitive Aβ oligomer assay discriminates alzheimer's and aged control cerebrospinal fluid. *J. Neurosci.* 34, 2884–2897. doi: 10.1523/JNEUROSCI.1675-13.2014

Shaw, L. M., Vanderstichele, H., Knapik-Czajka, M., Clark, C. M., Aisen, P. S., Petersen, R. C., et al. (2009). Cerebrospinal fluid biomarker signature in Alzheimer's disease neuroimaging initiative subjects. *Ann. Neurol.* 65, 403–413. doi: 10.1002/ana.21610

Sunderland, T., Linker, G., Mirza, N., Putnam, K. T., Friedman, D. L., Kimmel, L. H., et al. (2003). Decreased β-amyloid1-42 and increased tau levels in cerebrospinal fluid of patients with Alzheimer disease. *JAMA* 289, 2094–2103. doi: 10.1001/jama.289.16.2094

Wang-Dietrich, L., Funke, S. A., Kühbach, K., Wang, K., Besmehn, A., Willbold, S., et al. (2013). The amyloid-β oligomer count in cerebrospinal fluid is a biomarker for Alzheimer's disease. *J. Alzheimers Dis.* 34, 985–994. doi: 10.3233/JAD-122047

Conflict of Interest Statement: The authors declare that the research was conducted in the absence of any commercial or financial relationships that could be construed as a potential conflict of interest.

3.2 Bioconjugated Silica Nanoparticles: Standards in Amyloid-β Oligomer-based Diagnosis of Alzheimer's Disease

Autoren: Maren Hülsemann, Christian Zafiu, Katja Kühbach, Nicole Lühmann, Yvonne Herrmann, Luriano Peters, Christina Linnartz, Johannes Willbold, Kateryna Kravchenko, Andreas Kulawik, Sabine Willbold, Oliver Bannach und Dieter Willbold

Publiziert in: Journal of Alzheimer's Disease (Hülsemann et al., 2016)

DOI: http:\\dx.doi.org\10.3233\JAD-160253

Impact Factor (2015): 3.920

Eigener Anteil: 10%

Mitentwicklung der experimentellen Details des sFIDA-Ablaufes, Unterstützung bei der Auswertung des sFIDA-Assays und Unterstützung beim Schreiben des Manuskripts

Journal of Alzheimer's Disease 54 (2016) 79–88
DOI 10.3233/JAD-160253
IOS Press

Biofunctionalized Silica Nanoparticles: Standards in Amyloid-β Oligomer-Based Diagnosis of Alzheimer's Disease

Maren Hülsemann[a,1], Christian Zafiu[a], Katja Kühbach[a], Nicole Lühmann[b], Yvonne Herrmann[a], Luriano Peters[a], Christina Linnartz[a], Johannes Willbold[a], Kateryna Kravchenko[a], Andreas Kulawik[a], Sabine Willbold[b], Oliver Bannach[a,c] and Dieter Willbold[a,c,*]
[a]*Forschungszentrum Jülich, ICS-6, Institut für Strukturbiochemie, Jülich, Germany*
[b]*Forschungszentrum Jülich, ZEA-3, Zentralinstitut für Engineering, Elektronik und Analytik, Jülich, Germany*
[c]*Heinrich-Heine-Universität Düsseldorf, Institut für Physikalische Biologie, Düsseldorf, Germany*

Handling Associate Editor: Piotr Lewczuk

Accepted 23 May 2016

Abstract. Amyloid-β (Aβ) oligomers represent a promising biomarker for the early diagnosis of Alzheimer's disease (AD). However, state-of-the-art methods for immunodetection of Aβ oligomers in body fluids show a large variability and lack a reliable and stable standard that enables the reproducible quantitation of Aβ oligomers. At present, the only available standard applied in these assays is based on a random aggregation process of synthetic Aβ and has neither a defined size nor a known number of epitopes. In this report, we generated a highly stable standard in the size range of native Aβ oligomers that exposes a defined number of epitopes. The standard consists of a silica nanoparticle (SiNaP), which is functionalized with Aβ peptides on its surface (Aβ-SiNaP). The different steps of Aβ-SiNaP synthesis were followed by microscopic, spectroscopic and biochemical analyses. To investigate the performance of Aβ-SiNaPs as an appropriate standard in Aβ oligomer immunodetection, Aβ-SiNaPs were diluted in cerebrospinal fluid and quantified down to a concentration of 10 fM in the sFIDA (surface-based fluorescence intensity distribution analysis) assay. This detection limit corresponds to an Aβ concentration of 1.9 ng l^{-1} and lies in the sensitivity range of currently applied diagnostic tools based on Aβ oligomer quantitation. Thus, we developed a highly stable and well-characterized standard for the application in Aβ oligomer immunodetection assays that finally allows the reproducible quantitation of Aβ oligomers down to single molecule level and provides a fundamental improvement for the worldwide standardization process of diagnostic methods in AD research.

Keywords: Alzheimer's disease diagnosis, Aβ oligomer standards, assay standardization, biofunctionalized nanoparticles

INTRODUCTION

Alzheimer's disease (AD) is the most common form of dementia, affecting more than 33 million people worldwide and the case number is expected to triple over the next four decades [1, 2]. AD represents a multifactorial disorder with a yet poorly understood pathogenesis, which makes its early and accurate diagnosis a difficult challenge [3]. Currently, there is no causal therapy available and a reliable diagnosis can only be achieved by post mortem analysis of brain samples.

The 'amyloid cascade' hypothesis is widely accepted to explain development and progression of AD. It mainly postulates an imbalance between

[1]Current address: Albert Einstein College of Medicine, Institute of Anatomy and Structural Biology, Laboratory of Molecular and Cellular Biophysics, New York City, USA.

*Correspondence to: Prof. Dr. Dieter Willbold, ICS-6, Institut für Strukturbiochemie, Forschungszentrum Jülich, 52428 Jülich, Germany. Tel.: +49 2461 61 2100; Fax: +49 2461 61 2023; E-mail: d.willbold@fz-juelich.de.

expression and clearance of amyloid-β (Aβ) peptides in the brain. The Aβ overload favors Aβ aggregation, ultimately inducing neuronal and synaptic degeneration and leading to dementia [4]. More recent data suggest that soluble oligomers of Aβ, in particular, directly correlate with disease severity [5, 6]. Thus, Aβ oligomers represent a popular target in drug development as well as a promising biomarker candidate for both early diagnosis of AD and therapy monitoring, respectively. A broad range of diagnostic methods for detection and quantitation of Aβ oligomers is currently applied or under evaluation. The concentration of Aβ oligomers in human body fluids is commonly assayed by ELISA methods, using capture antibodies and detection antibodies that bind to the same or overlapping epitopes, or by application of oligomer-specific antibodies [7–14].

We previously described the surface-based fluorescence intensity distribution analysis (sFIDA) technology as a highly oligomer-specific detection and quantitation method for the early diagnosis of AD [15, 16].

In sFIDA, a glass surface is covalently coated with anti-Aβ capture antibodies (Nab228, Epitope $Aβ_{1–11}$) which immobilize Aβ species from the sample. In the next step, Aβ oligomers are labeled by at least two different fluorophore-coupled anti-Aβ antibodies. Since all three applied antibodies recognize overlapping epitopes in the N-terminal part of Aβ, only oligomeric structures can be immobilized and bound by both detection antibodies at the same time, which makes the sFIDA technique insensitive against Aβ monomers. The use of different antibodies with affinities to a pan-epitope (6E10-488, Epitope $Aβ_{3–8}$ and IC16-633, Epitope $Aβ_{1–8}$) enhances the specificity of the assay, since only co-localized signals are counted but not signals caused by cross-reactivity of the individual antibodies. Finally, the chip surface is imaged by dual-color TIRF microscopy. After application of an intensity threshold the number of colocalized pixels from both channels is counted and correlates with the number of oligomers in the samples and is referred to as sFIDA readout.

While assays quantitating total Aβ can readily be calibrated with synthetic Aβ monomers, it is very difficult to establish standards for oligomer-based diagnostic tests. Furthermore, there are large variations in Aβ oligomer measurements among and within laboratories [17].

Therefore the development of a reliable oligomer standard is highly needed, since the readouts of these quantitation tests are dependent on calibration curves of standard molecules. The use of oligomers or aggregates from synthetic Aβ is limited, as these structures are metastable, heterogeneous and in dynamic equilibrium with other assembly states, and hence do not have defined sizes or consistent molecular weights. Additionally, oligomers from synthetic Aβ are prone to further aggregation and susceptible to freeze/thaw cycles, making long-term storage and constant performance, as pre-requirements for any standard, impossible.

In this work we present a novel concept for the synthesis of Aβ oligomer standards, suitable for the application in Aβ oligomer-specific quantitation assays. The core and size-determining component of the standard is a SiNaP, which can be adjusted to any size required with nearly a monodisperse size distribution [18, 19]. SiNaPs are chemically inert, non-toxic, easy to modify and stable over months. These features make SiNaPs a highly favored substructure in the design of the standard. To simulate characteristics of a native oligomer, the size of the SiNaPs was tuned to the described size range of native oligomers of 3 to 20 nm [20–22]. The surface of the SiNaPs was functionalized, activated and finally coated with $Aβ_{42}$ peptides. These biofunctionalized Aβ-SiNaPs exhibit a defined number of Aβ epitopes on the surface and allow their application in quantitative oligomer-based detection assays.

To our knowledge no other available Aβ oligomer standard presents as defined characteristics as our standard, which will therefore have a major impact on the accurate and reproducible quantitation of Aβ oligomers in human samples. Aβ-SiNaPs are a helpful accomplishment for the urgently needed standardization process between different operators, laboratories, and clinical studies in AD research worldwide [17].

MATERIAL AND METHODS

Synthesis of SiNaPs according to the Stöber process

200 ml absolute ethanol (VWR, Darmstadt, Germany), 2.7 ml water, and 4.49 ml ammonia solution (25%, Carl Roth, Karlsruhe, Germany) were vigorously stirred in a round bottom flask. After 5 min 4.43 ml TEOS (tetraethylorthosilicate, Aldrich Chemistry, St. Louis, USA) were added and the solution was stirred further for 2 days at room temperature. The resulting SiNaPs were dialyzed (MWCO

3,500, Tubing Spectral Por7 Dialysis Membrane, Spektrum Laboratories, Rancho Dominguez, CA, USA) against fivefold the volume of ethanol for 2 days to remove non-reacted chemicals and the catalysts. The SiNaPs reached a concentration of about 10 g l^{-1} and were stored at 4°C in ethanol until further usage.

Particle characterization by TEM, XPS, and FTIR

The morphology of the SiNaPs was determined by transmission electron microscopy (TEM). TEM images were recorded using a Zeiss Libra 120 Transmission Electron Microscope (Carl Zeiss AG, Jena, Germany). The copper grids (S160, Plano GmbH, Wetzlar, Germany) were prepared without staining by placing a 5 µl drop of SiNaPs (1 to 0.1 mg ml^{-1}) in ethanol on the carbon film of the grid and letting it dry at room temperature for at least 3 h before measurement.

The different SiNaP functionalization steps were monitored by Fourier transformed Infrared Spectroscopy (FTIR) and X-ray photoelectron spectroscopy (XPS). FTIR spectra were obtained by a Bruker Tensor 27 (Bruker Optik GmbH, Ettlingen, Germany) equipped with an attenuated total reflection (ATR) unit (Golden Gate, diamond crystal, Specac Ltd, UK). A film of the particles was prepared by drop casting dispersion in ethanol onto the diamond crystal. The spectra were collected with 128 scans at resolution of 4 cm^{-1} after the solvent signals in the IR spectrum vanished. The beam path was purged with argon during the measurements.

XPS spectra were obtained by a PHI 5000 VersaProbe II emitting monochromatic Al-kα radiation at an angle of 46°. A film of particles was drop casted on glass slides and the solvent was evaporated over night before measurement. Spectra were obtained from three individual positions on the glass slides.

Calculations and assumptions

After size determination of the SiNaPs by TEM micrographs, the particle surface was calculated, assuming a spherical surface. The molecular weight of the SiNaP was calculated assuming an average density of 1.85 g cm^{-3} [23]. The concentration of the SiNaP solution was determined gravimetrically in triplicate and the mean concentration of the SiNaP was calculated after every functionalization step, so that chemicals for further functionalization steps were added accordingly.

The number of potential binding sites on the SiNaP surface was determined under the assumption that one APTES molecule occupies a surface of 0.6 nm^2 [24].

Synthesis of amino-functionalized SiNaPs

Amino-functionalized SiNaP were prepared via silanization with APTES ((3-aminopropyl) triethoxysilane, Sigma-Aldrich, St. Louis, USA). A 5-fold molar excess of APTES in relation to the number of potential binding sites on the particle surface was added to the SiNaPs in ethanol. The dispersion was sonicated for 10 min and incubated overnight on a shaker at ambient temperature. The resulting amino-functionalized SiNaPs were centrifuged (5,000 × *g*, 2 h) and the resulting pellet was dispersed in ethanol by sonication for 15 min. This washing step was repeated three times.

Synthesis of carboxylated SiNaPs

A pellet containing amino-functionalized SiNaP was re-dispersed in 0.1 M succinic anhydride (Aldrich Chemistry, St. Louis, USA) in DMF (AppliChem, Darmstadt, Germany) under argon atmosphere and stirred overnight. The resulting carboxylated SiNaPs were alternately washed with water and ethanol for three times by centrifugation (5,000 × *g*, 2 h) and pellet resuspension.

Peptide coupling to the SiNaP surface

The carboxylated SiNaPs (cSiNaP) were re-dispersed in 10 mM MES buffer, pH 5.7 (Sigma Aldrich, St. Louis, USA) and were activated by EDC (1-ethyl-3-(3-dimethylaminopropyl) carbodiimide, Fluka, Sigma Aldrich, St. Louis, USA) and NHS (N-hydroxysuccinimide, Aldrich Chemistry, St. Louis, USA). The chemicals were added to the particle solution in a 16-fold and 4-fold molar excess respectively, compared to the potentially bound APTES molecules, and the mixture was sonicated for 10 min. The dispersion was centrifuged for 1 h at 10,000 × *g* and the pellet was re-dissolved in 10 mM MES buffer (pH 5.7) again. The washing procedure was repeated once before the NHS-ester activated SiNaPs were added to the peptides.

The concentration of the pre-activated SiNaPs was gravimetrically determined and the theoretical number of NHS ester groups on the SiNaP surface was

calculated. The pre-activated SiNaPs were added to the peptide resulting in a 1 : 1 ratio of potential binding sites (i.e., NHS ester groups) versus peptides, whereas a complete binding of all peptides to the particle surface cannot be expected due to the size of the peptide. The Aβ monomer has a hydrodynamic radius of 0.9 nm ± 0.1 nm [25] which would allow a maximum surface coverage of 645 peptides per SiNaP.

The dispersion of SiNaPs and peptide was sonicated for 20 min and incubated under shaking overnight. On the next day the Aβ-coated SiNaPs were centrifuged again and the pellet was re-dispersed in aqueous 50% HFIP solution (hexafluoroisopropanol, Merck, Darmstadt, Germany) to remove non-covalently bound protein. The SiNaPs were sonicated in HFIP for 5 min, followed by centrifugation (5,000 × *g*, 1 h). The last washing step was performed in water and the peptide-coated SiNaPs were stored in water at 4°C until further usage.

Peptide preparation

1 mg $A\beta_{42}$ lyophilisates (Bachem, Bubendorf, Switzerland) were dissolved in 500 µl HFIP and incubated overnight. On the next day another 500 µl HFIP were added to the peptide solution and 200–500 µl (1 µg µl^{-1}) Aliquots were prepared and the solvent was evaporated. The dry aliquots were frozen at –20°C until further usage.

Determination of the peptide concentration by BCA assay

The Kit Extra Sense BCA Assay Protein Assay Kit (BioVision Incorporated, Catolog number K814-2500, *Microplate Procedure*) was used to determine the peptide load on the SiNaPs surface. Therefore 150 µl of $A\beta_{42}$ SiNaP were mixed with 150 µl 6 M Urea (Urea crystalline, AppliChem, Darmstadt, Germany) and the solution was incubated at 60°C for 30 min. 150 µl of working solution was added and the mixture was heated at 60°C for 1 h, before the absorption at 562 nm was measured by UV/VIS spectrometry. The protein concentration was calculated according to Beer-Lambert equation.

sFIDA protocol

Custom-made 96 well plates were manufactured by gluing a 170 µm thick glass bottom (Menzel Gläser, Thermo Fisher Scientific, MS, USA) to a 0.5 cm glass plate which was perforated with 96 holes. Prior to use, plates were cleaned with ethanol and water. For further purification and hydroxylation of the glass surface the wells were treated with 5 M NaOH (Karl Roth, Karlsruhe, Germany) for 3 h. Further washing with water and drying of the plate at 90°C was followed by H_2O-Plasma treatment (Diener electronics GmbH, Ebhausen, Germany). Afterwards a desiccator was flushed with argon gas and two trays containing 1 ml of APTES and 200 µl of TEA (triethylamine, Sigma Aldrich, St. Louis, USA), respectively, were added to the chamber. The 96 well full glass plate was placed into the desiccator with the wells facing the filled trays. The chamber was flushed with argon again and vapor deposition of APTES on the glass surface was performed overnight. Next day the chemicals were removed and the desiccator was again flushed with argon and the plate got cured inside for at least 4 h (storage possible up to one week).

Carboxyl groups of 20 mg ml^{-1} carboxymethyldextrane (CMD, Sigma Aldrich, St. Louis, USA) in water were activated by 200 mM EDC and 50 mM NHS for 0.5 h under shaking. Afterwards the mixture was added to the amino-functionalized glass plates to establish amide bonds between the CMD network and the glass surface. After 1.5 h the CMD solution was removed and the wells were washed with water three times.

The remaining carboxyl groups of the bound CMD were activated by 200 mM EDC and 50 mM NHS in water again for 0.5 h. After removing EDC/NHS and performing two washing steps with water, 1 mg l^{-1} anti-Aβ capture antibody (Nab 228, epitope $A\beta_{1-11}$, Sigma Aldrich, St. Louis, USA) in PBS was added to the wells. The incubation for 1.5 h led to the covalent binding of the capture antibody to the surface.

After removing the antibody solution the remaining active NHS-ester groups on the functionalized surface were quenched by 0.1 M ethanolamine hydrochloride (Sigma Aldrich, St. Louis, USA) in Tris-buffered saline, pH 7.4 (TBS). The solution was removed after 30 min and the wells were washed with TBS three times. Until sample application the plates were stored in TBS.

15 µl of samples were applied to the plate in triplicates and incubated overnight on the capture-antibody coated glass surface. Afterwards the wells were washed once with TBS-T (TBS supplemented with 0.05% Tween-20) and twice with TBS. In the next step, 1.25 mg/l of two fluorescence-labeled anti-Aβ antibodies IC16-Alexa 633 and 6E10-ATTO 488 (6E10: epitope $A\beta_{3-8}$, Covance, Princeton, USA;

dye: ATTO-Tec, Siegen, Germany) were added to the wells and incubated for 2 h. mAB IC16 (epitope $A\beta_{1-8}$) was kindly provided by the groups of Prof. Carsten Korth and Prof. Sascha Weggen, Heinrich Heine University Düsseldorf Medical School and labeled with Alexa 633 dye according to the manufactures instructions (Life Technologies, Carlsbad, USA). Finally, the wells were washed twice with TBS-T and twice with TBS. Prior to TIRF microscopy the wells were filled with water and sealed with a plastic foil.

Application of Aβ-SiNaPs in sFIDA

Aβ-SiNaPs were stored in water at 4°C until use. For sFIDA analysis, Aβ-SiNaPs were serially diluted in water and human AD-negative CSF (biochemed, Winchester, USA) to concentrations ranging from 100 pM down to 10 fM and analyzed by sFIDA in threefold determination.

Data acquisition

The surface of the sFIDA well plates was imaged by total internal reflection fluorescence (TIRF) microscopy (AM TIRF MC Leica TIRF microscope, Leica Microsystems, Wetzlar, Germany). The measurement was performed by the Leica Matrix screener software using a 100 × objective lens (1.47 oil CORR TIRF Leica), which enabled the detection of surface-near fluorescence. For each well, 25 images (112 × 112 µm, 1000 × 1000 pixels, 200 nm distance between the scan areas, 14 bit) were taken in channel 0 (Ex/Em 635/705 nm), and channel 1 (Ex/Em 488/525 nm), detecting IC16-Alexa 633 and 6E10-ATTO 488 respectively. Microscope settings of gain, laser power and exposure time were adjusted in a way that the intensity histogram still showed a detectable fluorescence signal for the lowest standard concentration. The microscope settings included a gain between 800 and 1000, a laser power of 100% and an exposure time between 1 and 1.8 s.

Data analysis

After data acquisition at the TIRF microscope the images were exported as tiff files and analyzed with a self-developed software designated sFIDAta. The performed image analysis was applied only to the central 700 × 700 pixels of each image. By this procedure, the border regions of all images, which are not uniformly illuminated, were excluded from the analysis. The software performed a separated histogram analysis for each channel and each SiNaP concentration. To exclude the background signal, intensity cutoffs were determined for each channel. Since the background signal can differ between different matrices (water or CSF), cutoffs were calculated individually for each matrix. The cutoff is defined as an intensity threshold that leaves 0.1% of the total pixel number in the images from the blank control measurement (i.e., 1,000 pixels out of a million pixels). Finally, images from both channels were merged and the number of colocalized pixels above the determined cutoffs was counted for each well. The mean number of colocalized pixels from the images of each concentration is referred to as 'sFIDA readout'.

RESULTS

Synthesis of SiNaPs

SiNaPs were produced as the core component of the standard. Synthesis of the SiNaPs was performed via the Stöber process, which describes a condensation reaction of tetraethylorthosilicate (TEOS) to a siloxane polymer network in the presence of water and ammonia, resulting in nearly monodisperse SiNaPs [18]. Since the diameter of a native oligomer is in the range of 3 to 20 nm, we aimed to synthesize the SiNaP core in an according size range. To determine the size and morphology of the obtained SiNaPs, transmission electron micrographs were recorded. Figure 1 shows SiNaPs with a mean diameter of 24 ± 4.6 nm exhibiting a rather polyhedral shape. It has been previously reported that the shape of very small SiNaPs (<50 nm) is not spherical due to the mechanism of particle formation [18, 23].

Synthesis strategy of biofunctionalized SiNaPs

For biofunctionalization of SiNaPs, three functionalization steps were performed as described in Fig. 2a-e. After synthesis of SiNaPs via the Stöber process (Fig. 2a) a primary amine group was introduced to the SiNaP surface by silanization with APTES (3-(aminopropyl)triethoxysilane) (Fig. 2b, aminated SiNaP = aSiNaP). In the next step aSiNaPs were transferred to a solution of succinic anhydride in DMF (dimethylformamide) under dry conditions. The amine group on the SiNaP surface attacked the succinic anhydride which led to a ring-opening of the anhydride, the formation of an amide bond and

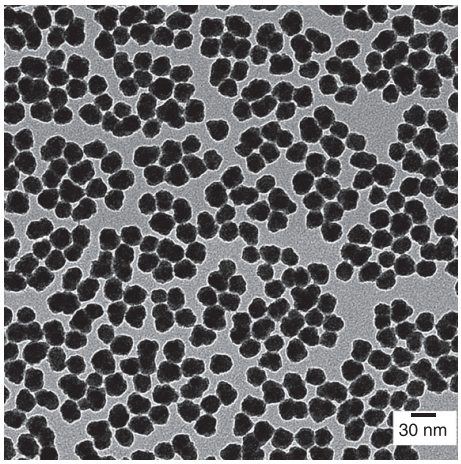

Fig. 1. Transmission electron micrographs of bare SiNaPs. A mean Feret diameter of 24 ± 4.6 nm was calculated from at least 250 SiNaPs.

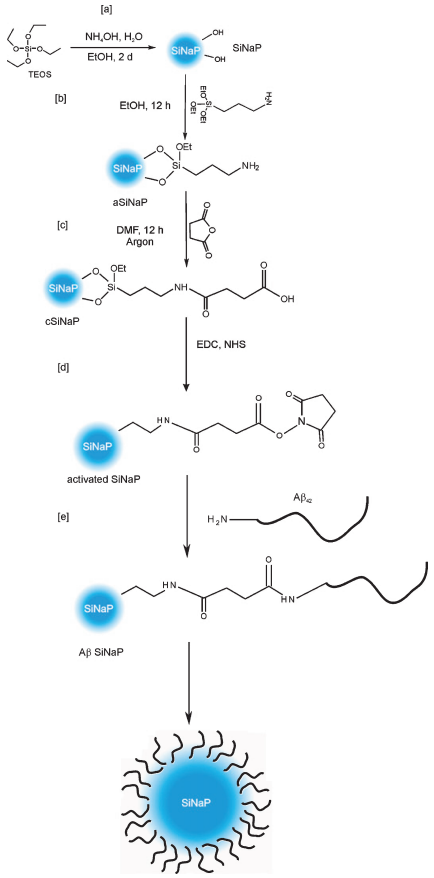

Fig. 2. Synthesis strategy of biofunctionalized SiNaPs. a) Stoeber synthesis of SiNaPs was followed by (b) silanization of the SiNaP surface with APTES (aSiNaP). c) Primary amines reacted with succinic anhydride via a nucleophilic addition and led to the introduction of carboxy functions on the SiNaP surface (cSiNaP). d) Carboxy groups became activated to reactive NHS esters by EDC/NHS (activated SiNaP) which (e) reacted with amine groups of biomolecules, such as Aβ peptides and led to their covalent binding on the SiNaP surface.

the exposure of free carboxyl groups on the SiNaP surface (Fig. 2c, carboxylated SiNaP = cSiNaP) [26].

The activation of the exposed carboxyl groups by EDC/NHS (1-ethyl-3-(3-dimethylaminopropyl) carbodiimide / N-hydroxysuccinimide) resulted in the formation of NHS ester groups (Fig. 2d, activated SiNaP) which could react with primary amine groups of chosen biomolecules (Fig. 2e) and led to their covalent binding on the SiNaP surface.

The successful modifications of the SiNaP surface was monitored by XPS and attenuated total reflection Fourier transform infrared spectroscopy (ATR-FTIR). Figure 3a shows the atomic composition of SiNaP and aSiNaP obtained from XPS spectra. Both nanoparticles exhibited high levels of oxygen and silicon atoms which originated from the dense silica core of the materials. Elevated levels of carbon and nitrogen in aSiNaP spectra suggest the surface modification with APTES as these signals were absent in the case of unmodified SiNaP.

Figure 3b shows full range FTIR spectra of different modification steps of SiNaP and a predominant band ranging from 1300 and 1000 cm^{-1} which corresponds to the Si-O and Si-OH bonds of amorphous silicate material. Another common feature of the spectra is a broad band between 3800 and 2700 cm^{-1} (Fig. 3c) which represents the O-H vibrations within the SiNaP core.

Unmodified SiNaP show two characteristic bands, one at 3650 cm^{-1} (free -O-H strech) and in Fig. 3d at 1650 cm^{-1} (-O-H bend) that represent the -O-H surface functionalities. Furthermore, the spectrum consisted of a broad band at 1450 cm^{-1} which could be assigned to carbonate anions as an insertion product of CO_2 into the silanol group of the silica surface.

After exposing SiNaP to APTES CH_2 scissoring bands at 1395 and 1445 cm^{-1} were observed together with C-H stretching bands between 2900 and 2980 cm^{-1}. In addition a weak band at 1620 cm^{-1}

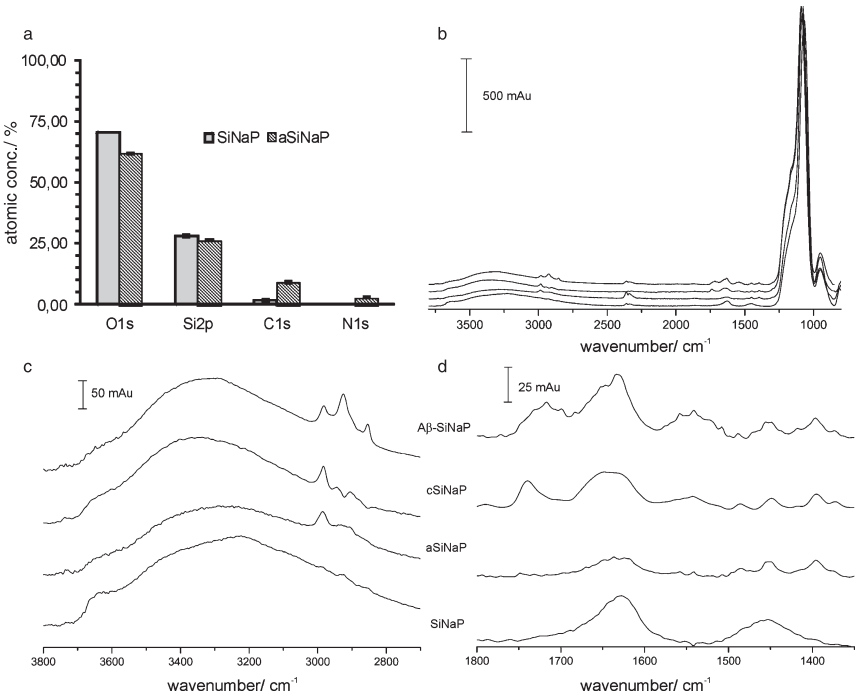

Fig. 3. a) XPS data analysis of SiNaP (grey) and aSiNaP (striped). b) ATR-FTIR spectra of different SiNaP functionalization steps. SiNaP: unmodified SiNaP, aSiNaP: aminated SiNaP functionalized with APTES, cSiNaP: carboxylated SiNaP functionalized with succinic anhydride; Aβ-SiNaP: SiNaP coated with Aβ. c) Expanded spectra from (b) in the range of 2700 – 3800 cm^{-1}. d) Expanded spectra from (b) in the range of 1300 – 1800 cm^{-1}.

represents the -N-H surface functionality which was also observed by XPS (Fig. 3a).

The modification of the SiNaPs by succinic acid was confirmed in the FTIR spectra by the appearance of two new bands at 1655 and 1723 cm^{-1} (COOH and COO^- vibrations respectively). The band at 1655 cm^{-1} overlaps with an additional one at 1630 cm^{-1}, which is typical for the amide I vibration.

Bioconjugation of SiNaPs with synthetic Aβ

The bioconjugation of SiNaPs with chosen biomolecules was enabled by previous functionalization and activation of the surfaces of SiNaPs by EDC/NHS treatment and the formation of NHS ester groups as reactive intermediates (Fig. 2d, e). The NHS esters on the surfaces of SiNaPs formed amide bonds with the exposed lysine residues of $A\beta_{42}$ at position 16 and/or 28 and led to coating of SiNaPs with Aβ peptides. An additional binding site is the N-terminus of the peptide, which we consider less reactive for the coupling reaction due to its vicinity to acidic amino acids and steric restraints. The successful attachment of $A\beta_{42}$ to the particles was demonstrated by FTIR (Fig. 3). Not only the bands assigned to CH_2 stretching vibrations (2925 cm^{-1} and 2855 cm^{-1}) showed an increased intensity for the peptide coated SiNaPs, but also the signals between 1580 and 1750 cm^{-1}. The increase of the band at 1720 cm^{-1} (COOH) appeared due to the presence of additional carboxyl groups by the amino acids of $A\beta_{42}$. Whereas the amide I vibration of the COOH-terminated SiNaPs was only visible as a shoulder which was increased to a maximum for the $A\beta_{42}$ functionalized SiNaPs. A new band positioned at 1542 cm^{-1} could be assigned to the amide II vibration of the peptide as well. Peptide quantitation by BCA assay revealed an $A\beta_{42}$ concentration of 24 $\mu g\ ml^{-1}$ in a 1 mg ml^{-1} SiNaPs solution. This corresponds to an average load of 44 peptides per 24 nm SiNaP,

which is only 7% of the theoretical maximal load of 645 peptides, probably as a consequence of repulsive interactions on the nanoparticle surface.

Aβ-SiNaP quantitation in water and cerebrospinal fluid by sFIDA

The sFIDA assay is designed to specifically determine the Aβ oligomer concentration in body fluids, such as cerebrospinal fluid (CSF). Apart from quantifying Aβ-SiNaPs in aqueous environment, we also analyzed possible matrix effects on the sFIDA readout by spiking Aβ-SiNaPs into CSF from AD-negative donors (Fig. 4).

Aβ-SiNaP concentrations ranging from 100 pM to 10 fM were subjected to sFIDA analysis, and the respective non-spiked fluids served as controls. All samples including blank controls were determined three-fold by sFIDA analysis. Aβ-SiNaPs diluted in water as well as in CSF revealed a correlation between the sFIDA readout and the Aβ-SiNaP concentration down to 10 fM. A concentration of 10 fM Aβ-SiNaPs in water and 100 fM in CSF could still be differentiated from the control demonstrating that Aβ-SiNaPs are a suitable standard in CSF-based AD diagnostics.

Considering a load of 44 $A\beta_{42}$ peptides per Aβ-SiNaP, 10 fM Aβ-SiNaP corresponded to an $A\beta_{42}$ peptide concentration of 1.9 ng l^{-1}. This limit of detection of $A\beta_{42}$ peptides is in the same range or one order of magnitude higher as reported for oligomer-specific ELISA-based assays [13, 14, 27]. By repetition of the experiment with the same Aβ-SiNaP batch stored at 4°C over a period of four months, we demonstrated constantly stable sFIDA readouts from the Aβ-SiNaP dilution series and therefore confirmed long-term stability of the standard (Fig. 5).

DISCUSSION

In this work we presented the synthesis and application of Aβ-SiNaPs as standard in sFIDA diagnostics. The successful synthesis and biofunctionalization of SiNaPs was shown by TEM, XPS micrographs and ATR-FTIR spectra. By sFIDA analysis we quantified Aβ-SiNaPs diluted in water and CSF over several orders of magnitude down to the femtomolar concentration range. A SiNaP standard of tunable, defined size and with an adjustable number of epitopes on the SiNaP surface might significantly contribute to the development, optimization and calibration of immuno-based diagnostic

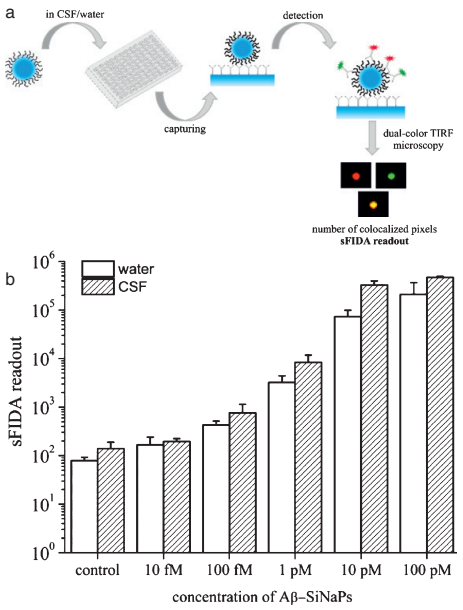

Fig. 4. sFIDA analysis of Aβ-SiNaPs. a) Schematic illustration of the experimental procedure of detecting Aβ-SiNaPs in the sFIDA assay. b) sFIDA analysis of Aβ-SiNaPs diluted in water and CSF sFIDA readout of Aβ-SiNaPs diluted in water and human CSF to concentrations of 100 pM to 10 fM. The respective diluent lacking Aβ-SiNaPs served as negative control. Shown are mean values and standard deviations from threefold determination.

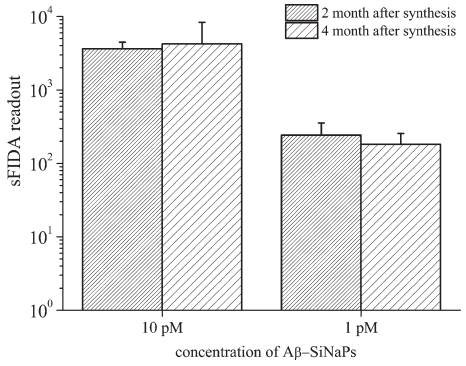

Fig. 5. sFIDA analysis of Aβ-SiNaPs diluted in water. sFIDA readout of Aβ-SiNaPs diluted in water to concentrations of 10 pM and 1 pM. Shown are two measurements of the same SiNaP batch at different time points, 2 and 4 months after synthesis. Plotted are mean values and standard deviations from threefold determination.

assays for protein misfolding diseases based on single-molecule detection.

In contrast to any other standard of Aβ aggregates, Aβ-SiNaPs exhibit a measurable number of accessible Aβ peptides on the SiNaP surface. These defined characteristics render Aβ-SiNaPs superior to the more heterogeneous oligomer standards prepared from a stochastic aggregation reaction of synthetic Aβ, as they have been used so far. In the presented case we bound 44 peptides per SiNaP.

In addition, Aβ-SiNaPs prepared by this method showed no observable aggregation after the excessive and non-covalently bound monomer was removed. This observation suggests that Aβ bound to the particle surface is not able to transmit to a conformation that is prone to form aggregates. Since the mid and C-terminal sections of the Aβ sequence are involved in the aggregation mechanism it appears very likely that the coupling of Lys16 and/or Lys28 is responsible for the inhibition of the aggregation of Aβ-SiNaP.

The chemically activated SiNaPs can be easily coated with any peptide of choice to serve also as standard in oligomer-based assays of other protein misfolding diseases, such as prion diseases or Parkinson's disease [28–31]. Additionally, hybrid aggregates consisting of different peptides, such as tau and Aβ, could be mimicked by a SiNaP standard to support explorative studies on hybrid oligomers as biomarkers, which might reflect the clinical diversity of many neurodegenerative disorders [32, 33]. For the described synthesis of biofunctionalized SiNaPs the chosen peptide needs to have a free primary amine group for the covalent coupling to the SiNaP outside the epitope, to enable detection of the peptide on the SiNaP. Alternatively other coupling methods, such as Biotin/Streptavidin could link peptides to the SiNaP platform.

Different approaches are developed for the oligomer-specific diagnosis of Alzheimer's disease based on immunodetection in liquid, such as ELISA-like methods as described above or flow cytometry combined with FRET [34]. However, these methods lack an appropriate standard molecule to enable the accurate and reproducible quantitation of Aβ oligomers in human samples. A calibration curve of a serial dilution of Aβ-SiNaPs in the respective body fluid should allow the quantitation of the analyte and also the number of detected epitopes by comparing the obtained fluorescence signals of the clinical sample and the standard.

We envisage the Aβ-SiNaP standard as an essential tool to cross-validate Aβ oligomers as AD biomarker on different platform technologies. It will allow the accurate determination of inter-assay variability and thereby be a valuable tool in the standardization process of various Aβ oligomer immunodetection assays.

ACKNOWLEDGMENTS

This work was supported by the Federal Ministry of Education and Research within the projects VIP (03V0641), KNDD (01GI1010A), and JPND/BIOMARKAPD (01ED1203H).

Authors' disclosures available online (http://www.j-alz.com/manuscript-disclosures/16-0253r2).

REFERENCES

[1] Prince M, Albanese E, Guerchet M, Prina M (2014) *World Alzheimer Report 2014, Dementia and Risk Reduction: An Analysis of Protective and Modifiable Factors*.

[2] Barnes DE, Yaffe K (2011) The projected effect of risk factor reduction on Alzheimer's disease prevalence. *Lancet Neurol* **10**, 819-828.

[3] Hardy J, Selkoe DJ (2002) The amyloid hypothesis of Alzheimer's disease: Progress and problems on the road to therapeutics. *Science* **297**, 353-356.

[4] Hardy J (2006) Has the amyloid cascade hypothesis for Alzheimer's disease been proved? *Curr Alzheimer Res* **3**, 71-73.

[5] Haass C, Selkoe DJ (2007) Soluble protein oligomers in neurodegeneration: Lessons from the Alzheimer's amyloid beta-peptide. *Nat Rev Mol Cell Biol* **8**, 101-112.

[6] Lesne S, Koh MT, Kotilinek L, Kayed R, Glabe CG, Yang A, Gallagher M, Ashe KH (2006) A specific amyloid-beta protein assembly in the brain impairs memory. *Nature* **440**, 352-357.

[7] El-Agnaf OM, Mahil DS, Patel BP, Austen BM (2000) Oligomerization and toxicity of beta-amyloid-42 implicated in Alzheimer's disease. *Biochem Biophys Res Commun* **273**, 1003-1007.

[8] Klaver AC, Patrias LM, Finke JM, Loeffler DA (2011) Specificity and sensitivity of the Abeta oligomer ELISA. *J Neurosci Methods* **195**, 249-254.

[9] Savage MJ, Kalinina J, Wolfe A, Tugusheva K, Korn R, Cash-Mason T, Maxwell JW, Hatcher NG, Haugabook SJ, Wu GX, Howell BJ, Renger JJ, Shughrue PJ, McCampbell A (2014) A sensitive A beta oligomer assay discriminates Alzheimer's and aged control cerebrospinal fluid. *J Neurosci* **34**, 2884-2897.

[10] Sian AK, Frears ER, El-Agnaf OM, Patel BP, Manca MF, Siligardi G, Hussain R, Austen BM (2000) Oligomerization of beta-amyloid of the Alzheimer's and the Dutch-cerebral-haemorrhage types. *Biochem J* **349**, 299-308.

[11] Xia W, Yang T, Shankar G, Smith IM, Shen Y, Walsh DM, Selkoe DJ (2009) A specific enzyme-linked immunosorbent assay for measuring beta-amyloid protein oligomers in human plasma and brain tissue of patients with Alzheimer disease. *Arch Neurol* **66**, 190-199.

[12] Yang T, O'Malley TT, Kanmert D, Jerecic J, Zieske LR, Zetterberg H, Hyman BT, Walsh DM, Selkoe DJ (2015) A

highly sensitive novel immunoassay specifically detects low levels of soluble A beta oligomers in human cerebrospinal fluid. *Alzheimers Res Ther* **7**, 14.

[13] Holtta M, Hansson O, Andreasson U, Hertze J, Minthon L, Nagga K, Andreasen N, Zetterberg H, Blennow K (2013) Evaluating amyloid-beta oligomers in cerebrospinal fluid as a biomarker for Alzheimer's disease. *PLoS One* **8**, e66381.

[14] Fukumoto H, Tokuda T, Kasai T, Ishigami N, Hidaka H, Kondo M, Allsop D, Nakagawa M (2010) High-molecular-weight beta-amyloid oligomers are elevated in cerebrospinal fluid of Alzheimer patients. *FASEB J* **24**, 2716-2726.

[15] Funke SA, Birkmann E, Henke F, Goertz P, Lange-Asschenfeldt C, Riesner D, Willbold D (2007) Single particle detection of A beta aggregates associated with Alzheimer's disease. *Biochem Biophys Res Commun* **364**, 902-907.

[16] Wang-Dietrich L, Funke SA, Kuhbach K, Wang K, Besmehn A, Willbold S, Cinar Y, Bannach O, Birkmann E, Willbold D (2013) The amyloid-beta oligomer count in cerebrospinal fluid is a biomarker for Alzheimer's disease. *J Alzheimers Dis* **34**, 985-994.

[17] Mattsson N, Andreasson U, Persson S, Carrillo MC, Collins S, Chalbot S, Cutler N, Dufour-Rainfray D, Fagan AM, Heegaard NH, Robin Hsiung GY, Hyman B, Iqbal K, Kaeser SA, Lachno DR, Lleo A, Lewczuk P, Molinuevo JL, Parchi P, Regeniter A, Rissman RA, Rosenmann H, Sancesario G, Schroder J, Shaw LM, Teunissen CE, Trojanowski JQ, Vanderstichele H, Vandijck M, Verbeek MM, Zetterberg H, Blennow K, Alzheimer's Association QCPWG (2013) CSF biomarker variability in the Alzheimer's Association quality control program. *Alzheimers Dement* **9**, 251-261.

[18] Stober W, Fink A, Bohn E (1968) Controlled growth of monodisperse silica spheres in micron size range. *J Colloid Interface Sci* **26**, 62-69.

[19] Thomassen LC, Aerts A, Rabolli V, Lison D, Gonzalez L, Kirsch-Volders M, Napierska D, Hoet PH, Kirschhock CE, Martens JA (2010) Synthesis and characterization of stable monodisperse silica nanoparticle sols for *in vitro* cytotoxicity testing. *Langmuir* **26**, 328-335.

[20] Glabe CG (2008) Structural classification of toxic amyloid oligomers. *J Biol Chem* **283**, 29639-29643.

[21] Mastrangelo IA, Ahmed M, Sato T, Liu W, Wang C, Hough P, Smith SO (2006) High-resolution atomic force microscopy of soluble Abeta42 oligomers. *J Mol Biol* **358**, 106-119.

[22] Sakono M, Zako T (2010) Amyloid oligomers: Formation and toxicity of Abeta oligomers. *FEBS J* **277**, 1348-1358.

[23] Masalov VM, Sukhinina NS, Kudrenko EA, Emelchenko GA (2011) Mechanism of formation and nanostructure of Stober silica particles. *Nanotechnology* **22**, 275718.

[24] Graf C, van Blaaderen A (2002) Metallodielectric colloidal core-shell particles for photonic applications. *Langmuir* **18**, 524-534.

[25] Nag S, Chen J, Irudayaraj J, Maiti S (2010) Measurement of the attachment and assembly of small amyloid-beta oligomers on live cell membranes at physiological concentrations using single-molecule tools. *Biophys J* **99**, 1969-1975.

[26] Qhobosheane M, Santra S, Zhang P, Tan W (2001) Biochemically functionalized silica nanoparticles. *Analyst* **126**, 1274-1278.

[27] Bruggink KA, Jongbloed W, Biemans EA, Veerhuis R, Claassen JA, Kuiperij HB, Verbeek MM (2013) Amyloid-beta oligomer detection by ELISA in cerebrospinal fluid and brain tissue. *Anal Biochem* **433**, 112-120.

[28] Bannach O, Birkmann E, Reinartz E, Jaeger KE, Langeveld JP, Rohwer RG, Gregori L, Terry LA, Willbold D, Riesner D (2012) Detection of prion protein particles in blood plasma of scrapie infected sheep. *PLoS One* **7**, e36620.

[29] Bannach O, Reinartz E, Henke F, Dressen F, Oelschlegel A, Kaatz M, Groschup MH, Willbold D, Riesner D, Birkmann E (2013) Analysis of prion protein aggregates in blood and brain from pre-clinical and clinical BSE cases. *Vet Microbiol* **166**, 102-108.

[30] Hubinger S, Bannach O, Funke SA, Willbold D, Birkmann E (2012) Detection of alpha-synuclein aggregates by fluorescence microscopy. *Rejuvenation Res* **15**, 213-216.

[31] Hansson O, Hall S, Ohrfelt A, Zetterberg H, Blennow K, Minthon L, Nagga K, Londos E, Varghese S, Majbour NK, Al-Hayani A, El-Agnaf OM (2014) Levels of cerebrospinal fluid alpha-synuclein oligomers are increased in Parkinson's disease with dementia and dementia with Lewy bodies compared to Alzheimer's disease. *Alzheimers Res Ther* **6**, 25.

[32] Clinton LK, Blurton-Jones M, Myczek K, Trojanowski JQ, LaFerla FM (2010) Synergistic Interactions between Abeta, tau, and alpha-synuclein: Acceleration of neuropathology and cognitive decline. *J Neurosci* **30**, 7281-7289.

[33] Guo JP, Arai T, Miklossy J, McGeer PL (2006) A beta and tau form soluble complexes that may promote self aggregation of both into the insoluble forms observed in Alzheimer's disease. *Proc Natl Acad Sci U S A* **103**, 1953-1958.

[34] Santos AN, Torkler S, Nowak D, Schlittig C, Goerdes M, Lauber T, Trischmann L, Schaupp M, Penz M, Tiller FW, Bohm G (2007) Detection of amyloid-beta oligomers in human cerebrospinal fluid by flow cytometry and fluorescence resonance energy transfer. *J Alzheimers Dis* **11**, 117-125.

3.3 Analysis of anti-coagulants for blood-based quantitation of amyloid-β oligomers in the sFIDA assay

Autoren: Kateryna Kravchenko, Andreas Kulawik, Maren Hülsemann, Katja Kühbach, Christian Zafiu, Yvonne Herrmann, Christina Linnartz, Luriano Peters, Tuyen Bujnicki, Johannes Willbold, Oliver Bannach und Dieter Willbold

Publiziert in: Biological Chemistry (Kravchenko et al., 2016)

DOI: https:\\doi.org\10.1515\hsz-2016-0153

Impact Factor (2015): 2.710

Eigener Anteil: 10%

Mitentwicklung der experimentellen Details des sFIDA-Ablaufes, Unterstützung bei der Auswertung des sFIDA-Assays und Unterstützung beim Schreiben des Manuskripts

DE GRUYTER Biol. Chem. 2016; aop

Kateryna Kravchenko, Andreas Kulawik, Maren Hülsemann, Katja Kühbach, Christian Zafiu, Yvonne Herrmann, Christina Linnartz, Luriano Peters, Tuyen Bujnicki, Johannes Willbold, Oliver Bannach and Dieter Willbold*

Analysis of anticoagulants for blood-based quantitation of amyloid β oligomers in the sFIDA assay

DOI 10.1515/hsz-2016-0153
Received March 18, 2016; accepted September 28, 2016

Abstract: Early diagnostics at the preclinical stage of Alzheimer's disease is of utmost importance for drug development in clinical trials and prognostic guidance. Since soluble Aβ oligomers are considered to play a crucial role in the disease pathogenesis, several methods aim to quantify Aβ oligomers in body fluids such as cerebrospinal fluid (CSF) and blood plasma. The highly specific and sensitive method surface-based fluorescence intensity distribution analysis (sFIDA) has successfully been established for oligomer quantitation in CSF samples. In our study, we explored the sFIDA method for quantitative measurements of synthetic Aβ particles in blood plasma. For this purpose, EDTA-, citrate- and heparin-treated blood plasma samples from five individual donors were spiked with Aβ coated silica nanoparticles (Aβ-SiNaPs) and were applied to the sFIDA assay. Based on the assay parameters linearity, coefficient of variation and limit of detection, we found that EDTA plasma yields the most suitable parameter values for quantitation of Aβ oligomers in sFIDA assay with a limit of detection of 16 fM.

Keywords: Alzheimer's disease diagnostic biomarkers; Amyloid beta oligomers; neurodegenerative diseases; blood plasma; sFIDA; silica nanoparticles.

***Corresponding author: Dieter Willbold,** ICS-6 Structural Biochemistry, Forschungszentrum Jülich, Wilhelm-Johnen-Str., D-52425 Jülich, Germany; and Institut für Physikalische Biologie, Heinrich-Heine-Universität Düsseldorf, Universitätsstraße 1, D-40225 Düsseldorf, Germany, e-mail: d.willbold@fz-juelich.de
Kateryna Kravchenko, Maren Hülsemann, Katja Kühbach, Christian Zafiu, Yvonne Herrmann, Christina Linnartz, Luriano Peters, Tuyen Bujnicki and Johannes Willbold: ICS-6 Structural Biochemistry, Forschungszentrum Jülich, Wilhelm-Johnen-Str., D-52425 Jülich, Germany
Andreas Kulawik and Oliver Bannach: ICS-6 Structural Biochemistry, Forschungszentrum Jülich, Wilhelm-Johnen-Str., D-52425 Jülich, Germany; and Institut für Physikalische Biologie, Heinrich-Heine-Universität Düsseldorf, Universitätsstraße 1, D-40225 Düsseldorf, Germany

Introduction

Alzheimer's disease (AD) is the most frequent form of dementia which affects more than 35 million people worldwide (Wimo et al., 2013). Since age is considered to be the major risk factor for AD, case numbers are expected to dramatically increase in the next decades as a consequence of the aging society. The clinical onset of AD is preceded by pathophysiological changes years before outbreak of the disease (Blennow, 2004). Early diagnostics at the preclinical stage of the disease is highly desired for drug development in clinical trials and prognostic guidance.

Major pathological hallmarks of AD are extracellular amyloid plaques consisting mainly of amyloid beta (Aβ) peptide as well as intracellular neurofibrillary tangles composed of tau protein (Selkoe, 1991). More recent data indicate that oligomeric Aβ is the most toxic species and is therefore of interest both as drug target and candidate biomarker (Haass and Selkoe, 2007; Blennow et al., 2015).

We developed a highly sensitive oligomer-specific diagnostic assay designated surface-based fluorescence intensity distribution analysis (sFIDA) (Birkmann et al., 2006, 2007; Funke et al., 2007, 2010; Bannach et al., 2012; Wang-Dietrich et al., 2013; Kühbach et al., 2016). In sFIDA, Aβ is captured to a functionalized glass surface by Aβ specific antibodies that recognize the N-terminus of the molecule. Subsequently, Aβ is decorated by two fluorescently labeled antibodies. Since the same or overlapping epitopes are recognized by both capture and detection antibodies, the assay is insensitive for monomeric Aβ which is also omnipresent in healthy subjects. Images from the surface are obtained using dual-color total internal reflection fluorescence microscopy (TIRFM). The number of colocalized pixels with signal intensities above background is referred to as sFIDA readout, which correlates with the number of Aβ oligomers in the sample. As a calibration standard in the sFIDA assay, 30 nm silica nanoparticles coated with $A\beta_{1-42}$ peptides (Aβ-SiNaPs) are

used. Aβ-SiNaPs have been shown to be a suitable standard in Aβ oligomer quantitation due to their uniform size and defined number of accessible epitopes. Moreover, the particles are not prone to aggregation and are stable over several months (Hülsemann et al., 2016).

sFIDA has been proven as a capable tool for the quantitation of Aβ oligomers from cerebrospinal fluid with a large sensitive range of detection. However, lumbar puncture, though generally considered to be safe, goes along with risks and is often experienced as uncomfortable for patients. Hence, the diagnosis from blood preparations after venipuncture is a worthwhile aim.

Blood can be processed either as serum or as plasma, which is the noncoagulated liquid component of blood after centrifugation. Coagulation is prevented by the addition of anticoagulants of which EDTA, citrate, and heparin are the most commonly used in clinical practice (Jambunathan and Galande, 2014). EDTA and citrate prevent the formation of thrombin by chelating calcium required for the blood clotting cascade (Davie and Ratnoff, 1964), whereas heparin functions by activating antithrombin (Olson and Chuang, 2002).

The choice of anticoagulant for blood plasma preparation is an important factor in the preanalytical phase of assay development and can have a considerable effect on the identification of biomarkers as shown for a variety of assays concerning the detection of cytokines (Riches et al., 1992), miRNA (Leidinger et al., 2015), proteins (Banks et al., 2005; Hsieh et al., 2006), enzymes (Gerlach et al., 2005), amino acid analysis (Parvy et al., 1983; Hubbard et al., 1988; Chuang et al., 1998) and other analytes (Fendl et al., 2016; Ribeiro et al., 2016).

The goal of the present study was to compare the effect of different anticoagulants on the sFIDA assay and identify the most suitable anticoagulant regarding assay standardization. Therefore, a dilution series of Aβ-SiNaPs was spiked in blood plasma supplemented with different anticoagulants (EDTA, citrate and heparin, respectively) and were subsequently applied to the sFIDA assay. Based on the assay parameters, linearity, coefficient of variance and limit of detection, the effect of the anticoagulants on the assay outcome was investigated.

Results

Aβ-SiNaPs were spiked in a log 10 dilution series to EDTA, citrate and heparin plasma, each of five individual healthy donors and subjected to sFIDA assay. As a preprocessing procedure all images underwent artifact detection. For Aβ-SiNaPs spiked in EDTA plasma, citrate plasma, heparin plasma and PBS 81.4%, 87.9%, 88.0% and 89.2% of the total number of images passed quality control, respectively.

Inspection of the images for sFIDA analysis revealed differences for the different anticoagulants (Figures 1 and 2). For channel 0 (em. 635 nm/exc. 705 nm) the major peak in intensity distribution for EDTA was approximately at 2400, for citrate at 1700 and for heparin at 900 on a 14-bit grayscale, and for channel 1 (em. 488 nm/exc. 525 nm) at approximately 1300, 1300 and 1000, respectively (Figure 2), as shown for blood plasma samples spiked in 1 pM Aβ-SiNaPs. This indicates that the overall intensity of images obtained from heparin treated blood plasma are considerably lower compared to EDTA and citrate, as can also be seen in representative images (Figure 1, left hand column). Furthermore, the variation in intensity distribution between the images is higher for heparin compared to EDTA and citrate plasma (Figure 1, middle and right hand column).

For deeper analysis, sFIDA readout was calculated, which is the number of colocalized pixels above background. A correlation between Aβ-SiNaP concentration and sFIDA readout was observed from 100 pM down to the lowest concentration of 10 fM for all plasma samples (Figure 3). In order to further characterize the effect of different anticoagulants on the sFIDA readout of Aβ-SiNaP spiked plasma samples, the linearity of the data was assessed as well as the coefficient of variation (CV) as a criterion for intra-assay precision and limit of detection (LOD) as a criterion for assay sensitivity were calculated.

Linearity

The sFIDA assay is known to have a wide detection range for Aβ oligomers. However, the linearity of the assay's readout is influenced by a variety of factors. To investigate the impact of anticoagulants in blood plasma samples on the linearity of the sFIDA readout, the Pearson's correlation coefficient, Mandel's fitting test, and the Lack-of-fit test were calculated (Table 1).

Nearly ideal linear relationship in terms of Pearson's correlation of $\rho = 0.94$ was found for EDTA blood plasma and PBS diluents, whereas considerably lower values of $\rho = 0.37$ and $\rho = 0.64$ were obtained for dilutions in citrate and heparin blood plasma, respectively (Table 2). As Pearson's correlation coefficient ρ has very limited significance as a criterion for linearity, Mandel's fitting test as well as Lack-of-fit test for the first and second order calibration

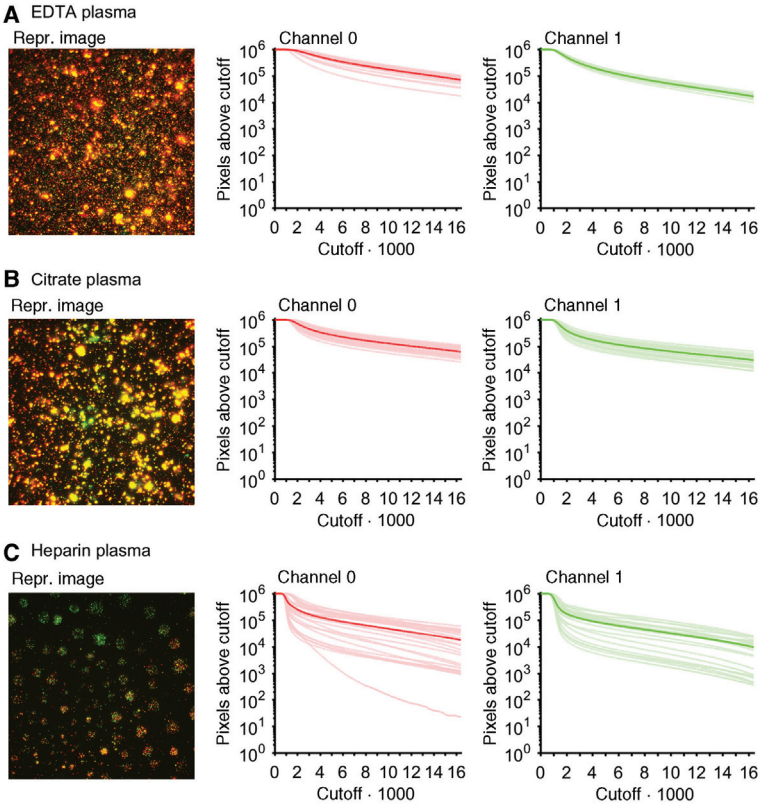

Figure 1: Representative images and cumulative histograms for 1 pM Aβ-SiNaP spiked in EDTA, citrate and heparin plasma.
1 pM Aβ-SiNaP was spiked in blood plasma treated with different anticoagulants from a single donor and subsequently applied to sFIDA assay. A representative image as a composition of channel 0 (exc.: 635 nm, em.: 705 nm) and channel 1 (exc.: 488 nm, em.: 525 nm) is given for (A) EDTA, (B) citrate and (C) heparin-treated plasma, respectively (left hand), as well as cumulative intensity histograms for channel 0 (middle) and channel 1 (right hand). Cumulative histograms for single images are depicted in a light color whereas the mean cumulative histogram is depicted in a dark color. The variation in intensity distribution between the images is higher for heparin compared to EDTA and citrate.

curve was performed which are recommended and well established methods for testing linearity (Van Loco et al., 2002; Sanagi et al., 2010). Likewise, Mandel's fitting test and Lack-of-fit test, respectively, indicate good linearity for EDTA plasma and PBS control, whereas for citrate and heparin a second order calibration curve is the function preferred (Table 1).

Coefficient of variation

CV was calculated to assess intra-assay precision, which differs between the anticoagulants (Figure 4). The lowest mean CV of 28% was obtained for EDTA plasma followed by 39% for citrate plasma and 67% for heparin plasma. For PBS a CV of 51% was obtained.

Limit of detection

LOD was calculated to investigate the effect of different anticoagulants on assay sensitivity as the mean for five donors. As each donor was measured in six replicates, the mean LOD calculation is based on 30 negative controls. Significant differences in mean LOD for Aβ-SiNaP dilution series in EDTA, citrate and heparin plasma

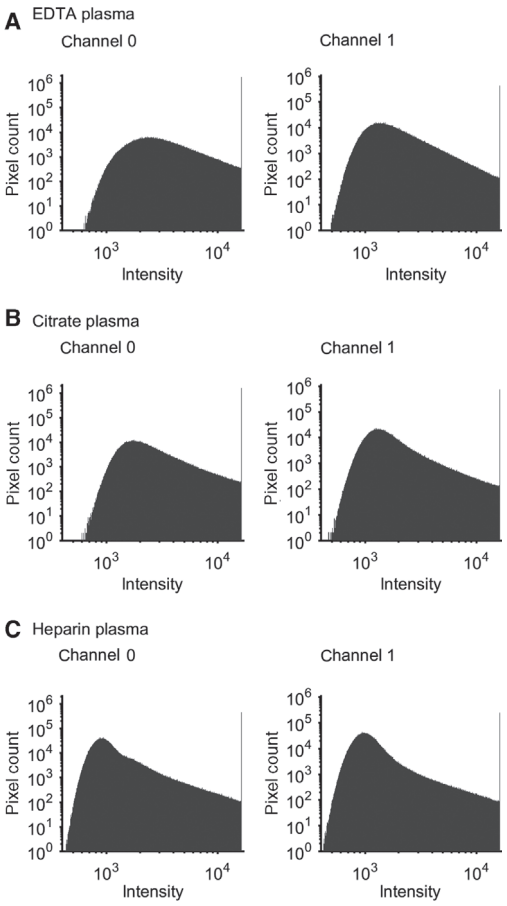

Figure 2: Intensity distribution for images obtained from 1 pM Aβ-SiNaPs spiked in EDTA, citrate and heparin plasma following sFIDA assay.
For channel 0 (exc.: 635 nm, em.: 705 nm) the major peak in intensity distribution for EDTA is approximately at 2400, for citrate at 1700 and for heparin plasma at 900 on a 14-bit grayscale, and for channel 1 (exc.: 488 nm, em.: 525 nm) at approximately 1300, 1300 and 1000, respectively.

as well as in PBS were observed (Figure 5). The lowest mean LOD of 16 fM was obtained for Aβ-SiNaPs spiked in EDTA plasma followed by 19 fM (incl. outlier: 34 fM) for citrate, 27 fM for PBS and 34 fM (incl. outlier: 280 fM) for heparin. Additionally, the median LOD was calculated being more robust towards outliers as observed for citrate and heparin. In agreement with mean LOD, the lowest median LOD of 16 fM was obtained for Aβ-SiNaP spiked in EDTA plasma followed by 22 fM for citrate plasma, 23 fM for PBS and 31 fM for heparin plasma (data not shown).

Summary

Mean Pearson's correlation coefficient between spiked Aβ-SiNaPs and sFIDA readout, mean CV (%) and mean LOD for all three anticoagulants and PBS are summarized in Table 2. Highest linearity, highest intra-assay precision and highest sensitivity of the sFIDA assay was obtained for Aβ-SiNaP-spiked EDTA plasma.

Discussion

The choice of anticoagulants for blood plasma preparation can have a significant impact on the detection of biomarkers. The aim of the present study was to compare the effect of different anticoagulants on the sFIDA readout and identify the most suitable anticoagulant regarding assay standardization. For this purpose, a dilution series of Aβ-SiNaPs was spiked in human blood plasma samples supplemented with different anticoagulants (EDTA, citrate and heparin, respectively) and was subsequently applied to the sFIDA assay. The assay outcome was evaluated by means of three parameters: the linearity of the sFIDA readout as a function of applied Aβ-SiNaP concentration, the coefficient of variation as well as the limit of detection.

The highest linearity for mean Pearson's correlation coefficient ρ of 0.94 was calculated for Aβ-SiNaPs spiked in EDTA plasma followed by heparin ($\rho = 0.94$) and citrate ($\rho = 0.37$) plasma. The lowest mean CV of 28% was obtained for EDTA followed by citrate (CV = 39%) and heparin plasma (CV = 67%). The lowest LOD of 16 fM was obtained for quantitation of Aβ-SiNaPs spiked in EDTA plasma followed by LOD of 19 fM and 34 fM for citrate and heparin plasma, respectively.

EDTA, citrate and heparin are the most common anticoagulants for blood plasma treatment in clinical practice. Whereas the anticoagulative effect of EDTA and citrate is attributed to the prevention of thrombin formation by chelating calcium required for the blood clotting cascade (Davie and Ratnoff, 1964), heparin functions by activating antithrombin (Olson and Chuang, 2002). Apart from this, heparin is known to bind to a variety of proteins including proteases, growth factors, chemokines, lipid binding proteins and adhesion proteins as summarized in Capila and

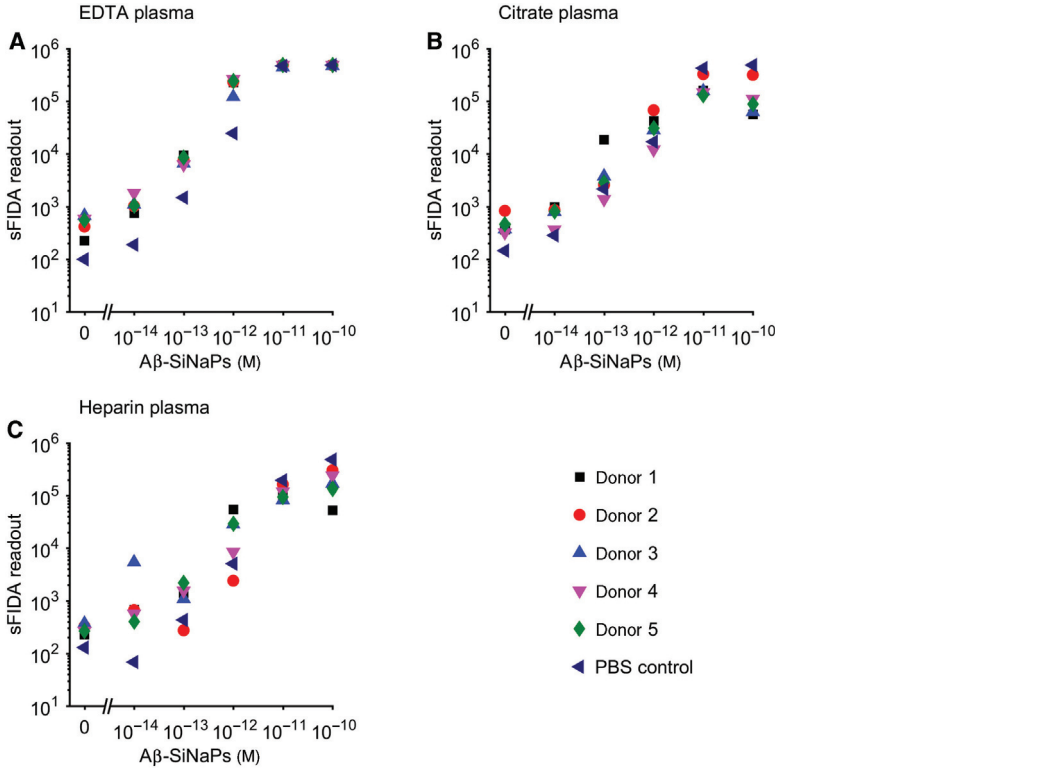

Figure 3: sFIDA readout for Aβ-SiNaPs spiked in EDTA, citrate and heparin plasma from five individual donors as well as in PBS. Aβ-SiNaPs were serially diluted to 100 pM, 10 pM, 1 pM, 100 fM and 10 fM. As negative controls, non-spiked plasma samples were used (respective 0 M Aβ-SiNaP data points). Black rectangular symbols represent the sFIDA readout for donor 1, red circular symbols for donor 2, blue up-top triangular symbols for donor 3, magenta down-top triangular symbols for donor 4, green rhombical symbol for donor 5 and dark blue left-top triangular symbols for PBS control.

Linhardt (2002) and thus might modulate matrix effects significantly by affecting the biochemical constitution of blood plasma. Moreover, it has been shown in several studies that heparin binds directly to Aβ species (Watson et al., 1997; Madine et al., 2012; Nguyen and Rabenstein, 2016) possibly interfering with Aβ oligomer quantitation and accounting for the attenuating effects in sFIDA assay presented here.

Altogether, this is in line with studies on quantitation of total Aβ levels from blood plasma. Vanderstichele et al. (2000) reported that plasma collected in citrate and heparin tubes did not result in any measurable Aβ levels, whereas Aβ levels in EDTA plasma could be readily detected (Vanderstichele et al., 2000). Lachno et al. (2009) determined total Aβ levels in serum, EDTA, citrate, heparin and fluoride plasma with highest Aβ levels in EDTA-treated plasma (Lachno et al., 2009).

The well-described binding of Aβ to various plasma proteins (Koudinov et al., 1994; Biere et al., 1996; Koudinov et al., 1998) might lead to a masking of epitopes and ultimately result in signal attenuation due to impaired capturing and probe detection. Previously, an interaction between prion protein aggregates and low density lipoproteins has been reported, making pretreatment with lipases and detergents necessary to counteract signal loss in sFIDA measurements (Safar et al., 2006; Bannach et al., 2012). In the present study, however, the presence of EDTA plasma did not have any adverse effect on detection and quantitation of Aβ-SiNaP down to the low femtomolar range.

Table 1: Analysis on linearity of sFIDA readout from Aβ-SiNaP dilution series.

	Pearson	Mandel's test		Lack-of-fit test (LRM)		Lack-of-fit test (QRM)	
	ρ	*PW*	*F*	LOF	*F*	LOF	*F*
EDTA 1	0.97	0.88	9.33	3.94	7.21	0.17	7.21
EDTA 2	0.98	1.16	10.04	6.35	8.02	0.12	8.02
EDTA 3	0.99	1.71	9.33	3.94	7.21	0.08	7.21
EDTA 4	0.78	0.13	9.33	3.17	7.21	2.33	7.21
EDTA 5	0.97	1.12	9.33	5.04	7.21	0.15	7.21
Citrate 1	0.1	138.29	8.28	52.22	4.89	1.88	4.89
Citrate 2	0.64	127.13	8.28	36.96	4.89	0.63	4.89
Citrate 3	0.19	204.31	8.28	56.76	4.89	0.34	4.89
Citrate 4	0.5	131.22	8.28	33.64	4.89	0.58	4.89
Citrate 5	0.42	69.77	8.28	21.01	4.89	0.86	4.89
Heparin 1	0.16	10.36	8.28	4.62	4.89	1.86	4.89
Heparin 2	0.87	46.14	8.28	11.79	4.89	5.80	4.89
Heparin 3	0.77	6.45	8.28	2.90	4.89	1.24	4.89
Heparin 4	0.70	3.92	8.28	2.36	4.89	1.58	4.89
Heparin 5	0.69	12.04	8.28	5.27	4.89	2.09	4.89
PBS 1	0.92	0.14	9.33	1.74	7.21	0.47	7.21
PBS 2	0.98	0.12	9.33	0.18	7.21	0.16	7.21
PBS 3	0.94	0.66	8.68	3.89	5.74	0.46	5.74

Pearson's correlation coefficient ρ, Mandel's test as well as Lack-of-fit test was calculated to analyze the linearity of sFIDA readout from SiNaP dilution series at a significance level of 99%. For the Mandel-test, H_0 assumes no significant difference between the residual variances. For $PW < F$ H_0 is accepted, the calibration function of choice is linear. For the Lack-of-fit test, H_0 assumes that the applied model is appropriate, lack of fit occurs at LOF > $F_{crit,99\%}$.

Table 2: Summary of analysis on the effect of different anitcoagulants on assay outcome parameters.

Anticoagulant	ρ	CV (%)	LOD (fM)
EDTA	0.94	28	16
Citrate	0.37	39	19
Heparin	0.64	67	34
PBS	0.94	51	27

The assay outcome was evaluated by means of three parameters: the linearity of the sFIDA readout as a function of applied Aβ-SiNaP concentration (mean Pearson's correlation coefficient ρ), the mean coefficient of variation (CV) as well as the mean limit of detection (LOD).

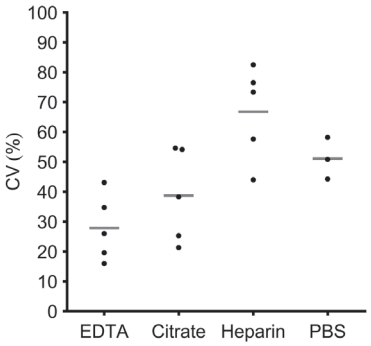

Figure 4: Coefficient of variation (CV) of sFIDA measurements for Aβ-SiNaPs diluted in EDTA, citrate and heparin plasma from five individual human donors.
The mean coefficient of variation [CV(%)] for the sFIDA readout was obtained for Aβ dilution series spiked in plasma samples from five different donors. The CV(%) was calculated as the standard deviation weighted by the mean sFIDA readout. The lowest and highest mean LOD is gained from EDTA and heparin treated blood plasma, respectively.

The achieved coefficient of variation of 28% is a severe issue for further improvement. Also, more validation parameters as suggested by Andreasson et al. (2015) (Andreasson et al., 2015) need to be addressed in future.

We conclude that EDTA is the most suitable anticoagulant for Aβ-SiNaP quantitation in blood plasma using the sFIDA assay. We therefore suggest that plasma samples for AD diagnosis in the sFIDA assay should be collected in EDTA tubes to ensure most accurate determination of Aβ oligomer levels in human blood plasma. Future investigations, however, will reveal whether humans do contain detectable amounts of Aβ oligomers and whether they correlate with disease progression or prognosis. Thus, further work will focus on sFIDA measurements of clinical EDTA plasma samples from AD patients and controls in order to

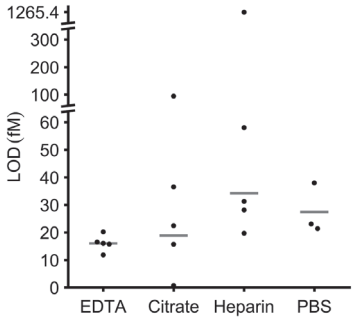

Figure 5: Limit of detection (LOD) from sFIDA measurements of Aβ-SiNaPs spiked in EDTA, citrate and heparin plasma from five donors as well as in PBS.
The mean limit of detection (LOD) for Aβ-SiNaPs spiked in blood plasma was obtained for six replicate measurements of each dilution series in samples from five different donors. The LOD was calculated from the sFIDA readout from the respective negative control plus three times the standard deviation. The lowest mean LOD of 16 fM was obtained for Aβ-SiNaPs spiked in EDTA plasma followed by 19 fM (incl. outlier: 34 fM) for citrate, 27 fM for PBS and 34 fM (incl. outlier: 280 fM) for heparin.

assess if Aβ oligomers can be exploited as a blood-based biomarker for AD.

Materials and methods

Plasma samples

A total of 15 blood plasma samples from five healthy donors were purchased from ZenBio, Inc. (BioCat GmbH, Heidelberg, Germany). Plasma samples were collected in BD Vacutainer tubes containing 12.15 mg K_2EDTA per 7.0 ml sample, 158 USP units Heparin per 10.0 ml sample or 1 ml acid-citrate-dextrose solution B (4.8 g/l citric acid; 13.2 g/l Na_3Citrate; 14.7 g/l dextrose) per 6 ml sample, respectively. To avoid repeated freeze/thaw cycles, plasma samples were directly aliquoted and stored at −80°C until usage. Prior to aliquoting, plasma samples were centrifuged for 10 min at 20 000 *g* and the supernatant was preserved.

Silica nanoparticles coated with $A\beta_{1-42}$ (Aβ-SiNaPs)

Aβ-SiNaPs were prepared as described previously (Hülsemann et al., 2016). Briefly, bare silica nanoparticles (SiNaPs) were synthesized via Stöber process and silanized with APTES to cover the surface with primary amino groups. Subsequent reaction with succinic anhydride resulted in carboxylated SiNaPs, which were activated by EDC/NHS for covalent coupling of $A\beta_{1-42}$. The same batch of Aβ-SiNaPs was used for all spiking experiments to ensure equal size (diameter of approx. 30 nm) of the particles and Aβ distribution on the surface. 1 nM Aβ-SiNaP stock solution was serially diluted to 100 pM, 10 pM, 1 pM, 100 fM and 10 fM in plasma samples and PBS.

sFIDA protocol

For sFIDA assay a 384-well multititer plate (SensoPlate plus, Greiner Bio-One International, Frickenhausen, Germany) was used. All of the protocol steps were carried out under the clean bench to avoid dust and microbial contamination. Prior to functionalization of the glass surface, wells were cleaned with sodium hydroxide and hydrochloric acid. 5 M NaOH (Carl Roth, Karlsruhe, Germany) was applied for 15 min to the wells (95 µl/well) followed by three washing steps with the same volume of water. Immediately, 1 M HCl (32%, AnalaR NORMAPUR, VWR Chemicals, France) was incubated for 15 min in the wells (95 µl/well) followed by three washing steps with water and two washing steps with 70% ethanol (AnalaR NORMAPUR, VWR Chemicals, France). Shortly after wells dried at room temperature (RT), 45 µl of a DMSO (Sigma-Aldrich, Steinheim, Germany) ethanolamine mixture (Sigma-Aldrich, Steinheim, Germany) (v/v 2:3) was added to the wells and incubated overnight at RT. Afterwards, the wells were washed twice with DMSO and twice with 95 µl/well 70% ethanol and left to dry. In the meantime, NHS-PEG-COOH (MW 5000, Laysan Bio, USA) was solved at 70°C in DMSO and cooled down to RT. 15 µl of 2 mM PEG solution were applied per well for 1 h followed by three washing steps with water. Activation of the PEG carboxyl groups was then performed by applying 30 µl/well of 100 mM EDC (Fluka, Buchs, Switzerland) and 100 mM NHS (Aldrich, Milwaukee, USA) mixture (v/v 1:1) in 0.1 M MES (Carl ROTH, Karlsruhe, Germany) buffer (pH 3.5) for 30 min. After washing the wells three times quickly with MES buffer, 15 µl/well capture antibody was added immediately for 1 h to the wells. As capture antibody, monoclonal anti-β-amyloid antibody NAB228 (Sigma-Aldrich, Steinheim, Germany) was diluted in PBS (Dulbecco's phosphate buffered saline 10×, Sigma-Aldrich, Steinheim, Germany) to a final concentration of 10 ng/µl and centrifuged at 15 000 *g* for 10 min to remove the unsoluble components. Hereafter, the wells were washed twice with PBS-T (PBS + 0.05% Tween-20, Sigma-Aldrich, Steinheim, Germany) and twice with PBS. Next the surface was blocked with 50 µl/well Smart Block solution (Candor Bioscience, Wangen, Germany) followed by two washing steps with PBS-T and two steps with PBS. 15 µl/well sample was then applied to the surface and incubated overnight. Unbound sample components were removed by two washing steps with PBS-T and two washing steps with PBS. Finally, fluorescently labeled detection antibodies 6E10 Alexa Fluor 488 (Covance, Princeton, USA) and NAB228 Alexa Fluor 647 (Santa Cruz, Dallas, USA) were combined to the final concentration of 1.25 ng/µl each, centrifuged at 100 000 *g* for 1 h and applied to the wells (15 µl/well). After final washing twice with PBS-T and twice with PBS, wells were filled with 95 µl PBS.

Data acquisition

Acquisition of 14-bit grayscale images was performed using total internal reflection microscopy (AM TIRF MC, Leica Microsystems, Wetzlar, Germany). A total of 50 images per well (25 positions per channel) containing 1000 × 1000 pixels each were obtained for channel 0 (excitation at 635 nm, emission filter 705/72 nm) and channel 1 (excitation at 488 nm, emission filter 525/36 nm). The image size

represents an area of 116 µm × 116 µm, thus in total 3.15% of the well surface (approximately 10 nm^2) were scanned. Laser intensity of 100%, exposure time between 1 s and 1.5 s and gain between 900 and 1000 were applied for image acquisition.

Artifact detection

Prior to data analysis, artificial images were removed from raw data pool applying two algorithms based on histogram analysis and cluster detection, respectively.

First, images were subjected to histogram artifact detection. This method is based on calculating the histogram for each image and counting the peaks by determination of local maxima in the histogram. Images with multimodal histograms (histograms containing more than one histogram maximum) were considered artificial and were excluded from further analysis. The image histogram was smoothed using 800 values for binning to eliminate background noise and thus avoid detection of local maxima. Via numerical differentiation the derivative of the smoothed histogram was calculated, which was then smoothed in the same way as the original histogram. After smoothing procedures, some rest noise can still cause local maxima especially at points where function overlaps the x-axis. In order to determine the parameters for exclusion of images based on their histogram, a threshold was defined that includes two components: α and β. α is the number of pixels that form a maximum, β is a number of pixels that form a minimum. Only if α and β of adjacent maximum and minimum are high enough to meet α and β limits, a maximum was treated as a maximum. α limit of 400 and β limit of 300 were chosen as parameters for maxima determination.

Second, images with unimodal histograms (histograms with a single maximum) can still contain artifacts in form of large and/or bright spots. To detect these spots, a cluster detection algorithm was applied to the images. This method is based on finding of agglomerations of pixels with intensities above a certain threshold. Depending on such parameters as cluster size, mean pixel intensity and standard deviation within a cluster, bright spots are identified as artifacts. Obtained grayscale images were transformed into binary images. The grayscale values with intensities ≤ mean grayscale value plus one standard deviation were set to 0, all others to 1. Using a rectangular structuring element with the size of 15 pixels × 15 pixels the images were eroded to identify large clusters and eliminate the small ones which represent Aβ-SiNaPs. To compensate pixel loss caused by erosion, dilation was applied to eroded images using the same structuring element.

An image was considered artificial and was excluded from further analysis, if at least one cluster fulfilled one of the following criteria: mean pixel intensity of more than 3000, a standard deviation of pixel intensity of more then 2800 or skewness of less than 0.

Data analysis

sFIDA readout: For data analysis of non-artificial images only a region of interest (ROI) consisting of the central 700 pixels × 700 pixels (corresponding to 490 000 pixels per image in total) was chosen in order to minimize the effects of inhomogeneous illumination of edge regions in TIRF microscopy images.

To reduce background noise, cutoffs were determined individually for each plasma sample based on the non-spiked control. This approach accounts for donor-specific background or signal by native Aβ oligomers which may influence the readout. For Aβ-SiNaPs diluted in PBS, the cutoff was determined from PBS control. The cutoff values for each channel were determined as the intensity, which was exceeded by 1% of total pixels. Number of colocalized pixels from both channels above the respective cutoff is referred to as sFIDA readout below.

The effects of different anticoagulants in plasma on sFIDA readouts were studied according to the criteria described below.

Linearity of the sFIDA readout

Pearson's correlation coefficient

Pearson's correlation coefficient (ρ) was calculated with MATLAB software as a criterion for linearity of the correlation between applied concentrations of Aβ-SiNaPs and obtained sFIDA readouts according to the formula:

$$\rho = \frac{N\sum xy - \sum x \sum y}{\sqrt{\left[N\sum x^2 - \left(\sum x\right)^2\right]\left[N\sum y^2 - \left(\sum y\right)^2\right]}}$$

where x is concentration of Aβ-SiNaPs, y is the sFIDA readout and N is the number of x,y pairs. Prior to mean value calculation, Olkin & Pratt correction was performed on Pearson's correlation coefficients (Olkin and Pratt, 1958; Eid et al., 2013). Briefly, ρ was transformed to G_i according to the formula:

$$G_i = \rho_i\left(1 + \frac{1-\rho_i^2}{2(n_i - 1 - 3)}\right)$$

where n is the number of samples in study i. Next, the weighted mean of G_i values was calculated for studies from $i = 1,\ldots,k$ according to the formula:

$$\overline{G} = \frac{\sum_{i=1}^{k} n_i G_i}{\sum_{i=1}^{k} n_i}$$

Thus, $\overline{G}$ is an estimator for mean correlation.

Test for linearity according to Mandel (Mandel's test)

The linearity of the sFIDA readout was further investigated using Mandel's fitting test (Mandel, 1964). This method provides evidence on linearity under consideration of the residual standard deviation for the first (linear) and second order (quadratic) calibration function. The H_0 hypothesis assumes no significant difference between the residual variances of the linear and quadratic calibration function. The Mandel's test was performed as follows (Funk et al., 2005; Bruggemann et al., 2006): the first and second order calibration functions are calculated including the residual standard deviations s_{y_1} and s_{y_2}:

$$s_{y_1} = \sqrt{\frac{\sum (y_i - \hat{y}_i)^2}{N-2}}, \quad \text{where } \hat{y}_i = a + bx_i$$

$$s_{y_2} = \sqrt{\frac{\sum (y_i - \hat{y}_i)^2}{N-3}}, \quad \text{where } \hat{y}_i = a + bx_i + cx_i^2$$

with:

y_i: observed sFIDA readout at each concentration level i

$\hat{y}_i$: estimation obtained from the respective regression analysis at i

N: total number of measurements

Next, the difference of the variances DS^2 is calculated based on the residual standard deviation s_{y_1} and s_{y_2}:

$$DS^2 = (N-2)s_{y_1}{}^2 - (N-3)s_{y_2}{}^2$$

Finally, the test value PW is calculated:

$$PW = \frac{DS^2}{s_{y_2}{}^2}$$

For the F-test, PW is compared with the corresponding value of the F-distribution $F_{\text{crit},99\%(f_1,f_2,\alpha)}$, with $f_1 = 1$ and $f_2 = N-3$ degrees of freedom at the significance level $\alpha = 0.01$.

For $PW < F_{\text{crit},99\%}$ H_0 is accepted. The second order calibration function will not provide a significantly better fit; the calibration function of choice is linear.

For $PW > F_{\text{crit},99\%}$ H_0 is retained, which indicates non-linearity (Bruggemann et al., 2006).

Lack-of-fit test

The Lack-of-fit test (Massart, 1997) is performed by comparing the ratio of the error due to lack of fit of the respective calibration function and the error due to pure error obtained from replicative measurements with $F_{\text{crit},99\%}$ at (k-2) and (n-k) degrees of freedom at the significance level $\alpha = 0.01$. The H_0 hypothesis assumes no lack of fit.

The Lack-of-fit test is calculated as follows: first, the sum of squares due to pure error and due to lack of fit are calculated, respectively:

$$SS_{\text{PE}} = \sum_i^k \sum_j^{n_i} (y_{ij} - \overline{y}_i)^2$$

$$SS_{\text{LOF}} = \sum_i^k n_i (\overline{y}_i - \hat{y}_i)^2$$

with:

i: concentration level, k: number of all concentration levels, n: number of replicates, $\overline{y}_i$ arithmetic mean of all observed values at i, $\hat{y}_i$: estimation obtained from the respective regression analysis at i. Next, the mean squares are calculated by dividing the sum of squares by the corresponding degrees of freedom (Massart, 1997).

$$MS_{\text{LOF}} = \frac{SS_{\text{LOF}}}{df}$$

$$MS_{\text{PE}} = \frac{SS_{\text{PE}}}{df}$$

For the F-test, the test value LOF is calculated as the arithmetic mean of both mean squares:

$$\text{LOF} = \frac{MS_{\text{LOF}}}{MS_{\text{PE}}}$$

For $\text{LOF} < F_{\text{crit},99\%}$ H_0 is accepted. There is no lack of fit. For $\text{LOF} > F_{\text{crit},99\%}$ H_0 is rejected. Saturated images for which sFIDA readout reached the maximum value of 490 000 (100 pM and 10 pM Aβ-SiNaPs in EDTA plasma as well as 100 pM Aβ-SiNaPs in PBS) were excluded from this analysis.

Coefficient of variation

CV was calculated as a criterion for intra-assay precision using Excel software. CV was calculated for each three replicate measurements for each standard concentration and negative control. The mean for each donor and each diluent was plotted using MATLAB software. Saturated images for 100 pM and 10 pM Aβ-SiNaPs in EDTA plasma as well as 100 pM Aβ-SiNaPs in PBS were excluded from this analysis.

Limit of detection

LOD was used as a criterion for sensitivity of the sFIDA assay. LOD was calculated as the mean from sFIDA readout for 6-fold replicate measurements of negative control (neg. control) from five individual donors (30 negative controls in total) and respective standard deviation (σ) according to the formula:

$$\text{LOD} = \text{sFIDA readout}_{(\text{neg. control})} + 3\sigma$$

Linear calibration curves for the correlation between concentrations of Aβ-SiNaPs and sFIDA readout for LOD determination were calculated with MATLAB software. Only values within the linear range of the obtained data were included for calculating the linear calibration curves (concentrations of 10 fM, 100 fM and 1 pM for all donors and anticoagulants). Using these calibration curves, the sFIDA readouts were correlated to their respective concentration.

Acknowledgments: This work was supported by the Federal Ministry of Education and Research within the projects 'Validierung des Innovationspotenzials wissenschaftlicher Forschung – VIP' (03V0641), 'Kompetenznetz Degenerative Demenzen' (01GI1010A), and the JPND 'Neurodegenerative Disease Research/Biomarkers for Alzheimer's and Parkinson's disease' (01ED1203H), as well as the Michael J. Fox Foundation for Parkinson's Research (11084).

References

Andreasson, U., Perret-Liaudet, A., van Waalwijk van Doorn, L.J., Blennow, K., Chiasserini, D., Engelborghs, S., Fladby, T., Genc, S., Kruse, N., Kuiperij, H.B., et al. (2015). A practical guide to immunoassay method validation. Front. Neurol. *6*, 179.

Banks, R.E., Stanley, A.J., Cairns, D.A., Barrett, J.H., Clarke, P., Thompson, D., and Selby, P.J. (2005). Influences of blood sample processing on low-molecular-weight proteome identified by surface-enhanced laser desorption/ionization mass spectrometry. Clin. Chem. *51*, 1637–1649.

Bannach, O., Birkmann, E., Reinartz, E., Jaeger, K.E., Langeveld, J.P., Rohwer, R.G., Gregori, L., Terry, L.A., Willbold, D., Riesner, D. (2012). Detection of prion protein particles in blood plasma of scrapie infected sheep. PLoS One *7*, e36620.

Biere, A.L., Ostaszewski, B., Stimson, E.R., Hyman, B.T., Maggio, J.E., and Selkoe, D.J. (1996). Amyloid beta-peptide is transported on lipoproteins and albumin in human plasma. J. Biol. Chem. *271*, 32916–32922.

Birkmann, E., Henke, F., Weinmann, N., Dumpitak, C., Groschup, M., Funke, A., Willbold, D., and Riesner, D. (2007). Counting of single prion particles bound to a capture-antibody surface (surface-FIDA). Vet. Microbiol. *123*, 294–304.

Birkmann, E., Schafer, O., Weinmann, N., Dumpitak, C., Beekes, M., Jackman, R., Thorne, L., and Riesner, D. (2006). Detection of prion particles in samples of BSE and scrapie by fluorescence correlation spectroscopy without proteinase K digestion. Biol. Chem. *387*, 95–102.

Blennow, K. (2004). CSF biomarkers for mild cognitive impairment. J. Intern. Med. *256*, 224–234.

Blennow, K., Mattsson, N., Scholl, M., Hansson, O., and Zetterberg, H. (2015). Amyloid biomarkers in Alzheimer's disease. Trends Pharmacol. Sci. *36*, 297–309.

Bruggemann, L., Quapp, W., and Wennrich, R. (2006). Test for non-linearity concerning linear calibrated chemical measurements. Accredit. Qual. Assur. *11*, 625–631.

Capila, I. and R. Linhardt, J. (2002). Heparin-protein interactions. Angew. Chem. Int. Ed. Engl. *41*, 391–412.

Chuang, C. K., Lin, S.P., Y. Lin, T., and Huang, F.Y. (1998). Effects of anticoagulants in amino acid analysis: comparisons of heparin, EDTA, and sodium citrate in vacutainer tubes for plasma preparation. Clin. Chem. *44*, 1052–1056.

Davie, E. W. and O. Ratnoff, D. (1964). Waterfall sequence for intrinsic blood clotting. Science *145*, 1310–1312.

Eid, M., Gollwitzer, M., and Schmitt, M. (2013). Statistik und Forschungsmethoden Lehrbuch; mit Online-Materialien. Weinheim, Wiley-VCH.

Fendl, B., Weiss, R., Fischer, M.B., Spittler, A., and Weber, V. (2016). Characterization of extracellular vesicles in whole blood: Influence of pre-analytical parameters and visualization of vesicle-cell interactions using imaging flow cytometry. Biochem. Biophys. Res. Commun. *478*, 168–173.

Funk, W., Dammann, V., and Donnevert, G. (2005). Qualitätssicherung in der Analytischen Chemie Anwendungen in der Umwelt-, Lebensmittel- und Werkstoffanalytik, Biotechnologie und Medizintechnik; Weinheim, Wiley-VCH.

Funke, S.A., Birkmann, E., Henke, F., Gortz, P., Lange-Asschenfeldt, C., Riesner, D., and Willbold, D. (2007). Single particle detection of Aβ aggregates associated with Alzheimer's disease. Biochem. Biophys. Res. Commun. *364*, 902–907.

Funke, S.A., Wang, L., Birkmann, E., and Willbold, D. (2010). Single-particle detection system for Aβ aggregates: adaptation of surface-fluorescence intensity distribution analysis to laser scanning microscopy. Rejuvenation Res. *13*, 206–209.

Gerlach, R. F., Uzuelli, J.A., Souza-Tarla, C.D., and Tanus-Santos, J.E. (2005). Effect of anticoagulants on the determination of plasma matrix metalloproteinase (MMP)-2 and MMP-9 activities. Anal. Biochem. *344*, 147–149.

Haass, C. and D. Selkoe, J. (2007). Soluble protein oligomers in neurodegeneration: lessons from the Alzheimer's amyloid β-peptide. Nat. Rev. Mol. Cell Biol. *8*, 101–112.

Hsieh, S.Y., Chen, R.K., Pan, Y.H., and Lee, H.L. (2006). Systematical evaluation of the effects of sample collection procedures on low-molecular-weight serum/plasma proteome profiling. Proteomics *6*, 3189–3198.

Hubbard, R.W., Chambers, J.G., Sanchez, A., Slocum, R., and Lee, P. (1988). Amino acid analysis of plasma: studies in sample preparation. J. Chromatogr. *431*, 163–169.

Hülsemann, M., Zafiu, C., Kühbach, K., Luhmann, N., Herrmann, Y., Peters, L., Linnartz, C., Willbold, J., Kravchenko, K., Kulawik, A., et al. (2016). Biofunctionalized silica nanoparticles: standards in amyloid-β oligomer-based diagnosis of Alzheimer's disease. J Alzheimers Dis. *54*, 79–98.

Jambunathan, K. and A. Galande, K. (2014). Sample collection in clinical proteomics–proteolytic activity profile of serum and plasma. Proteomics Clin. Appl. *8*, 299–307.

Koudinov, A., Matsubara, E., Frangione, B., and Ghiso, J. (1994). The soluble form of Alzheimer's amyloid β protein is complexed to high density lipoprotein 3 and very high density lipoprotein in normal human plasma. Biochem. Biophys. Res. Commun. *205*, 1164–1171.

Koudinov, A. R., Berezov, T.T., Kumar, A., and N. Koudinova, V. (1998). Alzheimer's amyloid β interaction with normal human plasma high density lipoprotein: association with apolipoprotein and lipids. Clin. Chim. Acta *270*, 75–84.

Kühbach, K., Hülsemann, M., Herrmann, Y., Kravchenko, K., Kulawik, A., Linnartz, C., Peters, L., Wang, K., Willbold, J., Willbold, D., et al. (2016). Application of an amyloid β oligomer standard in the sFIDA assay. Front. Neurosci. *10*, 8.

Lachno, D.R., Vanderstichele, H., De Groote, G., Kostanjevecki, V., De Meyer, G., Siemers, E.R., Willey, M.B., Bourdage, J.S., Konrad, R.J., Dean, R.A. (2009). The influence of matrix type, diurnal rhythm and sample collection and processing on the measurement of plasma β-amyloid isoforms using the INNO-BIA plasma Aβ forms multiplex assay. J. Nutr. Health. Aging *13*, 220–225.

Leidinger, P., Backes, C., Rheinheimer, S., Keller, A., and Meese, E. (2015). Towards clinical applications of blood-borne miRNA signatures: the influence of the anticoagulant EDTA on miRNA abundance. PLoS One *10*, e0143321.

Madine, J., Pandya, M.J., Hicks, M.R., Rodger, A., Yates, E.A., S. Radford, E., and D. Middleton, A. (2012). Site-specific identification of an Aβ fibril-heparin interaction site by using solid-state NMR spectroscopy. Angew. Chem. Int. Ed. Engl. *51*, 13140–13143.

Mandel, J. (1964). The statistical analysis of experimental data. New York [u.a.], Wiley Interscience.

Massart, D.L. (1997). Handbook of chemometrics and qualimetrics Elektronische Ressource. Amsterdam, New York, Elsevier.

Nguyen, K. and D. Rabenstein, L. (2016). Interaction of the heparin-binding consensus sequence of β-amyloid peptides with heparin and heparin-derived oligosaccharides. J. Phys. Chem. B *120*, 2187–2197.

Olkin, I. and J. Pratt, W. (1958). Unbiased Estimation of Certain Correlation Coefficients. Ann. Math. Statist. *29*, 201–211.

Olson, S.T. and Chuang, Y.J. (2002). Heparin activates antithrombin anticoagulant function by generating new interaction sites (exosites) for blood clotting proteinases. Trends Cardiovasc. Med. *12*, 331–338.

Parvy, P.R., J. Bardet, I., and Kamoun, P.P. (1983). EDTA in vacutainer tubes can interfere with plasma amino acid analysis. Clin. Chem. *29*, 735.

Ribeiro, A., Ritter, T., Griffin, M., and Ceredig, R. (2016). Development of a flow cytometry-based potency assay for measuring the *in vitro* immunomodulatory properties of mesenchymal stromal cells. Immunol. Lett. *177*: 38–46.

Riches, P., Gooding, R., Millar, B.C., and Rowbottom, A.W. (1992). Influence of collection and separation of blood samples on plasma IL-1, IL-6 and TNF-α concentrations. J. Immunol. Methods *153*, 125–131.

Safar, J. G., Wille, H., Geschwind, M.D., Deering, C., Latawiec, D., Serban, A., King, D.J., Legname, G., Weisgraber, K.H., Mahley, R.W., et al. (2006). Human prions and plasma lipoproteins. Proc. Natl. Acad Sci. USA *103*, 11312–11317.

Sanagi, M.M., Nasir, Z., Ling, S.L., Hermawan, D., Ibrahim, W.A., and Naim, A.A. (2010). A practical approach for linearity assessment of calibration curves under the International Union of Pure and Applied Chemistry (IUPAC) guidelines for an in-house validation of method of analysis. J. AOAC Int. *93*, 1322–1330.

Selkoe, D.J. (1991). The molecular pathology of Alzheimer's disease. Neuron *6*, 487–498.

Van Loco, J., Elskens, M., Croux, C., and Beernaert, H. (2002). Linearity of calibration curves: use and misuse of the correlation coefficient. Accredit. Qual. Assur. *7*, 281–285.

Vanderstichele, H., Van Kerschaver, E., Hesse, C., Davidsson, P., Buyse, M.A., Andreasen, N., Minthon, L., Wallin, A., Blennow, K., Vanmechelen, E. (2000). Standardization of measurement of β-amyloid(1-42) in cerebrospinal fluid and plasma. Amyloid *7*, 245–258.

Wang-Dietrich, L., Funke, S.A., Kuhbach, K., Wang, K., Besmehn, A., Willbold, S., Cinar, Y., Bannach, O., Birkmann, E, Willbold, D. (2013). The amyloid-β oligomer count in cerebrospinal fluid is a biomarker for Alzheimer's disease. J. Alzheimers Dis. *34*, 985–994.

Watson, D. J., A. Lander, D., and D. Selkoe, J. (1997). Heparin-binding properties of the amyloidogenic peptides Aβ and amylin. Dependence on aggregation state and inhibition by Congo red. J. Biol. Chem. *272*, 31617–31624.

Wimo, A., Jonsson, L., Bond, J., Prince, M., Winblad, B., and Alzheimer Disease International. (2013). The worldwide economic impact of dementia 2010. Alzheimer's Dement. *9*, 1–11.e13.

3.4 sFIDA automation yields sub-femtomolar limit of detection for Aβ aggregates in body liquids

Autoren: Yvonne Herrmann, Andreas Kulawik, Katja Kühbach, Maren Hülsemann, Luriano Peters, Tuyen Bujnicki, Kateryna Kravchenko, Christina Linnartz, Johannes Willbold, Christian Zafiu, Oliver Bannach und Dieter Willbold

Publiziert in: Clinical Biochemistry (Herrmann et al., 2016)

DOI: http:\\dx.doi.org\10.1016\j.clinbiochem.2016.11.001.

Impact Factor (2015): 2.382

Eigener Anteil: 65%

Implementierung, Etablierung und Durchführung der sFIDA-Studie mit Aβ-SiNaPs auf dem automatisierten System, Mitentwicklung der experimentellen Details des sFIDA-Ablaufes, Auswertung der sFIDA-Daten und Bestimmung der Intra-Assay Parameter und Schreiben des Manuskripts

ARTICLE IN PRESS

CLB-09404; No. of pages: 4; 4C:

Clinical Biochemistry xxx (2016) xxx–xxx

Contents lists available at ScienceDirect

Clinical Biochemistry

journal homepage: www.elsevier.com/locate/clinbiochem

Short Communication

sFIDA automation yields sub-femtomolar limit of detection for Aβ aggregates in body fluids

Yvonne Herrmann [a], Andreas Kulawik [a], Katja Kühbach [a], Maren Hülsemann [a], Luriano Peters [a], Tuyen Bujnicki [a], Kateryna Kravchenko [a], Christina Linnartz [a], Johannes Willbold [a], Christian Zafiu [a], Oliver Bannach [a,b], Dieter Willbold [a,b,*]

[a] Forschungszentrum Jülich, ICS-6 Structural Biochemistry, 52428 Jülich, Germany
[b] Heinrich-Heine-Universität Düsseldorf, Institut für Physikalische Biologie, 40225 Düsseldorf, Germany

ARTICLE INFO

Article history:
Received 13 June 2016
Received in revised form 22 October 2016
Accepted 2 November 2016
Available online xxxx

Keywords:
Alzheimer's disease
Amyloid β peptide
Diagnostic biomarker
Surface-based fluorescence intensity distribution analysis (sFIDA)
Silica nanoparticles
Automation

ABSTRACT

Objectives: Alzheimer's disease (AD) is a neurodegenerative disorder with yet non-existent therapeutic and limited diagnostic options. Reliable biomarker-based AD diagnostics are of utmost importance for the development and application of therapeutic substances. We have previously introduced a platform technology designated 'sFIDA' for the quantitation of amyloid β peptide (Aβ) aggregates as AD biomarker. In this study we implemented the sFIDA assay on an automated platform to enhance robustness and performance of the assay.

Design and methods: In sFIDA (surface-based fluorescence intensity distribution analysis) Aβ species are immobilized by a capture antibody to a glass surface. Aβ aggregates are then multiply loaded with fluorescent antibodies and quantitated by high resolution fluorescence microscopy. As a model system for Aβ aggregates, we used Aβ-conjugated silica nanoparticles (Aβ-SiNaPs) diluted in PBS buffer and cerebrospinal fluid, respectively. Automation of the assay was realized on a liquid handling system in combination with a microplate washer.

Results: The automation of the sFIDA assay results in improved intra-assay precision, linearity and sensitivity in comparison to the manual application, and achieved a limit of detection in the sub-femtomolar range.

Conclusions: Automation improves the precision and sensitivity of the sFIDA assay, which is a prerequisite for high-throughput measurements and future application of the technology in routine AD diagnostics.

1. Introduction

Alzheimer's disease (AD) is a neurodegenerative disorder that accounts for most cases of age-related dementia. AD is characterized by progressive neuronal loss in brain areas associated with cognitive learning and memory. There is neither a causative treatment nor a sufficiently reliable biomarker for an accurate diagnosis at the preclinical stage of the disease. The definitive diagnosis can only be made after the patients' death based on neuropathological features, such as neurodegeneration, neurofibrillary tangles and amyloid plaques, which mainly embody aggregated amyloid β (Aβ) deposits. However, recent evidence indicates that smaller and soluble Aβ oligomers are the most neurotoxic species and therefore represent a promising drug target in clinical studies and presumably the most direct biomarker for early AD diagnostics [1].

Previously, we have described the surface-based fluorescence intensity distribution analysis (sFIDA) technology as an oligomer-specific quantitation method for biomarker-based diagnostics of AD [2–9]. In sFIDA, Aβ species are captured by an N-terminal specific anti-Aβ-antibody on a glass surface, and Aβ oligomers are probed by two different fluorescence labelled antibodies. Since sFIDA employs overlapping epitopes in the capture and detection system, Aβ monomers are not detected. Images from the surface are obtained using dual-color total internal reflection fluorescence microscopy (TIRFM). The number of colocalized pixels in both channels is referred to as sFIDA readout and correlates with the concentration of Aβ oligomers in the sample. Recently, we have introduced Aβ-coated silica nanoparticles (Aβ-SiNaPs) as a model system for Aβ oligomers with respect to size and surface epitopes [9].

The low concentration of Aβ oligomers in body fluids such as cerebrospinal fluid (CSF) as well as excessive concentrations of monomeric Aβ and matrix components require highly sensitive and precise quantitation technologies. In this respect, assay automation provides stability and robustness by rendering underlying processes independent of human skill levels and error-proneness [10].

In this study, we automated the sFIDA assay on a liquid handling system combined with a microplate washer. From sFIDA measurements of Aβ-SiNaPs diluted in CSF and PBS, we determined essential assay parameters for sensitivity, precision and linearity.

* Corresponding author at: Forschungszentrum Jülich, Wilhelm-Johnen-Str., 52428 Jülich, Germany.
E-mail address: d.willbold@fz-juelich.de (D. Willbold).

http://dx.doi.org/10.1016/j.clinbiochem.2016.11.001
0009-9120/

Please cite this article as: Y. Herrmann, et al., sFIDA automation yields sub-femtomolar limit of detection for Aβ aggregates in body fluids, Clin Biochem (2016), http://dx.doi.org/10.1016/j.clinbiochem.2016.11.001

2. Material and methods

2.1. Synthesis of silica nanoparticles coated with $A\beta_{1-42}$ (Aβ-SiNaPs)

Aβ-SiNaPs were prepared as described previously by Hülsemann et al. [9]. Briefly, SiNaPs were synthesized via Stöber process and silanized with 4-amino-3,3-dimethylbutyltrimethoxysilan (ABCR GmbH & Co. KG, Karlsruhe, Germany) to functionalize the surface with primary amino groups. Reaction with succinic anhydride resulted in carboxylated SiNaPs, which were activated by EDC/NHS for covalent coupling of $A\beta_{1-42}$ to the particle surface. The SiNaPs used in this study have a diameter of approx. 19 nm and provide approx. 150 Aβ-epitopes per particle.

2.2. Automation devices

For automated sFIDA, a liquid handling system (Hamilton, NV, USA) [11] in combination with a microplate washer (BioTek, VT, USA) was used (Supplemental Section A.1.).

2.3. sFIDA

The automated sFIDA assay was performed with minor modifications as described previously by Kravchenko et al. [8]. The distribution of reagents and samples as well as the wash steps with 70% ethanol and DMSO were performed by the liquid handling system, whereas all other wash procedures were executed by the microplate washer (Supplemental Section A.2.). Cerebrospinal fluid (CSF) was pooled from healthy human donors (Biochemed Services, Winchester, USA).

2.4. Image data acquisition and analysis

Total internal reflection microscopy (TIRFM) of the assay surface was performed as described previously by Kühbach et al. [7]. Briefly, images were obtained in two channels (excitation: 635 nm, emission filter: 705/72 nm and excitation: 488 nm, emission filter: 525/36 nm). Within each well 25 positions were imaged. Each image represents an area of 116 μm × 116 μm.

Image data was analyzed with an in-house developed software featuring artifact filtering [8] (Supplemental Section A3) and sFIDA readout calculation. To account for uneven illumination of edge regions (vignetting), only a region of interest of the central 58 μm × 58 μm was analyzed. To reduce background noise, cutoffs were defined as the signal intensity exceeding 0.1% of total pixels and were determined on PBS and CSF samples without Aβ-SiNaPs (blank measurements).

Finally, colocalized pixels above the respective cutoffs were defined as the sFIDA readout which was determined for 12 replicates of each sample and for 24 replicates of blank measurements.

2.5. Determination of assay parameters

Coefficient of variation (CV), linearity (Pearson's r, Mandel's test, lack-of-fit test) and limit of detection (LOD) of the sFIDA readout was determined as described previously [8,12]. (Supplemental Section A.4/5).

The LOD is defined as the lowest reliably detectable analyte concentration with reasonable certainty for a given analytical procedure [12]. The criterion for significance is a pairwise comparison of a sample and blank measurements as calculated by p-value adjusted one-sided *t*-tests with a confidence level of 95%, where H_1: The readout of the sample is higher than the readout of blank measurements. As a mathematical model the LOD is calculated based on determinants of the distribution of blank measurements, i.e. the location (mean) and dispersion (standard deviation) with a reasonable confidence of 3σ.

$$\mathrm{LOD} = \mathrm{sFIDA\ readout}_{(\mathrm{blank\ measurements})} \times 3\sigma$$

3. Results

Automation of the sFIDA assay was implemented on a liquid handling system equipped with an eight channel head and a microplate washer with 96 needles for liquid aspirating and dispensing. No action from laboratory personnel was required within the whole procedure. Aβ-SiNaPs were serially diluted from 10 pM to 1 fM in CSF and PBS, respectively, and dispensed into the wells in a random layout.

High-throughput automation allowed processing a high number of replicates (12 sample replicates and 24 blank measurements), which in turn enables exclusion of minimum and maximum values. We investigated the effect of four iterations excluding minimum and maximum values on the assay outcome parameters intra-assay precision (coefficient of variation, CV), sensitivity (limit of detection, LOD) and linearity (Pearson's r, Mandel's test, lack-of-fit test) for each dilution series (CSF and PBS).

A correlation between Aβ-SiNaPs concentration and sFIDA readout was observed in both diluents CSF and PBS, respectively, with significance between blank measurements (0 M) and the Aβ-SiNaPs-containing samples without (0 iterations) and with one to four iterations of excluding minimum and maximum values (Fig. 1). The calculated LODs in the femtomolar range for CSF (5 fM) and PBS (22 fM) (Table 1) are largely in accordance with the pairwise comparisons. Remarkably, after three and four iterations of excluding minimum and maximum values, respectively, the calculated LOD is in the sub-femtomolar range for CSF (0.85 fM) and PBS (0.93 fM).

The mean CV is above 60% including all replicates, whereas four iterations of excluding minimum and maximum values resulted in lower standard deviation and consequently a lower mean CV of 32% in CSF and 18% in PBS.

The Pearson coefficient ($r > 0.94$) indicates linear correlation of the sFIDA readout with the applied Aβ-SiNaP concentration in both dilution

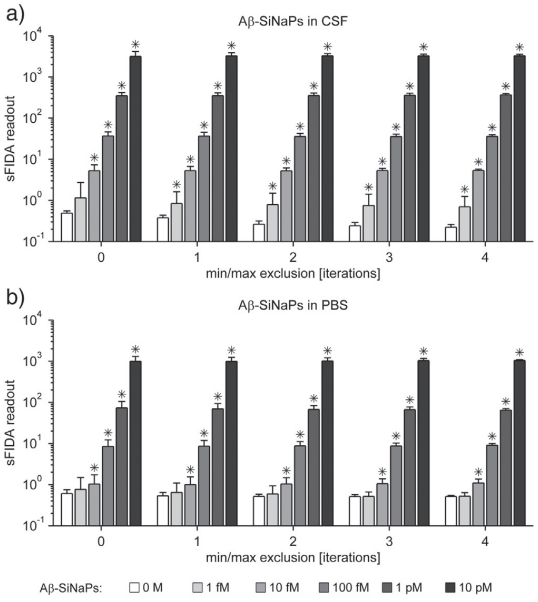

Fig. 1. sFIDA readout as a function of applied Aβ-SiNaP concentration. sFIDA readout as a function of applied Aβ-SiNaP concentration in a) CSF and in b) PBS without (0 iterations) and with iterative exclusion of minimum and maximum values (1–4 iterations). Significance between blank measurements (0 M Aβ-SiNaPs) and the samples (1 fM–10 pM Aβ-SiNaPs) was determined pairwise by p-value adjusted one-sided t-test (*: $p \le 0.05$, H_0 was rejected, i.e. the readout of the sample is higher than the readout of blank measurements).

Please cite this article as: Y. Herrmann, et al., sFIDA automation yields sub-femtomolar limit of detection for Aβ aggregates in body fluids, Clin Biochem (2016), http://dx.doi.org/10.1016/j.clinbiochem.2016.11.001

Table 1
Analysis of limit of detection, coefficient of variation and linearity of automated sFIDA assay.
Sensitivity of the automated sFIDA assay was calculated by the limit of detection (LOD), intra-assay precision was calculated by the coefficient of variation (CV), which is the percentage of standard deviation to the mean, correlation by Pearson's coefficient r and linearity by F-Test (Mandel's test, Lack-of-fit test) without or with iterative excluding minimum and maximum values. Mandel's test: The H_0 hypothesis assumes no significant difference between the residual variances of the linear and quadratic calibration function. For test value < $F_{(crit., 99\%)}$ H_0 is accepted. The second order calibration function will not provide a significantly better fit. The calibration function of choice is linear. For test value > $F_{(crit., 99\%)}$ H_0 is rejected, which indicates non-linearity. Lack-of-fit test for linear and quadratic regression model (LRM, QRM): The H_0 hypothesis assumes no lack of fit. For LRM, QRM < $F_{(crit., 99\%)}$ H_0 is accepted, i.e. there is no lack of fit.

Dilution matrix	Iterations of min/max exclusion	LOD [fM]	mean CV [%]	Pearson's r	Mandel's test		Lack-of-fit test		
					test value	$F_{(crit., 99\%)}$	LRM	QRM	$F_{(crit., 99\%)}$
CSF	0	5.4	72	0.947	0.004	7	0.001	7.2	3.6
	1	3.7	59	0.980	0.09	7	0.02	0.67	3.6
	2	0.94	42	0.992	0.23	7.1	0.06	0.18	3.7
	3	0.85	38	0.995	0.42	7.2	0.10	0.94	3.8
	4	0.91	32	0.996	0.68	7.5	0.16	0.05	4
PBS	0	22	62	0.950	0.53	7	0.13	2.4	3.6
	1	10	46	0.969	0.97	7	0.23	1.4	3.6
	2	4.7	35	0.980	1.8	7.1	0.42	0.57	3.7
	3	3.8	24	0.990	3.2	7.2	0.75	0.10	3.8
	4	0.93	18	0.990	23	7.5	5.2	0.05	4

series from 0 fM to 10 pM. The validity of the linear fitting model was checked more directly by F-test (Mandel's fitting test and lack-of-fit test) indicating that the data from dilution series in PBS and CSF fit to a linear regression model without (0 iterations) and with all iterations of excluding minimum and maximum values, respectively, except for four iterations for PBS (Table 1).

4. Discussion

In this study we successfully implemented the sFIDA assay on an automated platform. The sFIDA readout and Aβ-SiNaP concentration correlated linearly over four orders of magnitude, which is in line with previous reports [7–9]. Automation of the sFIDA assay decreased the CV for Aβ-SiNaPs dilutions in CSF and PBS to 32% and 18%, respectively, in comparison with manual preparation of the assay (40%) [8].

The improvement of the intra-assay precision was mainly accomplished by processing 12-fold replicates with iterative exclusion of minimum and maximum values from the analysis, which corresponds to the calculation of the trimmed mean ($\bar{x}_{\%}$). The trimmed mean proceeds a transition from the arithmetic mean $\bar{x}_{0\%}$ to the median $\bar{x}_{50\%}$ with increasing percentage of ending points to discard. According to the Analytical Methods Committee, exclusion of adjacent data points complies with both criteria of robust statistics: insensitivity to gross errors and unbiasedness for heavy-tailed distributions close to the normal. The mean fails the first, the median the second [13]. In particular the IQM ($\bar{x}_{25\%}$) is a reasonable compromise between the mean and the median, hedging a significant amount of outliers on the one hand and giving a sufficient sensitive estimate of the center of distribution on the other. In this respect, we suggest the use of the IQM for the quantitation of Aβ-SiNaPs and Aβ-oligomers in the sFIDA assay in practice with the automated system.

In this study, we significantly lowered the LOD into the sub-femtomolar range due to the high number of replicates feasible on an automation system in comparison to previous studies [8,9]. The lowest calculated LOD (0.85 fM) was observed for the dilution series in CSF after three iterations of excluding minimum and maximum values. The corresponding monomeric Aβ concentration was 0.56 ng/L assuming a load of 150 Aβ peptides per SiNaP. The observed LODs are similar to other studies using Aβ oligomer-specific ELISAs [14,15].

A major benefit of sFIDA assay automation is the elimination of human error. Manual distribution of a large number of samples in a non-systematic layout is almost impossible for an operator due to restrictions in working hours and the high physical and mental concentration effort. Additionally, the automated system provides a defined workflow and therefore costs and time for each experiment become reliably predictable.

In conclusion, automation of the sFIDA assay results in increased precision and sensitivity, which is a prerequisite for assay validation and future application of sFIDA in high-throughput AD diagnostics.

Acknowledgement

This work was supported by the Federal Ministry of Education and Research within the projects VIP (03V0641), KNDD (01GI1010A), and JPND/BIOMARKAPD (01ED1203H). We also received funding from the Program “Biomarkers Across Neurodegenerative Diseases” of The Alzheimer's Association, Alzheimer's Research UK, The Michael J. Fox Foundation for Parkinson's Research, and the Weston Brain Institute (11084).

Appendix A. Supplementary data

Supplementary data to this article can be found online at http://dx.doi.org/10.1016/j.clinbiochem.2016.11.001.

References

[1] J. Hardy, D.J. Selkoe, The amyloid hypothesis of alzheimer's disease: progress and problems on the road to therapeutics, Science 297 (2002) 353–356.
[2] E. Birkmann, F. Henke, N. Weinmann, C. Dumpitak, M. Groschup, A. Funke, et al., Counting of single prion particles bound to a capture-antibody surface (surface-fida), Vet. Microbiol. 123 (2007) 294–304.
[3] S.A. Funke, E. Birkmann, F. Henke, P. Gortz, C. Lange-Asschenfeldt, D. Riesner, et al., Single particle detection of abeta aggregates associated with alzheimer's disease, Biochem. Biophys. Res. Commun. 364 (2007) 902–907.
[4] S.A. Funke, E. Birkmann, F. Henke, P. Görtz, C. Lange-Asschenfeldt, D. Riesner, et al., Single-particle detection system for ab aggregates: adaptation of surface-fluorescence intensity distribution analysis to laser scanning microscopy, Rejuvenation Res. 13 (2007) 206–209.
[5] O. Bannach, E. Birkmann, E. Reinartz, K.E. Jaeger, J.P. Langeveld, R.G. Rohwer, et al., Detection of prion protein particles in blood plasma of scrapie infected sheep, PLoS One 7 (2012), e36620.
[6] L. Wang-Dietrich, S.A. Funke, K. Kühbach, K. Wang, A. Besmehn, S. Willbold, et al., The amyloid-beta oligomer count in cerebrospinal fluid is a biomarker for alzheimer's disease, J. Alzheimers Dis. 34 (2013) 985–994.
[7] K. Kühbach, M. Hülsemann, Y. Herrmann, K. Kravchenko, A. Kulawik, C. Linnartz, et al., Application of an amyloid beta oligomer standard in the sfida assay, Front. Neurosci. 10 (2016).
[8] K. Kravchenko, A. Kulawik, M. Hülsemann, K. Kühbach, C. Zafiu, Y. Herrmann, et al., Analysis of anti-coagulants for blood-based quantitation of amyloid beta oligomers in the sFIDA assay, Nov. 2 2016. Biol. Chem. http://dx.doi.org/10.1515/hsz-2016-0153.
[9] M. Hülsemann, C. Zafiu, K. Kühbach, N. Luhmann, Y. Herrmann, L. Peters, et al., Biofunctionalized silica nanoparticles: standards in amyloid-beta oligomer-based diagnosis of Alzheimer's disease, J. Alzheimers Dis. 54 (2016) 79–88.
[10] T. Chapman, Lab automation and robotics: automation on the move, Nature 421 (2003) 661–666.

Please cite this article as: Y. Herrmann, et al., sFIDA automation yields sub-femtomolar limit of detection for Aβ aggregates in body fluids, Clin Biochem (2016), http://dx.doi.org/10.1016/j.clinbiochem.2016.11.001

[11] M.E. DiLorenzo, C.F. Timoney, R.A. Felder, Technological advancements in liquid handling robotics, J. Assoc. Lab. Autom. 6 (2001) 36–40.
[12] A.D. McNaught, A. Wilkinson, M. Nic, J. Jirat, B. Kosata, A. Jenkins, IUPAC. Compendium of Chemical Terminology, 2nd ed. (the "Gold Book"), Blackwell Scientific Publications, Oxford, 1997.
[13] Analytical Methods C, Robust statistics-how not to reject outliers. Part 1. Basic concepts, Analyst 114 (1989) 1693–1697.
[14] M. Holtta, O. Hansson, U. Andreasson, J. Hertze, L. Minthon, K. Nagga, et al., Evaluating amyloid-beta oligomers in cerebrospinal fluid as a biomarker for alzheimer's disease, PLoS One 8 (2013), e66381.
[15] K.A. Bruggink, W. Jongbloed, E.A. Biemans, R. Veerhuis, J.A. Claassen, H.B. Kuiperij, et al., Amyloid-beta oligomer detection by elisa in cerebrospinal fluid and brain tissue, Anal. Biochem. 433 (2013) 112–120.

Please cite this article as: Y. Herrmann, et al., sFIDA automation yields sub-femtomolar limit of detection for Aβ aggregates in body fluids, Clin Biochem (2016), http://dx.doi.org/10.1016/j.clinbiochem.2016.11.001

Appendix A. Supplementary Material

A.1 Automation devices

The automation of the sFIDA assay was accomplished with a liquid handling system (Microlab Star, Hamilton, Reno, NV, USA) [1], in the following referred to as pipetting robot, in combination with a microplate washer 405 LS (BioTek, Winooski, VT, USA). The system was placed in a biological safety hood (BDK Luft- und Reinraumtechnik, Sonnenbühl-Genkingen, Germany) to avoid both dust contamination and exposure of biohazards to the operators.

The pipetting robot features eight pipetting channels with disposable tips, a transportation arm (iSWAP) and a deck for placement of microplates (MTP), reagent resevoirs and pipetting tips (Figure A.1). Reagent reservoirs of different volumes were available. The high-volume reservoir (Figure A.1b) was divided in 12 chambers with a volume of 21 mL per chamber. The low-volume reservoir (Figure A.1c) was divided in 24 chambers with a volume of 3.5 mL per chamber. Two further carriers contained five 50 mL reagent reservoirs (Figure A.1g) and three 120 mL reagent reservoirs (Figure A.1h), respectively. Additional carriers provided microplates (Figure A.1e) for the prepration of the assay as well as for the dipensation of prealiquote volumes. Futhermore, adapters for 1.5 mL tubes (Figure A.1a), lids (Figure A.1f, d) and three types of disposable pipetting tips with maximum volumes of 50 µL, 300 µL and 1000 µL (Figure A.1i, k, l) were provided.

The microplate washer has two manifolds with 96 needles for aspiration and 96 needles for dispensing to perform washing of 384-well plates in a shifted pattern in 4 steps. The washer employs a buffer switching system to allow the use of four different buffers.

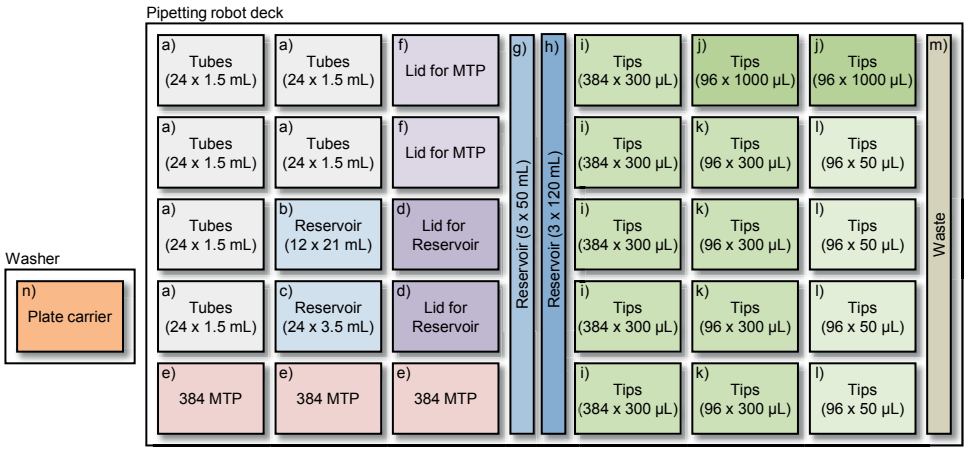

Figure A.1: Pipetting robot deck layout for sFIDA assay automation.

Carriers for laboratory equipment are placed on specific positions. a) Adapter for tubes (1.5 mL); b) Low-volume reagent reservoir for maximum volume of 3.5 mL per chamber; c) High-volume reagent reservoir for maximum volume of 21 mL per column; d) Lid for reservoir; e) 384-well-format microplates (MTP); f) Lid for MTP; g) Carrier with five 50 mL containers; h) Carrier with three 120 mL containers; i) 384 x 300 µL pipetting tips (stacked); j) 96 x 1000 µL pipetting tips; k) 96 x 300 µL pipetting tips; l) 96 x 50 µL pipetting tips; m) Waste; n) Position of plate carrier at the washer

A.2 sFIDA assay on the automated platform

The automated sFIDA assay consists of initiatory preparation steps by the operator, automated aspiration and dispensation procedures by the pipetting robot and the washer, automated TIRF microscopy as well as data analysis and reporting with an in-house developed software (Figure A.2).

In detail, 384-well microplates (SensoPlate Plus with 170 µm glass bottom; Greiner Bio-One, Kremsmünster, Austria) were placed on the pipetting robot deck and each well of the plate was treated with 5 M NaOH (AppliChem, Darmstadt, Germany) for 15 min and washed three times with 85 µL water (wash procedure 1). Subsequently, 1 M HCl (AppliChem, Darmstadt, Germany) was applied for 15 min followed by wash procedure 1. The plate was dried at room temperature. 10 M ethanolamine in DMSO (Sigma-Aldrich, St. Louis, MO, USA) was prepared manually and was provided in one chamber of the high-volume reagent reservoir, 45 µL were applied to each well and incubated overnight. During incubation, the microplate was covered with a lid.

On the next day, the pipetting robot performed three wash steps with DMSO provided in a 50 mL reagent reservoir and two wash steps with 70% ethanol (VWR Chemicals, Langenfeld, Germany) provided in a 120 mL reagent reservoir. Then the plate was dried at room temperature.

A solution of 2 mM SC-PEG-CM (MW 5,000 Da, Laysan Bio, Arab, AL, USA) was tempered to 70°C and provided in the low-volume reagent reservoir. After 20 min the solution cooled down to room temperature and 15 µL were applied to each well. After an incubation of 1 h the wells were washed (wash procedure 1).

Activation of the carboxyterminus of SC-PEG-CM was initiated by incubating 30 µL of freshly prepared 100 mM EDC (Fluka, Buchs, Switzerland) / 100 mM NHS (Aldrich, Milwaukee, WI, USA) in 0.1 M MES buffer, pH 4.7 (AppliChem, Darmstadt, Germany) in each well for 30 min. The prepared solution was placed in one chamber of the high-volume reagent reservoir. Next, the wells were washed three times with 0.1 M MES, pH 4.7 (wash procedure 2). The capture antibody solution containing 10 ng/µL mAb Nab228 (Sigma-Aldrich, St. Louis, MO, USA) in PBS was centrifuged at 15,000 g for 10 min to remove aggregated antibodies. The pipetting robot applied 15 µL of the supernatant to each well followed by incubation of 1 h. The following wash procedure 3 included three wash steps with PBS with 0.05% Tween20 (AppliChem, Darmstadt, Germany) (PBS-T) and three wash steps with PBS.

A blocking solution (Smart Block, CANDOR Biosciences, Wangen, Germany) was provided in one chamber of the high-volume reagent reservoir and 50 µL were applied to each well.

After 1 h incubation, the microplate was washed three times with PBS-T and three times with PBS, leaving 80 µL of PBS in each well after the final wash step (wash procedure 4).

Next, the pipetting robot prepared a ten-fold dilution series of Aβ-SiNaPs in CSF and PBS starting from a 1 nM Aβ-SiNaPs stock solution, emptied the PBS containing wells, and distributed 15 µl of each dilution sample in multiple replicates (12 sample replicates and 24 CSF and PBS samples, respectively, without Aβ-SiNaPs for blank measurements) to the microplate in a quasi-random layout followed by overnight incubation. Then, wash procedure 4 was applied leaving 80 µL PBS in each well.

The detection antibodies 6E10 labeled with Alexa Fluor 488 (Covance, Princeton, NJ, USA) and Nab228 labeled with Alexa Fluor 647 (Santa Cruz, Dallas, TX, USA) were combined to each 1.25 µg/mL in PBS and centrifuged (1 h, 100,000 g, 4°C). The supernatant was mixed and provided in one column of the low-volume reagent reservoir. The wells of the microplate were emptied and 15 µL of the antibody solution was added and incubated for 1 h. Next, the wells were washed five times with PBS-T and five times with PBS (wash procedure 5). Again, 80 µL PBS were left in the wells and the pipetting robot performed a column-wise exchange of PBS against 2 mM sodium azide (Sigma-Aldrich, St. Louis, MO, USA) in water prior to image acquisition by TIRF microscopy.

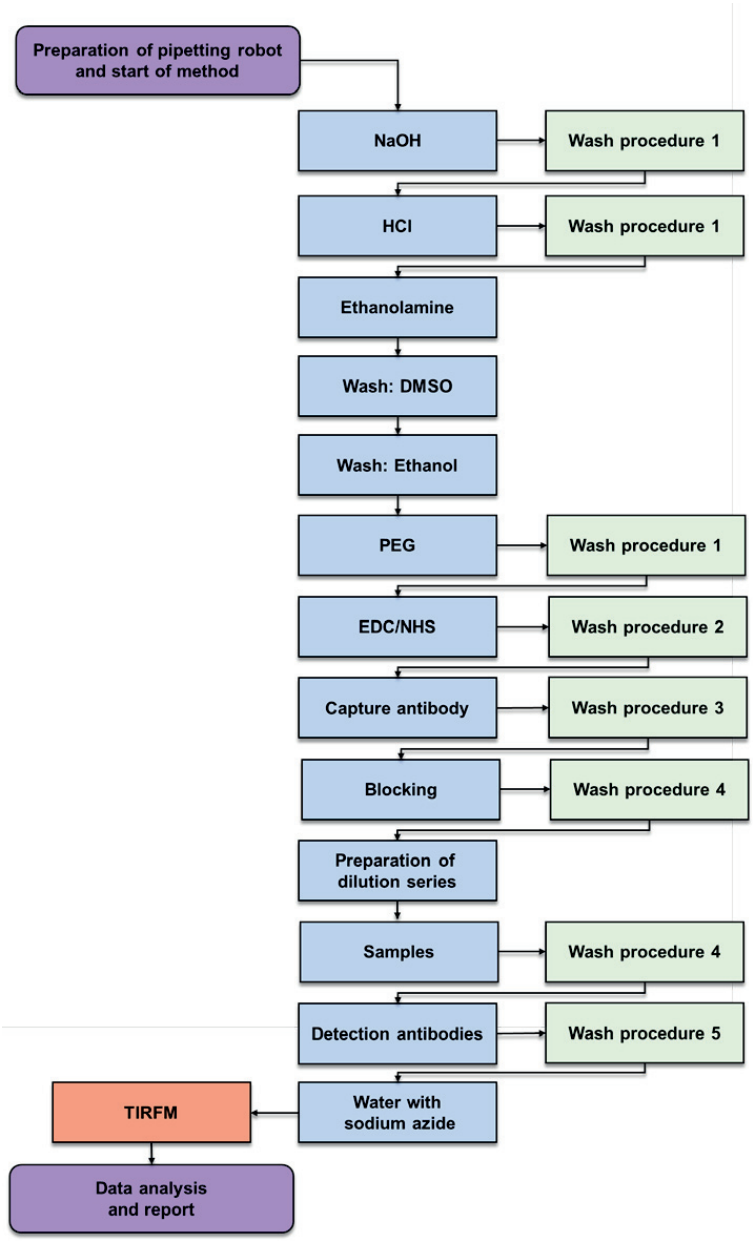

Figure A.2: Workflow of the automated sFIDA assay.

The automated sFIDA assay consists of initiatory preparation steps by the operator (upper purple rectangle), automated aspiration and dispensation procedures of reagents and washing solutions by the pipetting robot (blue rectangles) and the washer (green rectangles), image aquisition by automated TIRF microscopy (TIRFM) (orange rectangle) as well as data analysis and reporting with an in-house developed software (lower purple rectangle).

A.3 Artifact detection

Dust and other contaminations as well as mechanical damage of the assay surface become apparent as extraordinary large and bright spots in images obtained from TIRF microscopy which impair subsequent data analysis. To exclude artifact-afflicted images prior data analysis, cluster detection within each image was performed. To this end, the grayscale images were transformed to binary images. For the transformation the mean plus the standard deviation for each image was calculated as a threshold. If the pixel intensity was above the threshold the pixel intensity was set to 1 and if it was below or equals the threshold the pixel intensity was set to 0. Afterwards a rectangular structuring element of the size 4 µm x 4 µm was used to erode the images in order to identify large clusters. Afterwards dilation was applied with the same structuring element to compensate pixel loss in the eroded images. The identified clusters were tested based on mean pixel intensity, standard deviation and skewness. Each image containing at least one of the detected clusters with the following parameters was excluded from further analysis: mean pixel intensity of at least 3000, a standard deviation of at least 2800 or skewness of less than 0.

A.4 Calculation of coefficient of variation

Coefficient of variation (CV) was determined as a criterion for repeatability of the sFIDA assay according to the formula [2]:

Equation A.1: $\text{Coefficient of variation (CV) in \%} = \left(\frac{\sigma}{\text{mean sFIDA readout}}\right) * 100$

σ : standard deviation

The mean CVs for all concentrations and blank measurements, respectively, were calculated for each dilution series in CSF and in PBS.

A.5 Determination of linearity of the calibration curve

Pearson coefficient (r) was calculated as a criterion for correlation between the applied concentrations of Aβ-SiNaPs and obtained sFIDA readouts according to the formula [3]:

Equation A.3: $r = \frac{n\sum x_i y_i - \sum x_i \sum y_i}{\sqrt{n\sum (x_i)^2 (\sum x_i)^2}\sqrt{n\sum (y_i)^2 (\sum y_i)^2}}$;

n: number of values;

x_i: element i in dataset $\{x_i \ldots x_n\}$

y_i: element i in dataset $\{y_i \ldots y_n\}$

For further investigation of the linearity of the sFIDA readout, Mandel's fitting test was applied. This method evaluates linearity considering the residual standard deviation of the first and second order calibration function by determining as to whether the residual variances resulting from the linear and the quadratic calibration function significantly differ [4].

At first the calculation of the calibration functions of first and second order with their respective residual standard deviation were calculated:

Equation A.4: $s_{y1} = \sqrt{\frac{\sum (y_i - \hat{y}_i)^2}{N-2}}$, where $\hat{y}_i = a + bx_i$

Equation A.5: $s_{y2} = \sqrt{\frac{\sum (y_i - \hat{y}_i)^2}{N-3}}$, where $\hat{y}_i = a + bx_i + cx_i^2$

y_i: observed sFIDA readout at each concentration i

$\hat{y}_i$: estimation obtained from the respective regression analysis at i

N: total number of measurements

The residual standard deviation (s_{y1} and s_{y2}) were used to determine the difference of variance (DS^2) and calculation of the test value [4].

Equation A.6: Difference of variance $(DS^2) = (N - 2)(s_{y1})^2 - (N-3)(s_{y2})^2$

Equation A.7: test value $= \frac{DS^2}{(s_{y2})^2}$

The test value was compared to the corresponding value of the F-distribution with $f_1 = 1$, $f_2 = N - 3$ and $\alpha = 99\%$. If the test value ≤ F, the calibration function of choice is linear.

Furthermore, the lack-of-fit test for both datasets was calculated as an additional criterium for the linearity of sFIDA readout of the applied Aβ-SiNaP dilution series according to Massart et al [5]. At first the total sum of squares SS_T was calculated to determine the sum of squares due to pure error (SS_{PE}) and the sum of squares due to lack of fit (SS_{LOF}).

Equation A.8: $SS_T = \sum_{i=1}^{k} \sum_{j=1}^{n_i} \left(y_{ij} - \bar{y}\right)^2 = \sum_i^k \sum_j^{n_i} (y_{ij} - \bar{y}_i)^2 + \sum_i^k n_i(\bar{y}_i - \hat{y}_i)^2 + \sum_i^k n_i(\hat{y}_i - \bar{y}_i)^2$

y_{ij}: one of the n_i replicate measurements at x_i,

n_i: the number of replicate measurements at x_i,

$\sum_{i=1}^{k} n_i = n$, the total number of observations, including all replicate measurements,

k: the number of levels, i.e. different x values and

$\bar{y}$: the mean of all observations (grand mean)

Equation A.9: $SS_{PE} = \sum_i^k \sum_j^{n_i} (y_{ij} - \bar{y}_i)^2$

Equation A.10: $SS_{LOF} = \sum_i^k n_i (\bar{y}_i - \hat{y}_i)^2$

Then the values MS_{PE} and MS_{LOF} were calculated as follows:

Equation A.11: $MS_{PE} = \frac{SS_{PE}}{df}$

Equation A.12: $MS_{LOF} = \frac{SS_{LOF}}{df}$, with df degree of freedom

The lack-of-fit test is a one-sided test that compares the ratio of $F_{LOF} = \frac{MS_{LOF}}{MS_{PE}}$ with the F-distribution at (k - 2) and (n - k) degrees of freedom at a given error probability. If $F_{LOF} \leq F$, the lack-of-fit term is not significant, thus the linear model is adequate to describe the relationship between sFIDA readout and applied Aβ-SiNaP concentration.

A.5 References

[1] M.E. DiLorenzo, C.F. Timoney, R.A. Felder, Technological Advancements in Liquid Handling Robotics, Journal of the Association for Laboratory Automation 6(2) (2001) 36-40.

[2] B. Everitt, The Cambridge dictionary of statistics, Cambridge University Press, Cambridge, UK; New York, NY, USA, 1999.

[3] K. Pearson, Mathematical Contributions to the Theory of Evolution. III. Regression, Heredity, and Panmixia, Philosophical Transactions of the Royal Society of London A: Mathematical, Physical and Engineering Sciences 187 (1896) 253-318.

[4] J. Mandel, The statistical analysis of experimental data, Courier Corporation2012.

[5] B. Slutsky, Handbook of Chemometrics and Qualimetrics: Part A By D. L. Massart, B. G. M. Vandeginste, L. M. C. Buydens, S. De Jong, P. J. Lewi, and J. Smeyers-Verbeke. Data Handling in Science and Technology Volume 20A. Elsevier: Amsterdam. 1997., Journal of Chemical Information and Computer Sciences 38(6) (1998) 1254-1254.

3.5 Nanoparticle standards for immuno-based quantitation of α-synuclein oligomers in diagnostics of Parkinson's disease and other synucleopathies

Autoren: Yvonne Herrmann, Tuyen Bujnicki, Christian Zafiu, Luriano Peters, Andreas Kulawik, Katja Kühbach, Judith Fabig, Johannes Willbold, Oliver Bannach und Dieter Willbold

Publiziert in: Clinica Chimica Acta (Herrmann et al., 2017)

DOI: http:\\dx.doi.org\10.1016\j.cca.2017.01.010..

Impact Factor (2015): 2.799

Eigener Anteil: 55%

Mitentwicklung der experimentellen Details des sFIDA-Ablaufes, Durchführung der sFIDA-Studie mit α-syn-SiNaPs auf dem angepassten automatisierten System, Auswertung der sFIDA-Daten und Bestimmung der Intra-Assay Parameter beim Spiking Experiment und Schreiben des Manuskripts

Clinica Chimica Acta 466 (2017) 152–159

Contents lists available at ScienceDirect

Clinica Chimica Acta

journal homepage: www.elsevier.com/locate/clinchim

Nanoparticle standards for immuno-based quantitation of α-synuclein oligomers in diagnostics of Parkinson's disease and other synucleinopathies

Yvonne Herrmann [a], Tuyen Bujnicki [a], Christian Zafiu [a], Andreas Kulawik [a], Katja Kühbach [a], Luriano Peters [a], Judith Fabig [a], Johannes Willbold [a], Oliver Bannach [a,b], Dieter Willbold [a,b,*]

[a] Forschungszentrum Jülich GmbH, ICS-6 Structural Biochemistry, 52425 Jülich, Germany
[b] Heinrich-Heine-Universität Düsseldorf, Institut für Physikalische Biologie, 40225 Düsseldorf, Germany

ARTICLE INFO

Article history:
Received 14 November 2016
Received in revised form 22 December 2016
Accepted 10 January 2017
Available online 11 January 2017

Keywords:
Parkinson's disease
α-Synuclein
Diagnostic biomarker
Surface-based fluorescence intensity distribution analysis (sFIDA)
Silica nanoparticles (SiNaPs)
Automation
Protein aggregates
Neurodegenerative diseases

ABSTRACT

Parkinson's disease (PD) is a neurodegenerative disorder that is characterized by symptoms such as rigor, tremor and bradykinesia. A reliable and early diagnosis could improve the development of early therapeutic strategies before death of dopaminergic neurons leads to the first clinical symptoms.
The sFIDA (surface-based fluorescence intensity distribution analysis) assay is a highly sensitive method to determine the concentration of α-synuclein (α-syn) oligomers which are presumably the major toxic isoform of α-syn and potentially the most direct biomarker for PD.
Oligomer-based diagnostic tests require standard molecules that closely mimic the native oligomer. This is particularly important for calibration and assessment of inter-assay variation. In this study, we generated a standard in form of α-syn coated silica nanoparticles (α-syn-SiNaPs) that are in the size range of α-syn oligomers and provide a defined number of α-syn epitopes.
The preparation of the sFIDA assay was realized on an automated platform to allow handling of high number of samples and reduce the effects of human error. The assay outcome was analyzed by determination of coefficient of variation and linearity for the applied α-syn-SiNaPs concentrations. Additionally, the limit of detection and lower limit of quantification were determined yielding concentrations in the lower femtomolar range.

1. Introduction

Synucleinopathies are characterized by pathological accumulation of aggregated α-synuclein (α-syn) in the brain. The most prevalent form of synucleinopathies is Parkinson's disease (PD) affecting 1.5% of the over 65-year-old population [1]. Characteristic motoric symptoms in PD, including rigor, tremor, bradykinesia and postural instability, are linked to the death of dopaminergic neurons in the *substantia nigra pars compacta* [2]. Currently, the diagnosis of PD is based on the clinical symptoms that occur after the irrecoverable loss of the dopaminergic neurons, i.e. at a stage of the disease where causal treatments would have minor effects. Clinical PD diagnosis is usually guided by the patient's response to treatment with L-3,4-dihydroxy-phenylalanine. However, there is still a substantial rate of misdiagnoses based on the patient's clinical presentation [3].

A neuropathological hallmark of PD are Lewy bodies in the brain that are composed mostly of aggregated α-syn [4]. Physiologically, α-syn is involved in the regulation of synaptic plasticity and dopamine synthesis, as well as neuronal differentiation. The role of α-syn in PD pathogenesis is strongly supported by the discovery of point mutations in the SNCA gene that causes a familial form of PD [5]. It is widely accepted that accumulation of α-syn and formation of toxic oligomeric intermediates is a key event in the pathogenesis in PD [6–9]. Therefore, α-syn oligomers represent a popular therapeutic target as well as a promising biomarker for the early diagnosis of PD [9].

Recent studies have investigated the levels of α-syn oligomers in cerebrospinal fluid (CSF) and plasma of PD patients in comparison to non-diseased control cohorts [10–17]. In some of these reports elevated levels of α-syn oligomers in PD samples were observed. The studies are mainly based on enzyme-linked immunosorbent assays (ELISAs) which provide the specificity for α-syn oligomers by using the same monoclonal antibody for both capture and detection, respectively, or by applying a conformation-specific antibody which selectively captures oligomeric α-syn. These setups are therefore insensitive for the ubiquitous monomeric α-syn. In contrast to monomers, oligomers

* Corresponding author at: Forschungszentrum Jülich, Wilhelm-Johnen-Str., 52425 Jülich, Germany.
E-mail address: d.willbold@fz-juelich.de (D. Willbold).

http://dx.doi.org/10.1016/j.cca.2017.01.010
0009-8981/

exhibit multiple binding sites allowing the binding to capture antibodies and multiple detection by antibody probes.

Because only very low concentrations of α-syn oligomers can be expected in body fluids, any oligomer-based diagnostic test requires extreme sensitivity [17]. We have previously introduced the surface-based fluorescence intensity distribution analysis (sFIDA) assay which meets the requirements for sensitive and specific quantitation of Aβ oligomers as a potential biomarker of Alzheimer's disease (AD) [18–25]. In the present work we adapted the sFIDA technology for quantitation of α-syn oligomers. In sFIDA, α-syn species are captured by anti-α-syn-antibodies that are attached to a functionalized glass surface. Next, captured α-syn species are probed by two different detection antibodies targeting epitopes in the same region as the capture antibody and each antibody is labeled with a different fluorescent dye (Fig. 1). In contrast to canonical sandwich ELISAs, the surface is imaged by dual-color total internal reflection fluorescence microscopy (TIRFM). The sFIDA readout is the number of pixels with intensities above background-based cut-off intensities in the two channels. By using antibodies that are directed against overlapping epitopes, monomeric α-syn does not affect the sFIDA readout.

An unmet need for oligomer-based diagnostic tests is a suitable standard that allows calibration of the assay readout [26]. For quantitative analysis of Aβ oligomers we have recently introduced silica-based nanoparticles (SiNaPs) coated with Aβ peptides which mimic the properties of native oligomers with regard to size and epitope load [25].

In the present work a protocol was developed to synthesize SiNaPs coated with α-syn that are suited to serve as a stable standard for the quantitation of oligomeric α-syn. The standards were spiked into CSF and buffer, respectively, and were subjected to sFIDA analysis on an automated platform for which we determined several assay parameters, i.e. linearity, coefficient of variation (CV), limit of detection (LOD) and lower limit of quantification (LLOQ).

2. Material and methods

2.1. Expression and purification of recombinant α-syn

Recombinant human α-syn was expressed and purified according to Hoyer et al. [27]. Briefly, α-syn was expressed in *E. coli* using the plasmid pT7-7-α-syn wild type by cultivating the cells for 4 h at 37 °C after induction with 1 mM isopropyl-β-D-1-thiogalactopyranoside. The α-syn protein was purified using anion exchange chromatography on a HiTrap Q FF column (GE Healthcare, United Kingdom) by elution with a salt gradient at approximately 300 mM NaCl. Further purification was achieved by size exclusion chromatography on a Superdex 75 HR 10/30 column (GE Healthcare, United Kingdom) in phosphate-buffered saline, pH 7.4.

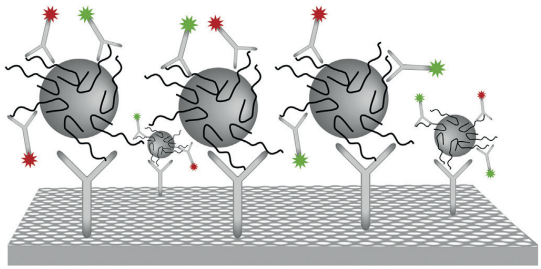

Fig. 1. Scheme of the sFIDA assay principle. α-syn-specific antibodies (Y symbols) are immobilized on a functionalized glass plate as capture antibodies. α-syn-SiNaPs (black lines as α-syn on gray silica nanoparticles) within the sample bind to capture antibodies and are detected by two different fluorescence labeled anti-α-syn-antibodies (Y symbols with colored stars). All three anti-α-syn-antibodies bind to the same region at the C-terminus of α-syn. The surface is imaged by dual-color TIRF microscopy. (For interpretation of the references to color in this figure legend, the reader is referred to the web version of this article.)

2.2. Synthesis of silica nanoparticles coated with α-syn (α-syn-SiNaPs)

Nanoparticle standards were synthesized according to a modified protocol that was previously described [25]. Briefly, 3.5 ml ddH_2O and 3.7 ml ammonia solution (30%, Carl Roth, Karlsruhe, Germany) were mixed in 200 ml absolute ethanol (VWR, Darmstadt, Germany) prior to adding 4.4 ml tetraethylorthosilicate (TEOS, Aldrich Chemistry, St. Louis, USA) and stirring for 4 days at room temperature (RT). The resulting alkaline suspension was neutralized with acetic acid and washed by three centrifugation/redispersion steps (5 min, 3,000 rpm and RT) in 96% ethanol. A size of 18 ± 4 nm was determined from TEM micrographs (Zeiss Libra 120 TEM, Carl Zeiss AG, Jena, Germany) as the mean diameter of 100 individual particles (Fig. 2 a and b). APTES ((3-aminopropyl) triethoxysilane, Sigma-Aldrich, St. Louis, USA) was added to the silica particle solution in 96% ethanol in a two-fold molar excess related the theoretical available particle surface sites and was stirred overnight at RT. The resulting amino-functionalized silica nanoparticles (aSiNaPs) were washed by three centrifugation/redispersion steps (2 h, 5,000 rpm and RT) in 96% ethanol (Fig. 2 d, ii). Carboxylated silica nanoparticles (cSiNaP) were obtained by transferring aSiNaP to 0.1 M succinic anhydride (Aldrich Chemistry, St. Louis, USA) in DMF (Sigma-Aldrich, Darmstadt, Germany) under argon atmosphere. The dispersion was heated to 80 °C for 1 h and stirred overnight at RT. The resulting dispersion was diluted in water (1:1 vol%) and washed by three centrifugation/redispersion steps (2 h, 5,000 rpm and RT) in water (Fig. 2 d, iii). Activated cSiNaP were prepared by dispersing 100 nM cSiNaP in 10 mM MES buffer, pH 5.7 (Sigma-Aldrich, St. Louis, USA) containing 40 μM EDC (1-ethyl-3-(3-dimethylaminopropyl) carbodiimide, Sigma-Aldrich, St. Louis, USA) and 10 μM NHS (*N*-hydroxysuccinimide, Aldrich Chemistry, St. Louis, USA) for 30 min at 600 rpm and 25 °C. After centrifugation (10,000 rpm, 15 min) and redispersion in 1 ml fresh 10 mM MES buffer the activated particles were (Fig. 2 d, iv) mixed with 27 nM recombinant α-syn incubated overnight (25 °C and 600 rpm). Finally, the particles were centrifuged (5,000 rpm, 10 min) and redispersed in 1 ml ddH_2O for three times (Fig. 2 d, v).

The particle concentrations in all steps were determined gravimetrically after evaporating the solvent in a concentrator (Eppendorf, Germany). The protein load on the particles was determined by bicinchoninic acid assay according to the manufacturer's instructions (Extra Sense, Bio Vision Incorporated) using cSiNaPs in the same concentration as α-syn-SiNaPs as control. The epitope load was calculated by forming the molar ratio of α-syn and SiNaP which yielded about 27 α-syn per particle. The particle solutions were stored at −20 °C as a 1:1 dilution in DMSO (dimethyl sulfoxide, Sigma-Aldrich, Steinheim, Germany).

2.3. Automation devices

The sFIDA assay preparation was performed on an automated system as previously described in Herrmann et al. [21] consisting of a liquid handling system Microlab Star (Hamilton, Reno, NV, USA) and a microplate washer 405 LS (BioTek, Winooski, VT, USA).

2.4. sFIDA assay

The sFIDA assay was based on a previously described protocol by Kravchenko et al. [19] that was adapted for the automated platform. The 384-well-format microplate was custom-assembled by PolyAn GmbH (Berlin, Germany) and exhibited a pre-functionalized amine reactive coating for capturing the monoclonal antibody (mAb) 4B12 (BioLegend, San Diego, CA, USA; epitope 103–108). We coated the surface with 1 pM of 4B12 as capture antibody to avoid any limitation for

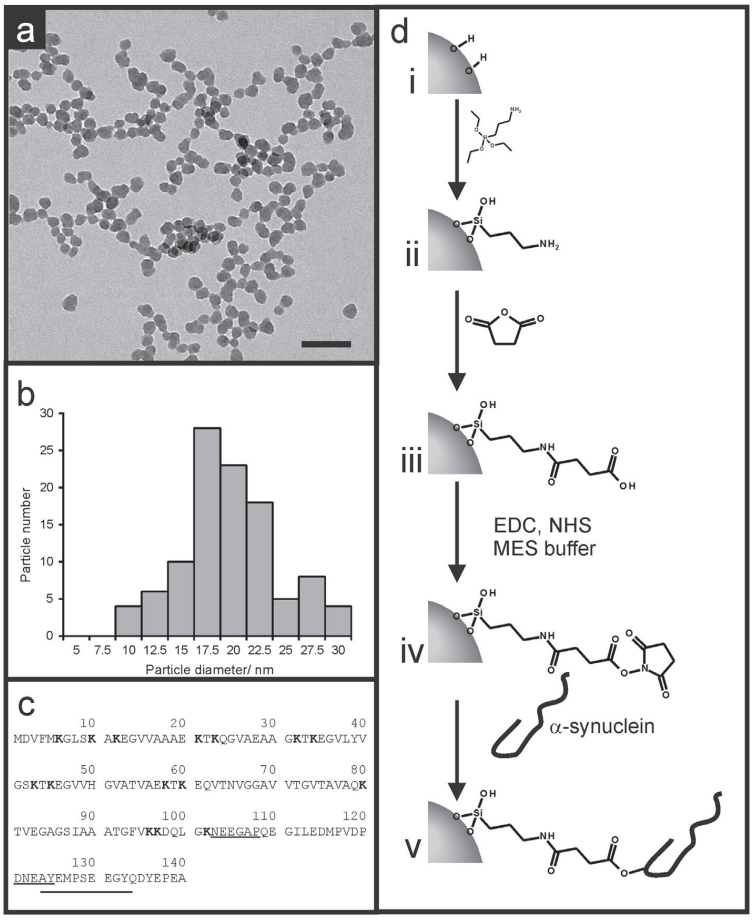

Fig. 2. Synthesis of α-syn-SiNaPs. a) Transmission electron micrographs of SiNaP were taken after synthesis (bar = 100 nm) to determine the particle size and shape, b) based on diameters from 100 individual particles taken from five transmission electron micrographs a size histogram is shown. c) Shows the sequence of α-syn highlighting Lysine K (bold) and epitope regions of mAb 4B12 (epitope 103–108), 211 (epitope 121–125) and 4D6 (epitope 124–134) (underlined). d) Surface modification of SiNaP showing the nanoparticle surface i) of bare SiNaP after Stöber synthesis, ii) aSiNaP after modification with APTES, iii) cSiNaP after modification with succinic anhydride, iv) activated SiNaP after treatment with EDC and NHS, and v) α-syn-SiNaP after conjugation with recombinant α-syn.

binding all α-syn species from native samples to the surface. A wide range of endogenous α-syn has been reported in the literature, ranging from 3.6 to 26 ng/ml [28] which corresponds to 0.3 to 28 fM considering a standard sample volume of 15 µl. CSF was pooled from healthy human donors (Biochemed Services, Winchester, USA). The detection antibodies 4D6 (BioLegend, San Diego, CA, USA) labeled with Atto 488 (ATTO-TEC, Siegen, Germany) and 211 (Santa Cruz Biotechnology Inc., TX, USA; epitope 121–125) labeled with Atto 633 (ATTO-TEC, Siegen, Germany) were used (Supplemental Section A.1).

2.5. Image data acquisition and analysis

For image data acquisition a TIRFM (DMI6000B AM TIRF MC, Leica microsystems, Wetzlar, Germany) was used as previously described by our group [20,25]. Briefly, the images of the assay surface were obtained in two different channels (channel 633: excitation at 635 nm, emission filter 705/72 nm; channel 488: excitation at 488 nm, emission filter 525/36 nm). The pixel size was 114 × 114 nm^2 that theoretically would cover 40 closely packed SiNaPs with a diameter of 18 nm.

Images were analyzed using an in-house developed software that offers an artifact detection for exclusion of artificial images (Supplemental Section A.2). For the minimization of inhomogeneous illumination of edge regions, only the central region of interest (ROI) of 58 µm × 58 µm was analyzed. The reduction of background noise in each channel was accomplished by applying cutoffs which were defined as the signal intensity at which 0.01% or 0.1% of all pixels in PBS and CSF controls, which were not spiked with α-syn-SiNaPs, remain. In the next step, colocalized pixels with intensity values above the cutoff in both color channels were counted for each image. The mean for all replicates of each sample was referred to as "sFIDA readout".

2.5.1. Application of trimmed mean

The sFIDA readout was determined in 12-fold replication for each sample with α-syn-SiNaPs and 20-fold replication for non-spiked controls. The arithmetic mean, further referred to as trimmed mean with trimming percentage 0% ($\bar{x}_{0\%}$), was calculated for all replicates of each sample. Furthermore, data points for each concentration were ordered from smallest to largest and a selected number of values from each end of the ordered list were excluded [30,31]. The trimming

percentages of 8%, 16%, 25% and 33% were selected in order to exclude one, two, three and four values from each end of the ranked data considering the samples with 12 replicates. The non-spiked control consisted of 20 replicates and therefore the same trimming percentages excluded two, four, five and seven values from each end of the ranked data. The remaining data points within each concentration were used for calculating the trimmed means $\bar{x}_{8\%}$, $\bar{x}_{16\%}$, $\bar{x}_{25\%}$ and $\bar{x}_{33\%}$.

2.5.2. Determination of assay parameters and determination of significant differences

For further investigation of the sFIDA assay performance on the automation platform the coefficient of variation (CV), limit of detection (LOD), lower limit of quantification (LLOQ) and linearity for both dilution series were calculated. The following calculations were applied on the previously determined $\bar{x}_{0\%}$ and the respective standard deviations, as well as for the trimmed means $\bar{x}_{8\%}$, $\bar{x}_{16\%}$, $\bar{x}_{25\%}$ and $\bar{x}_{33\%}$.

Briefly, CV in percent was determined for each concentration for both dilution series by calculation of the quotient of standard deviation and the mean for each concentration [32]. LODs were determined by calculating the mean of non-spiked control plus three times the respective standard deviation. The LLOQ values were determined by calculating the mean of non-spiked control plus ten times the respective standard deviation.

Statistical significance was determined as previously described by Herrmann et al. [21]. Briefly, a pairwise comparison of the sample from a respective concentration level and the non-spiked control was calculated by one-sided *t*-tests followed by *p*-value adjustment according to Benjamini and Hochberg [33] with a confidence level of 95%.

The resulting values of the calculation of LOD and LLOQ were then correlated to a concentration of α-syn-SiNaPs based on linear regression. The sFIDA readouts ranging from 0 fM to 1 pM of α-syn-SiNaPs were used as data points to calculate calibration curves for PBS and CSF.

Pearson coefficient (r) [34] as well as the lack-of-fit test [35] were calculated to assess the linearity of the sFIDA readout as a function of α-syn-SiNaP concentration in CSF and in PBS.

2.5.3. Single channel analysis

In channel 488, a cutoff value with signal intensity exceeding 0.01% of total pixels was possible due to a very low signal in the non-spiked controls and a single channel analysis was performed. For channel 633 the single channel analysis was accomplished with a cutoff at 0.1%. In this analysis the "single channel readout" was defined as the sum of pixels with intensities above the respective cutoff value for each channel. The previously described determination of assay parameters in Section 2.5.2 was also applied to the single channel readouts for channel 633 and channel 488.

2.6. sFIDA analysis of α-syn monomers

Monomers of the protein were obtained from human α-syn that was recombinant produced and purified according to a protocol from Hoyer and colleagues [27]. A concentration of the α-syn monomers of 270 pM was selected according to the calculated number of peptides for 10 pM α-syn-SiNaPs. The sFIDA assay was performed manually according to the sFIDA protocol described in Section 2.4.

3. Results

3.1. Synthesis of α-syn-SiNaPs

For generation of stable standards, α-syn-SiNaPs were adjusted to a diameter of 18 ± 4 nm by Stöber synthesis (Fig. 2) which was similar to previously reported size ranges of *in vitro* generated α-syn oligomers [16,36]. After a two-step surface modification the SiNaP exhibited carboxylic surface functionalities which were then activated by EDC and NHS. The NHS-activated particle surface was expected to react with one or more of the 15 lysines (K) and the N-terminal amino group of the recombinant α-syn (Fig. 2 c) by the formation of amide bonds. Twelve and therefore most of the coupling sites anchoring α-syn to the SiNaP are located in the N-terminal region (1–60) that was reported to form alpha helices and in turn only four are found at the beginning of the C-terminal part (Fig. 2 c: 80, 96, 97 and 102) of the protein. Due to the absence of coupling sites in the C-terminal region (103–140) our method ensures that the epitopes for the mAbs 4B12 (epitope 103–108), 211 (epitope 121–125) and 4D6 (epitope 124–134 [29]) are not affected. This means that the mean load of 27 α-syn molecules per particle correlated directly to the number of epitopes. However, the vicinity of the C-terminal coupling sites to the epitope of 4B12 may hamper an efficient binding towards a minority of the 27 proteins on the particle surface by steric factors.

3.2. sFIDA analysis of monomeric α-syn

For detection and quantitation of α-syn oligomers by sFIDA, we used mAb 4B12 as capture and mAbs 4D6 and 211 as detection probes. Both detection mAbs recognize overlapping epitopes close to the C-terminus of α-syn. The mAb 4B12 binds to a region nearby the epitopes recognized by the two detection antibodies. In order to demonstrate that the applied antibody combination did actually not detect monomeric α-syn, a sFIDA assay with α-syn monomers was performed. The applied molar concentration of 270 pM α-syn monomers corresponded to the calculated number of peptides on 10 pM α-syn-SiNaPs. As depicted in Fig. 3, the sFIDA readout of monomeric α-syn concentration exhibited the same signal level as the non-spiked control indicating that monomeric α-syn did not contribute to the readout values using the described sFIDA setup.

3.3. α-Syn-SiNaPs in the automated sFIDA assay

The α-syn-SiNaPs were evaluated as oligomer standard in the sFIDA assay by investigating parameters such as LOD, LLOQ, CV % and linearity. To this end, the α-syn-SiNaPs were diluted into CSF from healthy donors and PBS in a log10 dilution series with concentrations ranging from 10 pM to 1 fM. A correlation between the applied α-syn-SiNaP concentration and sFIDA readout was observed in CSF and PBS with

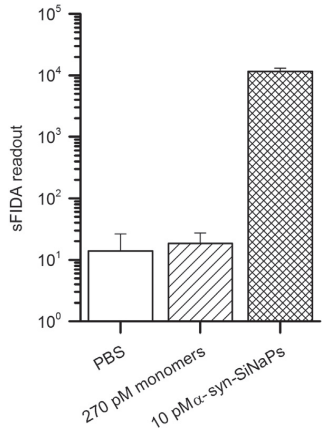

Fig. 3. sFIDA readouts of PBS control (white), 270 pM α-syn monomer (striped) and 10 pM α-syn-SiNaPs (checked). The α-syn monomer concentration of 270 pM corresponded to the applied concentration of 10 pM of α-syn-SiNaPs (27 α-syn-epitopes per SiNaP). After the exclusion of artificial images from the data analysis, a centered ROI with 58 μm × 58 μm of the images was analyzed. Cutoffs for each channel were set to minimize background signal by using the intensity in each channel where 0.1% of all pixels have intensity values above the cutoff in the non-spiked control in each channel. This led to following cutoff values for PBS: 7127 for channel 633 and 5040 for channel 488.

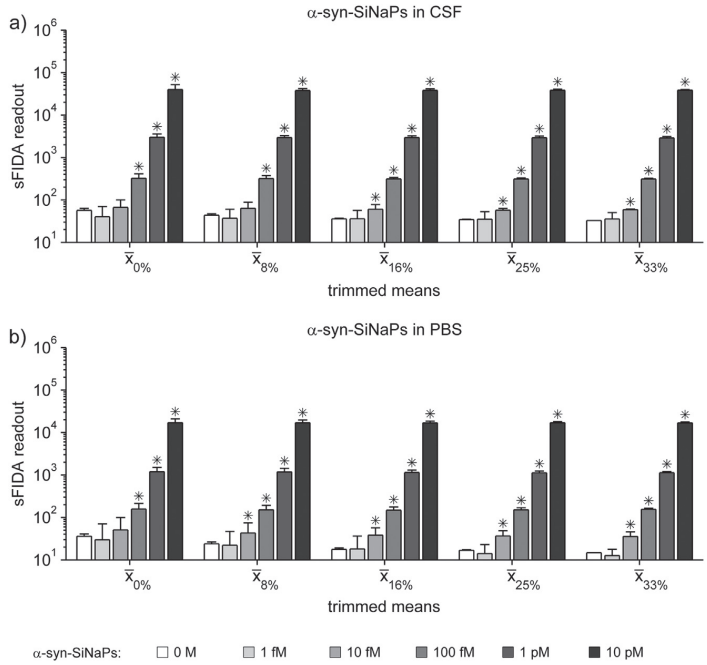

Fig. 4. sFIDA readouts for different concentrations of α-syn-SiNaPs in CSF (a) and in PBS (b). Columns and error bars represent the calculated arithmetic mean ($\bar{x}_0$), trimmed means for trimming percentage of 8%, 16%, 25% and 33% and respective standard deviations for each concentration. A centered ROI with 58 μm × 58 μm of the images was analyzed. Cutoffs for each channel were set to minimize background signal by using the intensity in each channel where 0.1% of all pixels have intensity values above the cutoff in the non-spiked control in each channel. This led to cutoff values for CSF (channel 633/channel 488): 4698/2140 and for PBS: 8573/1928. Significant differences between the non-spiked controls (0 fM α-syn-SiNaPs) and the samples were determined pairwise by *p*-value adjusted one-sided *t*-tests ($^*p \leq 0.05$).

significance between non-spiked controls and the spiked samples (Fig. 4). Interestingly, the non-spiked CSF control yielded less background compared to PBS which can be explained by a beneficial blocking effect of endogenous CSF components. Moreover, endogenous α-syn present in the CSF matrix does not interfere with SiNaP detection.

In order to investigate the performance of α-syn-SiNaPs as oligomeric standard and to obtain important intra-assay parameters, we automated the sFIDA assay which allowed the application of a high number of replicates for each concentration. This also allowed the calculation of the trimmed mean that is insensitive to small numbers of extreme outliers due to e.g. imperfect surface preparation and are known to be suitable for heavy-tailed distributions close to the normal [37]. The trimming percentage of 8% ($\bar{x}_{8\%}$), 16% ($\bar{x}_{16\%}$), 25% ($\bar{x}_{25\%}$) and 33% ($\bar{x}_{33\%}$) were applied in order to determine the contribution of different numbers of outliers (Comp. Fig. 4). Accordingly, the intra-assay parameters (LOD, LLOQ, CV % and linearity) were determined for the arithmetic mean ($\bar{x}_{0\%}$) and the trimmed means, respectively.

The calculated LODs show that the sFIDA readout reached a minimum of 3.8 fM in CSF for $\bar{x}_{33\%}$ and 13 fM in PBS for $\bar{x}_{25\%}$. LLOQs of 11 fM in CSF and in PBS were the lowest with an applied trimming percentage of 33% (Table 1). The calculated LODs and LLOQs were within the range that was significant different to the respective non-spiked control.

The exclusion of outliers upon mean trimming decreased standard deviation and consequently leads to improved intra-assay precision

Table 1
Sensitivity of the automated sFIDA assay was calculated by the limit of detection (LOD) and lower limit of quantification (LLOQ), correlation by Pearson's coefficient r, linearity by F-Test (Lack-of-fit test) and coefficient of variation in percent (CV %) for each concentration of α-syn-SiNaPs in CSF and PBS for arithmetic mean ($\bar{x}_{0\%}$) and trimmed means with trimming percentage of 8%, 16%, 25% and 33%. Lack-of-fit test for linear and quadratic regression model (LRM, QRM): The H_0 hypothesis assumes no lack of fit. For LRM/QRM < $F_{(crit.,\ 99\%)}$ H_0 is accepted (no lack of fit).

Dilution matrix	Trimmed means	LOD [fM]	LLOQ [fM]	Pearson's r	Lack-of-fit test			CV [%]					
					LRM	QRM	$F_{(crit.,\ 99\%)}$	0 fM	1 fM	10 fM	100 fM	1 pM	10 pM
CSF	$\bar{x}_{0\%}$	66	206	0.954	0.13	0.71	3.6	104	74	50	28	20	30
	$\bar{x}_{8\%}$	38	119	0.994	0.64	0.18	3.7	77	62	39	17	12	11
	$\bar{x}_{16\%}$	11	34	0.996	0.84	0.08	3.8	26	57	29	7.8	10	8.4
	$\bar{x}_{25\%}$	8.5	24	0.998	1.7	0.02	3.9	19	50	11	6.5	9.2	5.4
	$\bar{x}_{33\%}$	3.8	11	0.999	2.7	0.01	4.4	8.5	42	2.7	4.8	7.8	3.6
PBS	$\bar{x}_{0\%}$	146	488	0.974	0.36	0.84	3.6	157	137	96	36	26	22
	$\bar{x}_{8\%}$	55	193	0.987	0.59	0.31	3.7	94	112	73	27	22	15
	$\bar{x}_{16\%}$	17	71	0.994	1.2	0.12	3.8	49	101	48	19	15	9.7
	$\bar{x}_{25\%}$	13	56	0.999	2.9	0.04	3.9	41	63	33	12	9.3	5.9
	$\bar{x}_{33\%}$	n.d.[a]	11	0.999	3.2	0.03	4.4	14	41	28	5.8	7.2	4.4

[a] n.d.: not defined; LOD < 0 M.

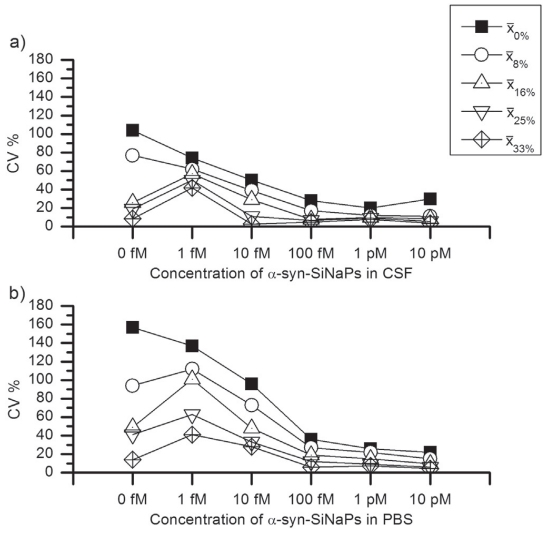

Fig. 5. Coefficient of variation in percent based on sFIDA readouts for each concentration of α-syn-SiNaPs in CSF (a) and in PBS (b) for the arithmetic mean ($\bar{x}_{0\%}$) and trimmed means for 8%, 16%, 25% and 33%.

reflected by lower CV % (Fig. 5 and Table 1). Higher α-syn-SiNaP concentrations, ranging from 10 pM to 100 fM in both dilution series, exhibited CV % values below 10% for $\bar{x}_{16\%}$, $\bar{x}_{25\%}$ and $\bar{x}_{33\%}$. Elevated CV % in lower concentrations were expected due to the low number of events [38].

The linear relationship of the correlation between sFIDA readout and the applied concentration of α-syn-SiNaPs was investigated by calculating the Pearson coefficient (r). The Pearson coefficient of $r > 0.95$ indicated a very strong linear correlation of the sFIDA readout and the applied α-syn-SiNaPs concentration for $\bar{x}_{0\%}$ which increased with the trimmed means (Table 1).

Furthermore, the linear relationship between α-syn-SiNaP concentrations in both matrices and the sFIDA readout was validated by lack-of-fit test. Here, the calculated test value according to lack-of-fit test that is lower than the calculated respective F-distribution value indicate that the data could be fitted to a linear regression model [39]. The results of lack-of-fit test showed that the sFIDA readout of the dilution series in CSF and PBS could be described by a linear regression model for $\bar{x}_{8\%}$, $\bar{x}_{16\%}$, $\bar{x}_{25\%}$ and $\bar{x}_{33\%}$ (Table 1).

3.4. Single channel analysis

The sFIDA design is based on dual probe detection to enhance specificity of the analysis. In principle, the sFIDA assay can also be used in single channel mode using the capture epitope and the epitope of a single detection probe, as long as both share an overlapping epitope to keep the assay insensitive to α-syn monomers. In this setup, only pixels with signal intensities above a noise threshold from one channel are evaluated. Based on the obtained image data we performed two separate single channel analyses for both dilution series. In CSF, for both channels 10 fM SiNaPs yielded higher readouts compared to the non-spiked control. However, a limited dynamic range of the single channel readout was observed in channel 633, probably as a consequence of a higher background noise compared to the 488 channel (Fig. 6). The determination of CV % and linearity for the single channel readouts for each channel in both dilution series are shown in the Supplemental material (Figs. A.3–A.4 and Tables A.1–A.2).

For channel 633, the LODs and LLOQs for CSF and PBS were in the high femtomolar range as a consequence of a high background noise in this channel. Moreover, the probe-capture combination mAb 211 and 4B12 yielded a slightly elevated signal from monomeric α-syn (Supplementary material Fig. A.5a), suggesting that this antibody combination is not suitable for single channel sFIDA. For channel 488, however, the combination of mAbs 4D6 and 4B12 was not sensitive to monomeric α-syn (Supplementary material Fig. A.5b). In both dilution series the LODs and LLOQs were in the lower femtomolar range for $\bar{x}_{33\%}$ (Table 2) and thus in the same order of magnitude as the ones obtained from the conventional dual channel analysis (Table 1). These results indicate that sFIDA can also be

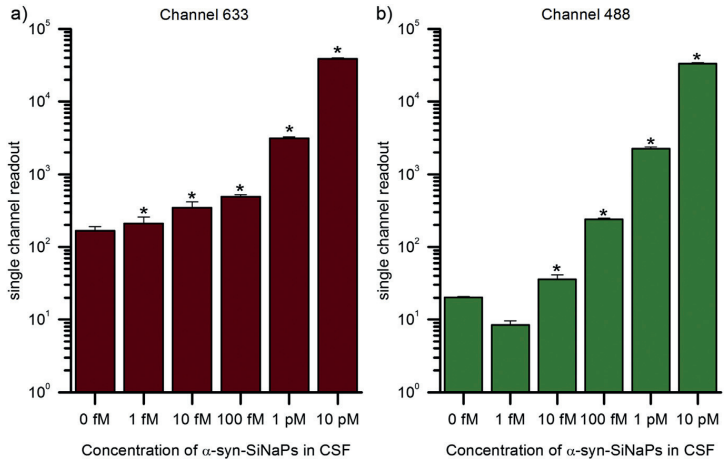

Fig. 6. Single channel readout of channel 633 (a) and channel 488 (b) for different concentrations of α-syn-SiNaPs in CSF. Columns and error bars represent the calculated trimmed mean for trimming percentage of 33% and respective standard deviations. A centered ROI with 58 μm × 58 μm of the images was analyzed. Cutoffs for each channel were set to minimize background signal by using the intensity in each channel where 0.1% (channel 633) and 0.01% (channel 488) of all pixels have intensity values above the cutoff in the non-spiked control in each channel. This led to following cutoff values for channel 633: 4698 and channel 488: 5335. Significant differences between non-spiked control (0 fM α-syn-SiNaPs) and samples were determined pairwise by *p*-value adjusted one-sided *t*-tests ($^*p \leq 0.05$). Data for $\bar{x}_{0\%}$ and the other trimmed means for each channel in both dilution series are illustrated in the Supplementary material (Figs. A.1–A.2).

Table 2
Sensitivity of the automated sFIDA assay was calculated by the limit of detection (LOD) and lower limit of quantification (LLOQ) for the single channel readout considering the pixel count above threshold in channel 488 and channel 633. Calculations are based on calibration curve of α-syn-SiNaPs in CSF and PBS and the respective non-spiked control. Shown are the arithmetic means ($\bar{x}_{0\%}$) and trimmed means with trimming percentage of 8%, 16%, 25% and 33%.

Dilution matrix	Trimmed means	LOD [fM]		LLOQ [fM]	
		Channel 488	Channel 633	Channel 488	Channel 633
CSF	$\bar{x}_{0\%}$	33	214	101	740
	$\bar{x}_{8\%}$	8.4	127	22	452
	$\bar{x}_{16\%}$	5.6	55	12	220
	$\bar{x}_{25\%}$	5.2	39	11	172
	$\bar{x}_{33\%}$	3.8	4.4	6.3	60
PBS	$\bar{x}_{0\%}$	26	618	76	2012
	$\bar{x}_{8\%}$	20	341	56	1102
	$\bar{x}_{16\%}$	15	171	42	542
	$\bar{x}_{25\%}$	9.4	119	27	343
	$\bar{x}_{33\%}$	2.5	84	6.8	184

performed with a single antibody probe and still yields meaningful results.

4. Discussion and summary

In this study we introduced α-syn-SiNaPs as calibration standard for immuno-based quantitation of α-syn oligomers. We validated the performance of the particle standard by automated sFIDA analysis.

Automation offers considerable advantages over manual operations, especially independence from human error-proneness and skill as well as the preparation of a high number of replicates. Furthermore, the application of robust statistics mitigates the impact of outliers and small departures from normal distribution, respectively, to estimates of the central tendency. In this context, the trimmed mean $\bar{x}_{\%}$, as an intermediate between the median and the mean, represents a compromise between robustness towards outliers and sensitivity. With a reasonable percentage of data points in a ranked data set to discard we propose the interquartile mean ($\bar{x}_{25\%}$) for future application of sFIDA based quantitation of α-syn-SiNaPs and α-syn oligomers in biological samples.

In previous studies on PD biomarkers the level of total α-syn has been investigated in CSF or blood plasma [26,28,40]. However, utility of total α-syn as a PD biomarker is still under debate and published data are conflicting both with regard to the reported α-syn levels in body fluids and its clinical significance.

Due to the limited utility of total α-syn as PD biomarker, the directly disease-related α-syn oligomers have been analyzed mainly with ELISA-based techniques [12,41,42]. However, the lack of suitable oligomeric standards has yet hampered rigorous quantitation of the absolute α-syn oligomer concentration in body fluids. Instead, the level of oligomers was estimated by comparing the ELISA signals from oligomers versus total α-syn [26].

The α-syn-SiNaPs standards described in this report could be basically applied in any immuno-based α-syn oligomer assay given that the same or overlapping epitopes, but not structural epitopes, are targeted by the capture and detection system. As for our previously described Aβ-oligomer standards [25], the α-syn-SiNaPs feature long term stability, a uniform and adjustable size and a tunable epitope load on the particle surface. Using an inorganic core material that determines the size allows in principle to modify the protein load on the surface simply by adjusting the protein concentration in the coupling step.

By sFIDA analysis we have demonstrated sensitive detection of α-syn-SiNaPs in CSF and PBS with LODs in the femtomolar range without interference of matrix components or endogenous α-syn. In a recently published study on biological samples, an oligomeric α-syn concentration of 116 pg/ml was reported for a PD cohort [17]. An assay LOD of 10 pg/ml was estimated on basis of recombinant oligomeric α-syn. In our present study we calculated an LOD of 2.5 fM for α-syn-SiNaPs which corresponds to an α-syn concentration of 0.98 pg/ml considering an α-syn load of 27 molecules per SiNaP.

Yet, there is little information available on the properties of native oligomers with regard to size and structure distribution, as well as the nature of epitopes available for immune-detection. However, from structural studies is known that the C-terminus is accessible in the aggregated conformation of α-syn [43–45]. Therefore, we hypothesize that sFIDA in its current version is capable of specifically quantitating α-syn oligomers in native patient samples which is subject of ongoing work.

We conclude that α-syn-SiNaPs are useful as a calibration standard for the sFIDA assay and potentially for any immuno-based method for the quantitation of native α-syn oligomers. As pathological accumulation of α-syn is per definition a hallmark of every synucleinopathy, such as multiple system atrophy and Lewy body dementia [40], our advanced sFIDA technology will allow future validation to answer the question if α-syn oligomers qualify as biomarkers for these diseases in clinical routine.

Acknowledgment

The authors thank Vera Bürger, Markus Mandler, and Achim Schneeberger (Affiris AG, Vienna, Austria) for fruitful discussions. This work was supported by the European Union Seventh Framework Programme (FP7/2007-2013) under grant agreement 602999 (SYMPATH project), the Federal Ministry of Education and Research within the projects VIP (03V0641), KNDD (01GI1010A), and JPND/BIOMARKAPD (01ED1203H). We also received funding from the Program "Biomarkers Across Neurodegenerative Diseases" (11084) of The Alzheimer's Association, Alzheimer's Research UK, The Michael J. Fox Foundation for Parkinson's Research, and the Weston Brain Institute.

Appendix A. Supplementary data

Supplementary data to this article can be found online at http://dx.doi.org/10.1016/j.cca.2017.01.010.

References

[1] W.G. Meissner, M. Frasier, T. Gasser, et al., Priorities in Parkinson's disease research, Nat. Rev. Drug Discov. 10 (2011) 377–393.
[2] J. Jankovic, Parkinson's disease: clinical features and diagnosis, J. Neurol. Neurosurg. Psychiatry 79 (2008) 368–376.
[3] A.J. Hughes, S.E. Daniel, A.J. Lees, Improved accuracy of clinical diagnosis of Lewy body Parkinson's disease, Neurology 57 (2001) 1497–1499.
[4] M.G. Spillantini, M.L. Schmidt, V.M. Lee, J.Q. Trojanowski, R. Jakes, M. Goedert, Alpha-synuclein in Lewy bodies, Nature 388 (1997) 839–840.
[5] M.H. Polymeropoulos, C. Lavedan, E. Leroy, et al., Mutation in the alpha-synuclein gene identified in families with Parkinson's disease, Science 276 (1997) 2045–2047.
[6] B. Winner, R. Jappelli, S.K. Maji, et al., In vivo demonstration that alpha-synuclein oligomers are toxic, Proc. Natl. Acad. Sci. U. S. A. 108 (2011) 4194–4199.

[7] D.P. Karpinar, M.B. Balija, S. Kugler, et al., Pre-fibrillar alpha-synuclein variants with impaired beta-structure increase neurotoxicity in Parkinson's disease models, EMBO J. 28 (2009) 3256–3268.
[8] E. Rockenstein, S. Nuber, C.R. Overk, et al., Accumulation of oligomer-prone α-synuclein exacerbates synaptic and neuronal degeneration, Brain – J. Neurol. (2014) 1–18.
[9] H.A. Lashuel, C.R. Overk, A. Oueslati, E. Masliah, The many faces of alpha-synuclein: from structure and toxicity to therapeutic target, Nat. Rev. Neurosci. 14 (2013) 38–48.
[10] O.M. El-Agnaf, S.A. Salem, K.E. Paleologou, et al., Detection of oligomeric forms of alpha-synuclein protein in human plasma as a potential biomarker for Parkinson's disease, FASEB J. 20 (2006) 419–425.
[11] M.J. Park, S.M. Cheon, H.R. Bae, S.H. Kim, J.W. Kim, Elevated levels of alpha-synuclein oligomer in the cerebrospinal fluid of drug-naive patients with Parkinson's disease, J. Clin. Neurol. 7 (2011) 215–222.
[12] T. Tokuda, M.M. Qureshi, M.T. Ardah, et al., Detection of elevated levels of α-synuclein oligomers in CSF from patients with Parkinson disease, Neurology 75 (2010) 1766–1770.
[13] O. Hansson, S. Hall, A. Öhrfelt, et al., Levels of cerebrospinal fluid α-synuclein oligomers are increased in Parkinson's disease with dementia and dementia with Lewy bodies compared to Alzheimer's disease, Alzheimers Res. Ther. 6 (2014) 25.
[14] M.R. Sierks, G. Chatterjee, C. McGraw, S. Kasturirangan, P. Schulz, S. Prasad, CSF levels of oligomeric alpha-synuclein and beta-amyloid as biomarkers for neurodegenerative disease, Integr. Biol. (Camb.) 3 (2011) 1188–1196.
[15] X. Wang, S. Yu, F. Li, T. Feng, Detection of alpha-synuclein oligomers in red blood cells as a potential biomarker of Parkinson's disease, Neurosci. Lett. 599 (2015) 115–119.
[16] M.H. Horrocks, S.F. Lee, S. Gandhi, et al., Single-molecule imaging of individual amyloid protein aggregates in human biofluids, ACS Chem. Neurosci. 7 (2016) 399–406.
[17] N.K. Majbour, N.N. Vaikath, K.D. van Dijk, et al., Oligomeric and phosphorylated alpha-synuclein as potential CSF biomarkers for Parkinson's disease, Mol. Neurodegener. 11 (2016) 7.
[18] S.A. Funke, E. Birkmann, F. Henke, et al., Single particle detection of Abeta aggregates associated with Alzheimer's disease, Biochem. Biophys. Res. Commun. 364 (2007) 902–907.
[19] K. Kravchenko, A. Kulawik, M. Hülsemann, et al., Analysis of anticoagulants for blood-based quantitation of amyloid beta oligomers in the sFIDA assay, Biol. Chem. (2016).
[20] K. Kühbach, M. Hülsemann, Y. Herrmann, et al., Application of an amyloid beta oligomer standard in the sFIDA assay, Front. Neurosci. 10 (2016) 8.
[21] Y. Herrmann, A. Kulawik, K. Kühbach, et al., sFIDA automation yields subfemtomolar limit of detection for Abeta aggregates in body fluids, Clin. Biochem. (2016).
[22] S.A. Funke, E. Birkmann, F. Henke, et al., An ultrasensitive assay for diagnosis of Alzheimer's disease, Rejuvenation Res. 11 (2008) 315–318.
[23] S.A. Funke, L. Wang, E. Birkmann, D. Willbold, Single-particle detection system for Aβ aggregates: adaptation of surface-fluorescence intensity distribution analysis to laser scanning microscopy, Rejuvenation Res. 13 (2009) 206–209.
[24] L. Wang-Dietrich, S.A. Funke, K. Kühbach, et al., The amyloid-beta oligomer count in cerebrospinal fluid is a biomarker for Alzheimer's disease, J. Alzheimers Dis. 34 (2013) 985–994.
[25] M. Hülsemann, C. Zafiu, K. Kühbach, et al., Biofunctionalized silica nanoparticles: standards in amyloid-beta oligomer-based diagnosis of Alzheimer's disease, J. Alzheimers Dis. 54 (2016) 79–88.
[26] A.H. Simonsen, B. Kuiperij, O. Mukhtar, et al., The utility of α-synuclein as biofluid marker in neurodegenerative diseases: a systematic review of the literature, Biomark. Med. (2015).
[27] W. Hoyer, T. Antony, D. Cherny, G. Heim, T.M. Jovin, V. Subramaniam, Dependence of α-synuclein aggregate morphology on solution conditions, J. Mol. Biol. 322 (2002) 383–393.
[28] B. Zhou, M. Wen, W.F. Yu, C.L. Zhang, L. Jiao, The diagnostic and differential diagnosis utility of cerebrospinal fluid alpha-synuclein levels in Parkinson's disease: a meta-analysis, Parkinsons Dis. 2015 (2015) 567386.
[29] B.R. Lee, Y. Matsuo, A.G. Cashikar, T. Kamitani, Role of Ser129 phosphorylation of alpha-synuclein in melanoma cells, J. Cell Sci. 126 (2013) 696–704.
[30] J.L. Devore, R. Peck, Introductory Statistics, West Publishing Company, 1990.
[31] W.M. Bolstad, Introduction to Bayesian Statistics: Wiley, 2007.
[32] B. Everitt, The Cambridge Dictionary of Statistics, Cambridge University Press, Cambridge, UK; New York, NY, USA, 1999.
[33] Y. Benjamini, Y. Hochberg, Controlling the false discovery rate: a practical and powerful approach to multiple testing, J. R. Stat. Soc. Ser. B Methodol. 57 (1995) 289–300.
[34] K. Pearson, Mathematical contributions to the theory of evolution. III. Regression, heredity, and panmixia, Philos. Trans. R. Soc. Lond. A: Math., Phys. Eng. Sci. 187 (1896) 253–318.
[35] B. Slutsky, in: D.L. Massart, B.G.M. Vandeginste, L.M.C. Buydens, S. De Jong, P.J. Lewi, J. Smeyers-Verbeke (Eds.), Handbook of Chemometrics and Qualimetrics: Part A, Data Handling in Science and Technology, Vol. 20A, Elsevier, Amsterdam 1997, p. 1254 Journal of Chemical Information and Computer Sciences 1998; 38.
[36] S.W. Chen, S. Drakulic, E. Deas, et al., Structural characterization of toxic oligomers that are kinetically trapped during alpha-synuclein fibril formation, Proc. Natl. Acad. Sci. U. S. A. 112 (2015) E1994–E2003.
[37] Robust statistics–how not to reject outliers. Part 1. Basic concepts, Analyst 114 (1989) 1693–1697.
[38] W. Horwitz, Evaluation of analytical methods used for regulation of foods and drugs, Anal. Chem. 54 (1982) 67A–76A.
[39] J. Van Loco, M. Elskens, C. Croux, H. Beernaert, Linearity of calibration curves: use and misuse of the correlation coefficient, Accred. Qual. Assur. 7 (2002) 281–285.
[40] B. Laurens, R. Constantinescu, R. Freeman, et al., Fluid biomarkers in multiple system atrophy: a review of the MSA biomarker initiative, Neurobiol. Dis. 80 (2015) 29–41.
[41] J.O. Aasly, K.K. Johansen, G. Bronstad, et al., Elevated levels of cerebrospinal fluid alpha-synuclein oligomers in healthy asymptomatic LRRK2 mutation carriers, Front. Aging Neurosci. 6 (2014) 248.
[42] L. Parnetti, D. Chiasserini, E. Persichetti, et al., Cerebrospinal fluid lysosomal enzymes and alpha-synuclein in Parkinson's disease, Mov. Disord. 29 (2014) 1019–1027.
[43] A. Der-Sarkissian, C.C. Jao, J. Chen, R. Langen, Structural organization of alpha-synuclein fibrils studied by site-directed spin labeling, J. Biol. Chem. 278 (2003) 37530–37535.
[44] H. Miake, H. Mizusawa, T. Iwatsubo, M. Hasegawa, Biochemical characterization of the core structure of alpha-synuclein filaments, J. Biol. Chem. 277 (2002) 19213–19219.
[45] R.A. Crowther, S.E. Daniel, M. Goedert, Characterisation of isolated alpha-synuclein filaments from substantia nigra of Parkinson's disease brain, Neurosci. Lett. 292 (2000) 128–130.

Supplementary material

A.1 sFIDA

The sFIDA assay was performed in a 384-well-format microplate. The microplates were custom-assembled by PolyAn GmbH (Berlin, Germany). In this process PolyAn modified the surface of glass plates (70 x 110 x 0.17 mm³; Menzel-Gläser, Braunschweig, Germany) with a 3-D antibiofouling polymer coating containing amine reactive NHS-Esters. This glass plates were glued by Grace Bio-Labs (Grace Bio-Labs, Oregon, USA) to bottomless 384-well microtiter plates (Greiner Bio One, Kremsmünster, Austria), sealed under inert atmosphere and stored at 4°C to maintain the surface reactivity.

During the incubations, a lid in microplate format (Forschungszentrum Jülich GmbH, Jülich, Germany) was placed on top of the processed microplate and transported back to the park position, before performing the next step in the assay.

The first step in the process of assay preparation was to functionalize surface with capture antibodies. The antibody 4B12 was prepared in a concentration of 10 ng/µl in 100 mM MES buffer, pH 4.7 (AppliChem, Darmstadt, Germany) and centrifuged at 15,000 g for 10 min before the liquid handling system applied 15 µl to each well. After overnight incubation wash procedure 1 was applied. This wash procedure consisted of three wash steps with 1 x PBS (Sigma-Aldrich, St. Louis, MO, USA) containing 0.05% Tween 20 (AppliChem, Darmstadt, Germany; PBS-T) and three wash steps with 1 x PBS (PBS).

A solution of 0.05 M ethanolamine hydrochloride (Sigma-Aldrich, St. Louis, MO, USA) in 0.1 M Tris at pH 9 was prepared to quench the remaining functional groups on the surface of the microplate. The liquid handling system applied 50 µl of the solution to each well. After 2 h incubation, the microplate was washed by wash procedure 1.

A blocking solution (Smart Block, CANDOR Biosciences, Wangen, Germany) was applied in a volume of 50 µl to each well. The blocking solution was incubated for 1 h before the microplate was washed three times with PBS-T, three times with PBS and leaving approx. 80 µl of PBS in each well after the final wash step (wash procedure 2) to prevent drying of the wells during sample application. The liquid handling system prepared a ten-fold dilution series of α-syn-SiNaPs in CSF and PBS starting from a 100 pM α-syn-SiNaPs stock solution. Each concentration of α-syn-SiNaPs was applied in 12 replicates and the non-spiked controls in 20 replicates for PBS and CSF, respectively. PBS was emptied from the wells by the liquid handling system just prior to the application of 15 µl sample per well. Both procedures, buffer removal and sample application, were performed column-wise. The samples were incubated overnight. On the next day the wells were washed three times with PBS-T, three times with PBS and leaving 10 µl PBS in each well (wash procedure 3).

The detection antibodies 4D6 labeled with Atto Fluor 488 (ATTO-TEC, Siegen, Germany) and 211 (Santa Cruz Biotechnology Inc., TX, USA) labeled with Atto Fluor 633 (ATTO-TEC, Siegen, Germany) were combined each to yield 1.87 µg ml^{-1} in PBS and centrifuged for 1 h at 100,000 g and 4°C. The liquid handling system applied 20 µl of the supernatant to each well, which resulted in a final concentration of 1.25 µg ml^{-1}. After an incubation time of 1 h, the wells were washed five times with PBS-T, five times with

PBS leaving 10 µl PBS in per well (wash procedure 4). Finally, the liquid handling system applied 90 µl of 2 mM sodium azide (Sigma-Aldrich, St. Louis, MO, USA) in water to preserve the samples during the measurements. Image acquisition was performed in a TIRFM with penetration depths of 200 nm and laser intensities of 100% for each channel. The exposure time was set to 400 ms in channel 633 and 1000 ms in channel 488 and EM gains of 300 (channel 633) and 800 (channel 488).

A.2 Artifact detection

The artifact detection was developed to exclude images that may contain extraordinary large and/or bright spots due to mechanical damage of the surface, dust, or other contamination. In order to detect and exclude such artifact afflicted images a cluster detection within each image was performed. The 14-bit grayscale images were transformed into binary images and a structuring element of 1 µm x 1 µm size was used to dilate and erode the images. This procedure was added to identify diffuse artifacts, which exhibited pixels with very low intensities that formed “gaps” in possible clusters, which then were not identified as artificial and lead to artificial sFIDA readouts during the image analysis. The next procedure applied a structuring element of size 4 µm x 4 µm to erode the images and identify large clusters. Finally, dilation was applied to compensate pixel loss in the eroded images. Each identified cluster was tested based on mean pixel intensity, standard deviation and skewness. An image containing at least one of the detected clusters with the following parameters was excluded from further analysis: mean pixel intensity ≥ 3000, a standard deviation ≥ 2800 or skewness of < 0. Altogether, 7.5% of the images were excluded from further analysis.

A.3 sFIDA with α-syn monomers

The sFIDA was performed manually with three replicates of samples containing 270 pM α-syn monomers, 10 pM α-syn-SiNaPs and six replicates of the non-spiked control following the sFIDA protocol (Supplemental Section A.1).

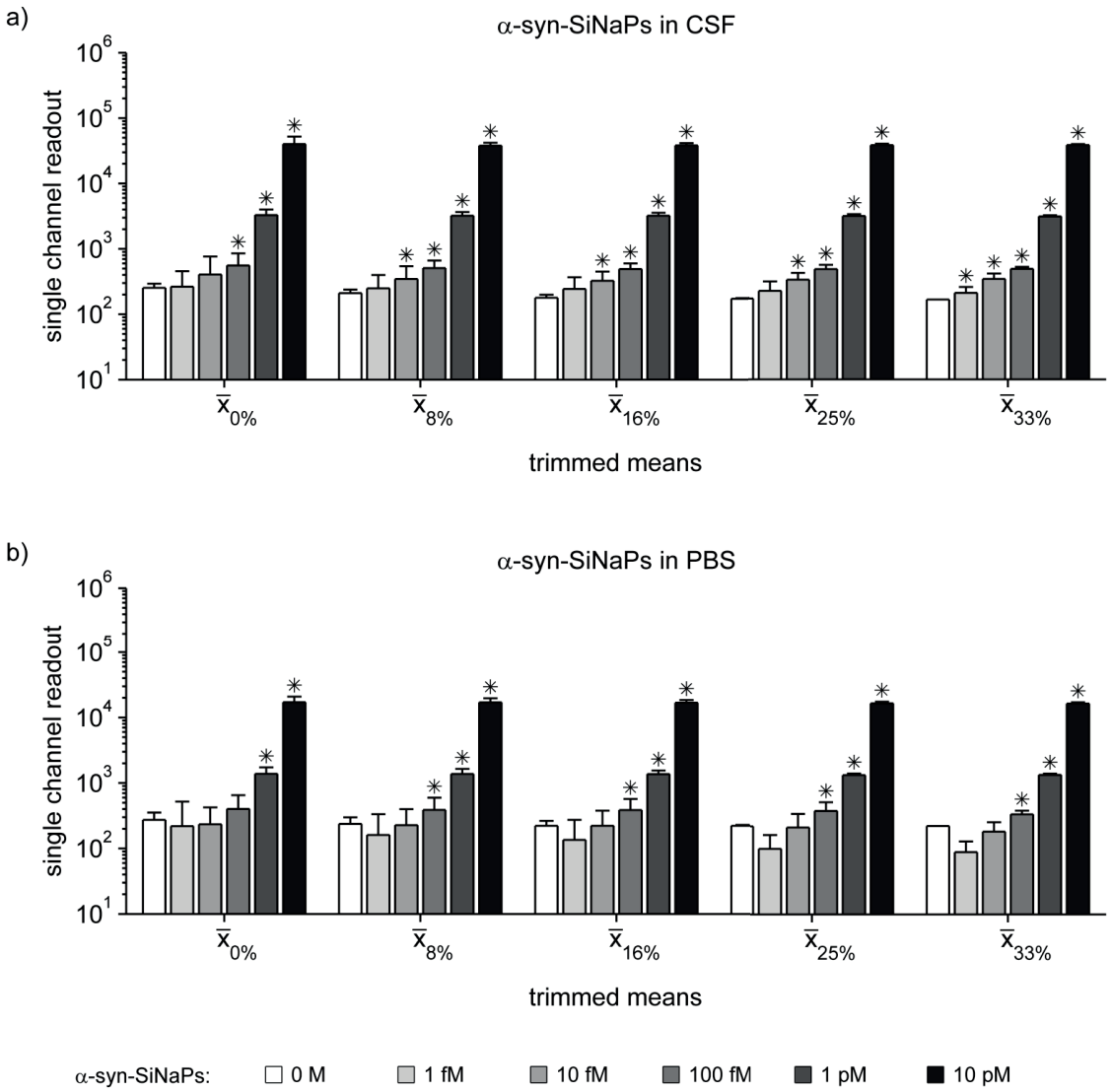

Figure A.1 Single channel readout considering channel 633 for different concentrations of α-syn-SiNaPs (a) in CSF and (b) in PBS. Columns and error bars represent the calculated arithmetic mean ($\bar{x}_0$), trimmed means for trimming percentage of 8%, 16%, 25% and 33% and respective standard deviations. A centered ROI with 58 µm x 58 µm of the images was analyzed. Cutoff for channel 633 was set to minimize background signal by using the intensity in each channel where only 0.1% of all pixels have intensity values above the cutoff in the negative control in each channel. This led to following cutoff values for CSF: 4698 and for PBS: 8573. Significant differences between the negative control (0 fM α-syn-SiNaPs) and the samples were determined pairwise by p-value adjusted one-sided t-tests (*$p \leq 0.05$).

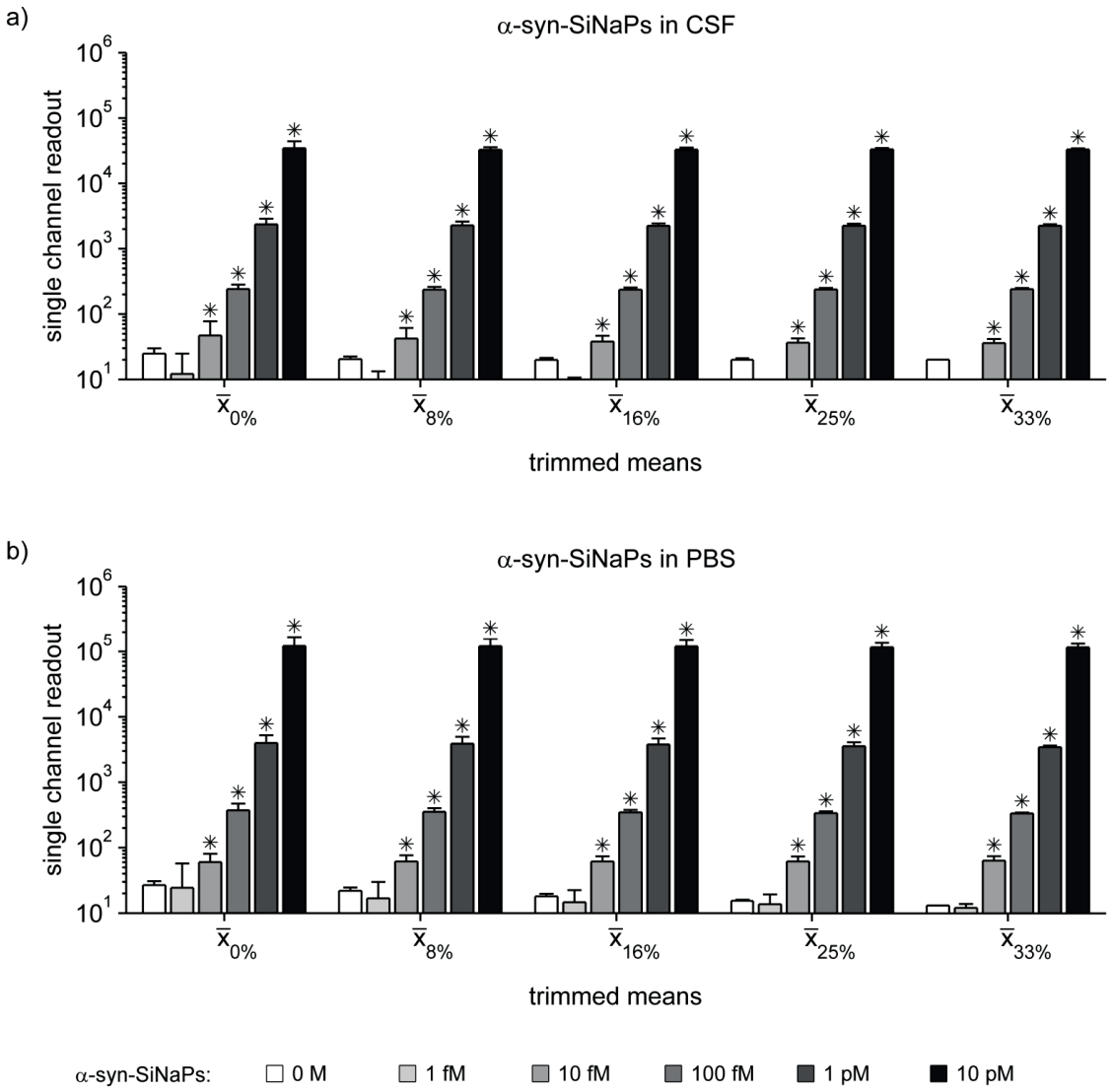

Figure A.2 Single channel readout considering channel 488 for different concentrations of α-syn-SiNaPs (a) in CSF and (b) in PBS. Columns and error bars represent the calculated arithmetic mean ($\bar{x}_0$), trimmed means for trimming percentage of 8%, 16%, 25% and 33% and respective standard deviations A centered ROI with 58 µm x 58 µm of the images was analyzed. Cutoff for channel 488 was set to minimize background signal by using the intensity in each channel where only 0.01% of all pixels have intensity values above the cutoff in the negative control in each channel. This led to following cutoff values for CSF: 5335 and for PBS: 3209. Significant differences between the negative control (0 fM α-syn-SiNaPs) and the samples were determined pairwise by p-value adjusted one-sided t-tests (*$p \leq 0.05$).

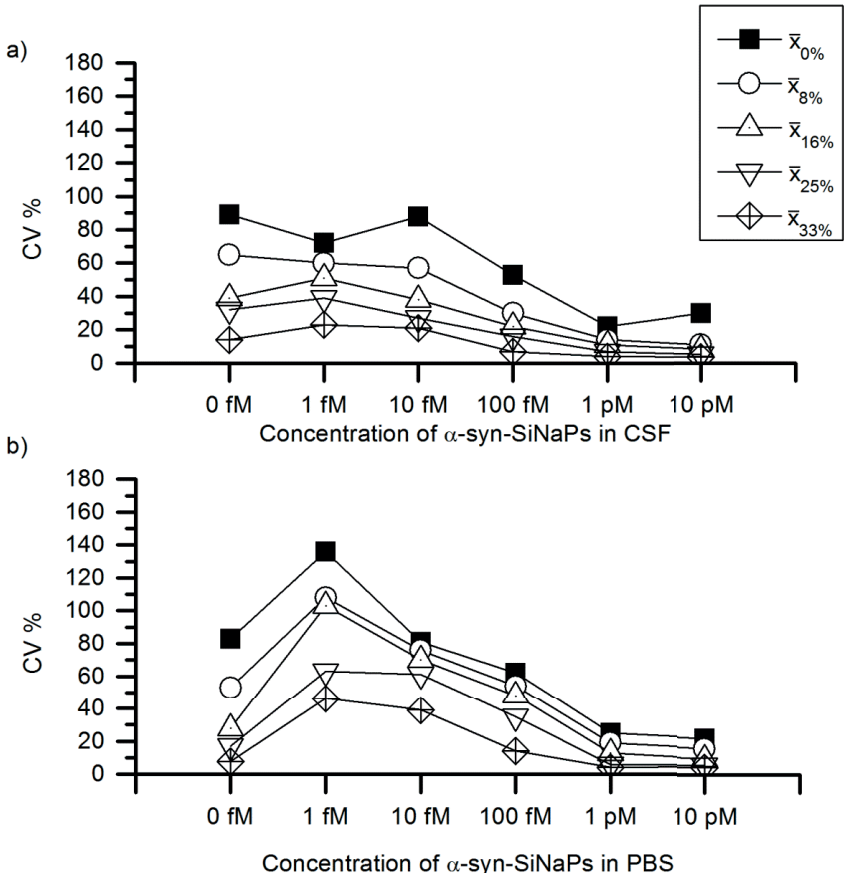

Figure A.3 Coefficient of variance in percent based on single channel readouts (channel 633) for each concentration of α-syn-SiNaPs (a) in CSF and (b) in PBS for the arithmetic mean ($\bar{x}_0$) and trimmed means for 8%, 16%, 25% and 33%.

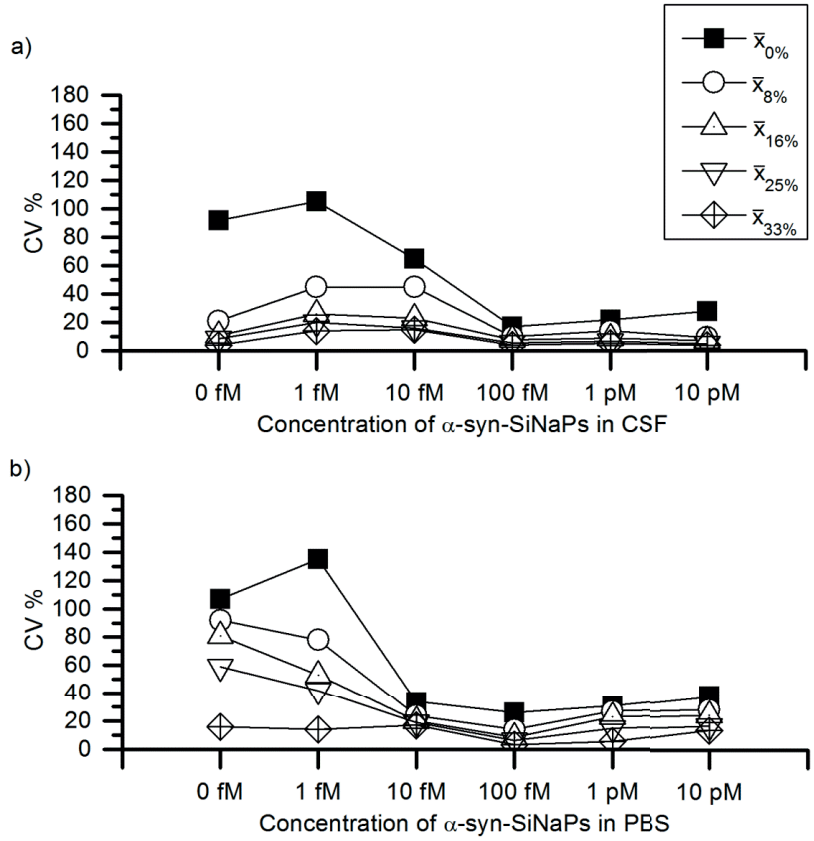

Figure A.4 Coefficient of variance in percent based on single channel readouts (channel 488) for each concentration of α-syn-SiNaPs (a) in CSF and (b) in PBS for the arithmetic mean ($\bar{x}_0$) and trimmed means for 8%, 16%, 25% and 33%.

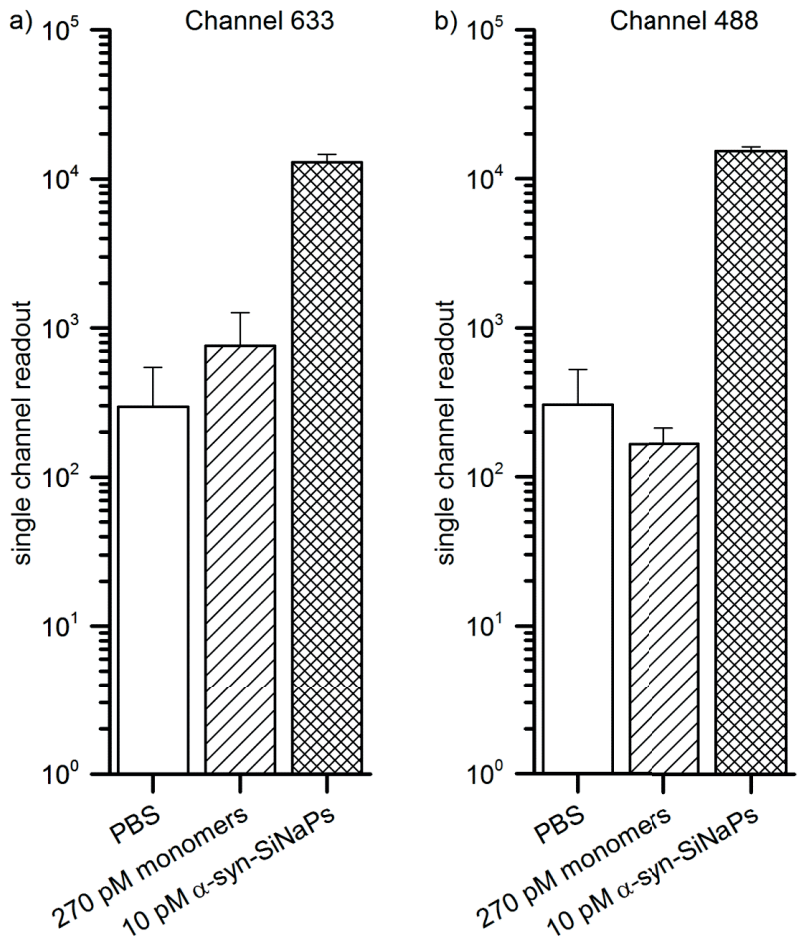

Figure A.5 Single channel readout of channel 633 (a) and channel 488 (b) for PBS control (white), 270 pM α-syn monomer (striped) and 10 pM α-syn-SiNaPs (checked). The α-syn monomer concentration of 270 pM corresponds to the applied concentration of 10 pM of α-syn-SiNaPs (27 α-syn-epitopes per SiNaP). After the exclusion of artificial images from the data analysis, a centered ROI with 58 µm x 58 µm of the images was analyzed. Cutoffs for each channel were set to minimize background signal by using the intensity in each channel where 0.1% of all pixels have intensity values above the cutoff in the non-spiked control in each channel. This led to following cutoff values for PBS: 7127 for channel 633 and 5040 for channel 488.

Table A.1 Correlation of the automated sFIDA assay for channel 633 was calculated by Pearson's coefficient r, linearity by F-Test (Lack-of-fit test) and coefficient of variation in percent (CV %) for each concentration for arithmetic mean ($\bar{x}_{0\%}$) and trimmed means with trimming percentage of 8%, 16%, 25% and 33%. Lack-of-fit test for linear and quadratic regression model (LRM, QRM): The H_0 hypothesis assumes no lack of fit. For LRM/QRM < $F_{(crit., 99\%)}$ H_0 is accepted (no lack of fit).

dilution matrix	trimmed means	Pearson's r	Lack-of-fit test			CV [%]					
			LRM	QRM	$F_{(crit., 99\%)}$	0 fM	1 fM	10 fM	100 fM	1 pM	10 pM
CSF	$\bar{x}_{0\%}$	0.953	0.11	0.72	3.6	89	72	88	53	22	30
	$\bar{x}_{8\%}$	0.993	0.52	0.20	3.7	65	60	57	30	14	11
	$\bar{x}_{16\%}$	0.996	0.67	0.10	3.8	39	51	38	22	11	8.4
	$\bar{x}_{25\%}$	0.998	1.5	0.06	3.9	32	39	27	16	6.7	5.3
	$\bar{x}_{33\%}$	0.999	2.4	0.06	4.4	14	23	21	7	3.9	3.7
PBS	$\bar{x}_{0\%}$	0.973	0.36	1.01	3.6	83	136	81	62	25	22
	$\bar{x}_{8\%}$	0.986	0.53	0.46	3.7	53	108	76	54	19	16
	$\bar{x}_{16\%}$	0.994	0.98	0.32	3.8	28	103	70	48	13	9.7
	$\bar{x}_{25\%}$	0.998	2.4	0.36	3.9	17	63	61	35	5.9	5.9
	$\bar{x}_{33\%}$	0.999	2.4	0.28	4.4	7.6	46	39	14	4.2	4.4

Table A.2 Correlation of the automated sFIDA assay for channel 488 was calculated by Pearson's coefficient r, linearity by F-Test (Lack-of-fit test) and coefficient of variation in percent (CV %) for each concentration for arithmetic mean ($\bar{x}_{0\%}$) and trimmed means with trimming percentage of 8%, 16%, 25% and 33%. Lack-of-fit test for linear and quadratic regression model (LRM, QRM): The H_0 hypothesis assumes no lack of fit. For LRM/QRM < $F_{(crit., 99\%)}$ H_0 is accepted (no lack of fit).

dilution matrix	trimmed means	Pearson's r	Lack-of-fit test			CV [%]					
			LRM	QRM	$F_{(crit., 99\%)}$	0 fM	1 fM	10 fM	100 fM	1 pM	10 pM
CSF	$\bar{x}_{0\%}$	0.960	0.22	0.59	3.6	92	105	65	17	22	28
	$\bar{x}_{8\%}$	0.995	1.4	0.14	3.7	21	45	45	10	14	9.5
	$\bar{x}_{16\%}$	0.997	2.1	0.06	3.8	11	26	23	8	9.1	7.3
	$\bar{x}_{25\%}$	0.998	3.5	0.02	3.9	8.7	20	16	5.7	6.9	5
	$\bar{x}_{33\%}$	0.999	4.0	0.01	4.4	4	14	15	4.3	5.4	3.8
PBS	$\bar{x}_{0\%}$	0.928	0.52	2.9	3.6	107	135	34	26	31	38
	$\bar{x}_{8\%}$	0.954	0.72	1.2	3.7	92	78	24	14	27	29
	$\bar{x}_{16\%}$	0.968	0.83	0.57	3.8	81	53	20	8.8	23	25
	$\bar{x}_{25\%}$	0.984	1.4	0.20	3.9	59	42	19	6.3	15	17
	$\bar{x}_{33\%}$	0.989	1.3	0.07	4.4	16	14	17	3.4	5.8	14

4. Diskussion und Zusammenfassung

Zurzeit gibt es weder eine zweifelsfreie Diagnose noch eine Therapie für die AD. Die Fehlfaltung und Aggregation von Aβ werden als Auslöser der AD genannt. Die löslichen Aggregationsspezies, Aβ-Oligomere, haben pathologische Effekte im Gehirn wodurch die AD entsteht. Die Aβ-Oligomere stehen daher im Fokus bei der Entwicklung eines Verfahrens zur frühzeitigen Diagnose der AD. Eine frühzeitige und sichere Diagnose kann den AD-Patienten helfen Vorkehrungen zu treffen. Insbesondere ist die Unterscheidung von AD-Patienten von anderen Demenzkranken wichtig bei der Medikamenten-Entwicklung, um die geeigneten Probanden für klinische Studien auszuwählen.

In Abschnitt 1.1.2.4 wurde die Notwendigkeit von Standardmolekülen zur Detektion von Aβ-Oligomeren erläutert. Im Rahmen der Optimierung des sFIDA-Assays wurden kommerziell erworbene, stabilisierte Aβ-Oligomere verwendet, aber zusätzlich die Entwicklung und Verwendung von Standardmolekülen in Form von $A\beta_{1-42}$-SiNaPs vorangetrieben. Darüber hinaus wurden die SiNaPs modifiziert, um als Kalibrierstandard im sFIDA-Assay zur Quantifizierung von α-syn-Oligomeren zur frühzeitigen Diagnose der PD verwendet zu werden.

Stabilisierte Aβ-Oligomere wurden in CSF, PBS und Blutplasma mit Gerinnungshemmer EDTA (Ethylendiamintetraessigsäure) verdünnt und erfolgreich im sFIDA-Assay gemessen (siehe Abschnitt 3.1). Der Hersteller gibt an, dass die CB-Oligomere folgende Eigenschaften besitzen: homogene Population mit einem hydrodynamischen Radius von 12 nm, ein überwiegend Monomer-freies Gemisch, $>$ 85% β-Faltblatt Konformation und ein Oligomer besteht aus circa 220 $A\beta_{1-42}$-Monomeren. Die Korrelation des *sFIDA readouts* mit der eingesetzten CB-Oligomer Konzentration wurde in CSF, PBS und im EDTA Plasma bis zum unteren femtomolaren Bereich gezeigt. Die Nachweisgrenzen betrugen 18 fM in CSF, 22 fM in PBS und 14 fM in EDTA Plasma. Die Nachweisgrenze von 14 fM in EDTA Plasma entspricht einer monomerischen Konzentration von 13.9 ng/l. Die stabilisierten Aβ-Oligomere bestehend aus circa 220 $A\beta_{1-42}$-Monomeren sind nicht vergleichbar mit *low molecular weight*-Oligomeren, die mit unter acht Aβ Einheiten definiert sind

(Bruggink et al., 2012). Im Gegensatz zu den LMW-Oligomeren haben die *high molecular weight*-Oligomere (HMW) ein molekular Gewicht von circa 42 kDa bis zu 1 mDa (Bruggink et al., 2012). Dementsprechend könnten die stabilisierten Aβ-Oligomere (circa 1 mDa) insbesondere als Kalibrierstandard für HMW-Oligomere untersucht werden.

Die Synthese, Charakterisierung und erfolgreiche Verwendung im sFIDA-Assay der $A\beta_{1-42}$-SiNaPs wurde in Abschnitt 3.2 vorgestellt. Die $A\beta_{1-42}$-SiNaPs wurden hergestellt durch die Biofunktionalisierung von SiNaPs. Zunächst wurden SiNaPs nach dem Stöber Prozess erzeugt und mit APTES silanisiert, um Amino-Gruppen auf der Oberfläche zu erzeugen. Daraufhin wurden carboxilierte SiNaPs durch die Reaktion mit Bernsteinsäure erstellt und im nächsten Schritt mit EDC/NHS aktiviert. Dadurch wird die Kopplung von $A\beta_{1-42}$ an die SiNaPs-Oberfläche realisiert. Der Durchmesser der SiNaPs ist circa 24 nm und wurde mit Transmissionselektronenmikroskop (TEM) bestimmt. Die Konzentration von $A\beta_{1-42}$ wurde auf 24 µg/ml in 1 mg/ml SiNaPs-Lösung bestimmt und entspricht 44 $A\beta_{1-42}$-Peptide pro SiNaP. Die $A\beta_{1-42}$-SiNaPs wurden in CSF und Wasser verdünnt und im sFIDA-Assay gemessen. Dabei wurde eine Korrelation des *sFIDA readouts* und der eingesetzten $A\beta_{1-42}$-SiNaPs Konzentration bis in den unteren femtomolaren Bereich gezeigt. Die Stabilität der $A\beta_{1-42}$-SiNaPs wurde durch weitere sFIDA-Assays bestimmt welche zeigten, dass die $A\beta_{1-42}$-SiNaPs über vier Monate in Wasser bei $4°C$ stabil sind. Die $A\beta_{1-42}$-SiNaPs besitzen eine definierte Anzahl an zugänglichen $A\beta_{1-42}$-Epitopen auf ihrer Oberfläche, die deutlich reduziert ist gegenüber den stabilisierten Oligomeren aus der vorherigen Studie. Dementsprechend können die $A\beta_{1-42}$-SiNaPs als Standard für Studien eingesetzt werden, die kleinere Aβ-Oligomere untersuchen möchten.

Die entwickelten $A\beta_{1-42}$-SiNaPs wurden bei der Untersuchung von Blutplasma mit verschiedenen Gerinnungshemmern (EDTA, Zitrat und Heparin) für die Detektion von Aβ-Oligomere eingesetzt (siehe Abschnitt 3.3). Die $A\beta_{1-42}$-SiNaPs in dieser Studien haben einen Durchmesser von 30 nm und circa 36 $A\beta_{1-42}$-Peptide pro SiNaP. Eine Korrelation des *sFIDA readouts* und der eingesetzten $A\beta_{1-42}$-SiNaPs Konzentration wurde in PBS, EDTA-, Zitrat- und Heparin-Plasma gezeigt. Die Berechnungen von CV $[\%]$, Nachweisgrenze basierend auf den *sFIDA readouts* weisen darauf hin, dass Plasma mit dem Gerinnungshemmer EDTA für den sFIDA-Assay am geeignetsten ist. In Abschnitt 1.1.2.2 wurde bereits erwähnt, dass die Untersuchung von Aβ als Biomarker in Blut oder Blutplasma optimiert werden könnte. Die $A\beta_{1-42}$-SiNaPs könnte eine Möglichkeit darstellen, um weitere Studien in Vollblut, Blutplasma oder Serum mit Gerinnungshemmern in EDTA durchzuführen

und somit die Validierung von Aβ als Biomarker für die AD in diesen Körperflüssigkeiten voran zu treiben.

Ein weiteres Ziel dieser Arbeit war es, die Automatisierung des sFIDA-Assays in einem *Liquid Handling System* umzusetzen, um den Durchsatz von Proben zu erhöhen und eine Standardisierung des Laborprozesses zu ermöglichen. Zusätzlich sollten negative Einflüsse durch Faktoren wie Fähigkeiten und Konzentrationsleistung der Anwender bei der Durchführung des sFIDA-Assays reduziert werden und gleichzeitig die Entlastung der Anwender realisiert werden. Somit soll die Präparation des sFIDA-Assays ökonomischer gestaltet werden. Im Kapitel 2 wurden die verwendeten Geräte, Waschautomat: BioTek Microplate Washer 405 Select LS (Washer) und Pipettierroboter: Microlab Star (ML Star), sowie die genutzten Softwareprogramme vorgestellt.

Die verwendeten Parameter beim Waschen der 384-*Well*-Format Mikrotiterplatten wurden erörtert und die Erstellung von Waschprotokollen erklärt. Der Washer kann unabhängig vom ML Star verwendet werden, um den Aufwand für den Anwender zu reduzieren und die gesamte Zeitersparnis des sFIDA-Assays zu erhöhen. Der Aufbau und die Eigenschaften vom ML Star wurden im Detail beschrieben und die Implementierung einer Roboter-Methode anhand eines Beispiels erklärt. Der Ablauf des sFIDA-Assays im automatisierten System wurde dargestellt und die damit verbundenen Kosten- und Zeitaufwand für ein Experiment mit hoher Probenanzahl bestimmt.

Die Implementierung des sFIDA-Assays wurde erfolgreich umgesetzt und Experimente im automatisierten System durchgeführt. Unter Verwendung der entwickelten Standardmoleküle $A\beta_{1-42}$-SiNaPs wurde der automatisierte sFIDA-Assay evaluiert (siehe Abschnitt 3.4). CSF und PBS wurden mit Konzentrationen von $A\beta_{1-42}$-SiNaPs versetzt (log10 Konzentrationsreihe) und im sFIDA-Assay gemessen. Es wurden Intra-Assay Parameter, wie Nachweisgrenze, Koeffizient der Varianz (CV) und Linearität zur Bewertung der Performanz des sFIDA-Assays im automatisierten System untersucht.

Die Automatisierung des sFIDA-Assays ermöglichte eine hohe Anzahl von Replikaten für jede eingesetzte $A\beta_{1-42}$-SiNaPs Konzentration (12-fach) und entsprechende negative Kontrollen (24-fach). Dadurch konnten Ausreißer durch den Ausschluss von Minimum- und Maximumwerten entfernt werden. Der Ausschluss wurde vier mal angewandt mit jeweils einem Minimum- und einem Maximumwert bezüglich des *sFIDA readouts* für die Replikate der eingesetzten Probe.

Der niedrigste Koeffizient der Varianz (CV in [%]) nach Ausschluss von vier Minimum- und vier Maximumwerten wurde für die Konzentrationsreihe in PBS mit

18% und in CSF mit 32% bestimmt. Im Vergleich zu den Ergebnissen bei manueller Durchführung des sFIDA-Assays von Kravchenko et al. 2016 (Abschnitt 3.3) konnten die CV % Werte weiter reduziert werden. Für beide Konzentrationsreihen wird ein Pearson Koeffizient von fast 1 bestimmt, dieser Wert weist auf eine lineare Korrelation zwischen *sFIDA readout* und eingesetzter $A\beta_{1-42}$-SiNaPs Konzentration hin. Neben dem Pearson Koeffizient konnte der Mandel's Test und *lack-of-fit* Test zeigen, dass die Kalibrationskurve erster Ordnung (linear) für die Konzentrationsreihe in CSF für jede Ebene des Ausschlusses von Minimum- und Maximumwerten gilt.

Die Nachweisgrenzen für $A\beta_{1-42}$-SiNaPs in CSF und Puffer wurden nach dem Ausschluss von drei bzw. vier Minimum- und Maximumwerte im niedrigen subfemtomolar-Bereich (CSF: 0.85 fM und PBS: 0.93 fM) bestimmt. Die Nachweisgrenze von 0.85 fM in CSF für die $A\beta_{1-42}$-SiNaPs mit ca. 47 $A\beta_{1-42}$-Epitopen entspricht einer monomerischen $A\beta_{1-42}$-Konzentration von 0.56 ng/l und ist damit niedriger als in den vergangen sFIDA-Studien. Die Nachweisgrenze ist weiterhin vergleichbar und höher als in Studien, die ELISAs verwendet haben (Savage et al., 2014; Hölttä et al., 2013; Bruggink et al., 2013; Fukumoto et al., 2010).

Die Automatisierung des sFIDA-Assays bietet nun eine standardisierte Ausführung des Experiments, um weitere Optimierungen im sFIDA-Assay zu testen. Dabei kann der Zeit- und Kostenaufwand des sFIDA-Assays anhand der verwendeten Anzahl von Mikrotiterplatten und Anzahl Proben präziser errechnet werden. Außerdem werden die Anwender entlastet und der Einfluss von Anwenderfehlern wird reduziert.

Die Verwendung von $A\beta_{1-42}$-SiNaPs als Aβ-Oligomer Standard bringt die Vorteile von einer definierten Größe der SiNaPs, die während der Stöber-Synthese gewählt werden kann. Die kugelförmige Geometrie der SiNaPs lässt eine gleichmäßige Verteilung der $A\beta_{1-42}$-Peptide zu. Wie bereits in Abschnitt 3.2 beschrieben, ist es möglich die SiNaPs mit anderen Proteinen herzustellen, sodass diese als Standard für oligomerbasierende Diagnostik anderer Proteinfehlfaltungserkrankungen eingesetzt werden können. Dementsprechend kann die Verwendung von Anti-α-syn-Antikörpern im sFIDA-Assay zur Detektion von α-syn-Oligomeren führen und die frühzeitige Diagnose von PD ermöglichen. Entsprechend wurden α-syn-SiNaPs erfolgreich synthetisiert und im sFIDA-Assay als Standard für α-syn-Oligomere getestet.

Im Abschnitt 3.5 wurden die Ergebnisse bei der Verwendung von α-syn-SiNaPs als Standardmolekül im automatisierten sFIDA-Assay vorgestellt. Dabei wurden die α-syn-SiNaPs in CSF und PBS seriell verdünnt und die obengenannten Intra-

Assay Parameter bestimmt.

Unter der Verwendung von gestutzten Mittelwerten (*trimmed mean*) mit 8%, 16%, 25% und 33% wurde der Einfluss von Ausreißern im sFIDA-Assay mit α-syn-SiNaPs untersucht. Hierbei wurde innerhalb einer Konzentration die Werte der Größe nach geordnet und durch die Prozentzahl wird bestimmt, wie viele Werte am oberen und unteren Ende der Liste herausgenommen wurden, um danach den gestutzten Mittelwert zu bilden.

Die CV-Werte für die höheren α-syn-SiNaPs Konzentrationen (10 pM bis 100 fM) in CSF und PBS liegen unter 10%. Während die unteren α-syn-SiNaPs Konzentrationen (10 fM bis 0 fM) ein Optimum von unter 45% erreichten. Die Linearität zwischen *sFIDA readout* und eingesetzter α-syn-SiNaP Konzentration in CSF und PBS wurde mit dem Pearson Koeffizient und dem *lack-of-fit* Test bestätigt.

Die eingesetzten α-syn-SiNaPs Konzentrationen resultierten in *sFIDA readouts*, die in CSF und PBS für die gestutzten Mittelwerte mit 16%, 25% und 33% signifikant von den negative Kontrollen unterscheidbar waren. Die berechneten Nachweisgrenzen in CSF und PBS bezüglich des *sFIDA readouts* lagen bei 3.8 fM in CSF und 13 fM in PBS.

Zusätzlich zum *sFIDA readout*, der die Kolokalisation der beiden Kanäle mit einbringt, wurde der *single channel readout* für Kanal 488 und 633 bestimmt. Für den Kanal 488 war es möglich einen Intensitätswert als Schwellwert zu bestimmen, bei dem die Anzahl der Pixel bei 0.01% in den negative Kontrollen lag. Die Relation von positiven Signal zum Hintergrund im Kanal 488 konnte dadurch verstärkt werden und der *single channel readout* beinhaltet dann nur noch die Anzahl der Pixel, die über diesem Schwellwert liegen. Im Kanal 633 konnte der Schwellwert nur bei 0.1% gesetzt werden und zeigte einen limitierten dynamischen Bereich für die Konzentrationsabhängigkeit.

Die Nachweisgrenzen für den *single channel readout* in Kanal 488 betrugen 3.8 fM in CSF und 2.5 fM in PBS. Die Nachweisgrenze von 2.5 fM in PBS für α-syn-SiNaPs mit ca. 27 α-syn Epitopen entspricht einer monomerischen Konzentration von 0.98 pg/ml. Die Nachweisgrenze liegt damit unter dem Bereich von 57 pg/ml bis 116 pg/ml, die in Kontrollgruppen bzw. PD-Patienten festgestellt wurden (Majbour et al., 2016). Somit sind die α-syn-SiNaPs als Kalibrierstandard im sFIDA-Assay geeignet, um die α-syn Oligomere in biologischen Proben zu quantifizieren. Der Vergleich mit weiteren Studien, die α-syn-Oligomere untersucht haben, erweist sich als schwierig, da diese keine vergleichbaren Standards eingesetzt haben oder das Signal der α-syn-Oligomere im Verhältnis zu α-syn-Monomeren angeben (Simonsen et al., 2015). In Zukunft könnte der Einsatz von α-syn-SiNaPs als Standard

die Validierung von oligomer-spezifischen Assays und die Vergleichbarkeit zwischen unterschiedlichen Methoden erleichtern.

Die Analyse für den *single channel readout* in Kanal 488 der α-syn-SiNaPs verdünnt in CSF und PBS weist auf die Möglichkeit hin den sFIDA-Assay weiter zu optimieren, um den Einsatz von einem Antikörper zur Detektion zu realisieren. Die Verwendung von zwei Antikörpern zur Detektion im sFIDA-Assay mit überlappenden Epitopen gewährleistet die spezifische Untersuchung von Oligomeren. Insbesondere bei der Auswertung der Bilddaten wird durch die Nutzung der Pixelposition (Kolokalisation) in den zwei aufgenommenen Kanälen die Spezifität auf Oligomere erhöht. Entsprechend sollte bei der Optimierung unter der Nutzung von nur einem Antikörper als Detektion darauf geachtet werden, dass die Spezifität zur Detektion von Oligomeren im sFIDA-Assay weiterhin gewährleisten wird. Insgesamt könnte die Einsparung auf nur einen Antikörper zur Detektion von Oligomeren im sFIDA-Assay die Kosten reduzieren.

Zusammenfassend zeigen die Ergebnisse dieser Arbeit das die Kalibration und Automatisierung des sFIDA-Assays zur die Detektion von $A\beta$- und α-syn-Oligomeren etabliert wurde. Die Verwendung des sFIDA-Assays ist nun mit einem hohen Durchsatz von Proben zur frühen Diagnose von AD und PD auf dem automatisierten System realisierbar. Zusätzlich kann die sFIDA-Technologie und der Einsatz der SiNaPs als Kalibrierstandard für weitere Proteinfehlfaltungserkrankungen angepasst werden, um eine frühzeitige und ökonomische Diagnose zu ermöglichen.

Literaturverzeichnis

Aasly, J. O., Johansen, K. K., Brønstad, G., Warø, B. J., Majbour, N. K., Varghese, S., Alzahmi, F., Paleologou, K. E., Amer, D. A. M., Al-Hayani, A., and El-Agnaf, O. M. A. (2014). Elevated levels of cerebrospinal fluid α-synuclein oligomers in healthy asymptomatic LRRK2 mutation carriers. *Frontiers in Aging Neuroscience*, 6(SEP):1–8.

Aerts, M., Esselink, R., Abdo, W., Bloem, B., and Verbeek, M. (2012). Csf α-synuclein does not differentiate between parkinsonian disorders. *Neurobiology of aging*, 33(2):430–e1.

Aguzzi, A. (2007). Unraveling prion strains with cell biology and organic chemistry. *Pnas*, 105(52):11–12.

Allinson, T. M. J., Parkin, E. T., Condon, T. P., Schwager, S. L. U., Sturrock, E. D., Turner, A. J., and Hooper, N. M. (2004). The role of ADAM10 and ADAM17 in the ectodomain shedding of angiotensin converting enzyme and the amyloid precursor protein. *European Journal of Biochemistry*, 271(12):2539–2547.

Alzheimer, A. (1911). Über eigenartige Krankheitsfälle des späteren Alters. *Zeitschrift für die gesamte Neurologie und Psychiatrie*, 4(1):356–385.

Andreasson, U., Perret-Liaudet, A., van Waalwijk van Doorn, L. J. C., Blennow, K., Chiasserini, D., Engelborghs, S., Fladby, T., Genc, S., Kruse, N., Kuiperij, H. B., Kulic, L., Lewczuk, P., Mollenhauer, B., Mroczko, B., Parnetti, L., Vanmechelen, E., Verbeek, M. M., Winblad, B., Zetterberg, H., Koel-Simmelink, M., and Teunissen, C. E. (2015). A practical guide to immunoassay method validation. *Frontiers in Neurology*, 6(Aug):1–8.

Armstrong, R. A. (2011). The pathogenesis of Alzheimer's disease: a reevaluation of the 'amyloid cascade hypothesis'. *Int J Alzheimers Dis*, 2011:630865.

Bailey, J. A., Maloney, B., Ge, Y.-W., and Lahiri, D. K. (2011). Functional activity of the novel Alzheimer's amyloid β-peptide interacting domain (AβID) in the

APP and BACE1 promoter sequences and implications in activating apoptotic genes and in amyloidogenesis. *Gene*, 488(1-2):13–22.

Barghorn, S., Nimmrich, V., Striebinger, A., Krantz, G., Keller, P., Janson, B., Bahr, M., Schmidt, M., Bitner, R. S., Harlan, J., Barlow, E., Ebert, U., and Hillen, H. (2005). Globular amyloid β-peptide1-42 oligomer - A homogenous and stable neuropathological protein in Alzheimer's disease. *Journal of Neurochemistry*, 95(3):834–847.

Bartoloni, A., Pizza, M., Bigio, M., Nucci, D., Ashworth, L., Irons, L., Robinson, A., Burns, D., Manclark, C., Sato, H., and Rappuoli, R. (1988). Automation of DNA sequencning reactions and related techniques: A workstation for micromanipulation of liquids. *Nature biotechnology*, 6:709–712.

Baruch-Suchodolsky, R. and Fischer, B. (2009). Aβ40, either soluble or aggregated, is a remarkably potent antioxidant in cell-free oxidative systems. *Biochemistry*, 48(20):4354–4370.

Beach, T. G., Monsell, S. E., and Kukull, W. A. (2012). Accuracy of the clinical diagnosis of alzheimer disease at national institute on aging alzheimer's disease centers, 2005-2010. *J Neuropathol Exp Neurol*, 71(4):266–273.

Bekris, L. M., Yu, C.-E., Bird, T. D., and Tsuang, D. W. (2010). Genetics of Alzheimer disease. *Journal of geriatric psychiatry and neurology*, 23(4):213–27.

Benilova, I., Karran, E., and De Strooper, B. (2012). The toxic β oligomer and Alzheimer's disease: an emperor in need of clothes. *Nature Neurosci*, 15(3):349–357.

Bibl, M., Esselmann, H., and Wiltfang, J. (2012). Neurochemical biomarkers in Alzheimer's disease and related disorders. *Ther Adv Neurol Disord*, 5(6):335–348.

BIOPRO Baden-Württemberg GmbH (2013). Biotechnology goes automated. https://www.gesundheitsindustrie-bw.de/en/article/dossier/biotechnology-goes-automated/
Last access: 2016-01-11.

BioTek Instruments, Inc. (2012). Microplate Washer - $405^{T}M$ LS - Operator's Manual.

BioTek Instruments, Inc. (2015a). Dual-action manifold. http://www.biotek.de/de/products/dual_action_manifold.html Last access: 2016-01-11.

BioTek Instruments, Inc. (2015b). Ultrasonic advantage. http://www.biotek.de/de/products/ultrasonic_advantage.html Last access: 2016-01-11.

Birkmann, E., Henke, F., Weinmann, N., Dumpitak, C., Groschup, M., Funke, A., Willbold, D., and Riesner, D. (2007). Counting of single prion particles bound to a capture-antibody surface (surface-FIDA). *Vet Microbiol*, 123(4):294–304.

Birkmann, E., Schäfer, O., Weinmann, N., Dumpitak, C., Beekes, M., Jackman, R., Thorne, L., and Riesner, D. (2006). Detection of prion particles in samples of BSE and scrapie by fluorescence correlation spectroscopy without proteinase K digestion. *Biological chemistry*, 387(1):95–102.

Bittner, T., Zetterberg, H., Teunissen, C. E., Jr., R. E. O., Militello, M., Andreasson, U., Hubeek, I., Gibson, D., Chu, D. C., Eichenlaub, U., Heiss, P., Kobold, U., Leinenbach, A., Madin, K., Manuilova, E., Rabe, C., and Blennow, K. (2016). Technical performance of a novel, fully automated electrochemiluminescence immunoassay for the quantitation of β-amyloid in human cerebrospinal fluid. *Alzheimer's and Dementia*, 12(5):517 – 526.

Blennow, K., Hampel, H., Weiner, M., and Zetterberg, H. (2010). Cerebrospinal fluid and plasma biomarkers in Alzheimer disease. *Nat Rev Neurol*, 6(3):131–144.

Blennow, K. and Zetterberg, H. (2015). The past and the future of Alzheimer's disease CSF biomarkers-a journey toward validated biochemical tests covering the whole spectrum of molecular events. *Front Neurosci*, 9:345.

Bolton, D., McKinley, M., and Prusiner, S. (1982). Identification of a protein that purifies with the scrapie prion. *Science*, 218(4579):1309–1311.

Brettschneider, J., Del Tredici, K., Lee, V. M.-Y., and Trojanowski, J. Q. (2015). Spreading of pathology in neurodegenerative diseases: a focus on human studies. *Nature reviews. Neuroscience*, 16(2):109–20.

Bruggink, K. A., Jongbloed, W., Biemans, E. A., Veerhuis, R., Claassen, J. A., Kuiperij, H. B., and Verbeek, M. M. (2013). Amyloid-β oligomer detection by ELISA in cerebrospinal fluid and brain tissue. *Anal Biochem*, 433(2):112–120.

Bruggink, K. A., Müller, M., Kuiperij, H. B., and Verbeek, M. M. (2012). Methods for analysis of amyloid-β aggregates. *Journal of Alzheimer's Disease*, 28(4):735–758.

Cardona, A.-m., Roth, Z., Raton, B., Raton, B., and Raton, B. (2009). Optimization of Multi-Centrifuge Steps in Biotechnology Automation. *Florida conference on recent advances in robotics (RCRAR)*, pages 1–10.

Chapman, T. (2003). Automation on the move. *Nature*, 421.

Compta, Y., Valente, T., Saura, J., Segura, B., Iranzo, Á., Serradell, M., Junqué, C., Tolosa, E., Valldeoriola, F., Muñoz, E., Santamaria, J., Cámara, A., Fernández, M., Fortea, J., Buongiorno, M., Molinuevo, J. L., Bargalló, N., and Martí, M. J. (2014). Correlates of cerebrospinal fluid levels of oligomeric- and total-α-synuclein in premotor, motor and dementia stages of Parkinson's disease. *Journal of Neurology*, 262(2):294–306.

Cox, J. C. and Rudolph, P. (1998). Automated RNA Selection. *Biotechnology Progress*, 14:845–850.

Craig, A. G. and Hoheisel, J. D., editors (1999). *Methods in Microbiology*. Academic Press, London.

Dehay, B., Bourdenx, M., Gorry, P., Przedborski, S., Vila, M., Hunot, S., Singleton, A., Olanow, C. W., Merchant, K. M., Bezard, E., Petsko, G. A., and Meissner, W. G. (2015). Targeting α-synuclein for treatment of Parkinson's disease: Mechanistic and therapeutic considerations. *The Lancet Neurology*, 14(8):855–866.

DiLorenzo, M. E., Timoney, C. F., and Felder, R. A. (2001). Technological Advancements in Liquid Handling Robotics. *Journal of Laboratory Automation*, 6:36–40.

Doecke, J. D., Laws, S. M., Faux, N., and et al (2012). Blood-based protein biomarkers for diagnosis of alzheimer disease. *Archives of Neurology*, 69(10):1318–1325.

Eisele, Y. S., Bolmont, T., Heikenwalder, M., Langer, F., Jacobson, L. H., Yan, Z.-X., Roth, K., Aguzzi, A., Staufenbiel, M., Walker, L. C., and Jucker, M. (2009). Induction of cerebral β-amyloidosis: intracerebral versus systemic Aβ inoculation. *Proceedings of the National Academy of Sciences of the United States of America*, 106(31):12926–12931.

El-Agnaf, O. M. a., Salem, S. a., Paleologou, K. E., Curran, M. D., Gibson, M. J., Court, J. a., Schlossmacher, M. G., and Allsop, D. (2006). Detection of oligomeric forms of α-synuclein protein in human plasma as a potential biomarker for Parkinson's disease. *The FASEB journal : official publication of the Federation of American Societies for Experimental Biology*, 20(3):419–425.

Elliott, P. and Peakman, T. C. (2008). The uk biobank sample handling and storage protocol for the collection, processing and archiving of human blood and urine. *International Journal of Epidemiology*, 37(2):234–244.

Esparza, T. J., Zhao, H., Cirrito, J. R., Cairns, N. J., Bateman, R. J., Holtzman, D. M., and Brody, D. L. (2013). Amyloidβ oligomerization in alzheimer dementia versus high pathology controls. *Annals of Neurology*, 73(1):104–119.

Finder, V. H. and Glockshuber, R. (2007). Amyloid-β Aggregation. *Neurodegenerative Diseases*, 4(1):13–27.

Folstein, M. F., Folstein, S. E., and McHugh, P. R. (1975). "Mini-mental state". A practical method for grading the cognitive state of patients for the clinician. *Journal of psychiatric research*, 12(3):189–198.

Førland, M. G., Öhrfelt, A., Oftedal, L. S., Tysnes, O.-B., Larsen, J. P., Blennow, K., Zetterberg, H., Alves, G., and Lange, J. (2016). Validation of a new assay for α-synuclein detection in cerebrospinal fluid. *Clinical Chemistry and Laboratory Medicine (CCLM)*, 0(0).

Foulds, P. G., Mitchell, J. D., Parker, A., Turner, R., Green, G., Diggle, P., Hasegawa, M., Taylor, M., Mann, D., and Allsop, D. (2011). Phosphorylated α-synuclein can be detected in blood plasma and is potentially a useful biomarker for parkinson's disease. *The FASEB Journal*, 25(12):4127–4137.

Foulds, P. G., Yokota, O., Thurston, A., Davidson, Y., Ahmed, Z., Holton, J., Thompson, J. C., Akiyama, H., Arai, T., Hasegawa, M., Gerhard, A., Allsop, D., and Mann, D. M. A. (2012). Post mortem cerebrospinal fluid α-synuclein levels are raised in multiple system atrophy and distinguish this from the other α-synucleinopathies, Parkinson's disease and Dementia with Lewy bodies. *Neurobiology of Disease*, 45(1):188–195.

Freir, D. B., Nicoll, A. J., Klyubin, I., Panico, S., Mc Donald, J. M., Risse, E., Asante, E. a., Farrow, M. a., Sessions, R. B., Saibil, H. R., Clarke, A. R., Rowan, M. J., Walsh, D. M., and Collinge, J. (2011). Interaction between prion protein

and toxic amyloid β assemblies can be therapeutically targeted at multiple sites. *Nature communications*, 2(May):336.

Fukumoto, H., Tokuda, T., Kasai, T., Ishigami, N., Hidaka, H., Kondo, M., Allsop, D., and Nakagawa, M. (2010). High-molecular-weight β-amyloid oligomers are elevated in cerebrospinal fluid of Alzheimer patients. *FASEB J*, 24(8):2716–2726.

Funke, S. A., Birkmann, E., Henke, F., Görtz, P., Lange-Asschenfeldt, C., Riesner, D., and Willbold, D. (2007). Single-Particle Detection System for Ab Aggregates: Adaptation of Surface-Fluorescence Intensity Distribution Analysis to Laser Scanning Microscopy. *Rejuvenation Res*, 13:206–209.

Funke, S. A., Wang, L., Birkmann, E., and Willbold, D. (2010). Single-Particle Detection System for Aβ Aggregates: Adaptation of Surface-Fluorescence Intensity Distribution Analysis to Laser Scanning Microscopy. *Rejuvenation Research*, 13(2-3):206–209.

Gilbert, B. J. (2014). Republished: the role of amyloid β in the pathogenesis of Alzheimer's disease. *Postgraduate medical journal*, 90(1060):113–7.

Goedert, M. (2001). Alpha-synuclein and neurodegenerative diseases. *Nature reviews. Neuroscience*, 2(7):492–501.

Golby, A., Silverberg, G., Race, E., Gabrieli, S., O'Shea, J., Knierim, K., Stebbins, G., and Gabrieli, J. (2005). Memory encoding in Alzheimer's disease: An fMRI study of explicit and implicit memory. *Brain*, 128(4):773–787.

Golde, T. E., Schneider, L. S., and Koo, E. H. (2011). Anti-Aβ therapeutics in Alzheimer's disease: the need for a paradigm shift. *Neuron*, 69(2):203–213.

Goldmann, W. (2008). PrP genetics in ruminant transmissible spongiform encephalopathies. *Vet Res*, 39(4):30.

Gorostidi, A., Bergareche, A., Ruiz-Martínez, J., Martí-Massó, J. F., Cruz, M., Varghese, S., Qureshi, M. M., Alzahmi, F., Al-Hayani, A., de Munain, A. L., et al. (2012). α-synuclein levels in blood plasma from lrrk2 mutation carriers. *PloS one*, 7(12):e52312.

Grady, C. L., McIntosh, A. R., Beig, S., Keightley, M. L., Burian, H., and Black, S. E. (2003). Evidence from functional neuroimaging of a compensatory prefrontal network in Alzheimer's disease. *The Journal of neuroscience : the official journal of the Society for Neuroscience*, 23(3):986–993.

Gralle, M. and Ferreira, S. T. (2007). Structure and functions of the human amyloid precursor protein: The whole is more than the sum of its parts. *Progress in Neurobiology*, 82(1):11 – 32.

greiner bio-one (2016). Sensoplate plus, 384 well, f-bottom, glass bottom, black, single packed; item no.: 781856. https://shop.gbo.com/en/row/articles/catalogue/article/0110_0040_0030_0050/14435/ Last access: 2016-01-16.

Haass, C., Schlossmacher, M., Hung, A., Vigo-Pelfrey, C., Mellon, A., Ostaszewski, B., Lieberburg, I., Koo, E., Schenk, D., Teplow, D., and Selkoe, D. (1992). Amyloid β-Peptide is Produced by Cultured Cells During Normal Metabolism. *Nature*, 356:133–135.

Haass, C. and Selkoe, D. J. (2007). Soluble protein oligomers in neurodegeneration: lessons from the Alzheimer's amyloid β-peptide. *Nat Rev Mol Cell Biol*, 8(2):101–112.

Hämäläinen, A., Pihlajamäki, M., Tanila, H., Hänninen, T., Niskanen, E., Tervo, S., Karjalainen, P. A., Vanninen, R. L., and Soininen, H. (2007). Increased fMRI responses during encoding in mild cognitive impairment. *Neurobiology of Aging*, 28(12):1889–1903.

Hamilton Bonaduz AG (2010a). Microlab star line operator's manual - venus two basepackage 4.3.

Hamilton Bonaduz AG (2010b). Microlab star line programmer's manual - venus two basepackage 4.3.

Hamilton Bonaduz AG (2015). Microlab star line. http://www.hamiltoncompany.com/products/automated-liquid-handling/liquid-handling-workstations/microlab-star-line Last access: 2016-01-13.

Hampel, H., Frank, R., Broich, K., Teipel, S. J., Katz, R. G., Hardy, J., Herholz, K., Bokde, A. L. W., Jessen, F., Hoessler, Y. C., Sanhai, W. R., Zetterberg, H., Woodcock, J., and Blennow, K. (2010). Biomarkers for Alzheimer's disease: academic, industry and regulatory perspectives. *Nature Reviews Drug Discovery*, 9(7):560–574.

Hansson, O., Hall, S., Öhrfelt, A., Zetterberg, H., Blennow, K., Minthon, L., Nägga, K., Londos, E., Varghese, S., Majbour, N. K., Al-Hayani, A., and El-Agnaf, O. (2014). Levels of cerebrospinal fluid α-synuclein oligomers are increased in

Parkinson's disease with dementia and dementia with Lewy bodies compared to Alzheimer's disease. *Alzheimer's Research & Therapy*, 6(3):25.

Hardy, J. and Selkoe, D. J. (2002). The amyloid hypothesis of Alzheimer's disease: progress and problems on the road to therapeutics. *Science*, 297(5580):353–356.

Hardy, J. A. and Higgins, G. A. (1992). Alzheimer's disease: the amyloid cascade hypothesis. *Science*, 256(5054):184.

Harper, J. D., Lieber, C. M., and Lansbury Jr., P. T. (1997). Atomic force microscopic imaging of seeded fibril formation and fibril branching by the Alzheimer's disease amyloid-β protein. *Chemistry & Biology*, 4(12):951–959.

Heilbronner, G., Eisele, Y. S., Langer, F., Kaeser, S. A., Novotny, R., Nagarathinam, A., Åslund, A., Hammarström, P., Nilsson, K. P. R., and Jucker, M. (2013). Seeded strain-like transmission of β-amyloid morphotypes in app transgenic mice. *EMBO reports*, 14(11):1017–1022.

Herrmann, Y., Bujnicki, T., Zafiu, C., Kulawik, A., Kühbach, K., Peters, L., Fabig, J., Willbold, J., Bannach, O., and Willbold, D. (2017). Nanoparticle standards for immuno-based quantitation of α-synuclein oligomers in diagnostics of Parkinson's disease and other synucleinopathies. *Clinica Chimica Acta*, 466:152–159.

Herrmann, Y., Kulawik, A., Kühbach, K., Hülsemann, M., Peters, L., Bujnicki, T., Kravchenko, K., Linnartz, C., Willbold, J., Zafiu, C., Bannach, O., and Willbold, D. (2016). sFIDA automation yields sub-femtomolar limit of detection for Aβ aggregates in body fluids. *Clinical Biochemistry*.

Herrup, K. (2015). The case for rejecting the amyloid cascade hypothesis. *Nature Neuroscience*, 18(6):794–799.

Herskovits, A. Z., Locascio, J. J., Peskind, E. R., Li, G., and Hyman, B. T. (2013). A Luminex Assay Detects Amyloid β Oligomers in Alzheimer's Disease Cerebrospinal Fluid. *PLoS ONE*, 8(7):e67898.

Hicks, D. A., Nalivaeva, N. N., and Turner, A. J. (2012). Lipid rafts and alzheimer's disease: protein-lipid interactions and perturbation of signalling. *Frontiers in Physiology*, 3(189).

Hiltunen, M., Van Groen, T., and Jolkkonen, J. (2009). Functional roles of amyloid-β protein precursor and amyloid-β peptides: Evidence from experimental studies. *Journal of Alzheimer's Disease*, 18(2):401–412.

Hölttä, M., Hansson, O., Andreasson, U., Hertze, J., Minthon, L., Nagga, K., Andreasen, N., Zetterberg, H., and Blennow, K. (2013). Evaluating amyloid-β oligomers in cerebrospinal fluid as a biomarker for Alzheimer's disease. *PLoS One*, 8(6):e66381.

Hübinger, S., Bannach, O., Funke, S. a., Willbold, D., and Birkmann, E. (2012). Detection of α-synuclein aggregates by fluorescence microscopy. *Rejuvenation research*, 15(2):213–6.

Hülsemann, M., Zafiu, C., Kühbach, K., Luhmann, N., Herrmann, Y., Peters, L., Linnartz, C., Willbold, J., Kravchenko, K., Kulawik, A., Willbold, S., Bannach, O., and Willbold, D. (2016). Biofunctionalized silica nanoparticles: Standards in amyloid-β oligomer-based diagnosis of Alzheimer's disease. *Journal of Alzheimer's Disease*, 54(1):79–88.

Humpel, C. (2011). Identifying and validating biomarkers for Alzheimer's disease. *Trends Biotechnol*, 29(1):26–32.

Igbavboa, U., Sun, G. Y., Weisman, G. A., He, Y., and Wood, W. G. (2009). Amyloid β-protein stimulates trafficking of cholesterol and caveolin-1 from the plasma membrane to the Golgi complex in mouse primary astrocytes. *Neuroscience*, 162(2):328–338.

Isenhour, T. L. (1985). Robotics in the Laboratory. *Journal of Chemical Information and Computer Sciences*, pages 292–295.

Jack, C. R., Knopman, D. S., Jagust, W. J., Shaw, L. M., Aisen, P. S., Weiner, M. W., Petersen, R. C., and Trojanowski, J. Q. (2010). Hypothetical model of dynamic biomarkers of the Alzheimer's pathological cascade. *Lancet neurology*, 9(1):119–28.

Jack Jr., C. R., Knopman, D. S., Jagust, W. J., Petersen, R. C., Weiner, M. W., Aisen, P. S., Shaw, L. M., Vemuri, P., Wiste, H. J., Weigand, S. D., Lesnick, T. G., Pankratz, V. S., Donohue, M. C., and Trojanowski, J. Q. (2013). Tracking pathophysiological processes in Alzheimer's disease: an updated hypothetical model of dynamic biomarkers. *Lancet Neurol*, 12(2):207–216.

Jankovic, J. (2008). Parkinson's disease: clinical features and diagnosis. *Journal of Neurology, Neurosurgery & Psychiatry*, 79(4):368–376.

Jesse, S., Steinacker, P., Lehnert, S., Gillardon, F., Hengerer, B., and Otto, M. (2009). Neurochemical approaches in the laboratory diagnosis of parkinson and

parkinson dementia syndromes: A review. *CNS Neuroscience and Therapeutics*, 15(2):157–182.

Johnson, K. A., Fox, N. C., Sperling, R. A., and Klunk, W. E. (2016). Brain Imaging in Alzheimer Disease. *Cold Spring Harbor Perspectives in Medicine*, pages 1–24.

Jongbloed, W., Bruggink, K. A., Kester, M. I., Visser, P. J., Scheltens, P., Blankenstein, M. A., Verbeek, M. M., Teunissen, C. E., and Veerhuis, R. (2015). Amyloid-β oligomers relate to cognitive decline in Alzheimer's disease. *J Alzheimers Dis*, 45(1):35–43.

Kempner, M. E. and Felder, R. A. (2002). A Review of Cell Culture Automation. *Journal of the Association for Laboratory Automation*, 7(2):56–62.

Kühbach, K., Hülsemann, M., Herrmann, Y., Kravchenko, K., Kulawik, A., Linnartz, C., Peters, L., Wang, K., Willbold, J., Willbold, D., and Bannach, O. (2016). Application of an amyloid-β oligomer standard in the sfida assay. *Frontiers in Neuroscience*, 10(8).

Klaver, A. C., Patrias, L. M., Finke, J. M., and Loeffler, D. A. (2011). Specificity and sensitivity of the abeta oligomer {ELISA}. *Journal of Neuroscience Methods*, 195(2):249 – 254.

Klein, W. L. (2002). Aβ toxicity in alzheimer's disease: globular oligomers (addls) as new vaccine and drug targets. *Neurochemistry International*, 41(5):345–352.

Klunk, W. E., Engler, H., Nordberg, A., Wang, Y., Blomqvist, G., Holt, D. P., Bergstro, M., Savitcheva, I., Debnath, M. L., Barletta, J., Price, J. C., Sandell, J., Lopresti, B. J., Wall, A., Koivisto, P., Antoni, G., Mathis, C. A., and Långstro, B. (2004). Imaging Brain Amyloid in Alzheimer's Disease with Pittsburgh Compound-B. *Annals of Neurology*, pages 306–319.

Kravchenko, K., Kulawik, A., Kühbach, K., Zafiu, C., Hülsemann, Maren Herrmann, Y., Linnartz, C., Peters, L., Willbold, J., Bannach, O., and Willbold, D. (2016). Influence of anti-coagulants on blood-based quantification of amyloid-β oligomers in the sfida assay. *Biological Chemistry*, 0(0).

Lansdall, C. J. (2014). An effective treatment for Alzheimer's disease must consider both amyloid and tau. *Bioscience Horizons*, 7:1–11.

Lashuel, H. A., Overk, C. R., Oueslati, A., and Masliah, E. (2013). The many faces of α-synuclein: from structure and toxicity to therapeutic target. *Nature reviews. Neuroscience*, 14(1):38–48.

Lehmann, R., Severitt, J. C., Roddelkopf, T., Junginger, S., and Thurow, K. (2015). Biomek Cell Workstation: A Variable System for Automated Cell Cultivation . *Journal of Laboratory Automation*.

Liscouski, J. G. (1985). Laboratory Automation. *Journal of Chemical Information and Computer Sciences*, 25(3):288–292.

Lücking, B. C. and Brice, A. (2000). α-synuclein and parkinson's disease. *Cellular and Molecular Life Sciences CMLS*, 57(13):1894–1908.

Luo, J., Wärmländer, S. K. T. S., Gräslund, A., and Abrahams, J. P. (2016). Cross-interactions between the Alzheimer disease amyloid-β peptide and other amyloid proteins: A further aspect of the amyloid cascade hypothesis. *Journal of Biological Chemistry*, 291(32):16485–16493.

Lutkemeyer, D., Poggendorf, I., Scherer, T., Zhang, J., Knoll, A., and Lehmann, J. (2000). First steps in robot automation of sampling and sample management during cultivation of mammalian cells in pilot scale. *Biotechnol Prog*, 16(5):822–828.

Majbour, N. K., Vaikath, N. N., van Dijk, K. D., Ardah, M. T., Varghese, S., Vesterager, L. B., Montezinho, L. P., Poole, S., Safieh-Garabedian, B., Tokuda, T., Teunissen, C. E., Berendse, H. W., van de Berg, W. D. J., and El-Agnaf, O. M. A. (2016). Oligomeric and phosphorylated α-synuclein as potential CSF biomarkers for Parkinson's disease. *Molecular neurodegeneration*, 11(1):7.

Malley, T. T. O., Oktaviani, N. A., Zhang, D., Lomakin, A., Nuallain, B. O., Linse, S., Benedek, G. B., Rowan, M. J., Mulder, F. A. A., and Walsh, D. M. (2014). A β dimers differ from monomers in structural propensity , aggregation paths and population of synaptotoxic assemblies. *The Biochemical journal*, 426:413–426.

McDowall, R. D. (1989). Review Sample Preparation for Biomedical. *Journal of Chromatography*, 492:3–58.

Meldrum, D. (2000). Automation for genomics, part one: Preparation for sequencing. *Genome Research*, 10(8):1081–1092.

Minoshima, S., Giordani, B., Berent, S., Frey, K. A., Foster, N. L., and Kuhl, D. E. (1997). Metabolic reduction in the posterior cingulate cortex in very early alzheimer's disease. *Annals of Neurology*, 42(1):85–94.

Mollenhauer, B. (2014). Quantification of α-synuclein in cerebrospinal fluid: How ideal is this biomarker for Parkinson's disease? *Parkinsonism and Related Disorders*, 20(SUPPL.1):S76–S79.

Mucke, L. (2009). Alzheimer's disease. *Nature*, 461(October):895–897.

Musiek, E. S. and Holtzman, D. M. (2015). Three dimensions of the amyloid hypothesis : time, space and wingmen. *Nature Neuroscience*, 18(6).

Nabers, A., Ollesch, J., Schartner, J., Kötting, C., Genius, J., Hafermann, H., Klafki, H., Gerwert, K., and Wiltfang, J. (2016). Amyloid-β-Secondary Structure Distribution in Cerebrospinal Fluid and Blood Measured by an Immuno-Infrared-Sensor: A Biomarker Candidate for Alzheimer's Disease. *Analytical Chemistry*, 88(5):2755–2762.

Nuallain, B. O., Freir, D. B., Nicoll, A. J., Risse, E., Ferguson, N., Herron, C. E., Collinge, J., and Walsh, D. M. (2010). Amyloid β-Protein Dimers Rapidly Form Stable Synaptotoxic Protofibrils. *Neurobiology of Disease*, 30(43):14411–14419.

Olanow, C. W. and Brundin, P. (2013). Parkinson's Disease and Alpha Synuclein: Is Parkinson's Disease a Prion-Like Disorder? *Movement Disorders*, 28(1):31–40.

Olsen, C. (2012). Maximizing cell wash performance with aquamax 2000/4000 microplate washers and cell wash heads. http://go.pardot.com/l/83942/2015-06-17/nf1/83942/4352/AquaMax_Washers_Datasheet_rev_E.pdf
Last access: 2016-01-06.

Olsson, B., Lautner, R., Andreasson, U., Öhrfelt, A., Portelius, E., Bjerke, M., Höltä, M., Rosen, C., Olsson, C., Strobel, G., Wu, E., Dakin, K., Petzold, M., Blennow, K., and Zetterberg, H. (2016). CSF and blood biomarkers for the diagnosis of Alzheimer's disease: A systematic review and meta-analysis. *The Lancet Neurology*, pages 673–684.

Park, M. J., Cheon, S. M., Bae, H. R., Kim, S. H., and Kim, J. W. (2011). Elevated levels of α-synuclein oligomer in the cerebrospinal fluid of drug-naïve patients with Parkinson's disease. *Journal of Clinical Neurology (Korea)*, 7(4):215–222.

Parkinson, J. (2002). An essay on the shaking palsy. 1817. *The Journal of neuropsychiatry and clinical neurosciences*, 14(2):223–236; discussion 222.

Parnetti, L., Castrioto, A., Chiasserini, D., Persichetti, E., Tambasco, N., El-Agnaf, O., and Calabresi, P. (2013). Cerebrospinal fluid biomarkers in Parkinson disease. *Nature reviews. Neurology*, 9(3):131–140.

Parnetti, L., Farotti, L., Eusebi, P., Chiasserini, D., De Carlo, C., Giannandrea, D., Salvadori, N., Lisetti, V., Tambasco, N., Rossi, A., Majbour, N. K., El-Agnaf, O., and Calabresi, P. (2014). Differential role of CSF α-synuclein species, tau, and Aβ42 in Parkinson's disease. *Frontiers in Aging Neuroscience*, 6(MAR):1–8.

Perl, D. and Brody, A. (1980). Alzheimer's disease: X-ray spectrometric evidence of aluminum accumulation in neurofibrillary tangle-bearing neurons. *Science*, 208(4441):297–299.

Price, J. L. and Morris, J. C. (1999). Tangles and plaques in nondemented aging and 'preclinical' alzheimer's disease. *Annals of Neurology*, 45(3):358–368.

Reesink, F. E., Lemstra, A. W., van Dijk, K. D., Berendse, H. W., van de Berg, W. D., Klein, M., Blankenstein, M. A., Scheltens, P., Verbeek, M. M., and van der Flier, W. M. (2010). Csf α-synuclein does not discriminate dementia with lewy bodies from alzheimer's disease. *Journal of Alzheimer's Disease*, 22(1):87–95.

Reiman, E. M., Caselli, R. J., Yun, L. S., Chen, K., Bandy, D., Minoshima, S., Thibodeau, S. N., and Osborne, D. (1996). Preclinical evidence of alzheimer's disease in persons homozygous for the ϵ4 allele for apolipoprotein e. *New England Journal of Medicine*, 334(12):752–758. PMID: 8592548.

Rombouts, S. A., Barkhof, F., Veltman, D. J., Machielsen, W. C., Witter, M. P., Bierlaagh, M. A., Lazeron, R. H., Valk, J., and Scheltens, P. (2000). Functional MR imaging in Alzheimer's disease during memory encoding. *AJNR Am J Neuroradiol*, 21(10):1869–1875.

Roychaudhuri, R., Yang, M., Hoshi, M. M., and Teplow, D. B. (2009). Amyloid β-protein assembly and Alzheimer disease. *The Journal of biological chemistry*, 284(8):4749–4753.

Sakono, M. and Zako, T. (2010). Amyloid oligomers: Formation and toxicity of Aβ oligomers. *FEBS Journal*, 277(6):1348–1358.

Sandbrink, R., Masters, C. L., and Beyreutherb, K. (1996). App gene family alternative splicing generates functionally related isoforms. *Annals of the New York Academy of Sciences*, 777:281–287.

Santi, S. D., de Leon, M. J., Rusinek, H., Convit, A., Tarshish, C. Y., Roche, A., Tsui, W. H., Kandil, E., Boppana, M., Daisley, K., Wang, G. J., Schlyer, D., and Fowler, J. (2001). Hippocampal formation glucose metabolism and volume losses in {MCI} and {AD}. *Neurobiology of Aging*, 22(4):529 – 539.

Saracchi, E., Fermi, S., and Brighina, L. (2014). Emerging candidate biomarkers for Parkinson's disease: a review. *Aging and disease*, 5(1):27–34.

Savage, M. J., Kalinina, J., Wolfe, A., Tugusheva, K., Korn, R., Cash-Mason, T., Maxwell, J. W., Hatcher, N. G., Haugabook, S. J., Wu, G., Howell, B. J., Renger, J. J., Shughrue, P. J., and McCampbell, A. (2014). A sensitive Aβ oligomer assay discriminates Alzheimer's and aged control cerebrospinal fluid. *J Neurosci*, 34(8):2884–2897.

Schaffer, C., Sarad, N., DeCrumpe, A., Goswami, D., Herrmann, S., Morales, J., Patel, P., and Osborne, J. (2014). Biomarkers in the Diagnosis and Prognosis of Alzheimer's Disease. *Journal of laboratory automation*, page 2211068214559979.

Schnieder, E., editor (1999). *Studium Technik*. Vieweg, Braunschweig.

Serrano-Pozo, A., Frosch, M. P., Masliah, E., and Hyman, B. T. (2011). Neuropathological alterations in Alzheimer disease. *Cold Spring Harbor perspectives in medicine*, 1(1):1–24.

Shaw, L. M., Vanderstichele, H., Knapik-Czajka, M., Clark, C. M., Aisen, P. S., Petersen, R. C., Blennow, K., Soares, H., Simon, A., Lewczuk, P., Dean, R., Siemers, E., Potter, W., Lee, V. M., Trojanowski, J. Q., and Alzheimer's Disease Neuroimaging Initiative (2009). Cerebrospinal fluid biomarker signature in Alzheimer's disease neuroimaging initiative subjects. *Ann Neurol*, 65(4):403–413.

Shoji, M., Golde, T. E., Ghiso, J., Cheung, T. T., Estus, S., Shaffer, L. M., Cai, X.-d., Mckay, D. M., Tintner, R., Frangione, B., and Younkin, S. G. (1992). Production of the Alzheimer Amyloid β Protein by Normal Proteolytic Processing. *Science*, 258(5079):126–129.

Sierks, M. R., Chatterjee, G., McGraw, C., Kasturirangan, S., Schulz, P., and Prasad, S. (2011). CSF levels of oligomeric alpha-synuclein and beta-amyloid as biomarkers for neurodegenerative disease. *Integrative biology : quantitative biosciences from nano to macro*, 3(12):1188–96.

Simonsen, A. H., Kuiperij, B., Ali El-Agnaf, O. M., Engelborghs, S., Herukka, S.-K., Parnetti, L., Rektorova, I., Vanmechelen, E., Kapaki, E., Verbeek, M., and Mollenhauer, B. (2015). The utility of α-synuclein as biofluid marker in neurodegenerative diseases: a systematic review of the literature. *Biomarkers in medicine*.

Solé-Padullés, C., Bartrés-Faz, D., Junqué, C., Vendrell, P., Rami, L., Clemente, I. C., Bosch, B., Villar, A., Bargalló, N., Jurado, M. A., Barrios, M., and Molinuevo, J. L. (2009). Brain structure and function related to cognitive reserve variables in normal aging, mild cognitive impairment and alzheimer's disease. *Neurobiology of Aging*, 30(7):1114 – 1124.

Soscia, S. J., Kirby, J. E., Washicosky, K. J., Tucker, S. M., Ingelsson, M., Hyman, B., Burton, M. A., Goldstein, L. E., Duong, S., Tanzi, R. E., and Moir, R. D. (2010). The Alzheimer's Disease-Associated Amyloid β-Protein Is an Antimicrobial Peptide. *PLoS ONE*, 5(3):e9505.

Soto, C. (2003). Unfolding the role of protein misfolding in neurodegenerative diseases. *Nature Reviews Neuroscience*, 4(1):49–60.

Sperling, R. A., Bates, J. F., Chua, E. F., Cocchiarella, A. J., Rentz, D. M., Rosen, B. R., Schacter, D. L., and Albert, M. S. (2003). fMRI studies of associative encoding in young and elderly controls and mild Alzheimer's disease. *J Neurol Neurosurg Psychiatry*, pages 44–51.

Stöhr, J., Watts, J. C., Mensinger, Z. L., Oehler, A., Grillo, S. K., DeArmond, S. J., Prusiner, S. B., and Giles, K. (2012). Purified and synthetic Alzheimer's amyloid β prions. *Proceedings of the National Academy of Sciences*, 109(27):11025–11030.

Sunderland, T., Linker, G., Mirza, N., Putnam, K. T., Friedman, D. L., Kimmel, L. H., Bergeson, J., Manetti, G. J., Zimmermann, M., Tang, B., Bartko, J. J., and Cohen, R. M. (2003). Decreased β-amyloid1-42 and increased tau levels in cerebrospinal fluid of patients with Alzheimer disease. *JAMA*, 289(16):2094–2103.

Swomley, A. M., Förster, S., Keeney, J. T., Triplett, J., Zhang, Z., Sultana, R., and Butterfield, D. A. (2014). Aβ, oxidative stress in Alzheimer disease: Evidence based on proteomics studies. *Biochimica et Biophysica Acta - Molecular Basis of Disease*, 1842(8):1248–1257.

Tabaton, M., Zhu, X., Perry, G., Smith, M. A., and Giliberto, L. (2011). Signaling Effect of Amyloid-β_{1-42} on the processing of aβpp. *Exp Neurol.*, 221(1):18–25.

Tecan Group Ltd. (2014). Application guide for Tecan plate washers. http://ww3.tecan.com/mandant/files/doc/303/BR_Application_Guide_for_Microplate_Washers_398255_V1-0.pdf Last access: 2016-01-06.

Thal, D. R., Walter, J., Saido, T. C., and Fändrich, M. (2015). Neuropathology and biochemistry of Aβ and its aggregates in Alzheimer's disease. *Acta Neuropathologica*, 129(2):167–182.

Tokuda, T., Qureshi, M., Ardah, M., Varghese, S., Shehab, S., Kasai, T., Ishigami, N., Tamaoka, A., Nakagawa, M., and El-Agnaf, O. (2010). Detection of elevated levels of α-synuclein oligomers in csf from patients with parkinson disease. *Neurology*, 75(20):1766–1770.

Tokuda, T., Salem, S. A., Allsop, D., Mizuno, T., Nakagawa, M., Qureshi, M. M., Locascio, J. J., Schlossmacher, M. G., and El-Agnaf, O. M. (2006). Decreased α-synuclein in cerebrospinal fluid of aged individuals and subjects with parkinson's disease. *Biochemical and biophysical research communications*, 349(1):162–166.

Uversky, V. N., Oldfield, C. J., and Dunker, a. K. (2008). Intrinsically Disordered Proteins in Human Diseases: Introducing the D 2 Concept. *Annual Review of Biophysics*, 37(1):215–246.

Verma, M., Vats, A., and Taneja, V. (2015). Toxic species in amyloid disorders: Oligomers or mature fibrils. *Annals of Indian Academy of Neurology*, 18(2):138–145.

Walker, L. C. and Jucker, M. (2015). Neurodegenerative diseases: Expanding the prion concept. *Annual Review of Neuroscience*, 38(1):87–103. PMID: 25840008.

Wang-Dietrich, L., Funke, S. A., Kuhbach, K., Wang, K., Besmehn, A., Willbold, S., Cinar, Y., Bannach, O., Birkmann, E., and Willbold, D. (2013). The amyloid-β oligomer count in cerebrospinal fluid is a biomarker for Alzheimer's disease. *J Alzheimers Dis*, 34(4):985–994.

World Health Organization (2015). International statistical classification of diseases and related health problems 10th revision (icd-10)-who version for 2016. http://apps.who.int/classifications/icd10/browse/2016/en#/F00-F09 Last access: 2015-11-27.

Xia, W., Yang, T., Shankar, G., and et al (2009). A specific enzyme-linked immunosorbent assay for measuring β-amyloid protein oligomers in human plasma and brain tissue of patients with alzheimer disease. *Archives of Neurology*, 66(2):190–199.

Yang, T., O'Malley, T. T., Kanmert, D., Jerecic, J., Zieske, L. R., Zetterberg, H., Hyman, B. T., Walsh, D. M., and Selkoe, D. J. (2015). A highly sensitive novel immunoassay specifically detects low levels of soluble Aβ oligomers in human cerebrospinal fluid. *Alzheimers Res Ther*, 7(1):14.

Zou, K., Gong, J.-s., Yanagisawa, K., Michikawa, M., and Dtpa, N. (2002). A Novel Function of Monomeric Amyloid β-Protein Serving as an Antioxidant Molecule against Metal-Induced Oxidative Damage. *The Journal of Neuroscience*, 22(12):4833–4841.

A. Anhang

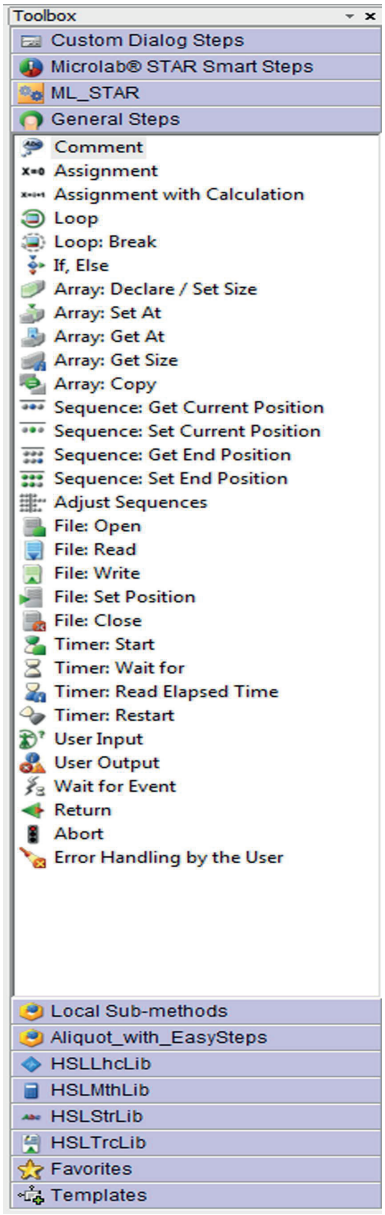

Abbildung A.1: Toolbox für Befehle im Microlab Star
Ausschnitt aus der Venus two-Software mit der Toolbox für mit einer Reihe von Befehlen zur Erstellung einer Methode im ML Star.

Abbildung A.2: Befehlabfolge zur Verteilung von Flüssigkeit mit einem Kanal im Microlab Star
Ausschnitt aus der Beispiel-Methode im ML Star. Die gefärbte Flüssigkeit wird von einem Pipettierkanal aufgenommen und dann in den acht Wells der Mikrotiterplatte verteilt.

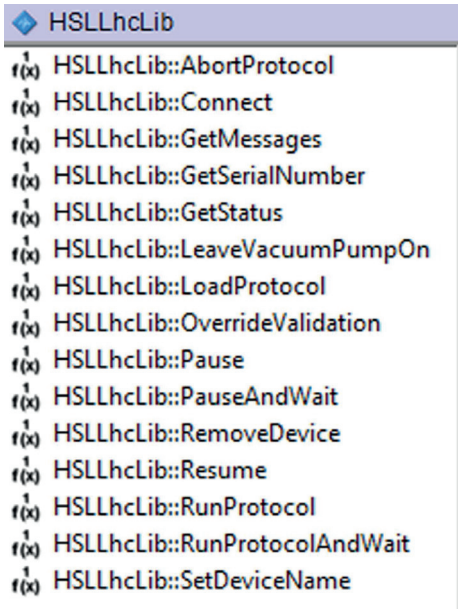

Abbildung A.3: *Liquid Handling Control Library* (LHC-Library) zur Nutzung des BioTek Washers innerhalb des Microlab Star
Die *LHC-Library* enthält eine Reihe von Befehlen, um den ML Star die Möglichkeit zu bieten, den BioTek Washer steuern zu können. Dabei muss der Washer erkannt, vorgefertigte Protokolle geladen und der Status während der Durchführung überprüft werden.

A.1 Implementierung vom Beispiel aus Abschnitt 2.2.4

Die folgenden Seiten zeigen die Implementierung vom beschriebenen Beispiel aus Abschnitt 2.2.4 im ML Star.

C:\Program Files (x86)\HAMILTON\Methods\2016-01-27_HelloWorld\DilutionSeriesOnMicrotiterplate.med

	Method
1	Initialize (Single Step) on ML_STAR Always initialize: Off 3 return value(s) .
2	Assignment 'volumeWater' = '50'
3	Assignment 'volumeColor' = '50'
4	Assignment 'numberCycles' = '12'
5	Assignment 'volumeToAspirate' = '0'
6	Assignment 'numberOfDispenses' = '0'
7	Assignment with Calculation 'endOfMicrotiterplate' = 'numberCycles' * '8'
8	Assignment 'nextPositionToAspirate' = '1'
9	Custom Dialog from Custom Dialog Steps Dialog Title: "User input"
10	Sequence: Set End Position end position of sequence 'ML_STAR.microplates_384_wells' = 'endOfMicrotiterplate'
11	1000µl Channel Tip Pick Up (Single Step) on ML_STAR Channel (1..8): 11111111, Optimized channel use: All sequence positions, Sequence: ML_STAR.MIStar1000ulHighVolumeTip, Sequence counting: (1) Automatic 3 return value(s) .
12	Loop over following sequences: - ML_STAR.microplates_384_wells (Controlling), Adjust for '1' times consumption 'loopCounterOverMicrotiterplate' used as loop counter variable
13	CalcAliquote of Aliquot_with_EasySteps ALIQUOT_WITH_EASYSTEPS::CalcAliquote(ML_STAR.microplates_384_wells, volumeWater, volumeWater, volumeWater, 1000, volumeToAspirate, numberOfDispenses, 1, 8)
14	1000µl Channel Aspirate (Single Step) on ML_STAR Channel (1..8): 11111111, Optimized channel use: All sequence positions, Sequence: ML_STAR.reagent_container_water, Sequence counting: (1) Automatic, Liquid class: "HighVolume_Water_DispenseJet_Part", Volume [µl]: volumeToAspirate, Mix volume [µl]: *, Cycles: 0, Position relative to liquid surface: * mm, LLD settings: On, Capacitive:5, Liquid following: On 3 return value(s)
15	Sequence: Set Current Position current position of sequence 'ML_STAR.reagent_container_water' = '1'
16	1000µl Channel Dispense (Single Step) on ML_STAR Channel (1..8): 11111111, Optimized channel use: All sequence positions, Sequence: ML_STAR.reagent_container_water, Sequence counting: (1) Automatic, Liquid class: As in first aspiration of cycle, Volume [µl]: volumeWater, Mix volume [µl]: *, Cycles: 0, Position relative to liquid surface: * mm, LLD settings: Off, Liquid following: On 3 return value(s)
17	Loop 'numberOfDispenses' times 'loopCounterOverNumberOfDispenses' used as loop counter variable
18	1000µl Channel Dispense (Single Step) on ML_STAR Channel (1..8): 11111111, Optimized channel use: All sequence positions, Sequence: ML_STAR.microplates_384_wells, Sequence counting: (1) Automatic, Liquid class: As in first aspiration of cycle, Volume [µl]: volumeWater, Mix volume [µl]: *, Cycles: 0, Position relative to liquid surface: * mm, LLD settings: Off, Liquid following: On 3 return value(s) .
19	End Loop
20	Sequence: Set Current Position current position of sequence 'ML_STAR.reagent_container_water' = '1'

C:\Program Files (x86)\HAMILTON\Methods\2016-01-27_HelloWorld\DilutionSeriesOnMicrotiterplate.med

	Method
21	1000µl Channel Dispense (Single Step) on ML_STAR Channel (1..8): 11111111, Optimized channel use: All sequence positions, Sequence: ML_STAR.reagent_container_water, Sequence counting: (1) Automatic, Liquid class: As in first aspiration of cycle, Volume [µl]: volumeWater, Mix volume [µl]: *, Cycles: 0, Position relative to liquid surface: * mm, LLD settings: Off, Liquid following: On 3 return value(s)
22	Sequence: Set Current Position current position of sequence 'ML_STAR.reagent_container_water' = '1'
23	End Loop - Reset sequence after loop: ML_STAR.microplates_384_wells
24	1000µl Channel Tip Eject (Single Step) on ML_STAR Channel (1..8): 11111111, Optimized channel use: All sequence positions, Use default waste: On 3 return value(s) .
25	1000µl Channel Tip Pick Up (Single Step) on ML_STAR Channel (1..8): 10000000, Optimized channel use: All sequence positions, Sequence: ML_STAR.MIStar300ulStandardVolumeTip, Sequence counting: (1) Automatic 3 return value(s) .
26	Sequence: Set Current Position current position of sequence 'ML_STAR.microplates_384_wells' = '1'
27	Sequence: Set End Position end position of sequence 'ML_STAR.microplates_384_wells' = '8'
28	Loop over following sequences: - ML_STAR.microplates_384_wells (Controlling), Adjust for '1' times consumption 'loopCounterOverFirstColumn' used as loop counter variable
29	CalcAliquote of Aliquot_with_EasySteps ALIQUOT_WITH_EASYSTEPS::CalcAliquote(ML_STAR.microplates_384_wells, volumeColor, volumeColor, volumeColor, 300, volumeToAspirate, numberOfDispenses, 1,
30	1000µl Channel Aspirate (Single Step) on ML_STAR Channel (1..8): 10000000, Optimized channel use: All sequence positions, Sequence: ML_STAR.tubes_colored_water, Sequence counting: (1) Automatic, Liquid class: "StandardVolume_Water_AliquotDispenseJet_Part", Volume [µl]: volumeToAspirate, Mix volume [µl]: *, Cycles: 0, Position relative to liquid surface: * mm, LLD settings: On, Capacitive:5, Liquid following: On 3 return value(s)
31	Sequence: Set Current Position current position of sequence 'ML_STAR.tubes_colored_water' = '1'
32	1000µl Channel Dispense (Single Step) on ML_STAR Channel (1..8): 10000000, Optimized channel use: All sequence positions, Sequence: ML_STAR.tubes_colored_water, Sequence counting: (1) Automatic, Liquid class: As in first aspiration of cycle, Volume [µl]: volumeColor, Mix volume [µl]: *, Cycles: 0, Position relative to liquid surface: * mm, LLD settings: Off, Liquid following: On 3 return value(s)
33	Loop 'numberOfDispenses' times 'loopCounterOverNumberOfDispenses' used as loop counter variable
34	1000µl Channel Dispense (Single Step) on ML_STAR Channel (1..8): 10000000, Optimized channel use: All sequence positions, Sequence: ML_STAR.microplates_384_wells, Sequence counting: (1) Automatic, Liquid class: As in first aspiration of cycle, Volume [µl]: volumeColor, Mix volume [µl]: *, Cycles: 0, Position relative to liquid surface: * mm, LLD settings: Off, Liquid following: On 3 return value(s)
35	End Loop
36	Sequence: Set Current Position current position of sequence 'ML_STAR.tubes_colored_water' = '1'
37	1000µl Channel Dispense (Single Step) on ML_STAR Channel (1..8): 10000000, Optimized channel use: All sequence positions, Sequence: ML_STAR.tubes_colored_water, Sequence counting: (1) Automatic, Liquid class: As in first aspiration of cycle, Volume [µl]: volumeWater, Mix volume [µl]: *, Cycles: 0, Position relative to liquid surface: * mm, LLD settings: Off, Liquid following: On 3 return value(s) .

C:\Program Files (x86)\HAMILTON\Methods\2016-01-27_HelloWorld\DilutionSeriesOnMicrotiterplate.med

	Method
38	Sequence: Set Current Position current position of sequence 'ML_STAR.tubes_colored_water' = '1'
39	End Loop - Reset sequence after loop: ML_STAR.microplates_384_wells
40	1000µl Channel Tip Eject (Single Step) on ML_STAR Channel (1..8): 10000000, Optimized channel use: All sequence positions, Use default waste: On 3 return value(s) .
41	Sequence: Set Current Position current position of sequence 'ML_STAR.microplates_384_wells' = '1'
42	Sequence: Set End Position end position of sequence 'ML_STAR.microplates_384_wells' = 'endOfMicrotiterplate'
43	Loop over following sequences: - ML_STAR.microplates_384_wells (Controlling), Adjust for '1' times consumption 'loopCounterOverWholePlate' used as loop counter variable
44	1000µl Channel Tip Pick Up (Single Step) on ML_STAR Channel (1..8): 11111111, Optimized channel use: All sequence positions, Sequence: ML_STAR.MIStar300ulStandardVolumeTip, Sequence counting: (1) Automatic 3 return value(s) .
45	1000µl Channel Aspirate (Single Step) on ML_STAR Channel (1..8): 11111111, Optimized channel use: All sequence positions, Sequence: ML_STAR.microplates_384_wells, Sequence counting: (1) Automatic, Liquid class: "StandardVolume_Water_DispenseJet_Empty", Volume [µl]: volumeColor, Mix volume [µl]: *, Cycles: 0, Position relative to liquid surface: * mm, LLD settings: On, Capacitive:5, Liquid following: On 3 return value(s) .
46	1000µl Channel Dispense (Single Step) on ML_STAR Channel (1..8): 11111111, Optimized channel use: All sequence positions, Sequence: ML_STAR.microplates_384_wells, Sequence counting: (1) Automatic, Liquid class: As in first aspiration of cycle, Volume [µl]: volumeColor, Mix volume [µl]: *, Cycles: 0, Position relative to liquid surface: * mm, LLD settings: Off, Liquid following: On 3 return value(s)
47	1000µl Channel Tip Eject (Single Step) on ML_STAR Channel (1..8): 11111111, Optimized channel use: All sequence positions, Use default waste: On 3 return value(s) .
48	Sequence: Get Current Position 'currentPositionOnPlate' = current position of sequence 'ML_STAR.microplates_384_wells'
49	If, Else (currentPositionOnPlate is less than OR equal to 0)
50	Assignment with Calculation 'nextPositionToAspirate' = 'endOfMicrotiterplate' - '7'
51	Sequence: Set Current Position current position of sequence 'ML_STAR.microplates_384_wells' = 'nextPositionToAspirate'
52	1000µl Channel Tip Pick Up (Single Step) on ML_STAR Channel (1..8): 11111111, Optimized channel use: All sequence positions, Sequence: ML_STAR.MIStar300ulStandardVolumeTip, Sequence counting: (1) Automatic 3 return value(s) .
53	1000µl Channel Aspirate (Single Step) on ML_STAR Channel (1..8): 11111111, Optimized channel use: All sequence positions, Sequence: ML_STAR.microplates_384_wells, Sequence counting: (1) Automatic, Liquid class: "StandardVolume_Water_DispenseJet_Empty", Volume [µl]: volumeColor, Mix volume [µl]: *, Cycles: 0, Position relative to liquid surface: * mm, LLD settings: On, Capacitive:5, Liquid following: On 3 return value(s) .
54	1000µl Channel Tip Eject (Single Step) on ML_STAR Channel (1..8): 11111111, Optimized channel use: All sequence positions, Use default waste: On 3 return value(s) .
55	Loop: Break

C:\Program Files (x86)\HAMILTON\Methods\2016-01-27_HelloWorld\DilutionSeriesOnMicrotiterplate.med

	Method
56	Else
57	Assignment with Calculation 'nextPositionToAspirate' = 'currentPositionOnPlate' - '8'
58	Sequence: Set Current Position current position of sequence 'ML_STAR.microplates_384_wells' = 'nextPositionToAspirate'
59	End If
60	End Loop - Reset sequence after loop: ML_STAR.microplates_384_wells
61	Timer: Start Start infinite timer 'WaitForUser'
62	Timer: Wait for Wait for timer 'WaitForUser', show timer display, is stoppable timer.
63	Use_Washer of DilutionSeriesOnMicrotiterplate Use_Washer()
64	

C:\Program Files (x86)\HAMILTON\Methods\2016-01-27_HelloWorld\DilutionSeriesOnMicrotiterplate.med

	Use_Washer
65	Sequence: Set Current Position current position of sequence 'ML_STAR.microplate_washer_position' = '1'
66	Sequence: Set Current Position current position of sequence 'ML_STAR.microplates_384_wells' = '1'
67	iSWAP Transport on ML_STAR Transport labware from 'ML_STAR.microplates_384_wells' to 'ML_STAR.microplate_washer_position' 1 return value(s)
68	Assignment 'WashProgramPath' = '"C:\\ProgramData\\BioTek\\Liquid Handling Control 2.13\\Protocols\\Washer Programme\\Roboter\\Greiner\\Wash3xWithWater\\"'
69	Connect of HSLLhcLib HSLLhcLib::Connect(HSLLhcLib::PRODUCT_TYPE_405TSLS, "USB 405 TS/LS sn:1309255", str_washer_version, str_washer_connect_msg)
70	SetDeviceName of HSLLhcLib HSLLhcLib::SetDeviceName("USB 405 TS/LS sn:1309255", "BioTek_Washer")
71	LoadProtocol of HSLLhcLib protocolSuccesful = HSLLhcLib::LoadProtocol("BioTek_Washer", HSLLhcLib::FILE, WashProgramPath)
72	Assignment 'washerStatus' = '"BUSY"'
73	Loop while '1' is equal to '1' 'loopCounterWasherStatus' used as loop counter variable
74	GetStatus of HSLLhcLib HSLLhcLib::GetStatus("BioTek_Washer", washerStatus)
75	Timer: Start Start timer 'washerStatusReport', set to relative time: '10' [s]
76	Timer: Wait for Wait for timer 'washerStatusReport', show timer display, is stoppable timer.
77	If, Else (washerStatus is equal to "Error")
78	User Output Dialog Title: '"Washer has an Error"', Return Value: '', Buttons: 'Only 'OK' button', Default: 'OK', Icons: 'Display information message icon', Sound: '', Timeout: 'infinite' Output: "Washer has an Error"
79	Loop: Break
80	End If
81	If, Else (washerStatus is equal to "Ready")
82	Loop: Break
83	End If
84	Assignment 'washerStatus' = '"Ready"'
85	End Loop
86	Sequence: Set Current Position current position of sequence 'ML_STAR.microplate_washer_position' = '1'
87	Sequence: Set Current Position current position of sequence 'ML_STAR.microplates_384_wells' = '1'
88	iSWAP Transport on ML_STAR Transport labware from 'ML_STAR.microplate_washer_position' to 'ML_STAR.microplates_384_wells' 1 return value(s)

C:\Program Files (x86)\HAMILTON\Methods\2016-01-27_HelloWorld\DilutionSeriesOnMicrotiterplate.med

	Use_Washer
89	

A.2 Implementierung des sFIDA-Assays im Microlab Star

Die folgenden Seiten zeigen die Implementierung des sFIDA-Assays von Dezember 2015. Diese Methode wurde beim Experiment beschrieben in Abschnitt 3.4 verwendet.

C:\Program Files (x86)\HAMILTON\Methods\sFIDA Greiner PEG\sFIDA_Greiner_PEG.med

	Method
1	Initialize (Single Step) on ML_STAR Always initialize: Off 3 return value(s)
2	_000_Settings of sFIDA_Greiner_PEG _000_Settings()
3	_0005_SelectStepDialog of sFIDA_Greiner_PEG _0005_SelectStepDialog()
4	_0004_InputDialog of sFIDA_Greiner_PEG _0004_InputDialog()
5	Loop 'g_NumPlates' times 'loopCounterOverExcel' used as loop counter variable
16	_0002_SetupSequences of sFIDA_Greiner_PEG _0002_SetupSequences()
17	Channels_TipCounter_Edit of Visual_NTR_library VISUAL_NTR_LIBRARY::Channels_TipCounter_Edit(ML_STAR, ML_STAR.NTR_300ulTips_All, "TipCounter300ulNTR", "Edit 300 ul NTR Tips", 1, 999)
18	Edit2 of HSLTipCountingLib TipCount::Edit2(ML_STAR.MlStar1000ulHighVolumeTip, "1000ulHighVolumeTip", ML_STAR, [illegible])
19	Edit2 of HSLTipCountingLib TipCount::Edit2(ML_STAR.MlStar300ulStandardVolumeTip, "300ulStandardVolumeTip", ML_STAR, 999999)
20	Edit2 of HSLTipCountingLib TipCount::Edit2(ML_STAR.MlStar50ulTip, "50ulStandardVolumeTip", ML_STAR, 999999)
21	If, Else (g_UserInputSelectStep is equal to 0)
22	User Output Dialog Title: '"Nothing to do"', Return Value: '', Buttons: 'Only 'OK' button', Default: 'OK', Icons: 'Display information message icon', Sound: '', Timeout: 'infinite' Output: "Nothing to do. You did not select a step. Method will abort"
23	Abort
24	End If
25	If, Else (g_UserInputSelectStep is equal to 1)
26	Comment <****************** sFIDA day 1 NaOH incubation 15 min Remove NaOH Wash 3x with water HCl incubation 15 min. Remove HCl Wash 3x with water Wash 2x with Ethanol in ML Star Wait till plate is dry Apply Ethanolamine over night *****************>
27	Comment <****** Apply NaOH *******>
28	Loop 'g_NumPlates' times 'loopCounterNaOHOverPlates' used as loop counter variable
36	_0008_MoveLidToPlate of sFIDA_Greiner_PEG _0008_MoveLidToPlate()
37	Timer: Wait for Wait for timer 'incubation_NaOH', show timer display, is stoppable timer.

C:\Program Files (x86)\HAMILTON\Methods\sFIDA Greiner PEG\sFIDA_Greiner_PEG.med

	Method
38	_0007_MoveLidToParkPosition of sFIDA_Greiner_PEG _0007_MoveLidToParkPosition()
39	Comment <****** Remove NaOH<br*******>
40	Loop 'g_NumPlates' times 'loopCounterRemoveLiquidOverPlates' used as loop counter variable
41	Assignment 'g_current_plate' = 'loopCounterRemoveLiquidOverPlates'
42	_0011_SetupAllForEachPlate of sFIDA_Greiner_PEG _0011_SetupAllForEachPlate()
43	_00002_RemoveLiquidFromPlate of sFIDA_Greiner_PEG _00002_RemoveLiquidFromPlate()
44	End Loop
45	_0003_UseWasher of sFIDA_Greiner_PEG _0003_UseWasher()
46	Comment <****** Apply HCl<br*******>
47	Loop 'g_NumPlates' times 'loopCounterHClOverPlates' used as loop counter variable
55	_0008_MoveLidToPlate of sFIDA_Greiner_PEG _0008_MoveLidToPlate()
56	Timer: Wait for Wait for timer 'incubation_HCl', show timer display, is stoppable timer.
57	_0007_MoveLidToParkPosition of sFIDA_Greiner_PEG _0007_MoveLidToParkPosition()
58	Comment <****** Remove HCl<br*******>
59	Loop 'g_NumPlates' times 'loopCounter2RemoveLiquidOverPlates' used as loop counter variable
60	Assignment 'g_current_plate' = 'loopCounter2RemoveLiquidOverPlates'
61	_0011_SetupAllForEachPlate of sFIDA_Greiner_PEG _0011_SetupAllForEachPlate()
62	_00002_RemoveLiquidFromPlate of sFIDA_Greiner_PEG _00002_RemoveLiquidFromPlate()
63	End Loop
64	_0003_UseWasher of sFIDA_Greiner_PEG _0003_UseWasher()
65	Comment <****** Wash Ethanol in ML Star<br*******>
66	Loop 'g_NumPlates' times 'loopCounterEthanolOverPlates' used as loop counter variable
67	Assignment 'g_current_plate' = 'loopCounterEthanolOverPlates'
68	_0011_SetupAllForEachPlate of sFIDA_Greiner_PEG _0011_SetupAllForEachPlate()

C:\Program Files (x86)\HAMILTON\Methods\sFIDA Greiner PEG\sFIDA_Greiner_PEG.med

	Method
69	_00004_WashEthanol of sFIDA_Greiner_PEG _00004_WashEthanol()
70	End Loop
71	Timer: Start Start infinite timer 'DryingPlate'
72	Timer: Wait for Wait for timer 'DryingPlate', show timer display, is stoppable timer.
73	Comment <****** Apply Ethanolamine *******>
74	Loop 'g_NumPlates' times 'loopCounterEthanolamineOverPlates' used as loop counter variable
75	Assignment 'g_current_plate' = 'loopCounterEthanolamineOverPlates'
76	_0011_SetupAllForEachPlate of sFIDA_Greiner_PEG _0011_SetupAllForEachPlate()
77	_00005_Ethanolamine of sFIDA_Greiner_PEG _00005_Ethanolamine()
78	End Loop
79	_0008_MoveLidToPlate of sFIDA_Greiner_PEG _0008_MoveLidToPlate()
80	Else
81	If, Else (g_UserInputSelectStep is equal to 2)
82	Comment <****************** sFIDA day 2 Remove Ethanolamine Wash 3x DMSO in ML Star Wash 2x Ethanol in ML Star Apply PEG incubation 1h Wash 3x with Water Apply EDC/NHS incubation 30 min Wash 3x with MES Apply Capture AB incubation 1 h Wash 3x PBS, 3x PBS-T Apply Blocking incubation 1 h Wash 3x PBS, 3x PBS-T Prepare dilution series for standards Apply Samples incubation ON ******************>
83	Comment <****** Remove Ethanolamine *******>
84	Loop 'g_NumPlates' times 'loopCounterRemoveLiquidOverPlates' used as loop counter variable
85	Assignment 'g_current_plate' = 'loopCounterRemoveLiquidOverPlates'
86	_0011_SetupAllForEachPlate of sFIDA_Greiner_PEG _0011_SetupAllForEachPlate()
87	_00002_RemoveLiquidFromPlate of sFIDA_Greiner_PEG _00002_RemoveLiquidFromPlate()
88	End Loop

C:\Program Files (x86)\HAMILTON\Methods\sFIDA Greiner PEG\sFIDA_Greiner_PEG.med

	Method
89	Comment <******* Wash with DMSO in ML Star *******>
90	Loop 'g_NumPlates' times 'loopCounterDMSOOverPlates' used as loop counter variable
91	Assignment 'g_current_plate' = 'loopCounterDMSOOverPlates'
92	_0011_SetupAllForEachPlate of sFIDA_Greiner_PEG _0011_SetupAllForEachPlate()
93	_00006_WashDMSO of sFIDA_Greiner_PEG _00006_WashDMSO()
94	End Loop
95	User Output Dialog Title: '"Pause"', Return Value: '', Buttons: 'Only 'OK' button', Default: 'OK', Icons: 'Display information message icon', Sound: '', Timeout: 'infinite' Output: "Please exchange liquid waste"
96	Comment <****** Wash Ethanol in ML Star *******>
97	Loop 'g_NumPlates' times 'loopCounterEthanolOverPlates' used as loop counter variable
98	Assignment 'g_current_plate' = 'loopCounterEthanolOverPlates'
99	_0011_SetupAllForEachPlate of sFIDA_Greiner_PEG _0011_SetupAllForEachPlate()
100	_00004_WashEthanol of sFIDA_Greiner_PEG _00004_WashEthanol()
101	End Loop
102	Timer: Start Start infinite timer 'DryingPlate'
103	Timer: Wait for Wait for timer 'DryingPlate', show timer display, is stoppable timer.
104	Comment <****** Apply PEG *******>
105	Loop 'g_NumPlates' times 'loopCounterPEGOverPlates' used as loop counter variable
106	Assignment 'g_current_plate' = 'loopCounterPEGOverPlates'
107	_0011_SetupAllForEachPlate of sFIDA_Greiner_PEG _0011_SetupAllForEachPlate()
108	_00007_SpacerCoating of sFIDA_Greiner_PEG _00007_SpacerCoating()
109	If, Else (loopCounterPEGOverPlates is equal to 1)
110	Timer: Start Start timer 'incubation_PEG', set to relative time: '3600' [s]
111	End If
112	End Loop

C:\Program Files (x86)\HAMILTON\Methods\sFIDA Greiner PEG\sFIDA_Greiner_PEG.med

	Method
113	_0008_MoveLidToPlate of sFIDA_Greiner_PEG _0008_MoveLidToPlate()
114	Timer: Wait for Wait for timer 'incubation_PEG', show timer display, is stoppable timer.
115	_0007_MoveLidToParkPosition of sFIDA_Greiner_PEG _0007_MoveLidToParkPosition()
116	_0003_UseWasher of sFIDA_Greiner_PEG _0003_UseWasher()
117	Comment <****** Apply EDC/NHS *******>
118	Loop 'g_NumPlates' times 'loopCounterActivationSurfaceOverPlates' used as loop counter variable
119	Assignment 'g_current_plate' = 'loopCounterActivationSurfaceOverPlates'
120	_0011_SetupAllForEachPlate of sFIDA_Greiner_PEG _0011_SetupAllForEachPlate()
121	_00008_ActivateSurface of sFIDA_Greiner_PEG _00008_ActivateSurface()
122	If, Else (loopCounterActivationSurfaceOverPlates is equal to 1)
123	Timer: Start Start timer 'incubation_Activation', set to relative time: '1800' [s]
124	End If
125	End Loop
126	_0008_MoveLidToPlate of sFIDA_Greiner_PEG _0008_MoveLidToPlate()
127	Timer: Wait for Wait for timer 'incubation_Activation', show timer display, is stoppable timer.
128	_0007_MoveLidToParkPosition of sFIDA_Greiner_PEG _0007_MoveLidToParkPosition()
129	_0003_UseWasher of sFIDA_Greiner_PEG _0003_UseWasher()
130	Comment <****** Apply Capture AB *******>
131	Loop 'g_NumPlates' times 'loopCounterCaptureOverPlates' used as loop counter variable
132	Assignment 'g_current_plate' = 'loopCounterCaptureOverPlates'
133	_0011_SetupAllForEachPlate of sFIDA_Greiner_PEG _0011_SetupAllForEachPlate()
134	_00009_CaptureAB of sFIDA_Greiner_PEG _00009_CaptureAB()
135	If, Else (loopCounterCaptureOverPlates is equal to 1)
138	End Loop
139	_0008_MoveLidToPlate of sFIDA_Greiner_PEG _0008_MoveLidToPlate()
140	Timer: Wait for Wait for timer 'incubation_CaptureAB', show timer display, is stoppable timer.

C:\Program Files (x86)\HAMILTON\Methods\sFIDA Greiner PEG\sFIDA_Greiner_PEG.med

	Method
141	_0007_MoveLidToParkPosition of sFIDA_Greiner_PEG _0007_MoveLidToParkPosition()
142	_0003_UseWasher of sFIDA_Greiner_PEG _0003_UseWasher()
143	Comment <****** Apply Blocking<br*******>
144	Loop 'g_NumPlates' times 'loopCounterBlockingOverPlates' used as loop counter variable
145	Assignment 'g_current_plate' = 'loopCounterBlockingOverPlates'
146	_0011_SetupAllForEachPlate of sFIDA_Greiner_PEG _0011_SetupAllForEachPlate()
147	_00010_Blocking of sFIDA_Greiner_PEG _00010_Blocking()
148	If, Else (loopCounterBlockingOverPlates is equal to 1)
149	Timer: Start Start timer 'incubation_Blocking', set to relative time: '3600' [s]
150	End If
151	End Loop
152	_0008_MoveLidToPlate of sFIDA_Greiner_PEG _0008_MoveLidToPlate()
153	Timer: Wait for Wait for timer 'incubation_Blocking', show timer display, is stoppable timer.
154	_0007_MoveLidToParkPosition of sFIDA_Greiner_PEG _0007_MoveLidToParkPosition()
155	_0003_UseWasher of sFIDA_Greiner_PEG _0003_UseWasher()
156	Comment <****** Dilute Standards<br*******>
157	Loop 'g_NumPlates' times 'loopCounterOverPossibleDilutions' used as loop counter variable
158	Assignment 'g_current_plate' = 'loopCounterOverPossibleDilutions'
159	_0011_SetupAllForEachPlate of sFIDA_Greiner_PEG _0011_SetupAllForEachPlate()
160	_00011_DiluteStandards of sFIDA_Greiner_PEG _00011_DiluteStandards()
161	End Loop
162	Comment <****** Distribute Samples<br*******>
163	Edit2 of HSLTipCountingLib TipCount::Edit2(ML_STAR.MIStar300ulStandardVolumeTip, "300ulStandardVolumeTip", ML_STAR, 999999)
164	Edit2 of HSLTipCountingLib TipCount::Edit2(ML_STAR.MIStar50ulTip, "50ulStandardVolumeTip", ML_STAR, 999999)

C:\Program Files (x86)\HAMILTON\Methods\sFIDA Greiner PEG\sFIDA_Greiner_PEG.med

	Method
165	Loop 'g_NumPlates' times 'loopCounterSamplesOverPlates' used as loop counter variable
166	Assignment 'sample_step' = '1'
167	Assignment 'g_current_plate' = 'loopCounterSamplesOverPlates'
168	_0011_SetupAllForEachPlate of sFIDA_Greiner_PEG _0011_SetupAllForEachPlate()
169	_00012_DistributeSamples of sFIDA_Greiner_PEG _00012_DistributeSamples()
170	End Loop
171	Assignment 'sample_step' = '0'
172	_0008_MoveLidToPlate of sFIDA_Greiner_PEG _0008_MoveLidToPlate()
173	Else
174	If, Else (g_UserInputSelectStep is equal to 3)
175	Comment <****************** sFIDA day 3 Apply Detection AB incubation 1 h Wash 5x PBS, 5 PBS-T Apply water with azid ******************>
176	Comment <******* Remove samples *******>
177	Channels_TipCounter_Edit of Visual_NTR_library VISUAL_NTR_LIBRARY::Channels_TipCounter_Edit(ML_STAR, ML_STAR.NTR_300ulTips_All, "TipCounter300ulNTR", "Edit 300 ul NTR Tips", 1, 999)
178	Loop 'g_NumPlates' times 'loopCounterExchangeLiquidOverPlates' used as loop counter variable
179	Assignment 'g_current_plate' = 'loopCounterExchangeLiquidOverPlates'
180	_0011_SetupAllForEachPlate of sFIDA_Greiner_PEG _0011_SetupAllForEachPlate()
181	_00015_ExchangeLiquidWithBuffer of sFIDA_Greiner_PEG _00015_ExchangeLiquidWithBuffer()
182	End Loop
183	StrConcat2 of HSLStrLib g_WashProgramPath = StrConcat2(g_GeneralPathToWasherPrograms, "Greiner_Sector1_3times_PBST_C_3times_PBS_B_remainingVol50µl.LH
184	_0003_UseWasher of sFIDA_Greiner_PEG _0003_UseWasher()
185	Comment <******* Apply detection ABs *******>
186	Edit2 of HSLTipCountingLib TipCount::Edit2(ML_STAR.MlStar300ulStandardVolumeTip, "300ulStandardVolumeTip", ML_STAR, 999999)

C:\Program Files (x86)\HAMILTON\Methods\sFIDA Greiner PEG\sFIDA_Greiner_PEG.med

	Method
187	Edit2 of HSLTipCountingLib TipCount::Edit2(ML_STAR.MIStar50ulTip, "50ulStandardVolumeTip", ML_STAR, 999999)
188	Loop 'g_NumPlates' times 'loopCounterDetectionABOverPlates' used as loop counter variable
189	Assignment 'g_current_plate' = 'loopCounterDetectionABOverPlates'
190	_0011_SetupAllForEachPlate of sFIDA_Greiner_PEG _0011_SetupAllForEachPlate()
191	_00013_DetectionAB of sFIDA_Greiner_PEG _00013_DetectionAB()
192	If, Else (loopCounterDetectionABOverPlates is equal to 1)
193	Timer: Start Start timer 'incubation_DetectionAB', set to relative time: '3600' [s]
194	End If
195	End Loop
196	_0008_MoveLidToPlate of sFIDA_Greiner_PEG _0008_MoveLidToPlate()
197	Timer: Wait for Wait for timer 'incubation_DetectionAB', show timer display, is stoppable timer
198	_0007_MoveLidToParkPosition of sFIDA_Greiner_PEG _0007_MoveLidToParkPosition()
199	Channels_TipCounter_Edit of Visual_NTR_library VISUAL_NTR_LIBRARY::Channels_TipCounter_Edit(ML_STAR, ML_STAR.NTR_300ulTips_All, "TipCounter300ulNTR", "Edit 300 ul NTR Tips", 1, 999)
200	Comment <****** Remove detection ABs<br*******>
201	Loop 'g_NumPlates' times 'loopCounterExchangeLiquidOverPlates' used as loop counter variable
202	Assignment 'g_current_plate' = 'loopCounterExchangeLiquidOverPlates'
203	_0011_SetupAllForEachPlate of sFIDA_Greiner_PEG _0011_SetupAllForEachPlate()
204	_00015_ExchangeLiquidWithBuffer of sFIDA_Greiner_PEG _00015_ExchangeLiquidWithBuffer()
205	End Loop
206	_0003_UseWasher of sFIDA_Greiner_PEG _0003_UseWasher()
207	Channels_TipCounter_Edit of Visual_NTR_library VISUAL_NTR_LIBRARY::Channels_TipCounter_Edit(ML_STAR, ML_STAR.NTR_300ulTips_All, "TipCounter300ulNTR", "Edit 300 ul NTR Tips", 1, 999)
208	Comment <****** Apply water with azid<br*******>
209	Loop 'g_NumPlates' times 'loopCounterWaterWithAzidOverPlates' used as loop counter variable

C:\Program Files (x86)\HAMILTON\Methods\sFIDA Greiner PEG\sFIDA_Greiner_PEG.med

	Method
210	Assignment 'g_current_plate' = 'loopCounterWaterWithAzidOverPlates'
211	_0011_SetupAllForEachPlate of sFIDA_Greiner_PEG _0011_SetupAllForEachPlate()
212	_00014_WaterWithAzid of sFIDA_Greiner_PEG _00014_WaterWithAzid()
213	End Loop
214	_0008_MoveLidToPlate of sFIDA_Greiner_PEG _0008_MoveLidToPlate()
215	Else
216	If, Else (g_UserInputSelectStep is equal to 4)
217	Comment <****************** sFIDA day 2 complete Remove Ethanolamine Wash 3x DMSO in ML Star Wash 2x Ethanol in ML Star Apply PEG incubation 1h Wash 3x with Water Apply EDC/NHS incubation 30 min Wash 3x with MES Apply Capture AB incubation 1 h Wash 3x PBS, 3x PBS-T Apply Blocking incubation 1 h Wash 3x PBS, 3x PBS-T Prepare dilution series for standards Apply Samples incubation 2 h Apply Detection AB incubation 1 h Wash 5x PBS, 5 PBS-T Apply water with azid *****************>
218	Comment <****** Remove Ethanolamine *******>
219	Loop 'g_NumPlates' times 'loopCounterRemoveLiquidOverPlates' used as loop counter
220	Assignment 'g_current_plate' = 'loopCounterRemoveLiquidOverPlates'
221	_0011_SetupAllForEachPlate of sFIDA_Greiner_PEG _0011_SetupAllForEachPlate()
222	_00002_RemoveLiquidFromPlate of sFIDA_Greiner_PEG _00002_RemoveLiquidFromPlate()
223	End Loop
224	Comment <****** Wash with DMSO in ML Star *******>
225	Loop 'g_NumPlates' times 'loopCounterDMSOOverPlates' used as loop counter variable
226	Assignment 'g_current_plate' = 'loopCounterDMSOOverPlates'
227	_0011_SetupAllForEachPlate of sFIDA_Greiner_PEG _0011_SetupAllForEachPlate()

C:\Program Files (x86)\HAMILTON\Methods\sFIDA Greiner PEG\sFIDA_Greiner_PEG.med

	Method
228	_00006_WashDMSO of sFIDA_Greiner_PEG _00006_WashDMSO()
229	End Loop
230	Comment <******* Wash Ethanol in ML Star *******>
231	Loop 'g_NumPlates' times 'loopCounterEthanolOverPlates' used as loop counter variable
232	Assignment 'g_current_plate' = 'loopCounterEthanolOverPlates'
233	_0011_SetupAllForEachPlate of sFIDA_Greiner_PEG _0011_SetupAllForEachPlate()
234	_00004_WashEthanol of sFIDA_Greiner_PEG _00004_WashEthanol()
235	End Loop
236	Timer: Start Start infinite timer 'DryingPlate'
237	Timer: Wait for Wait for timer 'DryingPlate', show timer display, is stoppable timer.
238	Comment <******* Apply PEG *******>
239	Loop 'g_NumPlates' times 'loopCounterPEGOverPlates' used as loop counter variable
247	_0008_MoveLidToPlate of sFIDA_Greiner_PEG _0008_MoveLidToPlate()
248	Timer: Wait for Wait for timer 'incubation_PEG', show timer display, is stoppable timer.
249	_0007_MoveLidToParkPosition of sFIDA_Greiner_PEG _0007_MoveLidToParkPosition()
250	_0003_UseWasher of sFIDA_Greiner_PEG _0003_UseWasher()
251	Comment <******* Apply EDC/NHS *******>
252	Loop 'g_NumPlates' times 'loopCounterActivationSurfaceOverPlates' used as loop counter variable
253	Assignment 'g_current_plate' = 'loopCounterActivationSurfaceOverPlates'
254	_0011_SetupAllForEachPlate of sFIDA_Greiner_PEG _0011_SetupAllForEachPlate()
255	_00008_ActivateSurface of sFIDA_Greiner_PEG _00008_ActivateSurface()
256	If, Else (loopCounterActivationSurfaceOverPlates is equal to 1)
259	End Loop
260	_0008_MoveLidToPlate of sFIDA_Greiner_PEG _0008_MoveLidToPlate()

C:\Program Files (x86)\HAMILTON\Methods\sFIDA Greiner PEG\sFIDA_Greiner_PEG.med

	Method
261	Timer: Wait for Wait for timer 'incubation_Activation', show timer display, is stoppable timer.
262	_0007_MoveLidToParkPosition of sFIDA_Greiner_PEG _0007_MoveLidToParkPosition()
263	_0003_UseWasher of sFIDA_Greiner_PEG _0003_UseWasher()
264	Comment <****** Apply Capture AB *******>
265	Loop 'g_NumPlates' times 'loopCounterCaptureOverPlates' used as loop counter variable
266	Assignment 'g_current_plate' = 'loopCounterCaptureOverPlates'
267	_0011_SetupAllForEachPlate of sFIDA_Greiner_PEG _0011_SetupAllForEachPlate()
268	_00009_CaptureAB of sFIDA_Greiner_PEG _00009_CaptureAB()
269	If, Else (loopCounterCaptureOverPlates is equal to 1)
272	End Loop
273	_0008_MoveLidToPlate of sFIDA_Greiner_PEG _0008_MoveLidToPlate()
274	Timer: Wait for Wait for timer 'incubation_CaptureAB', show timer display, is stoppable timer.
275	_0007_MoveLidToParkPosition of sFIDA_Greiner_PEG _0007_MoveLidToParkPosition()
276	_0003_UseWasher of sFIDA_Greiner_PEG _0003_UseWasher()
277	Comment <****** Apply Blocking *******>
278	Loop 'g_NumPlates' times 'loopCounterBlockingOverPlates' used as loop counter variable
279	Assignment 'g_current_plate' = 'loopCounterBlockingOverPlates'
280	_0011_SetupAllForEachPlate of sFIDA_Greiner_PEG _0011_SetupAllForEachPlate()
281	_00010_Blocking of sFIDA_Greiner_PEG _00010_Blocking()
282	If, Else (loopCounterBlockingOverPlates is equal to 1)
285	End Loop
286	_0008_MoveLidToPlate of sFIDA_Greiner_PEG _0008_MoveLidToPlate()
287	Timer: Wait for Wait for timer 'incubation_Blocking', show timer display, is stoppable timer.
288	_0007_MoveLidToParkPosition of sFIDA_Greiner_PEG _0007_MoveLidToParkPosition()
289	_0003_UseWasher of sFIDA_Greiner_PEG _0003_UseWasher()

C:\Program Files (x86)\HAMILTON\Methods\sFIDA Greiner PEG\sFIDA_Greiner_PEG.med

	Method
290	Comment <******* Dilute Standards *******>
291	Loop 'g_NumPlates' times 'loopCounterOverPossibleDilutions' used as loop counter variable
292	Assignment 'g_current_plate' = 'loopCounterOverPossibleDilutions'
293	_0011_SetupAllForEachPlate of sFIDA_Greiner_PEG _0011_SetupAllForEachPlate()
294	_00011_DiluteStandards of sFIDA_Greiner_PEG _00011_DiluteStandards()
295	End Loop
296	Comment <******* Distribute Samples *******>
297	Edit2 of HSLTipCountingLib TipCount::Edit2(ML_STAR.MIStar300ulStandardVolumeTip, "300ulStandardVolumeTip", ML_STAR, 999999)
298	Edit2 of HSLTipCountingLib TipCount::Edit2(ML_STAR.MIStar50ulTip, "50ulStandardVolumeTip", ML_STAR, 999999)
299	Loop 'g_NumPlates' times 'loopCounterSamplesOverPlates' used as loop counter variable
300	Assignment 'sample_step' = '1'
301	Assignment 'g_current_plate' = 'loopCounterSamplesOverPlates'
302	_0011_SetupAllForEachPlate of sFIDA_Greiner_PEG _0011_SetupAllForEachPlate()
303	_00012_DistributeSamples of sFIDA_Greiner_PEG _00012_DistributeSamples()
304	If, Else (loopCounterSamplesOverPlates is equal to 1)
307	End Loop
308	Assignment 'sample_step' = '0'
309	_0008_MoveLidToPlate of sFIDA_Greiner_PEG _0008_MoveLidToPlate()
310	Timer: Wait for Wait for timer 'incubation_samples', show timer display, is stoppable timer.
311	_0007_MoveLidToParkPosition of sFIDA_Greiner_PEG _0007_MoveLidToParkPosition()
312	Comment <******* Remove samples *******>
313	Channels_TipCounter_Edit of Visual_NTR_library VISUAL_NTR_LIBRARY::Channels_TipCounter_Edit(ML_STAR, ML_STAR.NTR_300ulTips_All, "TipCounter300ulNTR", "Edit 300 ul NTR Tips", 1, 999)
314	Loop 'g_NumPlates' times 'loopCounterExchangeLiquidOverPlates' used as loop counter variable

C:\Program Files (x86)\HAMILTON\Methods\sFIDA Greiner PEG\sFIDA_Greiner_PEG.med

	Method
315	Assignment 'g_current_plate' =
316	_0011_SetupAllForEachPlate of sFIDA_Greiner_PEG _0011_SetupAllForEachPlate()
317	_00015_ExchangeLiquidWithBuffer of sFIDA_Greiner_PEG
318	End Loop
319	_0003_UseWasher of sFIDA_Greiner_PEG _0003_UseWasher()
320	Comment <****** Apply detection ABs *******>
321	Edit2 of HSLTipCountingLib TipCount::Edit2(ML_STAR.MIStar300ulStandardVolumeTip, "300ulStandardVolumeTip", ML_STAR, 999999)
322	Edit2 of HSLTipCountingLib TipCount::Edit2(ML_STAR.MIStar50ulTip, "50ulStandardVolumeTip", ML_STAR, 999999)
323	Loop 'g_NumPlates' times 'loopCounterDetectionABOverPlates' used as loop counter variable
324	Assignment 'g_current_plate' = 'loopCounterDetectionABOverPlates'
325	_0011_SetupAllForEachPlate of sFIDA_Greiner_PEG _0011_SetupAllForEachPlate()
326	_00013_DetectionAB of sFIDA_Greiner_PEG _00013_DetectionAB()
327	If, Else (loopCounterDetectionABOverPlates is equal to 1)
330	End Loop
331	_0008_MoveLidToPlate of sFIDA_Greiner_PEG _0008_MoveLidToPlate()
332	Timer: Wait for Wait for timer 'incubation_DetectionAB', show timer display, is stoppable timer.
333	_0007_MoveLidToParkPosition of sFIDA_Greiner_PEG _0007_MoveLidToParkPosition()
334	Comment <****** Remove detection ABs *******>
335	Channels_TipCounter_Edit of Visual_NTR_library VISUAL_NTR_LIBRARY::Channels_TipCounter_Edit(ML_STAR, ML_STAR.NTR_300ulTips_All, "TipCounter300ulNTR", "Edit 300 ul NTR Tips", 1, 999)
336	Loop 'g_NumPlates' times 'loopCounterExchangeLiquidOverPlates' used as loop counter variable
337	Assignment 'g_current_plate' =
338	_0011_SetupAllForEachPlate of sFIDA_Greiner_PEG _0011_SetupAllForEachPlate()
339	_00015_ExchangeLiquidWithBuffer of sFIDA_Greiner_PEG
340	End Loop

C:\Program Files (x86)\HAMILTON\Methods\sFIDA Greiner PEG\sFIDA_Greiner_PEG.med

	Method
341	_0003_UseWasher of sFIDA_Greiner_PEG _0003_UseWasher()
342	Comment <****** Apply water with azid<br*******>
343	Channels_TipCounter_Edit of Visual_NTR_library VISUAL_NTR_LIBRARY::Channels_TipCounter_Edit(ML_STAR, ML_STAR.NTR_300ulTips_All, "TipCounter300ulNTR", "Edit 300 ul NTR Tips", 1, 999)
344	Loop 'g_NumPlates' times 'loopCounterWaterWithAzidOverPlates' used as loop counter variable
345	Assignment 'g_current_plate' = 'loopCounterWaterWithAzidOverPlates'
346	_0011_SetupAllForEachPlate of sFIDA_Greiner_PEG _0011_SetupAllForEachPlate()
347	_00014_WaterWithAzid of sFIDA_Greiner_PEG _00014_WaterWithAzid()
348	End Loop
349	_0008_MoveLidToPlate of sFIDA_Greiner_PEG _0008_MoveLidToPlate()
350	End If
351	End If
352	End If
353	End If
354	SendEMail of HSLUtilLib g_sentEmail = Util::SendEMail(g_emailAddress, g_emailSubject, g_emailBody)
355	Custom Dialog from Custom Dialog Steps Dialog Title: "Done!"
356	

C:\Program Files (x86)\HAMILTON\Methods\sFIDA Greiner PEG\sFIDA_Greiner_PEG.med

	_00001_NaOH
357	Comment <********** Distribute NaOH on current plate **********>
358	Assignment 'g_progressText' = '"Add NaOH to plate"'
359	AppendStatusText of HSLStatusWindow HSLStatusWindow::AppendStatusText(g_progressText)
360	1000µl Channel Tip Pick Up (Single Step) on ML_STAR Channel (1..8): 11111111, Optimized channel use: All sequence positions, Sequence: ML_STAR.MIStar1000ulHighVolumeTip, Sequence counting: (1) Automatic 3 return value(s) .
361	Write2 of HSLTipCountingLib TipCount::Write2(ML_STAR.MIStar1000ulHighVolumeTip, "1000ulHighVolumeTip", ML_STAR)
362	Assignment 'g_VolPreAliquot' = '100'
363	Assignment 'g_VolPostAliquot' = '100'
364	Assignment 'g_NaOH_volume' = '100'
365	Sequence: Set Current Position current position of sequence 'seq_current_plate' = '1'
366	Sequence: Set End Position end position of sequence 'seq_current_plate' = 'g_NumWells'
367	Loop over following sequences: - seq_current_plate (Controlling), Adjust for '1' times consumption 'loopCounterOverPlateNaOH' used as loop counter variable
368	CalcAliquote of Aliquot_with_EasySteps ALIQUOT_WITH_EASYSTEPS::CalcAliquote(seq_current_plate, g_NaOH_volume, g_VolPreAliquot, g_VolPostAliquot, g_maxVolPerTip1000, g_VolAspirate, numDispenseSteps, 1, 8)
369	Sequence: Set Current Position current position of sequence 'ML_STAR.LiqCar02_Pos05_NaOH' = '1'
370	1000µl Channel Aspirate (Single Step) on ML_STAR Channel (1..8): 11111111, Optimized channel use: All sequence positions, Sequence: ML_STAR.LiqCar02_Pos05_NaOH, Sequence counting: (1) Automatic, Liquid class: "HighVolume_Water_AliquotDispenseJet_Part", Volume [µl]: g_VolAspirate, Mix volume [µl]: *, Cycles: 0, Position relative to liquid surface: * mm, LLD settings: On, Capacitive:5, Liquid following: On 3 return value(s) .
371	1000µl Channel Dispense (Single Step) on ML_STAR Channel (1..8): 11111111, Optimized channel use: All sequence positions, Sequence: ML_STAR.dummyGreinerPlate, Sequence counting: (1) Automatic, Liquid class: As in first aspiration of cycle, Volume [µl]: g_VolPreAliquot, Mix volume [µl]: *, Cycles: 0, Position relative to liquid surface: * mm, LLD settings: Off, Liquid following: On 3 return value(s) .
372	Loop 'numDispenseSteps' times 'loopNumDispenseSteps' used as loop counter variable
373	1000µl Channel Dispense (Single Step) on ML_STAR Channel (1..8): 11111111, Optimized channel use: All sequence positions, Sequence: seq_current_plate, Sequence counting: (1) Automatic, Liquid class: As in first aspiration of cycle, Volume [µl]: g_NaOH_volume, Mix volume [µl]: *, Cycles: 0, Position relative to liquid surface: * mm, LLD settings: Off, Liquid following: On 3 return value(s) .
374	End Loop
375	Sequence: Set Current Position current position of sequence 'ML_STAR.LiqCar02_Pos05_NaOH' = '1'

C:\Program Files (x86)\HAMILTON\Methods\sFIDA Greiner PEG\sFIDA_Greiner_PEG.med

	_00001_NaOH
376	 1000µl Channel Dispense (Single Step) on ML_STAR Channel (1..8): 11111111, Optimized channel use: All sequence positions, Sequence: ML_STAR.LiqCar02_Pos05_NaOH, Sequence counting: (1) Automatic, Liquid class: As in first aspiration of cycle, Volume [µl]: Remaining volume inclusive blowout air, Mix volume [µl]: *, Cycles: 0, Position relative to liquid surface: * mm, LLD settings: On, Capacitive:5, Liquid following: On 3 return value(s) .
377	 End Loop - Reset sequence after loop: seq_current_plate
378	 1000µl Channel Tip Eject (Single Step) on ML_STAR Channel (1..8): 11111111, Optimized channel use: All sequence positions, Use default waste: On 3 return value(s) .
379	StrConcat2 of HSLStrLib g_WashProgramPath = StrConcat2(g_GeneralPathToWasherPrograms, "Greiner_Sector1_3times_Water_D.LHC")
380	

C:\Program Files (x86)\HAMILTON\Methods\sFIDA Greiner PEG\sFIDA_Greiner_PEG.med

	_00002_RemoveLiquidFromPlate
381	Comment <********** Remove liquid from plate **********>
382	Assignment 'g_progressText' = '"Remove Liquid from plate "'
383	AppendStatusText of HSLStatusWindow HSLStatusWindow::AppendStatusText(g_progressText)
384	1000µl Channel Tip Pick Up (Single Step) on ML_STAR Channel (1..8): 11111111, Optimized channel use: All sequence positions, Sequence: ML_STAR.MIStar1000ulHighVolumeTip, Sequence counting: (1) Automatic 3 return value(s)
385	Write2 of HSLTipCountingLib TipCount::Write2(ML_STAR.MIStar1000ulHighVolumeTip, "1000ulHighVolumeTip", ML_STAR)
386	Sequence: Set Current Position current position of sequence 'seq_current_plate' = '1'
387	Sequence: Set End Position end position of sequence 'seq_current_plate' = 'g_NumWells'
388	Assignment 'current_vol_in_tip' = '0'
389	Loop over following sequences: - seq_current_plate (Controlling), Adjust for '1' times consumption 'loopCounterOverPlateRemoveLiquid' used as loop counter variable
390	1000µl Channel Aspirate (Single Step) on ML_STAR Channel (1..8): 11111111, Optimized channel use: All sequence positions, Sequence: seq_current_plate, Sequence counting: (1) Automatic, Liquid class: "HighVolume_PBS_DispenseJet_Empty_Juelich", Volume [µl]: g_VolAspirateToEmptyWells, Mix volume [µl]: *, Cycles: 0, Position relative to liquid surface: * mm, LLD settings: Off, Liquid following: Off 3 return value(s)
391	Sequence: Set Current Position current position of sequence 'ML_STAR.LiqCar01_Pos01_LiquidWaste' = '1'
392	1000µl Channel Dispense (Single Step) on ML_STAR Channel (1..8): 11111111, Optimized channel use: All sequence positions, Sequence: ML_STAR.LiqCar01_Pos01_LiquidWaste, Sequence counting: (1) Automatic, Liquid class: As in first aspiration of cycle, Volume [µl]: Remaining volume inclusive blowout air, Mix volume [µl]: *, Cycles: 0, Position relative to liquid surface: * mm, LLD settings: On, Capacitive:5, Liquid following: Off 3 return value(s)
393	End Loop - Reset sequence after loop: seq_current_plate
394	1000µl Channel Tip Eject (Single Step) on ML_STAR Channel (1..8): 11111111, Optimized channel use: All sequence positions, Use default waste: On 3 return value(s)
395	

C:\Program Files (x86)\HAMILTON\Methods\sFIDA Greiner PEG\sFIDA_Greiner_PEG.med

	_00003_HCl
396	Comment <********** Distribute HCl on current plate **********>
397	Assignment 'g_progressText' = '"Add HCl to plate"'
398	AppendStatusText of HSLStatusWindow HSLStatusWindow::AppendStatusText(g_progressText)
399	1000µl Channel Tip Pick Up (Single Step) on ML_STAR Channel (1..8): 11111111, Optimized channel use: All sequence positions, Sequence: ML_STAR.MIStar1000ulHighVolumeTip, Sequence counting: (1) Automatic 3 return value(s) .
400	Write2 of HSLTipCountingLib TipCount::Write2(ML_STAR.MIStar1000ulHighVolumeTip, "1000ulHighVolumeTip", ML_STAR)
401	Assignment 'g_VolPreAliquot' = '100'
402	Assignment 'g_VolPostAliquot' = '100'
403	Assignment 'g_HCl_volume' = '100'
404	Sequence: Set Current Position current position of sequence 'seq_current_plate' = '1'
405	Sequence: Set End Position end position of sequence 'seq_current_plate' = 'g_NumWells'
406	Loop over following sequences: - seq_current_plate (Controlling), Adjust for '1' times consumption 'loopCounterOverPlateHCl' used as loop counter variable
407	CalcAliquote of Aliquot_with_EasySteps ALIQUOT_WITH_EASYSTEPS::CalcAliquote(seq_current_plate, g_HCl_volume, g_VolPreAliquot, g_VolPostAliquot, g_maxVolPerTip1000, g_VolAspirate, numDispenseSteps, 1, 8)
408	Sequence: Set Current Position current position of sequence 'ML_STAR.LiqCar02_Pos04_HCl' = '1'
409	1000µl Channel Aspirate (Single Step) on ML_STAR Channel (1..8): 11111111, Optimized channel use: All sequence positions, Sequence: ML_STAR.LiqCar02_Pos04_HCl, Sequence counting: (1) Automatic, Liquid class: "HighVolume_Water_AliquotDispenseJet_Part", Volume [µl]: g_VolAspirate, Mix volume [µl]: *, Cycles: 0, Position relative to liquid surface: * mm, LLD settings: On, Capacitive:5, Liquid following: On 3 return value(s) .
410	1000µl Channel Dispense (Single Step) on ML_STAR Channel (1..8): 11111111, Optimized channel use: All sequence positions, Sequence: ML_STAR.dummyGreinerPlate, Sequence counting: (1) Automatic, Liquid class: As in first aspiration of cycle, Volume [µl]: g_VolPreAliquot, Mix volume [µl]: *, Cycles: 0, Position relative to liquid surface: * mm, LLD settings: Off, Liquid following: On 3 return value(s) .
411	Loop 'numDispenseSteps' times 'loopNumDispenseSteps' used as loop counter variable
412	1000µl Channel Dispense (Single Step) on ML_STAR Channel (1..8): 11111111, Optimized channel use: All sequence positions, Sequence: seq_current_plate, Sequence counting: (1) Automatic, Liquid class: As in first aspiration of cycle, Volume [µl]: g_HCl_volume, Mix volume [µl]: *, Cycles: 0, Position relative to liquid surface: * mm, LLD settings: Off, Liquid following: On 3 return value(s) .
413	End Loop
414	Sequence: Set Current Position current position of sequence 'ML_STAR.LiqCar02_Pos04_HCl' = '1'

C:\Program Files (x86)\HAMILTON\Methods\sFIDA Greiner PEG\sFIDA_Greiner_PEG.med

	_00003_HCl
415	 1000µl Channel Dispense (Single Step) on ML_STAR Channel (1..8): 11111111, Optimized channel use: All sequence positions, Sequence: ML_STAR.LiqCar02_Pos04_HCl, Sequence counting: (1) Automatic, Liquid class: As in first aspiration of cycle, Volume [µl]: Remaining volume inclusive blowout air, Mix volume [µl]: *, Cycles: 0, Position relative to liquid surface: * mm, LLD settings: On, Capacitive:5, Liquid following: On 3 return value(s) .
416	 End Loop - Reset sequence after loop: seq_current_plate
417	 1000µl Channel Tip Eject (Single Step) on ML_STAR Channel (1..8): 11111111, Optimized channel use: All sequence positions, Use default waste: On 3 return value(s) .
418	StrConcat2 of HSLStrLib g_WashProgramPath = StrConcat2(g_GeneralPathToWasherPrograms, "Greiner_Sector1_3times_Water_D.LHC")
419	

C:\Program Files (x86)\HAMILTON\Methods\sFIDA Greiner PEG\sFIDA_Greiner_PEG.med

	_00004_WashEthanol
420	Comment <********** Wash current plate with ethanol **********>
421	1000µl Channel Tip Pick Up (Single Step) on ML_STAR Channel (1..8): 11111111, Optimized channel use: All sequence positions, Sequence: ML_STAR.MIStar1000ulHighVolumeTip, Sequence counting: (1) Automatic 3 return value(s)
422	Write2 of HSLTipCountingLib TipCount::Write2(ML_STAR.MIStar1000ulHighVolumeTip, "1000ulHighVolumeTip", ML_STAR)
423	Assignment 'g_progressText' = '"Wash ethanol: "'
424	AppendStatusText of HSLStatusWindow HSLStatusWindow::AppendStatusText(g_progressText)
425	Assignment 'g_VolPreAliquot' = '100'
426	Assignment 'g_VolPostAliquot' = '100'
427	Assignment 'g_wash_volume' = '100'
428	Sequence: Set End Position end position of sequence 'seq_current_plate' = 'g_NumWells'
429	Loop 'g_num_wash_steps_ethanol' times 'loopNumberWashStepsEthanol' used as loop counter variable
430	Sequence: Set Current Position current position of sequence 'seq_current_plate' = '1'
431	Assignment 'g_progressText' = '"Wash ethanol step: "'
432	StrConcat2 of HSLStrLib g_progressText = StrConcat2(g_progressText, loopNumberWashStepsEthanol)
433	AppendStatusText of HSLStatusWindow HSLStatusWindow::AppendStatusText(g_progressText)
434	Loop over following sequences: - seq_current_plate (Controlling), Adjust for '1' times consumption 'loopCounterOverPlateEthanol' used as loop counter variable
435	CalcAliquote of Aliquot_with_EasySteps ALIQUOT_WITH_EASYSTEPS::CalcAliquote(seq_current_plate, g_wash_volume, g_VolPreAliquot, g_VolPostAliquot, g_maxVolPerTip1000, g_VolAspirate, numDispenseSteps, 1, 8)
436	Sequence: Set Current Position current position of sequence 'ML_STAR.LiqCar01_Pos03_Ethanol' = '1'
437	1000µl Channel Aspirate (Single Step) on ML_STAR Channel (1..8): 11111111, Optimized channel use: All sequence positions, Sequence: ML_STAR.LiqCar01_Pos03_Ethanol, Sequence counting: (1) Automatic, Liquid class: "HighVolume_EtOH_DispenseJet_Part_Juelich", Volume [µl]: g_VolAspirate, Mix volume [µl]: *, Cycles: 0, Position relative to liquid surface: * mm, LLD settings: On, Capacitive:5, Liquid following: On 3 return value(s)
438	1000µl Channel Dispense (Single Step) on ML_STAR Channel (1..8): 11111111, Optimized channel use: All sequence positions, Sequence: ML_STAR.dummyGreinerPlate, Sequence counting: (1) Automatic, Liquid class: As in first aspiration of cycle, Volume [µl]: g_VolPreAliquot, Mix volume [µl]: *, Cycles: 0, Position relative to liquid surface: * mm, LLD settings: Off, Liquid following: On 3 return value(s)
439	Loop 'numDispenseSteps' times 'loopNumDispenseSteps' used as loop counter variable
442	Sequence: Set Current Position current position of sequence 'ML_STAR.LiqCar01_Pos01_LiquidWaste' = '1'

C:\Program Files (x86)\HAMILTON\Methods\sFIDA Greiner PEG\sFIDA_Greiner_PEG.med

	_00004_WashEthanol
443	1000µl Channel Dispense (Single Step) on ML_STAR Channel (1..8): 11111111, Optimized channel use: All sequence positions, Sequence: ML_STAR.LiqCar01_Pos01_LiquidWaste, Sequence counting: (1) Automatic, Liquid class: As in first aspiration of cycle, Volume [µl]: Remaining volume inclusive blowout air, Mix volume [µl]: *, Cycles: 0, Position relative to liquid surface: * mm, LLD settings: On, Capacitive:5, Liquid following: On 3 return value(s) .
444	End Loop - Reset sequence after loop: seq_current_plate
445	Sequence: Set Current Position current position of sequence 'seq_current_plate' = '1'
446	Assignment 'current_vol_in_tip' = '0'
447	Loop over following sequences: - seq_current_plate (Controlling), Adjust for '1' times consumption 'loopOverPlateToWash' used as loop counter variable
448	1000µl Channel Aspirate (Single Step) on ML_STAR Channel (1..8): 11111111, Optimized channel use: All sequence positions, Sequence: seq_current_plate, Sequence counting: (1) Automatic, Liquid class: "HighVolume_EtOH_DispenseJet_Empty", Volume [µl]: g_VolAspirateToEmptyWells, Mix volume [µl]: *, Cycles: 0, Position relative to liquid surface: * mm, LLD settings: Off, Liquid following: Off 3 return value(s) .
449	Sequence: Set Current Position current position of sequence 'ML_STAR.LiqCar01_Pos01_LiquidWaste' = '1'
450	1000µl Channel Dispense (Single Step) on ML_STAR Channel (1..8): 11111111, Optimized channel use: All sequence positions, Sequence: ML_STAR.LiqCar01_Pos01_LiquidWaste, Sequence counting: (1) Automatic, Liquid class: As in first aspiration of cycle, Volume [µl]: Remaining volume inclusive blowout air, Mix volume [µl]: *, Cycles: 0, Position relative to liquid surface: * mm, LLD settings: On, Capacitive:5, Liquid following: On 3 return value(s) .
451	End Loop - Reset sequence after loop: seq_current_plate
452	End Loop
453	1000µl Channel Tip Eject (Single Step) on ML_STAR Channel (1..8): 11111111, Optimized channel use: All sequence positions, Use default waste: On 3 return value(s) .
454	

C:\Program Files (x86)\HAMILTON\Methods\sFIDA Greiner PEG\sFIDA_Greiner_PEG.med

	_00005_Ethanolamine
455	Comment <********** Distribute Ethanolamine on current plate **********>
456	Assignment 'g_progressText' = '"Add Ethanolamine to plate"'
457	AppendStatusText of HSLStatusWindow HSLStatusWindow::AppendStatusText(g_progressText)
458	1000µl Channel Tip Pick Up (Single Step) on ML_STAR Channel (1..8): 11111111, Optimized channel use: All sequence positions, Sequence: ML_STAR.MIStar1000ulHighVolumeTip, Sequence counting: (1) Automatic 3 return value(s) .
459	Write2 of HSLTipCountingLib TipCount::Write2(ML_STAR.MIStar1000ulHighVolumeTip, "1000ulHighVolumeTip", ML_STAR)
460	Assignment 'g_VolPreAliquot' = '45'
461	Assignment 'g_VolPostAliquot' = '100'
462	Assignment 'g_Ethanolamine_volume' = '45'
463	Sequence: Set Current Position current position of sequence 'seq_current_plate' = '1'
464	Sequence: Set End Position end position of sequence 'seq_current_plate' = 'g_NumWells'
465	Loop over following sequences: - seq_current_plate (Controlling), Adjust for '1' times consumption 'loopCounterOverPlateEthanolamine' used as loop counter variable
466	CalcAliquote of Aliquot_with_EasySteps ALIQUOT_WITH_EASYSTEPS::CalcAliquote(seq_current_plate, g_Ethanolamine_volume, g_VolPreAliquot, g_VolPostAliquot, g_maxVolPerTip1000, g_VolAspirate, numDispenseSteps, 1, 8)
467	Sequence: Set Current Position current position of sequence 'seq_source_ethanolamine' = 'g_startPositionEthanolamine'
468	1000µl Channel Aspirate (Single Step) on ML_STAR Channel (1..8): 11111111, Optimized channel use: All sequence positions, Sequence: seq_source_ethanolamine, Sequence counting: (1) Automatic, Liquid class: "HighVolume_DMSO_DispenseJet_Part_sFIDA_Juelich", Volume [µl]: g_VolAspirate, Mix volume [µl]: *, Cycles: 0, Position relative to liquid surface: * mm, LLD settings: Off, Liquid following: Off 3 return value(s) .
469	1000µl Channel Dispense (Single Step) on ML_STAR Channel (1..8): 11111111, Optimized channel use: All sequence positions, Sequence: ML_STAR.dummyGreinerPlate, Sequence counting: (1) Automatic, Liquid class: As in first aspiration of cycle, Volume [µl]: g_VolPreAliquot, Mix volume [µl]: *, Cycles: 0, Position relative to liquid surface: * mm, LLD settings: Off, Liquid following: On 3 return value(s) .
470	Loop 'numDispenseSteps' times 'loopNumDispenseSteps' used as loop counter variable
471	1000µl Channel Dispense (Single Step) on ML_STAR Channel (1..8): 11111111, Optimized channel use: All sequence positions, Sequence: seq_current_plate, Sequence counting: (1) Automatic, Liquid class: As in first aspiration of cycle, Volume [µl]: g_Ethanolamine_volume, Mix volume [µl]: *, Cycles: 0, Position relative to liquid surface: * mm, LLD settings: Off, Liquid following: On 3 return value(s) .
472	End Loop
473	Sequence: Set Current Position current position of sequence 'seq_source_ethanolamine' = 'g_startPositionEthanolamine'

C:\Program Files (x86)\HAMILTON\Methods\sFIDA Greiner PEG\sFIDA_Greiner_PEG.med

	_00005_Ethanolamine
474	 1000µl Channel Dispense (Single Step) on ML_STAR Channel (1..8): 11111111, Optimized channel use: All sequence positions, Sequence: seq_source_ethanolamine, Sequence counting: (1) Automatic, Liquid class: As in first aspiration of cycle, Volume [µl]: Remaining volume inclusive blowout air, Mix volume [µl]: *, Cycles: 0, Position relative to liquid surface: * mm, LLD settings: On, Capacitive:5, Liquid following: On 3 return value(s) .
475	 End Loop - Reset sequence after loop: seq_current_plate
476	 1000µl Channel Tip Eject (Single Step) on ML_STAR Channel (1..8): 11111111, Optimized channel use: All sequence positions, Use default waste: On 3 return value(s) .
477	StrConcat2 of HSLStrLib g_WashProgramPath = StrConcat2(g_GeneralPathToWasherPrograms, "Greiner_Sector1_3times_Water_D.LHC")
478	

C:\Program Files (x86)\HAMILTON\Methods\sFIDA Greiner PEG\sFIDA_Greiner_PEG.med

	_00006_WashDMSO
479	Comment <********** Wash current plate with DMSO **********>
480	1000µl Channel Tip Pick Up (Single Step) on ML_STAR Channel (1..8): 11111111, Optimized channel use: All sequence positions, Sequence: ML_STAR.MIStar1000ulHighVolumeTip, Sequence counting: (1) Automatic 3 return value(s) .
481	Write2 of HSLTipCountingLib TipCount::Write2(ML_STAR.MIStar1000ulHighVolumeTip, "1000ulHighVolumeTip", ML_STAR)
482	Assignment 'g_VolPreAliquot' = '100'
483	Assignment 'g_VolPostAliquot' = '100'
484	Assignment 'g_wash_volume' = '100'
485	Sequence: Set End Position end position of sequence 'seq_current_plate' = 'g_NumWells'
486	Loop 'g_num_wash_steps_DMSO' times 'loopNumberWashStepsDMSO' used as loop counter variable
487	Sequence: Set Current Position current position of sequence 'seq_current_plate' = '1'
488	Assignment 'g_progressText' = '"Wash DMSO "'
489	StrConcat2 of HSLStrLib g_progressText = StrConcat2(g_progressText, loopNumberWashStepsDMSO)
490	AppendStatusText of HSLStatusWindow HSLStatusWindow::AppendStatusText(g_progressText)
491	Loop over following sequences: - seq_current_plate (Controlling), Adjust for '1' times consumption 'loopCounterOverPlateDMSO' used as loop counter variable
492	CalcAliquote of Aliquot_with_EasySteps ALIQUOT_WITH_EASYSTEPS::CalcAliquote(seq_current_plate, g_wash_volume, g_VolPreAliquot, g_VolPostAliquot, g_maxVolPerTip1000, g_VolAspirate, numDispenseSteps, 1, 8)
493	Sequence: Set Current Position current position of sequence 'ML_STAR.LiqCar02_Pos03_DMSO' = '1'
494	1000µl Channel Aspirate (Single Step) on ML_STAR Channel (1..8): 11111111, Optimized channel use: All sequence positions, Sequence: ML_STAR.LiqCar02_Pos03_DMSO, Sequence counting: (1) Automatic, Liquid class: "HighVolume_DMSO_DispenseJet_Part_sFIDA_Juelich", Volume [µl]: g_VolAspirate, Mix volume [µl]: *, Cycles: 0, Position relative to liquid surface: * mm, LLD settings: On, Capacitive:5, Liquid following: On 3 return value(s) .
495	1000µl Channel Dispense (Single Step) on ML_STAR Channel (1..8): 11111111, Optimized channel use: All sequence positions, Sequence: ML_STAR.dummyGreinerPlate, Sequence counting: (1) Automatic, Liquid class: As in first aspiration of cycle, Volume [µl]: g_VolPreAliquot, Mix volume [µl]: *, Cycles: 0, Position relative to liquid surface: * mm, LLD settings: Off, Liquid following: On 3 return value(s) .
496	Loop 'numDispenseSteps' times 'loopNumDispenseSteps' used as loop counter variable
499	Sequence: Set Current Position current position of sequence 'ML_STAR.LiqCar01_Pos01_LiquidWaste' = '1'

C:\Program Files (x86)\HAMILTON\Methods\sFIDA Greiner PEG\sFIDA_Greiner_PEG.med

	_00006_WashDMSO
500	1000µl Channel Dispense (Single Step) on ML_STAR Channel (1..8): 11111111, Optimized channel use: All sequence positions, Sequence: ML_STAR.LiqCar01_Pos01_LiquidWaste, Sequence counting: (1) Automatic, Liquid class: As in first aspiration of cycle, Volume [µl]: Remaining volume inclusive blowout air, Mix volume [µl]: *, Cycles: 0, Position relative to liquid surface: * mm, LLD settings: On, Capacitive:5, Liquid following: On 3 return value(s) .
501	End Loop - Reset sequence after loop: seq_current_plate
502	Sequence: Set Current Position current position of sequence 'seq_current_plate' = '1'
503	Assignment 'current_vol_in_tip' = '0'
504	Loop over following sequences: - seq_current_plate (Controlling), Adjust for '1' times consumption 'loopOverPlateToWash' used as loop counter variable
505	1000µl Channel Aspirate (Single Step) on ML_STAR Channel (1..8): 11111111, Optimized channel use: All sequence positions, Sequence: seq_current_plate, Sequence counting: (1) Automatic, Liquid class: "HighVolume_DMSO_DispenseJet_Empty_Juelich", Volume [µl]: g_VolAspirateToEmptyWells, Mix volume [µl]: *, Cycles: 0, Position relative to liquid surface: * mm, LLD settings: Off, Liquid following: Off 3 return value(s) .
506	Sequence: Set Current Position current position of sequence 'ML_STAR.LiqCar01_Pos01_LiquidWaste' = '1'
507	1000µl Channel Dispense (Single Step) on ML_STAR Channel (1..8): 11111111, Optimized channel use: All sequence positions, Sequence: ML_STAR.LiqCar01_Pos01_LiquidWaste, Sequence counting: (1) Automatic, Liquid class: As in first aspiration of cycle, Volume [µl]: Remaining volume inclusive blowout air, Mix volume [µl]: *, Cycles: 0, Position relative to liquid surface: * mm, LLD settings: On, Capacitive:5, Liquid following: On 3 return value(s) .
508	End Loop - Reset sequence after loop: seq_current_plate
509	End Loop
510	1000µl Channel Tip Eject (Single Step) on ML_STAR Channel (1..8): 11111111, Optimized channel use: All sequence positions, Use default waste: On 3 return value(s) .
511	

C:\Program Files (x86)\HAMILTON\Methods\sFIDA Greiner PEG\sFIDA_Greiner_PEG.med

	_00007_SpacerCoating
512	Comment <********** Distribution of spacer NHS-PEG-COOH on plate **********>
513	Assignment 'g_progressText' = '"Distribution of spacer NHS-PEG-COOH on plate"'
514	AppendStatusText of HSLStatusWindow HSLStatusWindow::AppendStatusText(g_progressText)
515	1000µl Channel Tip Pick Up (Single Step) on ML_STAR Channel (1..8): 11111111, Optimized channel use: All sequence positions, Sequence: ML_STAR.MIStar300ulStandardVolumeTip, Sequence counting: (1) Automatic 3 return value(s) .
516	Write2 of HSLTipCountingLib TipCount::Write2(ML_STAR.MIStar300ulStandardVolumeTip, "300ulStandardVolumeTip",
517	Assignment 'g_Volgeneral' = 'g_VolCapture'
518	Assignment 'g_VolPreAliquot' = 'g_VolCapture'
519	Assignment 'g_VolPostAliquot' = '30'
520	Sequence: Set Current Position current position of sequence 'seq_current_plate' = '1'
521	Sequence: Set End Position end position of sequence 'seq_current_plate' = 'g_NumWells'
522	Loop over following sequences: - seq_current_plate (Controlling), Adjust for '1' times consumption 'loopAspirate' used as loop counter variable
523	CalcAliquote of Aliquot_with_EasySteps ALIQUOT_WITH_EASYSTEPS::CalcAliquote(seq_current_plate, g_Volgeneral, g_VolPreAliquot, g_VolPostAliquot, g_maxVolPerTip300, g_VolAspirate, numDispenseSteps, 1, 8)
524	If, Else (loopAspirate is equal to 1)
525	Sequence: Set Current Position current position of sequence 'seq_source_spacer_PEG' = 'g_startPositionPEGSpacer'
526	1000µl Channel Aspirate (Single Step) on ML_STAR Channel (1..8): 11111111, Optimized channel use: All sequence positions, Sequence: seq_source_spacer_PEG, Sequence counting: (1) Automatic, Liquid class: "StandardVolume_PBS_DispenseJet_Empty_Juelich", Volume [µl]: 0, Mix volume [µl]: *, Cycles: 0, Position relative to liquid surface: * mm, LLD settings: On, Capacitive:5, Liquid following: On 3 return value(s) .
527	_0015_CheckLiquidLevel of sFIDA_Greiner_PEG _0015_CheckLiquidLevel()
528	End If
529	Sequence: Set Current Position current position of sequence 'seq_source_spacer_PEG' = 'g_startPositionPEGSpacer'
530	1000µl Channel Aspirate (Single Step) on ML_STAR Channel (1..8): 11111111, Optimized channel use: All sequence positions, Sequence: seq_source_spacer_PEG, Sequence counting: (1) Automatic, Liquid class: "StandardVolume_PBSLowVolume_DispenseJet_Part_Juelich_230714", Volume [µl]: g_VolAspirate, Mix volume [µl]: *, Cycles: 0, Position relative to liquid surface: * mm, LLD settings: Off, Liquid following: Off 3 return value(s) .

C:\Program Files (x86)\HAMILTON\Methods\sFIDA Greiner PEG\sFIDA_Greiner_PEG.med

	_00007_SpacerCoating
531	1000µl Channel Dispense (Single Step) on ML_STAR Channel (1..8): 11111111, Optimized channel use: All sequence positions, Sequence: ML_STAR.dummyGreinerPlate, Sequence counting: (1) Automatic, Liquid class: As in first aspiration of cycle, Volume [µl]: g_VolPreAliquot, Mix volume [µl]: *, Cycles: 0, Position relative to liquid surface: * mm, LLD settings: Off, Liquid following: Off 3 return value(s)
532	Loop 'numDispenseSteps' times 'loopDispense' used as loop counter variable
533	1000µl Channel Dispense (Single Step) on ML_STAR Channel (1..8): 11111111, Optimized channel use: All sequence positions, Sequence: seq_current_plate, Sequence counting: (1) Automatic, Liquid class: As in first aspiration of cycle, Volume [µl]: g_Volgeneral, Mix volume [µl]: *, Cycles: 0, Position relative to liquid surface: * mm, LLD settings: Off, Liquid following: Off 3 return value(s) .
534	End Loop
535	If, Else (g_VolPostAliquot is greater than 0)
536	Sequence: Set Current Position current position of sequence 'seq_source_spacer_PEG' = 'g_startPositionPEGSpacer'
537	1000µl Channel Dispense (Single Step) on ML_STAR Channel (1..8): 11111111, Optimized channel use: All sequence positions, Sequence: seq_source_spacer_PEG, Sequence counting: (1) Automatic, Liquid class: As in first aspiration of cycle, Volume [µl]: Remaining volume inclusive blowout air, Mix volume [µl]: *, Cycles: 0, Position relative to liquid surface: * mm, LLD settings: Off, Liquid following: On 3 return value(s) .
538	End If
539	End Loop - Reset sequence after loop: seq_current_plate
540	1000µl Channel Tip Eject (Single Step) on ML_STAR Channel (1..8): 11111111, Optimized channel use: All sequence positions, Use default waste: On 3 return value(s) .
541	StrConcat2 of HSLStrLib g_WashProgramPath = StrConcat2(g_GeneralPathToWasherPrograms, "Greiner_Sector1_3times_Water_D.LHC")
542	

C:\Program Files (x86)\HAMILTON\Methods\sFIDA Greiner PEG\sFIDA_Greiner_PEG.med

	_00008_ActivateSurface
543	Comment <********** Distribute EDC and NHS activation **********>
544	Assignment 'g_progressText' = '"Distribute EDC and NHS activation"'
545	AppendStatusText of HSLStatusWindow HSLStatusWindow::AppendStatusText(g_progressText)
546	1000µl Channel Tip Pick Up (Single Step) on ML_STAR Channel (1..8): 11111111, Optimized channel use: All sequence positions, Sequence: ML_STAR.MIStar1000ulHighVolumeTip, Sequence counting: (1) Automatic 3 return value(s) .
547	Write2 of HSLTipCountingLib TipCount::Write2(ML_STAR.MIStar1000ulHighVolumeTip, "1000ulHighVolumeTip", ML_STAR)
548	Assignment 'g_DispenseHeightEppi2ml' = '30'
549	Assignment 'g_Volgeneral' = '30'
550	Assignment 'g_VolPreAliquot' = 'g_Volgeneral'
551	Assignment 'g_VolPostAliquot' = '50'
552	Sequence: Set Current Position current position of sequence 'seq_current_plate' = '1'
553	Sequence: Set End Position end position of sequence 'seq_current_plate' = 'g_NumWells'
554	Loop over following sequences: - seq_current_plate (Controlling), Adjust for '1' times consumption 'loopAspirate' used as loop counter variable
555	CalcAliquote of Aliquot_with_EasySteps ALIQUOT_WITH_EASYSTEPS::CalcAliquote(seq_current_plate, g_Volgeneral, g_VolPreAliquot, g_VolPostAliquot, g_maxVolPerTip1000, g_VolAspirate, numDispenseSteps, 1, 8)
556	If, Else (loopAspirate is equal to 1)
557	Sequence: Set Current Position current position of sequence 'seq_source_EDC_NHS_Cap' = 'g_startPositionEDCNHSActivation'
558	1000µl Channel Aspirate (Single Step) on ML_STAR Channel (1..8): 11111111, Optimized channel use: All sequence positions, Sequence: seq_source_EDC_NHS_Cap, Sequence counting: (1) Automatic, Liquid class: "HighVolume_PBS_DispenseJet_Empty_Juelich", Volume [µl]: 0, Mix volume [µl]: *, Cycles: 0, Position relative to liquid surface: * mm, LLD settings: On, Capacitive:5, Liquid following: On 3 return value(s) .
559	_0015_CheckLiquidLevel of sFIDA_Greiner_PEG _0015_CheckLiquidLevel()
560	End If
561	Sequence: Set Current Position current position of sequence 'seq_source_EDC_NHS_Cap' = 'g_startPositionEDCNHSActivation'
562	1000µl Channel Aspirate (Single Step) on ML_STAR Channel (1..8): 11111111, Optimized channel use: All sequence positions, Sequence: seq_source_EDC_NHS_Cap, Sequence counting: (1) Automatic, Liquid class: "HighVolume_PBS_DispenseJet_Part_Juelich_230714", Volume [µl]: g_VolAspirate, Mix volume [µl]: *, Cycles: 0, Position relative to liquid surface: * mm, LLD settings: Off, Liquid following: Off 3 return value(s)

C:\Program Files (x86)\HAMILTON\Methods\sFIDA Greiner PEG\sFIDA_Greiner_PEG.med

	_00008_ActivateSurface
563	1000µl Channel Dispense (Single Step) on ML_STAR Channel (1..8): 11111111, Optimized channel use: All sequence positions, Sequence: ML_STAR.dummyGreinerPlate, Sequence counting: (1) Automatic, Liquid class: As in first aspiration of cycle, Volume [µl]: g_VolPreAliquot, Mix volume [µl]: *, Cycles: 0, Position relative to liquid surface: * mm, LLD settings: Off, Liquid following: Off 3 return value(s)
564	Loop 'numDispenseSteps' times 'loopDispense' used as loop counter variable
565	1000µl Channel Dispense (Single Step) on ML_STAR Channel (1..8): 11111111, Optimized channel use: All sequence positions, Sequence: seq_current_plate, Sequence counting: (1) Automatic, Liquid class: As in first aspiration of cycle, Volume [µl]: g_Volgeneral, Mix volume [µl]: *, Cycles: 0, Position relative to liquid surface: * mm, LLD settings: Off, Liquid following: Off 3 return value(s) .
566	End Loop
567	If, Else (g_VolPostAliquot is greater than 0)
568	Sequence: Set Current Position current position of sequence 'seq_source_EDC_NHS_Cap' = 'g_startPositionEDCNHSActivation'
569	1000µl Channel Dispense (Single Step) on ML_STAR Channel (1..8): 11111111, Optimized channel use: All sequence positions, Sequence: seq_source_EDC_NHS_Cap, Sequence counting: (1) Automatic, Liquid class: As in first aspiration of cycle, Volume [µl]: Remaining volume inclusive blowout air, Mix volume [µl]: *, Cycles: 0, Position relative to liquid surface: * mm, LLD settings: Off, Liquid following: On 3 return value(s) .
570	End If
571	End Loop - Reset sequence after loop: seq_current_plate
572	1000µl Channel Tip Eject (Single Step) on ML_STAR Channel (1..8): 11111111, Optimized channel use: All sequence positions, Use default waste: On 3 return value(s) .
573	StrConcat2 of HSLStrLib g_WashProgramPath = StrConcat2(g_GeneralPathToWasherPrograms, "Greiner_Sector1_3times_MES_A.LHC")
574	Assignment 'g_DispenseHeightEppi2ml' = '15'
575	

C:\Program Files (x86)\HAMILTON\Methods\sFIDA Greiner PEG\sFIDA_Greiner_PEG.med

	_00009_CaptureAB
576	Comment <********** Distribute capture antibody **********>
577	Assignment 'g_progressText' = '"Distribute capture antibody"'
578	AppendStatusText of HSLStatusWindow HSLStatusWindow::AppendStatusText(g_progressText)
579	Assignment 'g_endDialogErrorString' = '"Method: 0004 capture AB"'
580	1000µl Channel Tip Pick Up (Single Step) on ML_STAR Channel (1..8): 11111111, Optimized channel use: All sequence positions, Sequence: ML_STAR.MIStar300ulStandardVolumeTip, Sequence counting: (1) Automatic 3 return value(s)
581	Write2 of HSLTipCountingLib TipCount::Write2(ML_STAR.MIStar300ulStandardVolumeTip, "300ulStandardVolumeTip",
582	Assignment 'g_VolPreAliquot' = 'g_VolCapture'
583	Assignment 'g_VolPostAliquot' = '30'
584	Sequence: Set Current Position current position of sequence 'seq_current_plate' = '1'
585	Sequence: Set End Position end position of sequence 'seq_current_plate' = 'g_NumWells'
586	Loop over following sequences: - seq_current_plate (Controlling), Adjust for '1' times consumption 'loopAspirate' used as loop counter variable
587	CalcAliquote of Aliquot_with_EasySteps ALIQUOT_WITH_EASYSTEPS::CalcAliquote(seq_current_plate, g_VolCapture, g_VolPreAliquot, g_VolPostAliquot, g_maxVolPerTip300, g_VolAspirate, numDispenseSteps, 1, 8)
588	Comment <********** aspirate capture in eppi **********>
589	Assignment 'loopChannels' = '0'
590	If, Else (loopAspirate is equal to 1)
591	Sequence: Set Current Position current position of sequence 'seq_capture_source' = 'g_startPositionCapture'
592	1000µl Channel Aspirate (Single Step) on ML_STAR Channel (1..8): 11111111, Optimized channel use: All sequence positions, Sequence: seq_capture_source, Sequence counting: (1) Automatic, Liquid class: "StandardVolume_PBS_DispenseJet_Empty_Juelich", Volume [µl]: 0, Mix volume [µl]: *, Cycles: 0, Position relative to liquid surface: * mm, LLD settings: On, Capacitive:5, Liquid following: On 3 return value(s)
593	_0015_CheckLiquidLevel of sFIDA_Greiner_PEG _0015_CheckLiquidLevel()
594	End If
595	Sequence: Set Current Position current position of sequence 'seq_capture_source' = 'g_startPositionCapture'

C:\Program Files (x86)\HAMILTON\Methods\sFIDA Greiner PEG\sFIDA_Greiner_PEG.med

	_00009_CaptureAB
596	1000µl Channel Aspirate (Single Step) on ML_STAR Channel (1..8): 11111111, Optimized channel use: All sequence positions, Sequence: seq_capture_source, Sequence counting: (1) Automatic, Liquid class: "StandardVolume_PBSLowVolume_DispenseJet_Part_Juelich_230714", Volume [µl]: g_VolAspirate, Mix volume [µl]: *, Cycles: 0, Position relative to liquid surface: * mm, LLD settings: Off, Liquid following: Off 3 return value(s) .
597	1000µl Channel Dispense (Single Step) on ML_STAR Channel (1..8): 11111111, Optimized channel use: All sequence positions, Sequence: ML_STAR.dummyGreinerPlate, Sequence counting: (1) Automatic, Liquid class: As in first aspiration of cycle, Volume [µl]: g_VolPreAliquot, Mix volume [µl]: *, Cycles: 0, Position relative to liquid surface: * mm, LLD settings: Off, Liquid following: Off 3 return value(s) .
598	Loop 'numDispenseSteps' times 'loopDispense' used as loop counter variable
599	1000µl Channel Dispense (Single Step) on ML_STAR Channel (1..8): 11111111, Optimized channel use: All sequence positions, Sequence: seq_current_plate, Sequence counting: (1) Automatic, Liquid class: As in first aspiration of cycle, Volume [µl]: g_VolCapture, Mix volume [µl]: *, Cycles: 0, Position relative to liquid surface: * mm, LLD settings: Off, Liquid following: Off 3 return value(s) .
600	End Loop
601	If, Else (g_VolPostAliquot is greater than 0)
602	Sequence: Set Current Position current position of sequence 'seq_capture_source' = 'g_startPositionCapture'
603	1000µl Channel Dispense (Single Step) on ML_STAR Channel (1..8): 11111111, Optimized channel use: All sequence positions, Sequence: seq_capture_source, Sequence counting: (1) Automatic, Liquid class: As in first aspiration of cycle, Volume [µl]: Remaining volume inclusive blowout air, Mix volume [µl]: *, Cycles: 0, Position relative to liquid surface: * mm, LLD settings: Off, Liquid following: On 3 return value(s) .
604	End If
605	End Loop - Reset sequence after loop: seq_current_plate
606	1000µl Channel Tip Eject (Single Step) on ML_STAR Channel (1..8): 11111111, Optimized channel use: All sequence positions, Use default waste: On 3 return value(s) .
607	StrConcat2 of HSLStrLib g_WashProgramPath = StrConcat2(g_GeneralPathToWasherPrograms, "Greiner_Sector1_3times_PBST_C_3times_PBS_B.LHC")
608	

C:\Program Files (x86)\HAMILTON\Methods\sFIDA Greiner PEG\sFIDA_Greiner_PEG.med

	_00010_Blocking
609	Comment <********** Blocking **********>
610	Assignment 'g_progressText' = '"Blocking"'
611	AppendStatusText of HSLStatusWindow HSLStatusWindow::AppendStatusText(g_progressText)
612	Assignment 'g_endDialogErrorString' = '"Method: 0005 Blocking"'
613	1000µl Channel Tip Pick Up (Single Step) on ML_STAR Channel (1..8): 11111111, Optimized channel use: All sequence positions, Sequence: ML_STAR.MIStar1000ulHighVolumeTip, Sequence counting: (1) Automatic 3 return value(s)
614	Write2 of HSLTipCountingLib TipCount::Write2(ML_STAR.MIStar1000ulHighVolumeTip, "1000ulHighVolumeTip", ML_STAR)
615	Assignment 'g_Volgeneral' = '50'
616	Assignment 'g_VolPreAliquot' = 'g_Volgeneral'
617	Assignment 'g_VolPostAliquot' = '70'
618	Sequence: Set Current Position current position of sequence 'seq_current_plate' = '1'
619	Sequence: Set End Position end position of sequence 'seq_current_plate' = 'g_NumWells'
620	Loop over following sequences: - seq_current_plate (Controlling), Adjust for '1' times consumption 'loopAspirate' used as loop counter variable
621	CalcAliquote of Aliquot_with_EasySteps ALIQUOT_WITH_EASYSTEPS::CalcAliquote(seq_current_plate, g_Volgeneral, g_VolPreAliquot, g_VolPostAliquot, g_maxVolPerTip1000, g_VolAspirate, numDispenseSteps, 1, 8)
622	If, Else (loopAspirate is equal to 1)
623	Sequence: Set Current Position current position of sequence 'seq_source_blocking' = 'g_startPositionBlocking'
624	1000µl Channel Aspirate (Single Step) on ML_STAR Channel (1..8): 11111111, Optimized channel use: All sequence positions, Sequence: seq_source_blocking, Sequence counting: (1) Automatic, Liquid class: "HighVolume_PBS_DispenseJet_Empty_Juelich", Volume [µl]: 0, Mix volume [µl]: *, Cycles: 0, Position relative to liquid surface: * mm, LLD settings: On, Capacitive:5, Liquid following: On 3 return value(s)
625	_0015_CheckLiquidLevel of sFIDA_Greiner_PEG _0015_CheckLiquidLevel()
626	End If
627	Sequence: Set Current Position current position of sequence 'seq_source_blocking' = 'g_startPositionBlocking'
628	1000µl Channel Aspirate (Single Step) on ML_STAR Channel (1..8): 11111111, Optimized channel use: All sequence positions, Sequence: seq_source_blocking, Sequence counting: (1) Automatic, Liquid class: "HighVolume_PBS_DispenseJet_Part_Juelich_230714", Volume [µl]: g_VolAspirate, Mix volume [µl]: *, Cycles: 0, Position relative to liquid surface: * mm, LLD settings: Off, Liquid following: Off 3 return value(s)

C:\Program Files (x86)\HAMILTON\Methods\sFIDA Greiner PEG\sFIDA_Greiner_PEG.med

	_00010_Blocking
629	1000µl Channel Dispense (Single Step) on ML_STAR Channel (1..8): 11111111, Optimized channel use: All sequence positions, Sequence: ML_STAR.dummyGreinerPlate, Sequence counting: (1) Automatic, Liquid class: As in first aspiration of cycle, Volume [µl]: g_VolPreAliquot, Mix volume [µl]: *, Cycles: 0, Position relative to liquid surface: * mm, LLD settings: Off, Liquid following: Off 3 return value(s)
630	Loop 'numDispenseSteps' times 'loopDispense' used as loop counter variable
631	1000µl Channel Dispense (Single Step) on ML_STAR Channel (1..8): 11111111, Optimized channel use: All sequence positions, Sequence: seq_current_plate, Sequence counting: (1) Automatic, Liquid class: As in first aspiration of cycle, Volume [µl]: g_Volgeneral, Mix volume [µl]: *, Cycles: 0, Position relative to liquid surface: * mm, LLD settings: Off, Liquid following: Off 3 return value(s) .
632	End Loop
633	If, Else (g_VolPostAliquot is greater than 0)
634	Sequence: Set Current Position current position of sequence 'seq_source_blocking' = 'g_startPositionBlocking'
635	1000µl Channel Dispense (Single Step) on ML_STAR Channel (1..8): 11111111, Optimized channel use: All sequence positions, Sequence: seq_source_blocking, Sequence counting: (1) Automatic, Liquid class: As in first aspiration of cycle, Volume [µl]: Remaining volume inclusive blowout air, Mix volume [µl]: *, Cycles: 0, Position relative to liquid surface: * mm, LLD settings: Off, Liquid following: Off 3 return value(s) .
636	End If
637	End Loop - Reset sequence after loop: seq_current_plate
638	1000µl Channel Tip Eject (Single Step) on ML_STAR Channel (1..8): 11111111, Optimized channel use: All sequence positions, Use default waste: On 3 return value(s) .
639	StrConcat2 of HSLStrLib g_WashProgramPath = StrConcat2(g_GeneralPathToWasherPrograms, "Greiner_Sector1_3times_PBST_C_3times_PBS_B_remainingVol50µl.LHC")
640	Assignment 'g_DispenseHeightEppi2ml' = '15'
641	

C:\Program Files (x86)\HAMILTON\Methods\sFIDA Greiner PEG\sFIDA_Greiner_PEG.med

	_00011_DiluteStandards
642	If, Else (g_NumStds is greater than 0)
643	Assignment 'g_progressText' = '"Prepare dilution of standards"'
644	AppendStatusText of HSLStatusWindow HSLStatusWindow::AppendStatusText(g_progressText)
645	Assignment 'g_endDialogErrorString' = '"Method: 007 Standard Dilution"'
646	Comment <********** Dilute Standard **********>
647	Assignment 'allDilutionsDone' = '0'
648	Assignment 'dilutionCounter' = '0'
649	Array: Get Size 'sizeDilSeries1' = size of array 'arr_StdMolDil1'.
650	Array: Get Size 'sizeDilSeries2' = size of array 'arr_StdMolDil2'.
651	Array: Get Size 'sizeDilSeries3' = size of array 'arr_StdMolDil3'.
652	Comment <********** Dispense buffer **********>
653	Loop 'g_NumStds' times 'loopNumStandards' used as loop counter variable
654	Assignment 'current_vol' = '0'
655	If, Else (loopNumStandards is equal to 1)
656	Comment <********** Distribute buffer for dilution series 1 **********>
657	Sequence: Set Current Position current position of sequence 'ML_STAR.LiqCar01_Pos02_PBS' = '1'
658	Assignment 'g_numChannelsToUse' = 'sizeDilSeries1'
659	_0012_DefineChannelsToUse of sFIDA_Greiner_PEG _0012_DefineChannelsToUse()
660	1000µl Channel Tip Pick Up (Single Step) on ML_STAR Channel (1..8): g_channelPattern, Optimized channel use: All sequence positions, Sequence: ML_STAR.MIStar1000ulHighVolumeTip, Sequence counting: (1) Automatic 3 return value(s) .
661	Write2 of HSLTipCountingLib TipCount::Write2(ML_STAR.MIStar1000ulHighVolumeTip, "1000ulHighVolumeTip", ML_STAR)
662	Loop 'sizeDilSeries1' times 'loopSizeDilSeries1' used as loop counter variable
663	Assignment 'g_singleChannelNum' = 'loopSizeDilSeries1'
664	_0013_UseOneSpecificChannel of sFIDA_Greiner_PEG _0013_UseOneSpecificChannel()

C:\Program Files (x86)\HAMILTON\Methods\sFIDA Greiner PEG\sFIDA_Greiner_PEG.med

	_00011_DiluteStandards
665	Array: Get At 'current_vol' = element from array 'arr_VolBufferDilSeries1' at the index [loopSizeDilSeries1].
666	1000µl Channel Aspirate (Single Step) on ML_STAR Channel (1..8): g_singleChannelPatter, Optimized channel use: All sequence positions, Sequence: ML_STAR.LiqCar01_Pos02_PBS, Sequence counting: (1) Automatic, Liquid class: "HighVolume_PBS_DispenseJet_Part_Juelich_Dilution_27112014" , Volume [µl]: current_vol, Mix volume [µl]: *, Cycles: 0, Position relative to liquid surface: * mm, LLD settings: On, Capacitive:5, Liquid following: On 3 return value(s) .
667	End Loop
668	1000µl Channel Dispense (Single Step) on ML_STAR Channel (1..8): g_channelPattern, Optimized channel use: All sequence positions, Sequence: ML_STAR.CoolCar01_Pos03_04_DilutionSeries1, Sequence counting: (1) Automatic, Liquid class: As in first aspiration of cycle, Volume [µl]: Remaining volume inclusive blowout air, Mix volume [µl]: *, Cycles: 0, Position relative to liquid surface: * mm, LLD settings: Off, Liquid following: Off 3 return value(s) .
669	End If
670	1000µl Channel Tip Eject (Single Step) on ML_STAR Channel (1..8): 11111111, Optimized channel use: All sequence positions, Use default waste: On 3 return value(s) .
671	If, Else (loopNumStandards is equal to 2)
672	Comment <********** Distribute buffer for dilution series 2 **********>
673	Sequence: Set Current Position current position of sequence 'ML_STAR.SmallReservoir_CSF_for_Dilution' = '1'
674	Sequence: Set Current Position current position of sequence 'ML_STAR.LiqCar01_Pos02_PBS' = '1'
675	Assignment 'g_numChannelsToUse' = 'sizeDilSeries2'
676	_0012_DefineChannelsToUse of sFIDA_Greiner_PEG _0012_DefineChannelsToUse()
677	1000µl Channel Tip Pick Up (Single Step) on ML_STAR Channel (1..8): g_channelPattern, Optimized channel use: All sequence positions, Sequence: ML_STAR.MlStar1000ulHighVolumeTip, Sequence counting: (1) Automatic 3 return value(s) .
678	Write2 of HSLTipCountingLib TipCount::Write2(ML_STAR.MlStar1000ulHighVolumeTip, "1000ulHighVolumeTip", ML_STAR)
679	If, Else (g_DiluteWithCSF is equal to 1)
680	Loop 'sizeDilSeries2' times 'loopSizeDilSeries2' used as loop counter variable
681	Assignment 'g_singleChannelNum' = 'loopSizeDilSeries2'
682	_0013_UseOneSpecificChannel of sFIDA_Greiner_PEG _0013_UseOneSpecificChannel()
683	Array: Get At 'current_vol' = element from array 'arr_VolBufferDilSeries2' at the index [loopSizeDilSeries2].

C:\Program Files (x86)\HAMILTON\Methods\sFIDA Greiner PEG\sFIDA_Greiner_PEG.med

	_00011_DiluteStandards
684	1000µl Channel Aspirate (Single Step) on ML_STAR Channel (1..8): g_singleChannelPatter, Optimized channel use: All sequence positions, Sequence: ML_STAR.SmallReservoir_CSF_for_Dilution, Sequence counting: (1) Automatic, Liquid class: "HighVolume_PBS_DispenseJet_Part_Juelich_Dilution_27 112014", Volume [µl]: current_vol, Mix volume [µl]: *, Cycles: 0, Position relative to liquid surface: * mm, LLD settings: On, Capacitive:5, Liquid following: On 3 return value(s) .
685	End Loop
686	Else
687	Loop 'sizeDilSeries2' times 'loopSizeDilSeries2' used as loop counter variable
688	Assignment 'g_singleChannelNum' = 'loopSizeDilSeries2'
689	_0013_UseOneSpecificChannel of sFIDA_Greiner_PEG _0013_UseOneSpecificChannel()
690	Array: Get At 'current_vol' = element from array 'arr_VolBufferDilSeries2' at the index [loopSizeDilSeries2]
691	1000µl Channel Aspirate (Single Step) on ML_STAR Channel (1..8): g_singleChannelPatter, Optimized channel use: All sequence positions, Sequence: ML_STAR.LiqCar01_Pos02_PBS, Sequence counting: (1) Automatic, Liquid class: "HighVolume_PBS_DispenseJet_Part_Juelich_Dilution_27 112014", Volume [µl]: current_vol, Mix volume [µl]: *, Cycles: 0, Position relative to liquid surface: * mm, LLD settings: On, Capacitive:5, Liquid following: On 3 return value(s) .
692	End Loop
693	End If
694	1000µl Channel Dispense (Single Step) on ML_STAR Channel (1..8): g_channelPattern, Optimized channel use: All sequence positions, Sequence: ML_STAR.CoolCar01_Pos03_04_DilutionSeries2, Sequence counting: (1) Automatic, Liquid class: As in first aspiration of cycle, Volume [µl]: Remaining volume inclusive blowout air, Mix volume [µl]: *, Cycles: 0, Position relative to liquid surface: * mm, LLD settings: Off, Liquid following: Off 3 return value(s) .
695	End If
696	1000µl Channel Tip Eject (Single Step) on ML_STAR Channel (1..8): 11111111, Optimized channel use: All sequence positions, Use default waste: On 3 return value(s) .
697	If, Else (loopNumStandards is equal to 3)
698	Sequence: Set Current Position current position of sequence 'ML_STAR.SmallReservoir_Plasma_for_dilution' = '1'
699	Sequence: Set Current Position current position of sequence 'ML_STAR.LiqCar01_Pos02_PBS' = '1'
700	Assignment 'g_numChannelsToUse' = 'sizeDilSeries3'
701	_0012_DefineChannelsToUse of sFIDA_Greiner_PEG _0012_DefineChannelsToUse()

C:\Program Files (x86)\HAMILTON\Methods\sFIDA Greiner PEG\sFIDA_Greiner_PEG.med

	_00011_DiluteStandards
702	1000µl Channel Tip Pick Up (Single Step) on ML_STAR Channel (1..8): g_channelPattern, Optimized channel use: All sequence positions, Sequence: ML_STAR.MIStar1000ulHighVolumeTip, Sequence counting: (1) Automatic 3 return value(s) .
703	Write2 of HSLTipCountingLib TipCount::Write2(ML_STAR.MIStar1000ulHighVolumeTip, "1000ulHighVolumeTip", ML_STAR)
704	If, Else (g_dilutionWithPlasma is equal to 1)
705	Loop 'sizeDilSeries3' times 'loopSizeDilSeries3' used as loop counter variable
706	Assignment 'g_singleChannelNum' = 'loopSizeDilSeries3'
707	_0013_UseOneSpecificChannel of sFIDA_Greiner_PEG _0013_UseOneSpecificChannel()
708	Array: Get At 'current_vol' = element from array 'arr_VolBufferDilSeries3' at the index [loopSizeDilSeries3].
709	1000µl Channel Aspirate (Single Step) on ML_STAR Channel (1..8): g_singleChannelPatter, Optimized channel use: All sequence positions, Sequence: ML_STAR.SmallReservoir_Plasma_for_dilution, Sequence counting: (1) Automatic, Liquid class: "HighVolume_PBS_DispenseJet_Part_Juelich_Dilution_27112014", Volume [µl]: current_vol, Mix volume [µl]: *, Cycles: 0, Position relative to liquid surface: * mm, LLD settings: On, Capacitive:5, Liquid following: On 3 return value(s) .
710	End Loop
711	Else
712	Loop 'sizeDilSeries3' times 'loopSizeDilSeries3' used as loop counter variable
713	Assignment 'g_singleChannelNum' = 'loopSizeDilSeries3'
714	_0013_UseOneSpecificChannel of sFIDA_Greiner_PEG _0013_UseOneSpecificChannel()
715	Array: Get At 'current_vol' = element from array 'arr_VolBufferDilSeries3' at the index [loopSizeDilSeries3].
716	1000µl Channel Aspirate (Single Step) on ML_STAR Channel (1..8): g_singleChannelPatter, Optimized channel use: All sequence positions, Sequence: ML_STAR.LiqCar01_Pos02_PBS, Sequence counting: (1) Automatic, Liquid class: "HighVolume_PBS_DispenseJet_Part_Juelich_Dilution_27112014", Volume [µl]: current_vol, Mix volume [µl]: *, Cycles: 0, Position relative to liquid surface: * mm, LLD settings: On, Capacitive:5, Liquid following: On 3 return value(s) .
717	End Loop
718	End If

C:\Program Files (x86)\HAMILTON\Methods\sFIDA Greiner PEG\sFIDA_Greiner_PEG.med

	_00011_DiluteStandards
719	1000µl Channel Dispense (Single Step) on ML_STAR Channel (1..8): g_channelPattern, Optimized channel use: All sequence positions, Sequence: ML_STAR.CoolCar01_Pos03_04_DilutionSeries3, Sequence counting: (1) Automatic, Liquid class: As in first aspiration of cycle, Volume [µl]: Remaining volume inclusive blowout air, Mix volume [µl]: *, Cycles: 0, Position relative to liquid surface: * mm, LLD settings: Off, Liquid following: Off 3 return value(s)
720	End If
721	1000µl Channel Tip Eject (Single Step) on ML_STAR Channel (1..8): 11111111, Optimized channel use: All sequence positions, Use default waste: On 3 return value(s)
722	End Loop
723	1000µl Channel Tip Eject (Single Step) on ML_STAR Channel (1..8): 11111111, Optimized channel use: All sequence positions, Use default waste: On 3 return value(s) .
724	Comment <********** Dilute standards **********>
725	Loop 'g_NumStds' times 'loopNumStandards' used as loop counter variable
726	Assignment 'current_vol' = '50'
727	If, Else (loopNumStandards is equal to 1)
728	Sequence: Set Current Position current position of sequence 'ML_STAR.CoolCar01_Pos03_04_DilutionSeries1' = '1'
729	Comment <********** Make dilution series 1 **********>
730	1000µl Channel Tip Pick Up (Single Step) on ML_STAR Channel (1..8): 10000000, Optimized channel use: All sequence positions, Sequence: ML_STAR.MIStar300ulStandardVolumeTip, Sequence counting: (1) Automatic 3 return value(s) .
731	Write2 of HSLTipCountingLib TipCount::Write2(ML_STAR.MIStar300ulStandardVolumeTip, "300ulStandardVolumeTip", ML_STAR)
732	Loop 'sizeDilSeries1' times 'loopDiluteSeries1' used as loop counter variable
733	If, Else (loopDiluteSeries1 is greater than sizeDilSeries1)
734	Loop: Break
735	End If
736	If, Else (loopDiluteSeries1 is equal to 1)
737	Array: Get At 'currentVol' = element from array 'arr_EndVolDilSeries1' at the index [loopDiluteSeries1].
738	Array: Get At 'current_vol' = element from array 'arr_VolBufferDilSeries1' at the index [loopDiluteSeries1].

C:\Program Files (x86)\HAMILTON\Methods\sFIDA Greiner PEG\sFIDA_Greiner_PEG.med

	_00011_DiluteStandards
739	Assignment 'g_VolToMix_Dilutions' = 'current_vol'
740	Array: Get At 'current_vol' = element from array 'arr_VolsDilSeries1' at the index [loopDiluteSeries1].
741	HSL code. g_VolToMix_Dilutions=(g_VolToMix_Dilutions+current_vol)/2;
742	1000µl Channel Aspirate (Single Step) on ML_STAR Channel (1..8): 10000000, Optimized channel use: All sequence positions, Sequence: ML_STAR.CoolCar01_Pos03_Eppi22_StandardStock01, Sequence counting: (1) Automatic, Liquid class: "StandardVolume_PBS_DispenseJet_Empty_Juelich", Volume [µl]: current_vol, Cycles: g_NumMixing_Dilutions, LLD settings: Off, Liquid following: Off 3 return value(s) .
743	1000µl Channel Dispense (Single Step) on ML_STAR Channel (1..8): 10000000, Optimized channel use: All sequence positions, Sequence: ML_STAR.CoolCar01_Pos03_04_DilutionSeries1, Sequence counting: (1) Automatic, Liquid class: As in first aspiration of cycle, Volume [µl]: Remaining volume inclusive blowout air, Cycles: g_NumMixing_Dilutions, LLD settings: Off, Liquid following: On 3 return value(s) .
744	Sequence: Get Current Position 'dilSeries1currentPos' = current position of sequence 'ML_STAR.CoolCar01_Pos03_04_DilutionSeries1'
745	Else
746	Array: Get At 'currentVol' = element from array 'arr_EndVolDilSeries1' at the index [loopDiluteSeries1].
747	Assignment with Calculation 'setPosDilSeries1' = 'dilSeries1currentPos' - '1'
748	Sequence: Set Current Position current position of sequence 'ML_STAR.CoolCar01_Pos03_04_DilutionSeries1' = 'setPosDilSeries1'
749	Array: Get At 'current_vol' = element from array 'arr_VolBufferDilSeries1' at the index [loopDiluteSeries1].
750	Assignment 'g_VolToMix_Dilutions' = 'current_vol'
751	Array: Get At 'current_vol' = element from array 'arr_VolsDilSeries1' at the index [loopDiluteSeries1].
752	HSL code. g_VolToMix_Dilutions=(g_VolToMix_Dilutions+current_vol)/2;
753	1000µl Channel Aspirate (Single Step) on ML_STAR Channel (1..8): 10000000, Optimized channel use: All sequence positions, Sequence: ML_STAR.CoolCar01_Pos03_04_DilutionSeries1, Sequence counting: (1) Automatic, Liquid class: "StandardVolume_PBS_DispenseJet_Empty_Juelich", Volume [µl]: 0, Cycles: g_NumMixing_Dilutions, LLD settings: On, Capacitive:5, Liquid following: On 3 return value(s) .
754	Sequence: Get Current Position 'dilSeries1currentPos' = current position of sequence 'ML_STAR.CoolCar01_Pos03_04_DilutionSeries1'

C:\Program Files (x86)\HAMILTON\Methods\sFIDA Greiner PEG\sFIDA_Greiner_PEG.med

	_00011_DiluteStandards
755	1000µl Channel Tip Eject (Single Step) on ML_STAR Channel (1..8): 11111111, Optimized channel use: All sequence positions, Use default waste: On 3 return value(s) .
756	1000µl Channel Tip Pick Up (Single Step) on ML_STAR Channel (1..8): 10000000, Optimized channel use: All sequence positions, Sequence: ML_STAR.MlStar300ulStandardVolumeTip, Sequence counting: (1) Automatic 3 return value(s) .
757	Write2 of HSLTipCountingLib TipCount::Write2(ML_STAR.MlStar300ulStandardVolumeTip, "300ulStandardVolumeTip", ML_STAR)
758	Assignment with Calculation 'setPosDilSeries1' = 'dilSeries1currentPos' - '1'
759	Sequence: Set Current Position current position of sequence 'ML_STAR.CoolCar01_Pos03_04_DilutionSeries1' = 'setPosDilSeries1'
760	1000µl Channel Aspirate (Single Step) on ML_STAR Channel (1..8): 10000000, Optimized channel use: All sequence positions, Sequence: ML_STAR.CoolCar01_Pos03_04_DilutionSeries1, Sequence counting: (1) Automatic, Liquid class: "StandardVolume_PBS_DispenseJet_Empty_Juelich", Volume [µl]: current_vol, Mix volume [µl]: *, Cycles: 0, Position relative to liquid surface: * mm, LLD settings: On, Capacitive:5, Liquid following: On 3 return value(s) .
761	1000µl Channel Dispense (Single Step) on ML_STAR Channel (1..8): 10000000, Optimized channel use: All sequence positions, Sequence: ML_STAR.CoolCar01_Pos03_04_DilutionSeries1, Sequence counting: (1) Automatic, Liquid class: As in first aspiration of cycle, Volume [µl]: Remaining volume inclusive blowout air, Mix volume [µl]: *, Cycles: 0, Position relative to liquid surface: * mm, LLD settings: Off, Liquid following: On
762	Sequence: Get Current Position 'dilSeries1currentPos' = current position of sequence 'ML_STAR.CoolCar01_Pos03_04_DilutionSeries1'
763	If, Else (loopDiluteSeries1 is equal to sizeDilSeries1)
764	Comment <***** Mix last eppi*******>
765	Assignment with Calculation 'setPosDilSeries1' = 'dilSeries1currentPos' - '1'
766	Sequence: Set Current Position current position of sequence 'ML_STAR.CoolCar01_Pos03_04_DilutionSeries1' = 'sizeDilSeries1'
767	1000µl Channel Aspirate (Single Step) on ML_STAR Channel (1..8): 10000000, Optimized channel use: All sequence positions, Sequence: ML_STAR.CoolCar01_Pos03_04_DilutionSeries1, Sequence counting: (1) Automatic, Liquid class: "StandardVolume_PBS_DispenseJet_Empty_Juelich", Volume [µl]: 0, Cycles: g_NumMixing_Dilutions, LLD settings: On,
768	Loop: Break
769	End If

C:\Program Files (x86)\HAMILTON\Methods\sFIDA Greiner PEG\sFIDA_Greiner_PEG.med

	_00011_DiluteStandards
770	End If
771	End Loop
772	End If
773	1000µl Channel Tip Eject (Single Step) on ML_STAR Channel (1..8): 11111111, Optimized channel use: All sequence positions, Use default waste: On 3 return value(s)
774	If, Else (loopNumStandards is equal to 2)
775	Sequence: Set Current Position current position of sequence 'ML_STAR.CoolCar01_Pos03_04_DilutionSeries2' = '1'
776	Comment <********** Make dilution series 2 **********>
777	1000µl Channel Tip Pick Up (Single Step) on ML_STAR Channel (1..8): 10000000, Optimized channel use: All sequence positions, Sequence: ML_STAR.MIStar300ulStandardVolumeTip, Sequence counting: (1) Automatic 3 return value(s)
778	Write2 of HSLTipCountingLib TipCount::Write2(ML_STAR.MIStar300ulStandardVolumeTip, "300ulStandardVolumeTip", ML_STAR)
779	Loop 'sizeDilSeries2' times 'loopDiluteSeries2' used as loop counter variable
780	If, Else (loopDiluteSeries2 is greater than sizeDilSeries2)
781	Loop: Break
782	End If
783	If, Else (loopDiluteSeries2 is equal to 1)
784	Array: Get At 'current_vol' = element from array 'arr_VolBufferDilSeries2' at the index [loopDiluteSeries2].
785	Assignment 'g_VolToMix_Dilutions' = 'current_vol'
786	Array: Get At 'current_vol' = element from array 'arr_VolsDilSeries2' at the index [loopDiluteSeries2].
787	HSL code. g_VolToMix_Dilutions=(g_VolToMix_Dilutions+current_vol)/2;
788	1000µl Channel Aspirate (Single Step) on ML_STAR Channel (1..8): 10000000, Optimized channel use: All sequence positions, Sequence: ML_STAR.CoolCar01_Pos03_Eppi23_StandardStock02, Sequence counting: (1) Automatic, Liquid class: "StandardVolume_PBS_DispenseJet_Empty_Juelich", Volume [µl]: current_vol, Cycles: g_NumMixing_Dilutions, LLD settings: Off, Liquid following: Off 3 return value(s)

C:\Program Files (x86)\HAMILTON\Methods\sFIDA Greiner PEG\sFIDA_Greiner_PEG.med

	_00011_DiluteStandards
789	1000µl Channel Dispense (Single Step) on ML_STAR Channel (1..8): 10000000, Optimized channel use: All sequence positions, Sequence: ML_STAR.CoolCar01_Pos03_04_DilutionSeries2, Sequence counting: (1) Automatic, Liquid class: As in first aspiration of cycle, Volume [µl]: Remaining volume inclusive blowout air, Mix volume [µl]: *, Cycles: 0, Position relative to liquid surface: * mm, LLD settings: Off, Liquid following: On
790	Sequence: Get Current Position 'dilSeries2currentPos' = current position of sequence 'ML_STAR.CoolCar01_Pos03_04_DilutionSeries2'
791	Else
792	Array: Get At 'current_vol' = element from array 'arr_VolBufferDilSeries2' at the index [loopDiluteSeries2].
793	Assignment 'g_VolToMix_Dilutions' = 'current_vol'
794	Array: Get At 'current_vol' = element from array 'arr_VolsDilSeries2' at the index [loopDiluteSeries2].
795	HSL code. g_VolToMix_Dilutions=(g_VolToMix_Dilutions+current_vol)/2;
796	Assignment with Calculation 'setPosDilSeries2' = 'dilSeries2currentPos' - '1'
797	Sequence: Set Current Position current position of sequence 'ML_STAR.CoolCar01_Pos03_04_DilutionSeries2' = 'setPosDilSeries2'
798	If, Else (currentVol is less than g_bottomVolume2mlEppis)
799	1000µl Channel Aspirate (Single Step) on ML_STAR Channel (1..8): 10000000, Optimized channel use: All sequence positions, Sequence: ML_STAR.CoolCar01_Pos03_04_DilutionSeries2, Sequence counting: (1) Automatic, Liquid class: "StandardVolume_PBS_DispenseJet_Empty_Jueli ch", Volume [µl]: 0, Cycles: g_NumMixing_Dilutions, LLD settings: Off, Liquid
800	Else
801	1000µl Channel Aspirate (Single Step) on ML_STAR Channel (1..8): 10000000, Optimized channel use: All sequence positions, Sequence: ML_STAR.CoolCar01_Pos03_04_DilutionSeries2, Sequence counting: (1) Automatic, Liquid class: "StandardVolume_PBS_DispenseJet_Empty_Jueli ch", Volume [µl]: 0, Cycles: g_NumMixing_Dilutions, LLD settings: On,
802	End If
803	Sequence: Get Current Position 'dilSeries2currentPos' = current position of sequence 'ML_STAR.CoolCar01_Pos03_04_DilutionSeries2'
804	1000µl Channel Tip Eject (Single Step) on ML_STAR Channel (1..8): 11111111, Optimized channel use: All sequence positions, Use default waste: On 3 return value(s) .

C:\Program Files (x86)\HAMILTON\Methods\sFIDA Greiner PEG\sFIDA_Greiner_PEG.med

	_00011_DiluteStandards
805	1000µl Channel Tip Pick Up (Single Step) on ML_STAR Channel (1..8): 10000000, Optimized channel use: All sequence positions, Sequence: ML_STAR.MlStar300ulStandardVolumeTip, Sequence counting: (1) Automatic 3 return value(s)
806	Write2 of HSLTipCountingLib TipCount::Write2(ML_STAR.MlStar300ulStandardVolumeTip, "300ulStandardVolumeTip", ML_STAR)
807	Assignment with Calculation 'setPosDilSeries2' = 'dilSeries2currentPos' - '1'
808	Sequence: Set Current Position current position of sequence 'ML_STAR.CoolCar01_Pos03_04_DilutionSeries2' = 'setPosDilSeries2'
809	If, Else (currentVol is less than g_bottomVolume2mlEppis)
810	1000µl Channel Aspirate (Single Step) on ML_STAR Channel (1..8): 10000000, Optimized channel use: All sequence positions, Sequence: ML_STAR.CoolCar01_Pos03_04_DilutionSeries2, Sequence counting: (1) Automatic, Liquid class: "StandardVolume_PBS_DispenseJet_Empty_Jueli ch", Volume [µl]: current_vol, Mix volume [µl]: *, Cycles: 0, Position relative to liquid surface: * mm, LLD settings: Off, Liquid following: Off
811	Else
812	1000µl Channel Aspirate (Single Step) on ML_STAR Channel (1..8): 10000000, Optimized channel use: All sequence positions, Sequence: ML_STAR.CoolCar01_Pos03_04_DilutionSeries2, Sequence counting: (1) Automatic, Liquid class: "StandardVolume_PBS_DispenseJet_Empty_Jueli ch", Volume [µl]: current_vol, Mix volume [µl]: *, Cycles: 0, Position relative to liquid surface: * mm, LLD settings: On, Pressure:5, Liquid following: On
813	End If
814	1000µl Channel Dispense (Single Step) on ML_STAR Channel (1..8): 10000000, Optimized channel use: All sequence positions, Sequence: ML_STAR.CoolCar01_Pos03_04_DilutionSeries2, Sequence counting: (1) Automatic, Liquid class: As in first aspiration of cycle, Volume [µl]: Remaining volume inclusive blowout air, Mix volume [µl]: *, Cycles: 0, Position relative to liquid surface: * mm, LLD settings: Off, Liquid following: On
815	Sequence: Get Current Position 'dilSeries2currentPos' = current position of sequence 'ML_STAR.CoolCar01_Pos03_04_DilutionSeries2'
816	If, Else (loopDiluteSeries2 is equal to sizeDilSeries2)
817	Assignment with Calculation 'setPosDilSeries2' = 'dilSeries2currentPos' - '1'
818	Sequence: Set Current Position current position of sequence 'ML_STAR.CoolCar01_Pos03_04_DilutionSeries2' = 'setPosDilSeries2'

C:\Program Files (x86)\HAMILTON\Methods\sFIDA Greiner PEG\sFIDA_Greiner_PEG.med

	_00011_DiluteStandards
819	1000µl Channel Aspirate (Single Step) on ML_STAR Channel (1..8): 10000000, Optimized channel use: All sequence positions, Sequence: ML_STAR.CoolCar01_Pos03_04_DilutionSeries2, Sequence counting: (1) Automatic, Liquid class: "StandardVolume_PBS_DispenseJet_Empty_Jueli ch", Volume [µl]: 0, Cycles: g_NumMixing_Dilutions, LLD settings: On,
820	Loop: Break
821	End If
822	End If
823	End Loop
824	End If
825	1000µl Channel Tip Eject (Single Step) on ML_STAR Channel (1..8): 11111111, Optimized channel use: All sequence positions, Use default waste: On 3 return value(s)
826	If, Else (loopNumStandards is equal to 3)
827	Sequence: Set Current Position current position of sequence 'ML_STAR.CoolCar01_Pos03_04_DilutionSeries3' = '1'
828	Comment <********** Make dilution series 3 **********>
829	1000µl Channel Tip Pick Up (Single Step) on ML_STAR Channel (1..8): 10000000, Optimized channel use: All sequence positions, Sequence: ML_STAR.MlStar300ulStandardVolumeTip, Sequence counting: (1) Automatic 3 return value(s) .
830	Write2 of HSLTipCountingLib TipCount::Write2(ML_STAR.MlStar300ulStandardVolumeTip, "300ulStandardVolumeTip", ML_STAR)
831	Loop 'sizeDilSeries3' times 'loopDiluteSeries3' used as loop counter variable
832	If, Else (loopDiluteSeries3 is greater than sizeDilSeries3)
833	Loop: Break
834	End If
835	If, Else (loopDiluteSeries3 is equal to 1)
836	Array: Get At 'current_vol' = element from array 'arr_VolBufferDilSeries3' at the index [loopDiluteSeries3]
837	Assignment 'g_VolToMix_Dilutions' = 'current_vol'
838	Array: Get At 'current_vol' = element from array 'arr_VolsDilSeries3' at the index [loopDiluteSeries3]
839	HSL code. g_VolToMix_Dilutions=(g_VolToMix_Dilutions+current_vol) /2;

C:\Program Files (x86)\HAMILTON\Methods\sFIDA Greiner PEG\sFIDA_Greiner_PEG.med

	_00011_DiluteStandards	
840		1000µl Channel Aspirate (Single Step) on ML_STAR Channel (1..8): 10000000, Optimized channel use: All sequence positions, Sequence: ML_STAR.CoolCar01_Pos03_Eppi24_StandardStock04, Sequence counting: (1) Automatic, Liquid class: "StandardVolume_PBS_DispenseJet_Empty_Juelich", Volume [µl]: current_vol, Cycles: g_NumMixing_Dilutions, LLD settings: Off, Liquid following: Off 3 return value(s) .
841		1000µl Channel Dispense (Single Step) on ML_STAR Channel (1..8): 10000000, Optimized channel use: All sequence positions, Sequence: ML_STAR.CoolCar01_Pos03_04_DilutionSeries3, Sequence counting: (1) Automatic, Liquid class: As in first aspiration of cycle, Volume [µl]: Remaining volume inclusive blowout air, Cycles: g_NumMixing_Dilutions, LLD settings: Off, Liquid following: On 3 return value(s) .
842		Sequence: Get Current Position 'dilSeries3currentPos' = current position of sequence 'ML_STAR.CoolCar01_Pos03_04_DilutionSeries3'
843	Else	
844		Assignment with Calculation 'setPosDilSeries3' = 'dilSeries3currentPos' - '1'
845		Sequence: Set Current Position current position of sequence 'ML_STAR.CoolCar01_Pos03_04_DilutionSeries3' = 'setPosDilSeries3'
846		Array: Get At 'current_vol' = element from array 'arr_VolBufferDilSeries3' at the index [loopDiluteSeries3].
847		Assignment 'g_VolToMix_Dilutions' = 'current_vol'
848		Array: Get At 'current_vol' = element from array 'arr_VolsDilSeries3' at the index [loopDiluteSeries3].
849		HSL code. g_VolToMix_Dilutions=(g_VolToMix_Dilutions+current_vol)/2;
850		1000µl Channel Aspirate (Single Step) on ML_STAR Channel (1..8): 10000000, Optimized channel use: All sequence positions, Sequence: ML_STAR.CoolCar01_Pos03_04_DilutionSeries3, Sequence counting: (1) Automatic, Liquid class: "StandardVolume_PBS_DispenseJet_Empty_Juelich", Volume [µl]: 0, Cycles: g_NumMixing_Dilutions, LLD settings: On, Capacitive:5, Liquid following: On 3 return value(s) .
851		Sequence: Get Current Position 'dilSeries3currentPos' = current position of sequence 'ML_STAR.CoolCar01_Pos03_04_DilutionSeries3'
852		1000µl Channel Tip Eject (Single Step) on ML_STAR Channel (1..8): 11111111, Optimized channel use: All sequence positions, Use default waste: On 3 return value(s) .
853		1000µl Channel Tip Pick Up (Single Step) on ML_STAR Channel (1..8): 10000000, Optimized channel use: All sequence positions, Sequence: ML_STAR.MIStar300ulStandardVolumeTip, Sequence counting: (1) Automatic 3 return value(s) .
854		Write2 of HSLTipCountingLib TipCount::Write2(ML_STAR.MIStar300ulStandardVolumeTip, "300ulStandardVolumeTip", ML_STAR)

C:\Program Files (x86)\HAMILTON\Methods\sFIDA Greiner PEG\sFIDA_Greiner_PEG.med

	_00011_DiluteStandards
855	Assignment with Calculation 'setPosDilSeries3' = 'dilSeries3currentPos' - '1'
856	Sequence: Set Current Position current position of sequence 'ML_STAR.CoolCar01_Pos03_04_DilutionSeries3' = 'setPosDilSeries3'
857	1000µl Channel Aspirate (Single Step) on ML_STAR Channel (1..8): 10000000, Optimized channel use: All sequence positions, Sequence: ML_STAR.CoolCar01_Pos03_04_DilutionSeries3, Sequence counting: (1) Automatic, Liquid class: "StandardVolume_PBS_DispenseJet_Empty_Juelich", Volume [µl]: current_vol, Mix volume [µl]: *, Cycles: 0, Position relative to liquid surface: * mm, LLD settings: On, Capacitive:5, Liquid following: On 3 return value(s) .
858	1000µl Channel Dispense (Single Step) on ML_STAR Channel (1..8): 10000000, Optimized channel use: All sequence positions, Sequence: ML_STAR.CoolCar01_Pos03_04_DilutionSeries3, Sequence counting: (1) Automatic, Liquid class: As in first aspiration of cycle, Volume [µl]: Remaining volume inclusive blowout air, Cycles: g_NumMixing_Dilutions, LLD settings: Off, Liquid following: On 3 return value(s) .
859	Sequence: Get Current Position 'dilSeries3currentPos' = current position of sequence 'ML_STAR.CoolCar01_Pos03_04_DilutionSeries3'
860	If, Else (loopDiluteSeries3 is equal to sizeDilSeries3)
861	Assignment with Calculation 'setPosDilSeries3' = 'dilSeries3currentPos' - '1'
862	Sequence: Set Current Position current position of sequence 'ML_STAR.CoolCar01_Pos03_04_DilutionSeries3' = 'setPosDilSeries3'
863	1000µl Channel Aspirate (Single Step) on ML_STAR Channel (1..8): 10000000, Optimized channel use: All sequence positions, Sequence: ML_STAR.CoolCar01_Pos03_04_DilutionSeries3, Sequence counting: (1) Automatic, Liquid class: "StandardVolume_PBS_DispenseJet_Empty_Jueli ch", Volume [µl]: 0, Cycles: g_NumMixing_Dilutions, LLD settings: On,
864	Loop: Break
865	End If
866	End If
867	End Loop
868	End If
869	1000µl Channel Tip Eject (Single Step) on ML_STAR Channel (1..8): 11111111, Optimized channel use: All sequence positions, Use default waste: On 3 return value(s) .
870	End Loop
871	Sequence: Set Current Position current position of sequence 'ML_STAR.LiqCar01_Pos02_PBS' = '1'

C:\Program Files (x86)\HAMILTON\Methods\sFIDA Greiner PEG\sFIDA_Greiner_PEG.med

	_00011_DiluteStandards
872	End If
873	

C:\Program Files (x86)\HAMILTON\Methods\sFIDA Greiner PEG\sFIDA_Greiner_PEG.med

	_00012_DistributeSamples
1084	Comment <********** Distribute samples with 50µl tips randomly over columns ********** >
1085	Assignment 'g_progressText' = '"Distribute sample"'
1086	AppendStatusText of HSLStatusWindow HSLStatusWindow::AppendStatusText(g_progressText)
1087	Sequence: Set Current Position current position of sequence 'seq_current_plate' = '1'
1088	Sequence: Set End Position end position of sequence 'seq_current_plate' = 'g_NumWells'
1089	Assignment 'g_VolPreAliquot' = 'g_VolSample'
1090	Assignment 'g_VolPostAliquot' = '20'
1091	Assignment 'liquidClassSamples' = '"StandardVolume_CSF_DispenseJet_Part_Juelich"'
1092	Assignment 'g_VolAspirateToEmptyWells' = '120'
1093	Assignment with Calculation 'VolumeSampleReplicates' = 'g_VolSample' * 'g_NumReplicates'
1094	Assignment with Calculation 'aliquotVolumeSample' = 'VolumeSampleReplicates' + 'g_VolPreAliquot'
1095	Assignment with Calculation 'aliquotVolumeSample' = 'aliquotVolumeSample' + 'g_VolPostAliquot'
1096	Assignment 'liquidClassSamples' = '"Tip_50ul_PBS_DispenseJet_Empty_sFIDA_Juelich"'
1097	Assignment 'end_reading_excel_file' = '0'
1098	Comment <********** samples are distrubuted column wise **********>
1099	Loop 'g_NumColumns' times 'loopOverColumns' used as loop counter variable
1100	If, Else (end_reading_excel_file is equal to 1)
1101	Loop: Break
1102	End If
1103	Array: Declare / Set Size Set array 'positions_current_sample' to empty size.
1104	Array: Declare / Set Size Set array 'current_positions_on_plate' to empty size.
1105	Assignment 'current_plate_positions_excel' = '"Column "'
1106	Assignment 'current_sample_excel' = '"Samples in Column "'
1107	StrConcat2 of HSLStrLib current_sample_excel = StrConcat2(current_sample_excel, loopOverColumns)
1108	StrConcat2 of HSLStrLib current_plate_positions_excel = StrConcat2(current_plate_positions_excel, loopOverColumns)

C:\Program Files (x86)\HAMILTON\Methods\sFIDA Greiner PEG\sFIDA_Greiner_PEG.med

	_00012_DistributeSamples
1109	Assignment 'g_dataTransferSheet' = '"sample_positions_columnwise$"'
1110	File: Open File handle 'input_positions_sample' (File name: 'g_inputPath', Table name: 'g_dataTransferSheet'), Mode: 'Append'. Columns: current_position = current_sample_excel (Float) current_position_plate = current_plate_positions_excel (Float)
1111	TrcTrace of HSLTrcLib TrcTrace("excel column to read sample position ", current_sample_excel)
1112	TrcTrace of HSLTrcLib TrcTrace("excel column to read plate position ", current_plate_positions_excel)
1113	Loop 'g_NumRows' times 'loopCounterOverExcelColumn' used as loop counter variable
1114	File: Read Read from file 'input_positions_sample'
1115	Array: Set At Set 'current_position' within the array 'positions_current_sample', add to the end.
1116	Array: Set At Set 'current_position_plate' within the array 'current_positions_on_plate', add to the end.
1117	TrcTrace of HSLTrcLib TrcTrace("current position ", current_position)
1118	End Loop
1119	File: Close Close file 'input_positions_sample'
1120	Array: Get Size 'array_size_positions' = size of array 'positions_current_sample'.
1121	TrcTrace of HSLTrcLib TrcTrace("size of array ", array_size_positions)
1122	Loop '2' times 'loopCounterOverColumn' used as loop counter variable
1123	Comment <********** Remove liquid **********>
1124	Sequence: Get Current Position 'current_position_plate' = current position of sequence 'seq_current_plate'
1125	If, Else (current_position_plate is greater than OR equal to g_NumWells)
1126	Assignment 'end_reading_excel_file' = '1'
1127	Loop: Break
1128	Else
1129	If, Else (current_position_plate is less than OR equal to 0)
1130	Assignment 'end_reading_excel_file' = '1'
1131	Loop: Break
1132	End If
1133	End If

C:\Program Files (x86)\HAMILTON\Methods\sFIDA Greiner PEG\sFIDA_Greiner_PEG.med

	_00012_DistributeSamples
1134	1000µl Channel Tip Pick Up (Single Step) on ML_STAR Channel (1..8): 11111111, Optimized channel use: All sequence positions, Sequence: ML_STAR.MlStar300ulStandardVolumeTip, Sequence counting: (1) Automatic 3 return value(s)
1135	Write2 of HSLTipCountingLib TipCount::Write2(ML_STAR.MlStar300ulStandardVolumeTip, "300ulStandardVolumeTip", ML_STAR)
1136	1000µl Channel Aspirate (Single Step) on ML_STAR Channel (1..8): 11111111, Optimized channel use: All sequence positions, Sequence: seq_current_plate, Sequence counting: (1) Automatic, Liquid class: "StandardVolume_PBS_DispenseJet_Empty_Juelich", Volume [µl]: g_VolAspirateToEmptyWells, Mix volume [µl]: *, Cycles: 0, Position relative to liquid surface: * mm, LLD settings: Off, Liquid following: Off 3 return value(s)
1137	1000µl Channel Tip Eject (Single Step) on ML_STAR Channel (1..8): 11111111, Optimized channel use: All sequence positions, Use default waste: On 3 return value(s)
1138	TrcTrace of HSLTrcLib TrcTrace("during pipetting current_position_plate ", current_position_plate)
1139	Sequence: Set Current Position current position of sequence 'seq_current_plate' = 'current_position_plate'
1140	TrcTrace of HSLTrcLib TrcTrace("during pipetting current_position_plate ", current_position_plate)
1141	If, Else (loopCounterOverColumn is equal to 1)
1142	Assignment 'loopCounterOverArrayPositions' = '1'
1143	End If
1144	1000µl Channel Tip Pick Up (Single Step) on ML_STAR Channel (1..8): 11111111, Optimized channel use: All sequence positions, Sequence: ML_STAR.MlStar50ulTip, Sequence counting: (1) Automatic 3 return value(s)
1145	Write2 of HSLTipCountingLib TipCount::Write2(ML_STAR.MlStar50ulTip, "50ulStandardVolumeTip", ML_STAR)
1146	Assignment 'numberOfChannels' = '0'
1147	Assignment 'current_channel' = '1'
1148	Loop 'array_size_positions' times 'loopCounterOverArrayPositions' used as loop counter variable
1149	If, Else (loopCounterOverColumn is equal to 2)
1150	If, Else (loopCounterOverArrayPositions is equal to 1)
1151	Assignment 'loopCounterOverArrayPositions' = '2'
1152	End If
1153	End If
1154	Array: Get At 'current_sample_postion' = element from array 'positions_current_sample' at the index [loopCounterOverArrayPositions].
1155	MthFloor of HSLMthLib current_sample_postion = MthFloor(current_sample_postion)

C:\Program Files (x86)\HAMILTON\Methods\sFIDA Greiner PEG\sFIDA_Greiner_PEG.med

	_00012_DistributeSamples
1156	If, Else (current_sample_postion is less than 9999)
1157	Assignment 'g_singleChannelNum' = 'current_channel'
1158	TrcTrace of HSLTrcLib TrcTrace("during pipetting current_sample_postion ", current_sample_postion)
1159	Sequence: Set Current Position current position of sequence 'ML_STAR.all_possible_samples' = 'current_sample_postion'
1160	_0013_UseOneSpecificChannel of sFIDA_Greiner_PEG _0013_UseOneSpecificChannel()
1161	1000µl Channel Aspirate (Single Step) on ML_STAR Channel (1..8): g_singleChannelPatter, Optimized channel use: All sequence positions, Sequence: ML_STAR.all_possible_samples, Sequence counting: (1) Automatic, Liquid class: liquidClassSamples, Volume [µl]: g_VolSample, Mix volume [µl]: *, Cycles: 0, Position relative to liquid surface: * mm, LLD settings: On, Capacitive:5, Liquid following: On 3 return value(s) .
1162	Assignment with Calculation 'current_channel' = 'current_channel' + '1'
1163	Assignment with Calculation 'numberOfChannels' = 'numberOfChannels' + '1'
1164	End If
1165	Assignment with Calculation 'loopCounterOverArrayPositions' = 'loopCounterOverArrayPositions' + '1'
1166	End Loop
1167	TrcTrace of HSLTrcLib TrcTrace("anzahl kanal: ", numberOfChannels)
1168	Assignment 'g_numChannelsToUse' = 'numberOfChannels'
1169	_0012_DefineChannelsToUse of sFIDA_Greiner_PEG _0012_DefineChannelsToUse()
1170	1000µl Channel Dispense (Single Step) on ML_STAR Channel (1..8): g_channelPattern, Optimized channel use: All sequence positions, Sequence: seq_current_plate, Sequence counting: (1) Automatic, Liquid class: As in first aspiration of cycle, Volume [µl]: Remaining volume inclusive blowout air, Mix volume [µl]: *, Cycles: 0, Position relative to liquid surface: * mm, LLD settings: Off, Liquid following: On 3 return value(s) .
1171	1000µl Channel Tip Eject (Single Step) on ML_STAR Channel (1..8): 11111111, Optimized channel use: All sequence positions, Use default waste: On 3 return value(s) .
1172	End Loop
1173	End Loop
1174	StrConcat2 of HSLStrLib g_WashProgramPath = StrConcat2(g_GeneralPathToWasherPrograms, "Greiner_Sector1_3times_PBST_C_3times_PBS_B_remainingVol50µl.LHC")
1175	

C:\Program Files (x86)\HAMILTON\Methods\sFIDA Greiner PEG\sFIDA_Greiner_PEG.med

	_00013_DetectionAB
1077	Comment <********** Distribute detection antibodies **********>
1078	Assignment 'g_progressText' = '"Distribute detection antibodies"'
1079	AppendStatusText of HSLStatusWindow HSLStatusWindow::AppendStatusText(g_progressText)
1080	Assignment 'g_endDialogErrorString' = '"Method: 0009 DetectionAB"'
1081	Sequence: Set Current Position current position of sequence 'seq_current_plate' = '1'
1082	Sequence: Set End Position end position of sequence 'seq_current_plate' = 'g_NumWells'
1083	Loop over following sequences: - seq_current_plate (Controlling), Adjust for '1' times consumption 'loopCounterOverPlate' used as loop counter variable
1084	Comment <********** Remove liquid **********>
1085	Sequence: Get Current Position 'current_position_plate' = current position of sequence 'seq_current_plate'
1086	1000µl Channel Tip Pick Up (Single Step) on ML_STAR Channel (1..8): 11111111, Optimized channel use: All sequence positions, Sequence: ML_STAR.MIStar300ulStandardVolumeTip, Sequence counting: (1) Automatic 3 return value(s) .
1087	Write2 of HSLTipCountingLib TipCount::Write2(ML_STAR.MIStar300ulStandardVolumeTip, "300ulStandardVolumeTip", ML_STAR)
1088	1000µl Channel Aspirate (Single Step) on ML_STAR Channel (1..8): 11111111, Optimized channel use: All sequence positions, Sequence: seq_current_plate, Sequence counting: (1) Automatic, Liquid class: "StandardVolume_PBS_DispenseJet_Empty_Juelich", Volume [µl]: g_VolAspirateToEmptyWells, Mix volume [µl]: *, Cycles: 0, Position relative to liquid surface: * mm, LLD settings: Off, Liquid following: Off 3 return value(s)
1089	1000µl Channel Tip Eject (Single Step) on ML_STAR Channel (1..8): 11111111, Optimized channel use: All sequence positions, Use default waste: On 3 return value(s) .
1090	If, Else (current_position_plate is less than OR equal to 0)
1091	Assignment with Calculation 'current_position_plate' = 'g_NumWells' - '8'
1092	MthFloor of HSLMthLib current_position_plate = MthFloor(current_position_plate)
1093	End If
1094	Sequence: Set Current Position current position of sequence 'seq_current_plate' = 'current_position_plate'
1095	1000µl Channel Tip Pick Up (Single Step) on ML_STAR Channel (1..8): 11111111, Optimized channel use: All sequence positions, Sequence: ML_STAR.MIStar50ulTip, Sequence counting: (1) Automatic 3 return value(s) .
1096	Write2 of HSLTipCountingLib TipCount::Write2(ML_STAR.MIStar50ulTip, "50ulStandardVolumeTip", ML_STAR)
1097	If, Else (loopCounterOverPlate is equal to 1)

C:\Program Files (x86)\HAMILTON\Methods\sFIDA Greiner PEG\sFIDA_Greiner_PEG.med

	_00013_DetectionAB
1098	Sequence: Set Current Position current position of sequence 'seq_detection_source' = 'g_startPositionDetectionAB'
1099	1000µl Channel Aspirate (Single Step) on ML_STAR Channel (1..8): 11111111, Optimized channel use: All sequence positions, Sequence: seq_detection_source, Sequence counting: (1) Automatic, Liquid class: "Tip_50ul_PBS_DispenseJet_Empty_sFIDA_Juelich", Volume [µl]: 0, Mix volume [µl]: *, Cycles: 0, Position relative to liquid surface: * mm, LLD settings: On, Capacitive:5, Liquid following: On 3 return value(s) .
1100	_0015_CheckLiquidLevel of sFIDA_Greiner_PEG _0015_CheckLiquidLevel()
1101	End If
1102	Sequence: Set Current Position current position of sequence 'seq_detection_source' = 'g_startPositionDetectionAB'
1103	1000µl Channel Aspirate (Single Step) on ML_STAR Channel (1..8): 11111111, Optimized channel use: All sequence positions, Sequence: seq_detection_source, Sequence counting: (1) Automatic, Liquid class: "Tip_50ul_PBS_DispenseJet_Empty_sFIDA_Juelich", Volume [µl]: g_VolSample, Mix volume [µl]: *, Cycles: 0, Position relative to liquid surface: * mm, LLD settings: Off, Liquid following: Off 3 return value(s)
1104	1000µl Channel Dispense (Single Step) on ML_STAR Channel (1..8): 11111111, Optimized channel use: All sequence positions, Sequence: seq_current_plate, Sequence counting: (1) Automatic, Liquid class: As in first aspiration of cycle, Volume [µl]: g_VolCapture, Mix volume [µl]: *, Cycles: 0, Position relative to liquid surface: * mm, LLD settings: Off, Liquid following: On 3 return value(s)
1105	1000µl Channel Tip Eject (Single Step) on ML_STAR Channel (1..8): 11111111, Optimized channel use: All sequence positions, Use default waste: On 3 return value(s)
1106	End Loop - Reset sequence after loop: seq_current_plate
1107	StrConcat2 of HSLStrLib g_WashProgramPath = StrConcat2(g_GeneralPathToWasherPrograms, "Greiner_Sector1_5times_PBST_C_5times_PBS_B_remainingVol50µl_Water_D.LHC")
1108	

C:\Program Files (x86)\HAMILTON\Methods\sFIDA Greiner PEG\sFIDA_Greiner_PEG.med

	_00014_WaterWithAzid
1109	Comment <********** Remove Liquid and add water with azid **********>
1110	Assignment 'g_progressText' = '"Distribute Water with azid"'
1111	AppendStatusText of HSLStatusWindow HSLStatusWindow::AppendStatusText(g_progressText)
1112	Assignment 'g_endDialogErrorString' = '"Method: 025 Distribute water with azid"'
1113	Sequence: Set Current Position current position of sequence 'seq_current_plate' = '1'
1114	Sequence: Set End Position end position of sequence 'seq_current_plate' = 'g_NumWells'
1115	Loop over following sequences: - seq_current_plate (Controlling), Adjust for '1' times consumption 'loopCounterOverPlate' used as loop counter variable
1116	Comment <********** Remove liquid **********>
1117	Sequence: Get Current Position 'current_position_plate' = current position of sequence 'seq_current_plate'
1118	Channels_TipCounter_Write of Visual_NTR_library VISUAL_NTR_LIBRARY::Channels_TipCounter_Write(ML_STAR, ML_STAR.NTR_300ulTips_All, "TipCounter300ulNTR", default, ML_STAR.dummyGreinerPlate, 0, 1, 0, ML_STAR.NTR_300ulTips_All, 1, 0, 1, 0, "Please
1119	1000µl Channel Tip Pick Up (Single Step) on ML_STAR Channel (1..8): 11111111, Optimized channel use: All sequence positions, Sequence: ML_STAR.NTR_300ulTips_All, Sequence counting: (1) Automatic 3 return value(s)
1120	1000µl Channel Aspirate (Single Step) on ML_STAR Channel (1..8): 11111111, Optimized channel use: All sequence positions, Sequence: seq_current_plate, Sequence counting: (1) Automatic, Liquid class: "StandardVolume_PBS_DispenseJet_Empty_Juelich", Volume [µl]: g_VolAspirateToEmptyWells, Mix volume [µl]: *, Cycles: 0, Position relative to liquid surface: * mm, LLD settings: Off, Liquid following: Off 3 return value(s) .
1121	1000µl Channel Tip Eject (Single Step) on ML_STAR Channel (1..8): 11111111, Optimized channel use: All sequence positions, Use default waste: On 3 return value(s) .
1122	Sequence: Set Current Position current position of sequence 'seq_current_plate' = 'current_position_plate'
1123	Channels_TipCounter_Write of Visual_NTR_library VISUAL_NTR_LIBRARY::Channels_TipCounter_Write(ML_STAR, ML_STAR.NTR_300ulTips_All, "TipCounter300ulNTR", default, ML_STAR.dummyGreinerPlate, 0, 1, 0, ML_STAR.NTR_300ulTips_All, 1, 0, 1, 0, "Please
1124	1000µl Channel Tip Pick Up (Single Step) on ML_STAR Channel (1..8): 11111111, Optimized channel use: All sequence positions, Sequence: ML_STAR.NTR_300ulTips_All, Sequence counting: (1) Automatic 3 return value(s)
1125	Sequence: Set Current Position current position of sequence 'ML_STAR.LiqCar02_Pos01_WaterWithAzid' = '1'
1126	1000µl Channel Aspirate (Single Step) on ML_STAR Channel (1..8): 11111111, Optimized channel use: All sequence positions, Sequence: ML_STAR.LiqCar02_Pos01_WaterWithAzid, Sequence counting: (1) Automatic, Liquid class: "StandardVolume_PBS_DispenseJet_Empty_Juelich", Volume [µl]: g_wash_volume, Mix volume [µl]: *, Cycles: 0, Position relative to liquid surface: * mm, LLD settings: On, Pressure:5, Liquid following: Off 3 return value(s) .

C:\Program Files (x86)\HAMILTON\Methods\sFIDA Greiner PEG\sFIDA_Greiner_PEG.med

	_00014_WaterWithAzid
1127	 1000µl Channel Dispense (Single Step) on ML_STAR Channel (1..8): 11111111, Optimized channel use: All sequence positions, Sequence: seq_current_plate, Sequence counting: (1) Automatic, Liquid class: As in first aspiration of cycle, Volume [µl]: g_wash_volume, Mix volume [µl]: *, Cycles: 0, Position relative to liquid surface: * mm, LLD settings: Off, Liquid following: On 3 return value(s) .
1128	 1000µl Channel Tip Eject (Single Step) on ML_STAR Channel (1..8): 11111111, Optimized channel use: All sequence positions, Use default waste: On 3 return value(s) .
1129	 End Loop - Reset sequence after loop: seq_current_plate
1130	

C:\Program Files (x86)\HAMILTON\Methods\sFIDA Greiner PEG\sFIDA_Greiner_PEG.med

	_00015_ExchangeLiquidWithBuffer
1131	Comment <********** Remove Liquid and add buffer **********>
1132	Assignment 'g_progressText' = '"Remove liquid and add buffer"'
1133	AppendStatusText of HSLStatusWindow HSLStatusWindow::AppendStatusText(g_progressText)
1134	Assignment 'g_endDialogErrorString' = '"Method: 024 Exchange liquid against buffer"'
1135	Sequence: Set Current Position current position of sequence 'seq_current_plate' = '1'
1136	Sequence: Set End Position end position of sequence 'seq_current_plate' = 'g_NumWells'
1137	Loop over following sequences: - seq_current_plate (Controlling), Adjust for '1' times consumption 'loopCounterOverPlate' used as loop counter variable
1138	Comment <********** Remove liquid **********>
1139	Sequence: Get Current Position 'current_position_plate' = current position of sequence 'seq_current_plate'
1140	Channels_TipCounter_Write of Visual_NTR_library VISUAL_NTR_LIBRARY::Channels_TipCounter_Write(ML_STAR, ML_STAR.NTR_300ulTips_All, "TipCounter300ulNTR", default, ML_STAR.dummyGreinerPlate, 0, 1, 0, ML_STAR.NTR_300ulTips_All, 1, 0, 1, 0, "Please
1141	1000µl Channel Tip Pick Up (Single Step) on ML_STAR Channel (1..8): 11111111, Optimized channel use: All sequence positions, Sequence: ML_STAR.NTR_300ulTips_All, Sequence counting: (1) Automatic 3 return value(s) .
1142	1000µl Channel Aspirate (Single Step) on ML_STAR Channel (1..8): 11111111, Optimized channel use: All sequence positions, Sequence: seq_current_plate, Sequence counting: (1) Automatic, Liquid class: "StandardVolume_PBS_DispenseJet_Empty_Juelich", Volume [µl]: g_VolAspirateToEmptyWells, Mix volume [µl]: *, Cycles: 0, Position relative to liquid surface: * mm, LLD settings: Off, Liquid following: Off 3 return value(s) .
1143	1000µl Channel Tip Eject (Single Step) on ML_STAR Channel (1..8): 11111111, Optimized channel use: All sequence positions, Use default waste: On 3 return value(s) .
1144	Sequence: Set Current Position current position of sequence 'seq_current_plate' = 'current_position_plate'
1145	Sequence: Set Current Position current position of sequence 'ML_STAR.LiqCar01_Pos02_PBS' = '1'
1146	Channels_TipCounter_Write of Visual_NTR_library VISUAL_NTR_LIBRARY::Channels_TipCounter_Write(ML_STAR, ML_STAR.NTR_300ulTips_All, "TipCounter300ulNTR", default, ML_STAR.dummyGreinerPlate, 0, 1, 0, ML_STAR.NTR_300ulTips_All, 1, 0, 1, 0, "Please
1147	1000µl Channel Tip Pick Up (Single Step) on ML_STAR Channel (1..8): 11111111, Optimized channel use: All sequence positions, Sequence: ML_STAR.NTR_300ulTips_All, Sequence counting: (1) Automatic 3 return value(s) .
1148	1000µl Channel Aspirate (Single Step) on ML_STAR Channel (1..8): 11111111, Optimized channel use: All sequence positions, Sequence: ML_STAR.LiqCar01_Pos02_PBS, Sequence counting: (1) Automatic, Liquid class: "StandardVolume_PBS_DispenseJet_Empty_Juelich", Volume [µl]: g_wash_volume, Mix volume [µl]: *, Cycles: 0, Position relative to liquid surface: * mm, LLD settings: On, Pressure:5, Liquid following: Off 3 return value(s) .

C:\Program Files (x86)\HAMILTON\Methods\sFIDA Greiner PEG\sFIDA_Greiner_PEG.med

	_00015_ExchangeLiquidWithBuffer
1149	 1000µl Channel Dispense (Single Step) on ML_STAR Channel (1..8): 11111111, Optimized channel use: All sequence positions, Sequence: seq_current_plate, Sequence counting: (1) Automatic, Liquid class: As in first aspiration of cycle, Volume [µl]: g_wash_volume, Mix volume [µl]: *, Cycles: 0, Position relative to liquid surface: * mm, LLD settings: Off, Liquid following: On 3 return value(s) .
1150	 1000µl Channel Tip Eject (Single Step) on ML_STAR Channel (1..8): 11111111, Optimized channel use: All sequence positions, Use default waste: On 3 return value(s) .
1151	 End Loop - Reset sequence after loop: seq_current_plate
1152	

C:\Program Files (x86)\HAMILTON\Methods\sFIDA Greiner PEG\sFIDA_Greiner_PEG.med

	_000_Settings
1433	Comment <********** General settings and intialize global variables **********>
1434	Assignment 'g_dataTransferSheet' = '"DataTransferSector1$"'
1435	Init of HSLStatusWindow g_return_progress = HSLStatusWindow::Init()
1436	Assignment 'g_progressText' = '"Initializing variables"'
1437	SetStatusText of HSLStatusWindow HSLStatusWindow::SetStatusText(g_progressText)
1438	Assignment 'g_VolPreAliquot' = '15'
1439	Assignment 'g_VolPostAliquot' = '30'
1440	Assignment 'g_Volgeneral' = '45'
1441	Assignment 'g_maxVolPerTip300' = '300'
1442	Assignment 'g_maxVolPerTip1000' = '1000'
1443	Assignment 'g_inputPath' = '"C:\\Users\\technical_support\\Documents\\sFIDA-assay Input excel files\\20151117-sFIDA-Greiner-PEG-Standard.xls"'
1444	Assignment 'g_emailSubject' = '"Your experiment is done on the ML-Star!"'
1445	Assignment 'g_emailBody' = '"Experiment is done! Please come and clean me up"'
1446	Assignment 'g_emailAddress' = '"y.herrmann@fz-juelich.de"'
1447	GetUserName of HSLUtilLib currentUser = Util::GetUserName()
1448	If, Else (currentUser is NOT equal to "administrator")
1449	StrLeft of HSLStrLib firstLetter = StrLeft(currentUser, 1)
1450	StrTrimLeft of HSLStrLib currentUser = StrTrimLeft(currentUser, firstLetter)
1451	StrConcat4 of HSLStrLib g_emailAddress = StrConcat4(firstLetter, ".", currentUser, "@fz-juelich.de")
1452	TrcTrace of HSLTrcLib TrcTrace("email adresse ", g_emailAddress)
1453	End If
1454	StrConcat2 of HSLStrLib currentUser = StrConcat2(firstLetter, currentUser)
1455	Assignment 'g_GeneralPathToWasherPrograms' = '"C:\\ProgramData\\BioTek\\Liquid Handling Control 2.13\\Protocols\\Washer Programme\\Roboter\\Greiner\\PEG protocol wash steps\\All sectors flipped\\"'
1456	Assignment 'g_VolToMix_Dilutions' = '150'
1457	Assignment 'g_NumMixing_DissolveSteps' = '10'
1458	Assignment 'g_AspirateHeightGlassPlate' = '0,3'

C:\Program Files (x86)\HAMILTON\Methods\sFIDA Greiner PEG\sFIDA_Greiner_PEG.med

	_000_Settings	
1459	X=0	Assignment 'g_DispenseHeightGlassPlate' = '0,3'
1460	X=0	Assignment 'g_AspirateHeightReservoirs' = '0,8'
1461	X=0	Assignment 'g_DispenseHeightEppi2ml' = '15'
1462	X=0	Assignment 'g_DispenseHeightReagentReservoirs' = '50'
1463	X=0	Assignment 'g_gripHeightGlassPlate' = '3'
1464	X=0	Assignment 'g_endDialogErrorString' = '""'
1465	X=0	Assignment 'g_liquidClassBlood' = '0'
1466	X=0	Assignment 'g_liquidClassPlasma' = '0'
1467	X=0	Assignment 'g_liquidClassCSF' = '1'
1468	X=0	Assignment 'g_noneSamples' = '0'
1469	X=0	Assignment 'g_typeSample' = '"no special type"'
1470	X=0	Assignment 'g_VolAspirateToEmptyWells' = '150'
1471	X=0	Assignment 'g_dilutionWithPlasma' = '0'
1472	X=0	Assignment 'g_DiluteWithCSF' = '0'
1473	X=0	Assignment 'g_EndVolStdDilSeries1' = '0'
1474	X=0	Assignment 'g_EndVolStdDilSeries2' = '0'
1475	X=0	Assignment 'g_EndVolStdDilSeries3' = '0'
1476	X=0	Assignment 'g_startPositionPEGSpacer' = '1'
1477	X=0	Assignment 'g_startPositionEthanolamine' = '89'
1478	X=0	Assignment 'g_startPositionCapture' = '9'
1479	X=0	Assignment 'g_startPositionDetectionAB' = '17'
1480	X=0	Assignment 'g_startPositionEDCNHSActivation' = '1'
1481	X=0	Assignment 'g_startPositionBlocking' = '9'
1482	X=0	Assignment 'g_NumSamples' = '12'
1483	X=0	Assignment 'g_NumReplicates' = '12'
1484	X=0	Assignment 'g_NumWells' = '0'
1485	X=0	Assignment 'g_WashProgramPath' = '""'
1486	X=0	Assignment 'g_NumPlates' = '1'

C:\Program Files (x86)\HAMILTON\Methods\sFIDA Greiner PEG\sFIDA_Greiner_PEG.med

	_000_Settings	
1487	X=0	Assignment 'g_DispenseHeightPlate' = '1'
1488	X=0	Assignment 'g_UserInputSelectStep' = '0'
1489	X=0	Assignment 'g_num_wash_steps_ethanol' = '2'
1490	X=0	Assignment 'g_wash_volume' = '100'
1491	X=0	Assignment 'g_Ethanolamine_volume' = '45'
1492	X=0	Assignment 'g_num_wash_steps_DMSO' = '3'
1493	Abc	StrConcat2 of HSLStrLib currentUser = StrConcat2(firstLetter, currentUser)
1494	X=0	Assignment 'g_current_plate' = '1'
1495	X=0	Assignment 'g_singleChannelNum' = '1'
1496	X=0	Assignment 'g_numChannelsToUse' = '1'
1497	X=0	Assignment 'g_singleChannelPatter' = '"10000000"'
1498	X=0	Assignment 'g_NumMixing_Dilutions' = '10'
1499	X=0	Assignment 'g_NumStds' = '1'
1500	X=0	Assignment 'g_bottomVolume2mlEppis' = '200'
1501	X=0	Assignment 'g_spacer_pos_plate_1' = '1'
1502	X=0	Assignment 'g_spacer_pos_plate_2' = '25'
1503	X=0	Assignment 'g_EDCNHS_pos_plate_1' = '1'
1504	X=0	Assignment 'g_EDCNHS_pos_plate_2' = '17'
1505	X=0	Assignment 'g_cap_pos_plate_1' = '9'
1506	X=0	Assignment 'g_cap_pos_plate_2' = '33'
1507	X=0	Assignment 'g_block_pos_plate_1' = '9'
1508	X=0	Assignment 'g_block_pos_plate_2' = '25'
1509	X=0	Assignment 'g_dec_pos_plate_1' = '17'
1510	X=0	Assignment 'g_dec_pos_plate_2' = '41'
1511	X=0	Assignment 'g_ethanolamine_pos_plate_1' = '17'
1512	X=0	Assignment 'g_ethanolamine_pos_plate_2' = '41'
1513	X=0	Assignment 'g_column_wise' = '1'
1514	X=0	Assignment 'g_NumColumns' = '24'

C:\Program Files (x86)\HAMILTON\Methods\sFIDA Greiner PEG\sFIDA_Greiner_PEG.med

	_000_Settings
1515	X=0 Assignment 'g_NumRows' = '16'
1516	

C:\Program Files (x86)\HAMILTON\Methods\sFIDA Greiner PEG\sFIDA_Greiner_PEG.med

	_0001_ImportExcel
1153	Comment <********** Import user input from excel **********>
1154	Assignment 'g_progressText' = '"Read excel input file"'
1155	AppendStatusText of HSLStatusWindow HSLStatusWindow::AppendStatusText(g_progressText)
1156	Comment <********** Read first line of each column and save in global variables **********>
1157	File: Open File handle 'input_excel' (File name: 'g_inputPath', Table name: 'g_dataTransferSheet'), Mode: 'Append'. Columns: g_NumStds = "NumStds" (Integer) g_NumStdsConc = "NumStdsConc" (Integer) g_NumSamples = "NumSamples" (Integer) g_NumWells = "NumTotalWells" (Integer) g_NumReplicates = "NumReplicates" (Integer) g_VolCapture = "VolCapture" (Integer) g_VolSample = "VolSample" (Integer) g_VolDetection = "VolDetection" (Integer)
1158	File: Read Read from file 'input_excel'
1159	File: Close Close file 'input_excel'
1160	Comment <********** Read multiple lines in one column (number of concentrations) and save in global array **********>
1161	Assignment 'numStdConc' = '0'
1162	Assignment 'numConcString' = """"
1163	File: Open File handle 'input_excel_num_conc' (File name: 'g_inputPath', Table name: 'g_dataTransferSheet'), Mode: 'Append'. Columns: g_NumStdsConc = "NumStdsConc" (Float)
1164	Array: Declare / Set Size Set array 'NumConcEachStd' to empty size.
1165	Loop 'g_NumStds' times 'loopNumStds' used as loop counter variable
1173	File: Close Close file 'input_excel'
1174	Array: Declare / Set Size Set array 'arr_StdMolDil1' to empty size.
1175	Array: Declare / Set Size Set array 'arr_StdMolDil2' to empty size.
1176	Array: Declare / Set Size Set array 'arr_StdMolDil3' to empty size.
1177	Comment <********** Read multiple lines in one column (number of dilutions for each standard) and save in global arrays **********>
1178	Assignment 'concDilSeries1' = """"
1179	Assignment 'concDilSeries2' = """"

C:\Program Files (x86)\HAMILTON\Methods\sFIDA Greiner PEG\sFIDA_Greiner_PEG.med

	_0001_ImportExcel
1180	Assignment 'concDilSeries3' = """"
1181	Loop 'g_NumStds' times 'loopNumStds2' used as loop counter variable
1182	Assignment 'StdMolDilCol' = "'StdDilSeries"'
1183	Assignment with Calculation 'loopNumStds2Add1' = 'loopNumStds2' + '0'
1184	StrConcat2 of HSLStrLib StdMolDilCol = StrConcat2(StdMolDilCol, loopNumStds2Add1)
1185	File: Open File handle 'input_excel_num_dil' (File name: 'g_inputPath', Table name: 'g_dataTransferSheet'), Mode: 'Append'. Columns: g_NumStdMolDil = StdMolDilCol (Float)
1186	Array: Get At 'numStdConc' = element from array 'NumConcEachStd' at the index [loopNumStds2].
1187	Loop 'numStdConc' times 'loopCounter1' used as loop counter variable
1188	File: Read Read from file 'input_excel_num_dil'
1189	If, Else (loopNumStds2 is equal to 1)
1190	TrcTrace of HSLTrcLib TrcTrace("array 1 ", g_NumStdMolDil)
1191	Array: Set At Set 'g_NumStdMolDil' within the array 'arr_StdMolDil1', add to the end.
1192	StrConcat2 of HSLStrLib concDilSeries1 = StrConcat2(concDilSeries1, g_NumStdMolDil)
1193	StrConcat2 of HSLStrLib concDilSeries1 = StrConcat2(concDilSeries1, "\n")
1194	Else
1195	If, Else (loopNumStds2 is equal to 2)
1196	TrcTrace of HSLTrcLib TrcTrace("array 2 ", g_NumStdMolDil)
1197	Array: Set At Set 'g_NumStdMolDil' within the array 'arr_StdMolDil2', add to the end.
1198	StrConcat2 of HSLStrLib concDilSeries2 = StrConcat2(concDilSeries2, g_NumStdMolDil)
1199	StrConcat2 of HSLStrLib concDilSeries2 = StrConcat2(concDilSeries2, "\n")
1200	End If
1201	If, Else (loopNumStds2 is equal to 3)
1202	Array: Set At Set 'g_NumStdMolDil' within the array 'arr_StdMolDil3', add to the end.
1203	TrcTrace of HSLTrcLib TrcTrace("array 3 ", g_NumStdMolDil)
1204	StrConcat2 of HSLStrLib concDilSeries3 = StrConcat2(concDilSeries3, g_NumStdMolDil)
1205	StrConcat2 of HSLStrLib concDilSeries3 = StrConcat2(concDilSeries3, "\n")

C:\Program Files (x86)\HAMILTON\Methods\sFIDA Greiner PEG\sFIDA_Greiner_PEG.med

	_0001_ImportExcel
1206	End If
1207	End If
1208	End Loop
1209	File: Close Close file 'input_excel_num_dil'
1210	End Loop
1211	File: Close Close file 'input_excel'
1212	Assignment 'BufferVolDilSeries1' = '""'
1213	Assignment 'BufferVolDilSeries2' = '""'
1214	Assignment 'BufferVolDilSeries3' = '""'
1215	Array: Declare / Set Size Set array 'arr_VolsDilSeries1' to empty size.
1216	Array: Declare / Set Size Set array 'arr_VolsDilSeries2' to empty size.
1217	Array: Declare / Set Size Set array 'arr_VolsDilSeries3' to empty size.
1218	Comment <********* Read multiple lines in one column (volume for each standard dilution step) and save in global arrays
1219	Loop 'g_NumStds' times 'loopNumStds2' used as loop counter variable
1220	Assignment 'StdDilVolsCol' = '"VolDilutionSeries"'
1221	Assignment with Calculation 'loopNumStds2Add1' = 'loopNumStds2' + '0'
1222	StrConcat2 of HSLStrLib StdDilVolsCol = StrConcat2(StdDilVolsCol, loopNumStds2Add1)
1223	File: Open File handle 'input_excel_Vols_dil' (File name: 'g_inputPath', Table name: 'g_dataTransferSheet'), Mode: 'Append'. Columns: current_VolStdDil = StdDilVolsCol (Float)
1224	Array: Get At 'numStdConc' = element from array 'NumConcEachStd' at the index [loopNumStds2].
1225	Loop 'numStdConc' times 'loopCounter1' used as loop counter variable
1226	File: Read Read from file 'input_excel_Vols_dil'
1227	If, Else (loopNumStds2 is equal to 1)
1228	TrcTrace of HSLTrcLib TrcTrace("array 1 ", current_VolStdDil)
1229	Array: Set At Set 'current_VolStdDil' within the array 'arr_VolsDilSeries1', add to the end.
1230	StrConcat2 of HSLStrLib BufferVolDilSeries1 = StrConcat2(BufferVolDilSeries1, current_VolStdDil)

C:\Program Files (x86)\HAMILTON\Methods\sFIDA Greiner PEG\sFIDA_Greiner_PEG.med

	_0001_ImportExcel
1231	StrConcat2 of HSLStrLib BufferVolDilSeries1 = StrConcat2(BufferVolDilSeries1, "\n")
1232	Else
1233	If, Else (loopNumStds2 is equal to 2)
1234	TrcTrace of HSLTrcLib TrcTrace("array 2 ", current_VolStdDil)
1235	Array: Set At Set 'current_VolStdDil' within the array 'arr_VolsDilSeries2', add to the end.
1236	StrConcat2 of HSLStrLib BufferVolDilSeries2 = StrConcat2(BufferVolDilSeries2, current_VolStdDil)
1237	StrConcat2 of HSLStrLib BufferVolDilSeries2 = StrConcat2(BufferVolDilSeries2, "\n")
1238	End If
1239	If, Else (loopNumStds2 is equal to 3)
1240	Array: Set At Set 'current_VolStdDil' within the array 'arr_VolsDilSeries3', add to the end.
1241	TrcTrace of HSLTrcLib TrcTrace("array 3 ", current_VolStdDil)
1242	StrConcat2 of HSLStrLib BufferVolDilSeries3 = StrConcat2(BufferVolDilSeries3, current_VolStdDil)
1243	StrConcat2 of HSLStrLib BufferVolDilSeries3 = StrConcat2(BufferVolDilSeries3, "\n")
1244	End If
1245	End If
1246	End Loop
1247	File: Close Close file 'input_excel_num_dil'
1248	End Loop
1249	File: Close Close file 'input_excel'
1250	Assignment 'VolDilSeries1' = """"
1251	Assignment 'VolDilSeries2' = """"
1252	Assignment 'VolDilSeries3' = """"
1253	Array: Declare / Set Size Set array 'arr_VolBufferDilSeries1' to empty size.
1254	Array: Declare / Set Size Set array 'arr_VolBufferDilSeries2' to empty size.
1255	Array: Declare / Set Size Set array 'arr_VolBufferDilSeries3' to empty size.
1256	Array: Declare / Set Size Set array 'arr_EndVolDilSeries1' to empty size.
1257	Array: Declare / Set Size Set array 'arr_EndVolDilSeries2' to empty size.

C:\Program Files (x86)\HAMILTON\Methods\sFIDA Greiner PEG\sFIDA_Greiner_PEG.med

	_0001_ImportExcel
1258	Array: Declare / Set Size Set array 'arr_EndVolDilSeries3' to empty size.
1259	Comment <********** Read multiple lines in one column (volume of buffer for each standard dilution step) and save in global arrays **********>
1260	Loop 'g_NumStds' times 'loopNumStds2' used as loop counter variable
1261	Assignment 'StdDilVolsBufferCol' = '"VolDilutionSeriesBuffer"'
1262	Assignment with Calculation 'loopNumStds2Add1' = 'loopNumStds2' + '0'
1263	StrConcat2 of HSLStrLib StdDilVolsBufferCol = StrConcat2(StdDilVolsBufferCol, loopNumStds2Add1)
1264	File: Open File handle 'input_excel_num_VolBuffer' (File name: 'g_inputPath', Table name: 'g_dataTransferSheet'), Mode: 'Append'. Columns: current_VolBufferStdDil = StdDilVolsBufferCol (Float)
1265	Array: Get At 'numStdConc' = element from array 'NumConcEachStd' at the index [loopNumStds2].
1266	Loop 'numStdConc' times 'loopCounter1' used as loop counter variable
1267	File: Read Read from file 'input_excel_num_VolBuffer'
1268	If, Else (loopNumStds2 is equal to 1)
1269	TrcTrace of HSLTrcLib TrcTrace("array 1 ", current_VolBufferStdDil)
1270	Array: Set At Set 'current_VolBufferStdDil' within the array 'arr_VolBufferDilSeries1', add to the end.
1271	StrConcat2 of HSLStrLib VolDilSeries1 = StrConcat2(VolDilSeries1, current_VolBufferStdDil)
1272	StrConcat2 of HSLStrLib VolDilSeries1 = StrConcat2(VolDilSeries1, "\n")
1273	Assignment with Calculation 'g_EndVolStdDilSeries1' = 'current_VolBufferStdDil' + 'current_VolStdDil'
1274	Array: Set At Set 'g_EndVolStdDilSeries1' within the array 'arr_EndVolDilSeries1', add to the end.
1275	Else
1276	If, Else (loopNumStds2 is equal to 2)
1277	TrcTrace of HSLTrcLib TrcTrace("array 2 ", current_VolBufferStdDil)
1278	Array: Set At Set 'current_VolBufferStdDil' within the array 'arr_VolBufferDilSeries2', add to the end.
1279	StrConcat2 of HSLStrLib VolDilSeries2 = StrConcat2(VolDilSeries2,
1280	StrConcat2 of HSLStrLib VolDilSeries2 = StrConcat2(VolDilSeries2, "\n")
1281	Assignment with Calculation 'g_EndVolStdDilSeries2' = 'current_VolBufferStdDil' + 'current_VolStdDil'

C:\Program Files (x86)\HAMILTON\Methods\sFIDA Greiner PEG\sFIDA_Greiner_PEG.med

	_0001_ImportExcel
1282	Array: Set At Set 'g_EndVolStdDilSeries2' within the array 'arr_EndVolDilSeries1', add to the end.
1283	End If
1284	If, Else (loopNumStds2 is equal to 3)
1285	Array: Set At Set 'current_VolBufferStdDil' within the array 'arr_VolBufferDilSeries3', add to the end.
1286	TrcTrace of HSLTrcLib TrcTrace("array 3 ", current_VolBufferStdDil)
1287	StrConcat2 of HSLStrLib VolDilSeries3 = StrConcat2(VolDilSeries3,
1288	StrConcat2 of HSLStrLib VolDilSeries3 = StrConcat2(VolDilSeries3, "\n")
1289	Assignment with Calculation 'g_EndVolStdDilSeries3' = 'current_VolBufferStdDil' + 'current_VolStdDil'
1290	Array: Set At Set 'g_EndVolStdDilSeries3' within the array 'arr_EndVolDilSeries1', add to the end.
1291	End If
1292	End If
1293	End Loop
1294	File: Close Close file 'input_excel_num_dil'
1295	End Loop
1296	File: Close Close file 'input_excel'
1297	Comment <********** Import reagent positions for each plate **********>
1298	File: Open File handle 'input_excel_position_sheet' (File name: 'g_inputPath', Table name: '"DataTransferStartPositions$"'), Mode: 'Append'. Columns: g_spacer_pos_plate_1 = "PEG_Plate_1" (Float) g_EDCNHS_pos_plate_1 = "EDC_Plate_1" (Float) g_cap_pos_plate_1 = "Cap_Plate_1" (Float) g_block_pos_plate_1 = "Blocking_Plate_1" (Float) g_dec_pos_plate_1 = "Dec_Plate_1" (Float) g_spacer_pos_plate_2 = "PEG_Plate_2" (Float) g_EDCNHS_pos_plate_2 = "EDC_Plate_2" (Float) g_cap_pos_plate_2 = "Cap_Plate_2" (Float) g_block_pos_plate_2 = "Blocking_Plate_2" (Float) g_dec_pos_plate_2 = "Dec_Plate_2" (Float) g_ethanolamine_pos_plate_1 = "Ethanolamine_Plate_1" (Float) g_ethanolamine_pos_plate_2 = "Ethanolamine_Plate_2" (Float)
1299	File: Read Read from file 'input_excel_position_sheet'
1300	File: Close Close file 'input_excel_position_sheet'
1301	MthFloor of HSLMthLib g_NumWells = MthFloor(g_NumWells)

C:\Program Files (x86)\HAMILTON\Methods\sFIDA Greiner PEG\sFIDA_Greiner_PEG.med

	_0001_ImportExcel
1302	

C:\Program Files (x86)\HAMILTON\Methods\sFIDA Greiner PEG\sFIDA_Greiner_PEG.med

	_0002_SetupSequences
1303	Comment <********** Setup sequences according to plate number **********>
1304	Assignment 'g_progressText' = '"Setup sequences"'
1305	AppendStatusText of HSLStatusWindow HSLStatusWindow::AppendStatusText(g_progressText)
1306	SeqCopySequence of HSLSeqLib SeqCopySequence(seq_capture_source, ML_STAR.Carrier01_Antibodies_SmallReservoirRack)
1307	SeqCopySequence of HSLSeqLib SeqCopySequence(seq_detection_source, ML_STAR.Carrier01_Antibodies_SmallReservoirRack)
1308	SeqCopySequence of HSLSeqLib SeqCopySequence(seq_source_spacer_PEG, ML_STAR.Carrier01_Antibodies_SmallReservoirRack)
1309	Sequence: Set Current Position current position of sequence 'seq_capture_source' = 'g_startPositionCapture'
1310	Sequence: Set Current Position current position of sequence 'seq_detection_source' = 'g_startPositionDetectionAB'
1311	Sequence: Set Current Position current position of sequence 'seq_source_spacer_PEG' = 'g_startPositionPEGSpacer'
1312	SeqCopySequence of HSLSeqLib SeqCopySequence(seq_source_EDC_NHS_Cap,
1313	SeqCopySequence of HSLSeqLib SeqCopySequence(seq_source_ethanolamine,
1314	SeqCopySequence of HSLSeqLib SeqCopySequence(seq_source_blocking, ML_STAR.Carrier01_Reagents_TallReservoirRack)
1315	Sequence: Set Current Position current position of sequence 'seq_source_EDC_NHS_Cap' = 'g_startPositionEDCNHSActivation'
1316	Sequence: Set Current Position current position of sequence 'seq_source_blocking' = 'g_startPositionBlocking'
1317	Sequence: Set Current Position current position of sequence 'seq_source_spacer_PEG' = 'g_startPositionEthanolamine'
1318	SeqCopySequence of HSLSeqLib SeqCopySequence(seq_current_plate, ML_STAR.CoolCar01_Pos05_Greiner_allSectors)
1319	Sequence: Set Current Position current position of sequence 'seq_current_plate' = '1'
1320	

C:\Program Files (x86)\HAMILTON\Methods\sFIDA Greiner PEG\sFIDA_Greiner_PEG.med

	_0003_UseWasher
1321	Comment <********** Start washer program **********>
1322	Assignment 'g_progressText' = '"Washing step with protocol: "'
1323	AppendStatusText of HSLStatusWindow HSLStatusWindow::AppendStatusText(g_progressText)
1324	TrcTrace of HSLTrcLib TrcTrace("Washer program started: ", g_WashProgramPath)
1325	Assignment 'g_progressText' = 'g_WashProgramPath'
1326	AppendStatusText of HSLStatusWindow HSLStatusWindow::AppendStatusText(g_progressText)
1327	Assignment 'g_endDialogErrorString' = '"Washing step\n"'
1328	iSWAP Transport on ML_STAR Transport labware from 'ML_STAR.CoolCar01_Pos05_Greiner_allSectors' to 'ML_STAR.Greiner_WasherPlate_rotated180' 1 return value(s) .
1329	TrcTrace of HSLTrcLib TrcTrace("Washer program started: ", g_WashProgramPath)
1330	Connect of HSLLhcLib HSLLhcLib::Connect(HSLLhcLib::PRODUCT_TYPE_405TSLS, "USB 405 TS/LS sn:1309255", str_washer_version, str_washer_connect_msg)
1331	SetDeviceName of HSLLhcLib HSLLhcLib::SetDeviceName("USB 405 TS/LS sn:1309255", "BioTek_Washer")
1332	LoadProtocol of HSLLhcLib protocolSuccesful = HSLLhcLib::LoadProtocol("BioTek_Washer", HSLLhcLib::FILE, g_WashProgramPath)
1333	RunProtocol of HSLLhcLib HSLLhcLib::RunProtocol("BioTek_Washer")
1334	Assignment 'washerStatus' = '"BUSY"'
1335	Loop while '1' is equal to '1' 'loopCounterWasherStatus' used as loop counter variable
1336	GetStatus of HSLLhcLib HSLLhcLib::GetStatus("BioTek_Washer", washerStatus)
1337	TrcTrace of HSLTrcLib TrcTrace("washer status ", washerStatus)
1338	Timer: Start Start timer 'washerStatusReport', set to relative time: '10' [s]
1339	Timer: Wait for Wait for timer 'washerStatusReport', show timer display, is stoppable timer.
1340	If, Else (washerStatus is equal to "Error")
1341	StrConcat4 of HSLStrLib g_endDialogErrorString = StrConcat4(g_endDialogErrorString, washerStatus, "\n", str_washer_connect_msg)
1342	_0006_ErrorHandeling of sFIDA_Greiner_PEG _0006_ErrorHandeling()
1343	Loop: Break
1344	End If
1345	If, Else (washerStatus is equal to "Ready")

C:\Program Files (x86)\HAMILTON\Methods\sFIDA Greiner PEG\sFIDA_Greiner_PEG.med

	_0003_UseWasher
1346	Loop: Break
1347	End If
1348	If, Else (loopCounterWasherStatus is greater than 500)
1349	Assignment 'g_endDialogErrorString' = '"Washer has a problem!"'
1350	_0006_ErrorHandeling of sFIDA_Greiner_PEG _0006_ErrorHandeling()
1351	End If
1352	End Loop
1353	GetMessages of HSLLhcLib HSLLhcLib::GetMessages("BioTek_Washer", str_washer_connect_msg)
1354	TrcTrace of HSLTrcLib TrcTrace("Report from washer ", str_washer_connect_msg)
1355	MoveSeq of VirtualLabware_V2 VIRTUALLABWARE_V2::MoveSeq(ML_STAR, ML_STAR.CoolCar01_Pos05_Greiner_allSectors, 0, -1, 0)
1356	iSWAP Transport on ML_STAR Transport labware from 'ML_STAR.Greiner_WasherPlate_rotated180' to 'ML_STAR.CoolCar01_Pos05_Greiner_allSectors' 1 return value(s) .
1357	MoveSeq of VirtualLabware_V2 VIRTUALLABWARE_V2::MoveSeq(ML_STAR, ML_STAR.CoolCar01_Pos05_Greiner_allSectors, 0, 1, 0)
1358	If, Else (washerStatus is equal to "Error")
1359	User Output Dialog Title: '"Washer has an error"', Return Value: '', Buttons: "OK' and 'Cancel' button', Default: 'OK', Icons: 'Display information message icon', Sound: '', Timeout: 'infinite' Output: "Washer has problem. Do manual wash and then click ok.", <New Line>, "Or Abort method with cancel"
1360	End If
1361	If, Else (g_NumPlates is equal to 2)
1362	Comment <********** Redo washing step for second plate **********>
1363	StrConcat2 of HSLStrLib g_WashProgramPath = StrConcat2(g_GeneralPathToWasherPrograms, "Greiner_Sector1_3times_Water_D.LHC")
1364	iSWAP Transport on ML_STAR Transport labware from 'ML_STAR.CoolCar02_Pos05_Greiner_allSectors' to 'ML_STAR.GreinerWasherPlate' 1 return value(s)
1365	TrcTrace of HSLTrcLib TrcTrace("Washer program started: ", g_WashProgramPath)
1366	Connect of HSLLhcLib HSLLhcLib::Connect(HSLLhcLib::PRODUCT_TYPE_405TSLS, "USB 405 TS/LS sn:1309255", str_washer_version, str_washer_connect_msg)
1367	SetDeviceName of HSLLhcLib HSLLhcLib::SetDeviceName("USB 405 TS/LS sn:1309255", "BioTek_Washer")
1368	LoadProtocol of HSLLhcLib protocolSuccesful = HSLLhcLib::LoadProtocol("BioTek_Washer", HSLLhcLib::FILE, g_WashProgramPath)

C:\Program Files (x86)\HAMILTON\Methods\sFIDA Greiner PEG\sFIDA_Greiner_PEG.med

	_0003_UseWasher
1369	RunProtocol of HSLLhcLib HSLLhcLib::RunProtocol("BioTek_Washer")
1370	Loop while '1' is equal to '1' 'loopCounterWasherStatus' used as loop counter variable
1371	GetStatus of HSLLhcLib HSLLhcLib::GetStatus("BioTek_Washer", washerStatus)
1372	TrcTrace of HSLTrcLib TrcTrace("washer status ", washerStatus)
1373	Timer: Start Start timer 'washerStatusReport', set to relative time: '10' [s]
1374	Timer: Wait for Wait for timer 'washerStatusReport', show timer display, is stoppable timer.
1375	If, Else (washerStatus is equal to "Ready")
1376	Loop: Break
1377	End If
1378	If, Else (washerStatus is equal to "Error")
1379	StrConcat4 of HSLStrLib g_endDialogErrorString = StrConcat4(g_endDialogErrorString, washerStatus, "\n", str_washer_connect_msg)
1380	Loop: Break
1381	End If
1382	If, Else (loopCounterWasherStatus is greater than 1000)
1383	Assignment 'g_endDialogErrorString' = "'Washer has a problem!"'
1384	Loop: Break
1385	End If
1386	End Loop
1387	GetMessages of HSLLhcLib HSLLhcLib::GetMessages("BioTek_Washer", str_washer_connect_msg)
1388	TrcTrace of HSLTrcLib TrcTrace("Report from washer ", str_washer_connect_msg)
1389	iSWAP Transport on ML_STAR Transport labware from 'ML_STAR.GreinerWasherPlate' to 'ML_STAR.CoolCar02_Pos05_Greiner_allSectors' 1 return value(s) .
1390	If, Else (washerStatus is equal to "Error")
1391	User Output Dialog Title: "'Washer has an error"', Return Value: '', Buttons: "OK' and 'Cancel' button', Default: 'OK', Icons: 'Display information message icon', Sound: '', Timeout: 'infinite' Output: "Washer has problem. Do manual wash and then click ok.", <New Line>, "Or Abort method with cancel"
1392	End If
1393	End If

C:\Program Files (x86)\HAMILTON\Methods\sFIDA Greiner PEG\sFIDA_Greiner_PEG.med

	_0003_UseWasher
1394	

C:\Program Files (x86)\HAMILTON\Methods\sFIDA Greiner PEG\sFIDA_Greiner_PEG.med

	_0004_InputDialog
1395	Comment <********** Input Dialog for excel file **********>
1396	Assignment 'g_progressText' = '"Input dialog is shown"'
1397	AppendStatusText of HSLStatusWindow HSLStatusWindow::AppendStatusText(g_progressText)
1398	Custom Dialog from Custom Dialog Steps Dialog Title: "Dialog"
1399	CheckIfFileExists of HSLFileDirectoryLib fileCheck = FileDirectoryLib::CheckIfFileExists(g_inputPath)
1400	If, Else (fileCheck is equal to 0)
1401	Custom Dialog from Custom Dialog Steps Dialog Title: "File does not exist"
1402	Abort
1403	End If
1404	

C:\Program Files (x86)\HAMILTON\Methods\sFIDA Greiner PEG\sFIDA_Greiner_PEG.med

	_0007_MoveLidToParkPosition
1408	Comment <********** Move "lid" plate to greiner plate **********>
1409	Assignment 'g_progressText' = ""Move lid to park position""
1410	AppendStatusText of HSLStatusWindow HSLStatusWindow::AppendStatusText(g_progressText)
1411	iSWAP Transport on ML_STAR Transport labware from 'ML_STAR.Gre_Lid_OnPlate01' to 'ML_STAR.Gre_Lid_ParkPos04' 1 return value(s)
1412	If, Else (g_NumPlates is equal to 2)
1413	iSWAP Transport on ML_STAR Transport labware from 'ML_STAR.Gre_Lid_OnPlate02' to 'ML_STAR.Gre_Lid_ParkPos02' 1 return value(s)
1414	End If
1415	

C:\Program Files (x86)\HAMILTON\Methods\sFIDA Greiner PEG\sFIDA_Greiner_PEG.med

	_0008_MoveLidToPlate
1416	Comment <********** Move "lid" plate to greiner plate **********>
1417	Assignment 'g_progressText' = ""Lid to plate"'
1418	AppendStatusText of HSLStatusWindow HSLStatusWindow::AppendStatusText(g_progressText)
1419	If, Else (g_NumPlates is equal to 2)
1420	iSWAP Transport on ML_STAR Transport labware from 'ML_STAR.Gre_Lid_ParkPos02' to 'ML_STAR.Gre_Lid_OnPlate02' 1 return value(s)
1421	End If
1422	MoveSeq of VirtualLabware_V2 VIRTUALLABWARE_V2::MoveSeq(ML_STAR, ML_STAR.Gre_Lid_OnPlate01, 0, -2,5, 0)
1423	iSWAP Transport on ML_STAR Transport labware from 'ML_STAR.Gre_Lid_ParkPos04' to 'ML_STAR.Gre_Lid_OnPlate01' 1 return value(s)
1424	MoveSeq of VirtualLabware_V2 VIRTUALLABWARE_V2::MoveSeq(ML_STAR, ML_STAR.Gre_Lid_OnPlate01, 0, 2,5, 0)
1425	

C:\Program Files (x86)\HAMILTON\Methods\sFIDA Greiner PEG\sFIDA_Greiner_PEG.med

	_0011_SetupAllForEachPlate
1522	Comment <********** Setup sequences and number of wells for each plate **********>
1523	If, Else (g_current_plate is equal to 1)
1524	SeqCopySequence of HSLSeqLib SeqCopySequence(seq_current_plate, ML_STAR.CoolCar01_Pos05_Greiner_allSectors)
1525	Sequence: Set Current Position current position of sequence 'seq_current_plate' = '1'
1526	Assignment 'g_dataTransferSheetBody' = '"DataTransferPlate"'
1527	Assignment 'g_dataTransferSheet' = 'g_dataTransferSheetBody'
1528	StrConcat2 of HSLStrLib g_dataTransferSheet = StrConcat2(g_dataTransferSheet, 1)
1529	StrConcat2 of HSLStrLib g_dataTransferSheet = StrConcat2(g_dataTransferSheet, "$")
1530	TrcTrace of HSLTrcLib TrcTrace("Import sheet: ", g_dataTransferSheet)
1531	_0001_ImportExcel of sFIDA_Greiner_PEG _0001_ImportExcel()
1532	MthFloor of HSLMthLib g_ethanolamine_pos_plate_1 = MthFloor(g_ethanolamine_pos_plate_1)
1533	MthFloor of HSLMthLib g_spacer_pos_plate_1 = MthFloor(g_spacer_pos_plate_1)
1534	MthFloor of HSLMthLib g_EDCNHS_pos_plate_1 = MthFloor(g_EDCNHS_pos_plate_1)
1535	MthFloor of HSLMthLib g_cap_pos_plate_1 = MthFloor(g_cap_pos_plate_1)
1536	MthFloor of HSLMthLib g_block_pos_plate_1 = MthFloor(g_block_pos_plate_1)
1537	MthFloor of HSLMthLib g_dec_pos_plate_1 = MthFloor(g_dec_pos_plate_1)
1538	Assignment 'g_startPositionEthanolamine' = 'g_ethanolamine_pos_plate_1'
1539	Assignment 'g_startPositionPEGSpacer' = 'g_spacer_pos_plate_1'
1540	Assignment 'g_startPositionEDCNHSActivation' = 'g_EDCNHS_pos_plate_1'
1541	Assignment 'g_startPositionCapture' = 'g_cap_pos_plate_1'
1542	Assignment 'g_startPositionBlocking' = 'g_block_pos_plate_1'
1543	Assignment 'g_startPositionDetectionAB' = 'g_dec_pos_plate_1'
1544	If, Else (sample_step is equal to 1)
1545	Assignment 'g_progressText' = '"Setup sample sequence"'
1546	SetStatusText of HSLStatusWindow HSLStatusWindow::SetStatusText(g_progressText)
1547	Comment <********** Select sample sequence **********>

C:\Program Files (x86)\HAMILTON\Methods\sFIDA Greiner PEG\sFIDA_Greiner_PEG.med

	_0011_SetupAllForEachPlate
1548	SeqEdit2 of HSLSeqLib SeqEdit2(ML_STAR.all_possible_samples, ML_STAR, "Edit sequence for Sample distribution", "Edit sequence", 999999999, "", 0, ML_STAR.all_possible_samples, 1, "")
1549	End If
1550	Else
1551	SeqCopySequence of HSLSeqLib SeqCopySequence(seq_current_plate, ML_STAR.CoolCar02_Pos05_Greiner_allSectors)
1552	Sequence: Set Current Position current position of sequence 'seq_current_plate' = '1'
1553	Assignment 'g_dataTransferSheetBody' = '"DataTransferPlate"'
1554	Assignment 'g_dataTransferSheet' = 'g_dataTransferSheetBody'
1555	StrConcat2 of HSLStrLib g_dataTransferSheet = StrConcat2(g_dataTransferSheet, 2)
1556	StrConcat2 of HSLStrLib g_dataTransferSheet = StrConcat2(g_dataTransferSheet, "$")
1557	TrcTrace of HSLTrcLib TrcTrace("Import sheet: ", g_dataTransferSheet)
1558	_0001_ImportExcel of sFIDA_Greiner_PEG _0001_ImportExcel()
1559	MthFloor of HSLMthLib g_ethanolamine_pos_plate_2 = MthFloor(g_ethanolamine_pos_plate_2)
1560	MthFloor of HSLMthLib g_spacer_pos_plate_2 = MthFloor(g_spacer_pos_plate_2)
1561	MthFloor of HSLMthLib g_EDCNHS_pos_plate_2 = MthFloor(g_EDCNHS_pos_plate_2)
1562	MthFloor of HSLMthLib g_cap_pos_plate_2 = MthFloor(g_cap_pos_plate_2)
1563	MthFloor of HSLMthLib g_block_pos_plate_2 = MthFloor(g_block_pos_plate_2)
1564	MthFloor of HSLMthLib g_dec_pos_plate_2 = MthFloor(g_dec_pos_plate_2)
1565	Assignment 'g_startPositionEthanolamine' = 'g_ethanolamine_pos_plate_2'
1566	Assignment 'g_startPositionPEGSpacer' = 'g_spacer_pos_plate_2'
1567	Assignment 'g_startPositionEDCNHSActivation' = 'g_EDCNHS_pos_plate_2'
1568	Assignment 'g_startPositionCapture' = 'g_cap_pos_plate_2'
1569	Assignment 'g_startPositionBlocking' = 'g_block_pos_plate_2'
1570	Assignment 'g_startPositionDetectionAB' = 'g_dec_pos_plate_2'
1571	If, Else (sample_step is equal to 1)
1572	Assignment 'g_progressText' = '"Setup sample sequence"'
1573	SetStatusText of HSLStatusWindow HSLStatusWindow::SetStatusText(g_progressText)

C:\Program Files (x86)\HAMILTON\Methods\sFIDA Greiner PEG\sFIDA_Greiner_PEG.med

	_0011_SetupAllForEachPlate
1574	Comment <********** Select sample sequence **********>
1575	SeqEdit2 of HSLSeqLib SeqEdit2(ML_STAR.all_possible_samples, ML_STAR, "Edit sequence for Sample distribution", "Edit sequence", 999999999, "", 0, ML_STAR.all_possible_samples, 1, "")
1576	End If
1577	End If
1578	

C:\Program Files (x86)\HAMILTON\Methods\sFIDA Greiner PEG\sFIDA_Greiner_PEG.med

	_0014_CheckExcelInput
1633	Comment <********** Show dialog with experiment summary. (Input from excel) *********>
1634	Assignment 'g_StorageWater' = """"
1635	Custom Dialog from Custom Dialog Steps Dialog Title: "Last check before running"
1636	If, Else (checkedInput is equal to 3)
1637	Abort
1638	End If
1639	

C:\Program Files (x86)\HAMILTON\Methods\sFIDA Greiner PEG\sFIDA_Greiner_PEG.med

	_0015_CheckLiquidLevel
1640	Comment <***************** Check liquid level ******************>
1641	1000µl Channel Get Last Liquid Level (Single Step) on ML_STAR 3 return value(s) . connect_instrument = Connected instrument name_curr_step = Name of current step LLD_each_Channel = Liquid level for each channel.
1642	GetNumberOfPositions of HSLMlStarStepReturnLib number_positions_LLD = StepReturn::GetNumberOfPositions(LLD_each_Channel)
1643	GetLastLiquidLevel of HSLMlStarStepReturnLib LLD_specific_pos = StepReturn::GetLastLiquidLevel(1, LLD_each_Channel)
1644	Loop 'number_positions_LLD' times 'loopCounterOverChannels' used as loop counter variable
1645	GetLastLiquidLevel of HSLMlStarStepReturnLib LLD_specific_pos = StepReturn::GetLastLiquidLevel(loopCounterOverChannels, LLD_each_Channel)
1646	Assignment with Calculation 'row_id_based_on_counter' = 'loopCounterOverChannels' + '1'
1647	StrConcat12 of HSLStrLib str_update_col_sql = StrConcat12("UPDATE ", "[Sheet1$]", " SET [Col", loopCounter_number_pos, "] ='", LLD_specific_pos, "' WHERE ", "[row-ID]", "='row", loopCounterOverChannels, "'", "")
1648	TrcTrace of HSLTrcLib TrcTrace("SQL Command update: ", str_update_col_sql)
1649	If, Else (LLD_specific_pos is less than OR equal to 112)
1650	User Output Dialog Title: '"Pause"', Return Value: '', Buttons: 'Only 'OK' button', Default: 'OK', Icons: 'Display information message icon', Sound: '', Timeout: 'infinite' Output: "Please check liquid for current step"
1651	Loop: Break
1652	End If
1653	End Loop
1654	

A.3 *Reprint permissions* für Publikationen

Von: Carry Koolbergen
An: Herrmann, Yvonne
Thema: RE: Letter of permission to reprint an article in a cumulative dissertation
Datum: Dienstag, 14. Februar 2017 15:43:44
Anlagen: image001.png

DOI: 10.3233/JAD-160253
Citation: Journal of Alzheimer's Disease, vol. 54, no. 1, pp. 79-88, 2016

Dear Yvonne Herrmann,

We hereby grant you permission to reproduce the below mentioned material in **print and electronic format** at no charge subject to the following conditions:

1. If any part of the material to be used (for example, figures) has appeared in our publication with credit or acknowledgement to another source, permission must also be sought from that source. If such permission is not obtained then that material may not be included in your publication/copies.

2. Suitable acknowledgement to the source must be made, either as a footnote or in a reference list at the end of your publication, as follows:

   "Reprinted from Publication title, Vol number, Author(s), Title of article, Pages No., Copyright (Year), with permission from IOS Press".
   The publication is available at IOS Press through http://dx.doi.org/10.3233/JAD-160253

3. This permission is granted for non-exclusive world **English** rights only. For other languages please reapply separately for each one required.

4. Reproduction of this material is confined to the purpose for which permission is hereby given.

Yours sincerely

Carry Koolbergen (Mrs.)
Contracts, Rights & Permissions Coordinator
Not in the office on Wednesdays

IOS Press BV
Nieuwe Hemweg 6B
1013 BG Amsterdam
The Netherlands
Tel.: +31 (0)20 687 0022
Fax: +31 (0)20 687 0019
Email: c.koolbergen@iospress.nl / publisher@iospress.nl
URL: www.iospress.nl

Van: Herrmann, Yvonne [mailto:y.herrmann@fz-juelich.de]
Verzonden: dinsdag 31 januari 2017 18:21
Aan: Carry Koolbergen <C.Koolbergen@iospress.nl>
Onderwerp: Letter of permission to reprint an article in a cumulative dissertation

Copyright Clearance Center RightsLink®

My Orders My Library My Profile

Welcome y.herrmann@fz-juelich.de Log out | Help

My Orders > Orders > All Orders

License Details

This Agreement between Yvonne Herrmann ("You") and De Gruyter ("De Gruyter") consists of your license details and the terms and conditions provided by De Gruyter and Copyright Clearance Center.

printable details

License Number	4047691163742
License date	Feb 14, 2017
Licensed Content Publisher	De Gruyter
Licensed Content Publication	Biological Chemistry
Licensed Content Title	Analysis of anticoagulants for blood-based quantitation of amyloid β oligomers in the sFIDA assay
Licensed Content Author	Kateryna Kravchenko, Andreas Kulawik, Maren Hülsemann, et al.
Licensed Content Date	Dec 20, 2016
Licensed Content Volume	0
Licensed Content Issue	0
I would like to...	Thesis/Dissertation
Requestor type	Academic institution
Format	Print, Electronic
Portion	chapter/article
Page range of chapter/article	1-11
Number of pages in chapter/article	11
Rights for	Main product
Duration of use	Life of current edition
Creation of copies for the disabled	no
With minor editing privileges	no
For distribution to	Worldwide
In the following language(s)	Original language of publication
With incidental promotional use	no
Lifetime unit quantity of new product	0 to 499
The requesting person/organization	Co-author on the requested article
Order reference number	
Title of your thesis / dissertation	Automatisierung und Kalibrierung des sFIDA-Assays zur frühzeitigen Diagnose von neurodegenerativen Krankheiten
Expected completion date	Apr 2017
Expected size (number of pages)	200
Publisher VAT	
Requestor Location	Yvonne Herrmann Wilhelm-Johnen-Str. Juelich, NRW 52426 Germany Attn: Yvonne Herrmann
Billing Type	Credit Card
Credit card info	Visa ending in 3329
Credit card expiration	04/2020
Total	**124.49 EUR**

BACK

Copyright Clearance Center RightsLink®

My Orders My Library My Profile

Welcome y.herrmann@fz-juelich.de Log out | Help

My Orders > Orders > All Orders

License Details

This Agreement between Yvonne Herrmann ("You") and Elsevier ("Elsevier") consists of your license details and the terms and conditions provided by Elsevier and Copyright Clearance Center.

printable details

License Number	4040620591218
License date	Feb 02, 2017
Licensed Content Publisher	Elsevier
Licensed Content Publication	Clinical Biochemistry
Licensed Content Title	sFIDA automation yields sub-femtomolar limit of detection for Aβ aggregates in body fluids
Licensed Content Author	Yvonne Herrmann,Andreas Kulawik,Katja Kühbach,Maren Hülsemann,Luriano Peters,Tuyen Bujnicki,Kateryna Kravchenko,Christina Linnartz,Johannes Willbold,Christian Zafiu,Oliver Bannach,Dieter Willbold
Licensed Content Date	Available online 5 November 2016
Licensed Content Volume	n/a
Licensed Content Issue	n/a
Licensed Content Pages	1
Type of Use	reuse in a thesis/dissertation
Portion	full article
Format	both print and electronic
Are you the author of this Elsevier article?	Yes
Will you be translating?	No
Order reference number	
Title of your thesis/dissertation	Automatisierung und Kalibrierung des sFIDA-Assays zur frühzeitigen Diagnose von neurodegenerativen Krankheiten
Expected completion date	Apr 2017
Estimated size (number of pages)	200
Elsevier VAT number	GB 494 6272 12
Requestor Location	Yvonne Herrmann Wilhelm-Johnen-Str. Juelich, NRW 52426 Germany Attn: Yvonne Herrmann
Billing Type	Invoice
Billing address	Yvonne Herrmann Wilhelm-Johnen-Str. Juelich, Germany 52426 Attn: Yvonne Herrmann
Total	**0.00 EUR**

BACK

Copyright Clearance Center RightsLink®

Meine Aufträge MyLibrary Mein Profil

Welcome y.herrmann@fz-juelich.de Log out | Help

My Orders > Orders > All Orders

License Details

This Agreement between Yvonne Herrmann ("You") and Elsevier ("Elsevier") consists of your license details and the terms and conditions provided by Elsevier and Copyright Clearance Center.

printable details

License Number	4039401093999
License date	Jan 31, 2017
Licensed Content Publisher	Elsevier
Licensed Content Publication	Clinica Chimica Acta
Licensed Content Title	Nanoparticle standards for immuno-based quantitation of α-synuclein oligomers in diagnostics of Parkinson's disease and other synucleopathies
Licensed Content Author	Yvonne Herrmann,Tuyen Bujnicki,Christian Zafiu,Andreas Kulawik,Katja Kühbach,Luriano Peters,Judith Fabig,Johannes Willbold,Oliver Bannach,Dieter Willbold
Licensed Content Date	March 2017
Licensed Content Volume	466
Licensed Content Issue	n/a
Licensed Content Pages	8
Type of Use	reuse in a thesis/dissertation
Portion	full article
Format	both print and electronic
Are you the author of this Elsevier article?	Yes
Will you be translating?	No
Order reference number	
Title of your thesis/dissertation	Automatisierung und Kalibrierung des sFIDA-Assays zur frühzeitigen Diagnose von neurodegenerativen Krankheiten
Expected completion date	Apr 2017
Estimated size (number of pages)	200
Elsevier VAT number	GB 494 6272 12
Requestor Location	Yvonne Herrmann Wilhelm-Johnen-Str. Juelich, NRW 52426 Germany Attn: Yvonne Herrmann
Total	**0.00 EUR**

BACK

Eidesstattliche Erklärung

Ich erkläre an Eides Statt, dass ich meine Dissertation mit dem Titel *Automatisierung und Kalibrierung des sFIDA-Assays zur frühzeitigen Diagnose von neurodegenerativen Krankheiten* selbständig und ohne Benutzung anderer als der angegebenen Hilfsmittel angefertigt habe und dass ich alle Stellen, die ich wörtlich oder sinngemäß aus Veröffentlichungen entnommen habe, als solche kenntlich gemacht habe. Die Arbeit hat bisher in gleicher oder ähnlicher Form oder auszugsweise noch keiner Prüfungsbehörde vorgelegen.
Ich versichere, dass die eingereichte schriftliche Fassung der auf dem beigefügten Medium gespeicherten Fassung entspricht.

Jülich, den 15. Februar 2017

(Yvonne Nelly Herrmann)